Dissertation zur Erlangung des Doktorgrades
der Fakultät für Biologie
der Ludwig-Maximilians-Universität München

Histone H3 lysine 9 methylation: A signature for chromatin function

Ragnhild Eskeland
aus
Stord, Norwegen

Dezember 2006

Ehrenwörtliche Versicherung

Diese Dissertation wurde selbständig, ohne unerlaubte Hilfe erarbeitet.

München, 21.12.2006

Ragnhild Eskeland

Dissertation eingereicht am: 21.12.2006

1. Gutachter: Prof. Dr. Peter B. Becker
2. Gutachter: Prof. Dr. med. Thomas Cremer

Mündliche Prüfung am: **19.04.2007**

Til mor og far

"The mind is not a vessel to be filled but a fire to be kindled." Mestrius Plutarchus

The results presented in this PhD thesis have been published in following publications:

Eskeland, R.*, Czermin, B.*, Boeke, J., Bonaldi, T., Regula, J. T., and Imhof, A. (2004). The N-terminus of Drosophila SU(VAR)3-9 mediates dimerization and regulates its methyltransferase activity. *Biochemistry* **43,** 3740-9.

Eskeland, R., Eberharter, A., and Imhof, A. (2007). HP1 binding to chromatin methylated at H3K9 is enhanced by auxiliary factors. Mol Cell Biol 27, 453-465.

Greiner, D., Bonaldi, T., Eskeland, R., Roemer, E., and Imhof, A. (2005). Identification of a specific inhibitor of the histone methyltransferase SU(VAR)3-9. *Nat Chem Biol* **1,** 143-5.

Stabell, M., Eskeland, R., Bjorkmo, M., Larsson, J., Aalen, R. B., Imhof, A., and Lambertsson, A. (2006). The Drosophila G9a gene encodes a multi-catalytic histone methyltransferase required for normal development. *Nucleic Acids Res* **34,** 4609-21.

*Co-first author.

These publications can be found in the Appendix.

Acknowledgements

I would like to thank my supervisor Axel Imhof for giving me the opportunity to work in his lab. You have taught me a lot the last four years and given me the freedom to develop my own ideas.

My gratitude is also to Peter Becker for being my official supervisor and providing an excellent scientific environment in the lab. Thank you for following up on my work, I have learned a lot from your critical comments.

Prof. Dr.Thomas Cremer I would like to thank for being my "Zweitgutachter".

Many thanks to Cristina for corrections on my thesis. Thank you for always encouraging me:-) I am also grateful to Jan Postberg for corrections.

I would also like to thank the Imhof lab for the nice every day life in the lab. Thank you all for the wonderful leaving present! It will be hanging in my living room and always remind me of my time here. Birgit for sharing your knowledge and reagents. Annette for everyday chats, I had a great time with you in DomRep. Tizi for help with the mass spec and support in the lab. Also thanks to: Jörn, Irene, Lars, Pierre, Ana, Tilman and Doro.

Thanks goes to Anton Eberharter for scientific discussions and for providing me with active ACF and ACF1 plus viral stocks and constructs. I am grateful to Alex Brehm and Gernot Längst for always being available for questions and comments on my work. Andreas Hocheimer for many inspiring discussions and showing me the excellent NE protocol.

I also wish to thank the rest of the Becker lab, both for the nice environment you have created and help and advices throughout my time here.

I am grateful to the International graduate program of Elitenetzwerk Bayern for supporting me to visit a Chromatin Structure and Function Conference in December 2006.

A special thanks goes to Even. Thank you for always being understanding, supportive and for all the late dinners you have had ready for me. I will never forget that you came here to be with me. My life in Munich would not have been the same without you!

Mange takk til familien heime. Mor og far for at dåke forstod kor viktig dette var for meg og for støtte heile vegen. Det har vore langt heim. og eg har savna dåke mykje. Heldigvis blir turen heim mykje kortare etter jul.

I am also very grateful to all my friends here in Munich. Simone and Silvia for a wonderful holiday in Italy and many, many cinema memories. Isabel and Armin for all the times at Mozart and for introducing us to good German wine. Juliane and Ingo for lending me the laptop and for all the nice dinners. Birgit for borrowing me the bike. It was nice to have you around in the lab and I am happy we managed to stay in touch after you left. Many thanks go also to Mattia and Anna, Marica and Thomas, Javier and Robert for all the great nights out in Munich. Warm thanks goes to Jo, Ina and Dan who was here the first years of my time in Munich. Lastly, many thanx goes to friends at home that I did not get to see very much these years.

1. Summary

In most eukaryotes the histone methyltransferases SU(VAR)3-9, G9a and their orthologues play major roles in transcriptional regulation. Histone H3 lysine 9 methylation is associated to transcriptional silencing *in vivo*. SU(VAR)3-9 is the main H3K9 HMTase in *Drosophila* heterochromatin whereas G9a was found to be an euchromatic H3K9 methyltransferase in mammalian cells. In this work SU(VAR)3-9 and a new HMTase homologous to G9a were characterized *in vitro*.

A detailed analysis of the reaction products shows that recombinant SU(VAR)3-9 adds three methylgroups to full-length H3 and only two methylgroups to an H3-tail peptide. The transfer of two methylgroups to an unmethylated H3-tail peptide is achieved in a nonprocessive manner. The full-length enzyme elutes with an apparent molecular weight of 160 kDa from a gel filtration column, which indicates the formation of a dimer. The N-terminus was shown to be required for this dimerisation and to retrieve full activity *in vitro*. We show that the interaction occurs by domain swapping of two motifs within the N-terminus. The fact that the N-terminus is responsible for a concentration dependent dimerisation of SU(VAR)3-9 may indicate a role for this domain in the dosage-dependent effect on position effect variegation.

Drosophila G9a adds three methyl groups to unmethylated H3 *in vitro* as has been described for mouse G9a. *In vitro*, a N-terminal truncation of dG9a adds three methylgroups toward H3K9 and K27, with a preference for K9. Surprisingly, dG9a also methylates H4 with specificity for K8, K12 or K16. *In vivo*, dG9a is present in complexes with a molecular mass of 440-670 kDa and we show that it specifically interacts with the histone deacetylase Rpd3.

HP1a is predominantly associated with centromeric heterochromatin in *Drosophila*. Supporting the histone code hypothesis, the chromo domain of HP1 recognises and binds H3K9 methylated peptides. Here we show the mechanism for binding to H3K9Me chromatin by recombinant *Drosophila* HP1a. HP1a requires a bimodal interaction of the chromo domain with H3K9Me and a simultaneous interaction of the chromo shadow domain with auxiliary factors (SU(VAR)3-9 and ACF) for stable association with H3K9Me chromatin. The two HP1 paralogs HP1a and HP1c bind to distinct chromatin structures and we identify distinct interaction partners for these two proteins.

2. Introduction

2.1 Chromatin

The compaction of eukaryotic DNA into a complex structure known as chromatin is necessary to fit it into the nucleus. More than thirty years ago a proposal was made that the structural repeating unit of chromatin in eukaryote organisms is the nucleosome (Kornberg, 1974). The nucleosome consists of an octamer, containing a central tetramer of histones H3 and H4 and two dimers of histones H2A and H2B. Wrapped around each histone octamer is 146 bp of DNA in 1.65 turns of flat, left-handed superhelix (Luger et al., 1997). The DNA connecting two nucleosome core particles is called linker DNA and can vary in length. Linker histone H1 binds to linker DNA, and DNA entering and exiting nucleosome (Thomas, 1999). Histone H1 facilitates the transition from the 10 nm filament to the 30 nm chromatin fiber and stabilizes both the nucleosome and chromatin higher order structure (Figure 2.1) (Ramakrishnan, 1997). The core histones are small basic proteins with N-terminal tail domain, a central histone fold and a C-terminal tail. The N-terminal tail domains and some C-terminal tail domains of the core histones protrude out of the nucleosome (Luger et al., 1997). Particularly the core histones are among the most conserved proteins known, suggesting for a strong selective pressure against mutations. Histone H4 has evolved the slowest, however different H4 genes coding for the same polypeptide sequence have been shown to have differential regulated expression during the cell cycle (Akhmanova et al., 1996). Within the classes of histones H1, H2A, H2B and H3, there are amino acid variations resulting in histone variants (Doenecke et al., 1997; Malik and Henikoff, 2003). Some histone variants are more diverse in sequence, for example, CENP-A is a H3 variant specifically localizing to centromeres (Palmer et al., 1991). Another such variant is macroH2A, which is enriched on the inactive human X-chromosome (Chadwick and Willard, 2002). Histone variants have different expression patterns, some are highly expressed during replication others has a low expression throughout the cell cycle, and the different histone variants participate in many nuclear events such as DNA repair, transcriptional regulation, heterochromatin barriers and genome stability (For recent review, see (Kamakaka and Biggins, 2005).

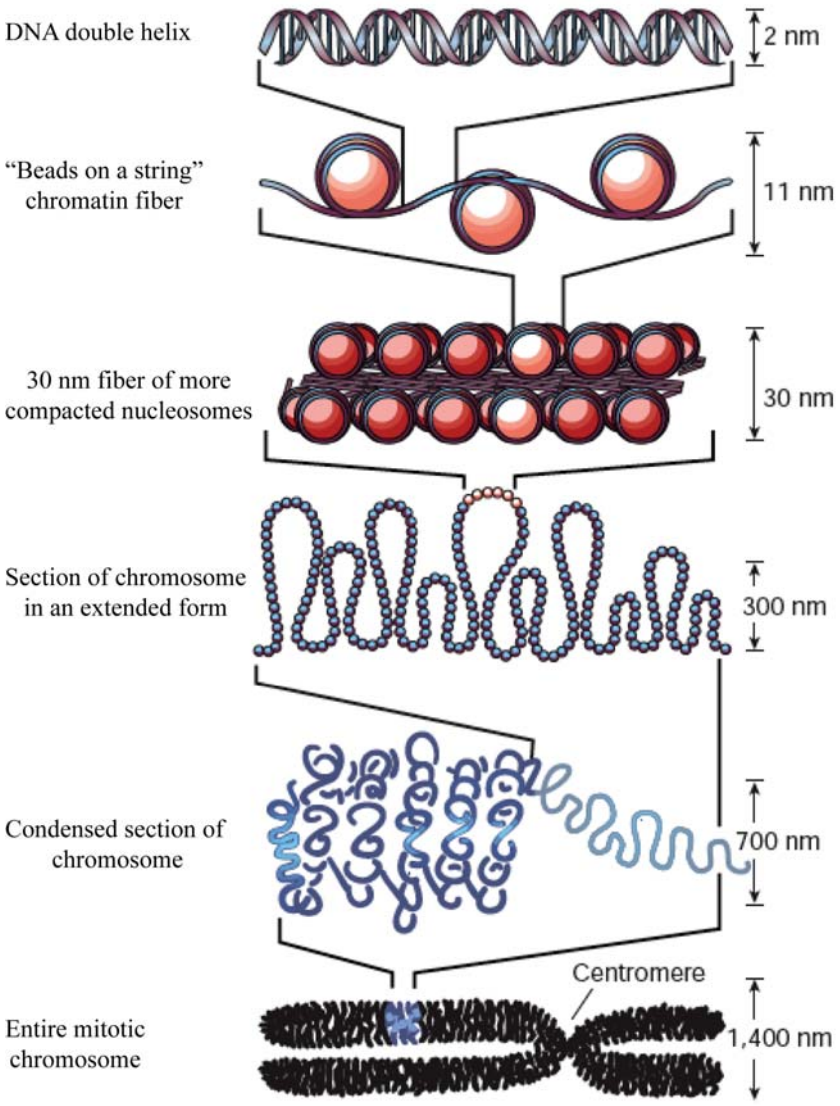

Figure 2.1 Packaging of eukaryotic DNA, from (Felsenfeld and Groudine, 2003).

Chromatin within the eukaryotic nucleus can be cytologically divided into euchromatin and heterochromatin (Elgin and Grewal, 2003; Henikoff, 2000; Richards and Elgin, 2002). If a gene is located in a domain where the DNA is less densly packed (euchromatin) it has the potential to be transcriptionally active. Often when a gene is within or adjacent to a more densly compact domain (heterochromatin) it is silenced. A significant portion of the genome with low gene density is permanently packed in an inactive form called constitutive heterochromatin and this silenced state persists through cell divisions. Changes in gene expression alter the relationship between euchromatin and heterochromatin and therefore correlate with cellular differentiation. Control of individual gene expression may involve local changes in nucleosomal compaction. The nucleosome structure can be regulated through

assembly/disassembly by histone chaperones, replacement of histone variants, nucleosome remodeling and post-translational modifications of the histones (Becker and Horz, 2002; Fischle et al., 2003b; Workman, 2006).

The chromosomes in the nucleus are organized into distinct territories (chromosome territory; CT) (For recent review see (Cremer et al., 2006)). Actively transcribed genes are often at the CT surface and adjacent to mostly DNA-free channels and lacunas between the CTs (interchromatin compartment; IC) where it is presumed that the transcription factories travel to access DNA (Cremer and Cremer, 2001; Cremer et al., 2006; Mahy et al., 2002). It has recently been shown that these ICs are dynamic and that the size of ICs depend upon compaction of the surrounding chromosome domains (Albiez et al., 2006).

Transcriptionally active and silent regions may be positioned adjacent to each other: Therefore boundaries must exist to prevent two neighboring regions from influencing each other. These borders are called insulators and are DNA elements that prevent stimulation of transcription or silencing from one region to another (West et al., 2002). Binding of proteins to the insulator sequences is necessary for effective borders. In *Drosophila* an example of such a protein is a zink finger protein Su(Hw), which binds *gypsy* retrotransposon sequences (Gerasimova et al., 2000). In vertebrates a conserved zink finger protein, CTCF, is shown to bind to the chromatin insulator domain of the *H19* imprinting control region (ICR) (Pant et al., 2004) but also many other genome wide target sites (Mukhopadhyay et al., 2004). There are two alternative molecular mechanisms proposed for how an insulator works to prevent repression, a passive barrier model or a active anti-silencing model (Fourel et al., 2004). The passive model suggests that a large and stable bound protein complex function as a physical block, whereas the active model suggests that insulator sequences and proteins serve as binding sites for enzymatic activities that actively interfere with silencing (Fourel et al., 2004). Insulators also blocks enhancers for transcription, and it was shown that the enhancer blocking of the insulator *gypsy* in *Drosophila* depends on the number of binding sites for Su(Hw) and the strength of the enhancer (Scott et al., 1999).

2.2 Position-Effect Variegation

Position-Effect Variegation (PEV) is a observed phenomenon when a euchromatic gene is artificially relocated next to heterochromatin, and the gene that get in close proximity to heterochromatin has variegated expression. Silencing of certain genes may lead to phenotypic variegation in tissues.

In *Drosophila*, expression of the gene *white* gives red eye pigments. However, the *In(1)w^{m4}* strain features a phenotype red-white mottled eyes (Figure 2.2). *In(1)w^{m4}* stands for white mottled four and was obtained by X-irradiation of *Drosophila melanogaster* (Muller, 1930). A segment containing the *white* gene on the X chromosome got inverted, such that the *white* gene was only 25 kb from centromeric heterochromatin (Tartof et al., 1984). *White* was repressed due to spreading of heterochromatin factors over the region. The inactivation of the relocated euchromatic gene occurs early in development and is inherited through cell division (Becker, 1957).

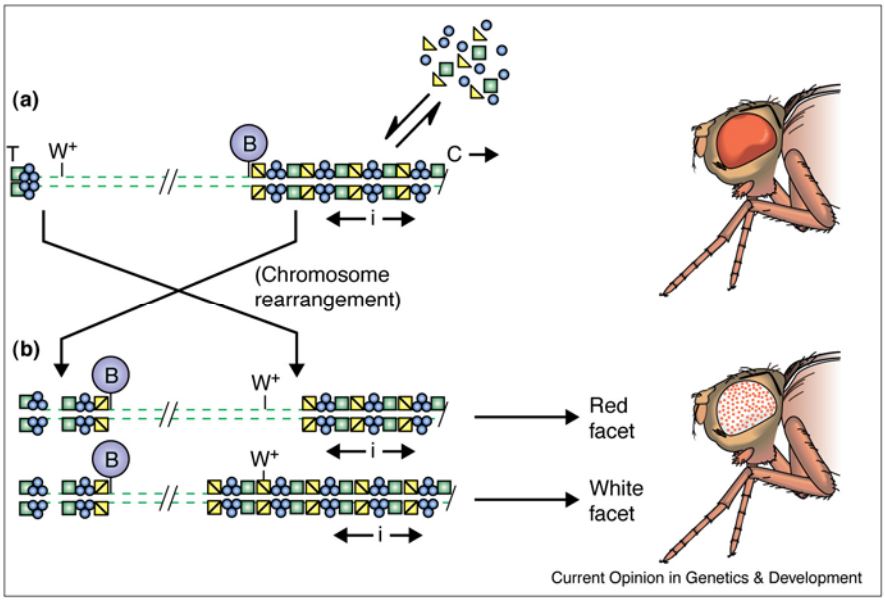

Figure 2.2 A schematic illustration of *white* variegation in the X chromosome of the *Drosophila* line *In(1)w^{m4}*. (A) Wild type flies have red-pigmented eyes, because *white* (W+) is expressed and positioned distal to heterochromatic centromeres (C) and telomeres (T). Heterochromatin-specific complexes (illustrated by colored symbols) cannot spread due to the presence of a barrier (B). **(B)** In *In(1)w^{m4}*, the *white* gene brought close to heterochromatin by chromosome rearrangement. This results in variegated expression of the *white* gene and the eye has a mottled appearance. Some groups of ommatidia (facets) become colorless because *white* is repressed by spreading of heterochromatin-proteins from the proximal heterochromatin. The illustration is taken from (Grewal and Elgin, 2002).

Position-effect variegation of *white* in *Drosophila* is an excellent genetic tool to screen for functions of chromosomal proteins. The *In(1)w^{m4}* line can be used for secondary site mutations that either suppress or enhance variegation in the fly eyes. Mutation in genes for suppressor of position-effect variegation (SU(VAR)) results in increased expression of *white* and thereby red eyes. Colorless/white eyes are the effect of mutations of enhancer of position-effect variegation (E(VAR)) genes (reviewed in (Reuter and Spierer, 1992)). Selective screens allowed the isolation of PEV modifier mutations that led to about 150 genes, not all of them are known (Schotta et al., 2003).

Suppressor of position effect variegation 2-5 (SU(VAR)2-5) encodes for a heterochromatin protein (HP1a) and was isolated as dominant suppressor of PEV (Eissenberg et al., 1990). Two other dominant suppressors of PEV are *SU(VAR)3-9* (Tschiersch et al., 1994) and *SU(VAR)3-7* (Cleard et al., 1997; Reuter et al., 1990). *SU(VAR)3-9* encodes the major heterochromatin histone H3K9 methyltransferase (Aagaard et al., 1999; Schotta et al., 2002), whereas the SU(VAR)3-7 protein contains seven zink fingers and was shown to interact with HP1a (Cleard et al., 1997; Delattre et al., 2000). All these three genes were characterized to have haplo-suppressor and triplo-enhancer dosage dependent effect on PEV (Locke et al., 1988; Wustmann et al., 1989). An extra copy of *SU(VAR)2-5, SU(VAR)3-7* or *SU(VAR)3-9* results in reduced expression of the *white* gene, therefore an enhancer effect.

The genetic interactions between *SU(VAR)3-9, SU(VAR)2-5* and *SU(VAR)3-7* can be tested by adding additional gene copies of one gene (three instead of two; triplo) to a null mutation of another gene. The suppressor effect of *SU(VAR)3-9* is dominant over the triplo-dependent enhancer effects of *SU(VAR)2-5* and *SU(VAR)3-7*, indicating its importance in heterochromatin formation. However, *SU(VAR)3-9* is not an essential gene because homozygous null mutants are viable and fertile (Schotta et al., 2002). Interestingly *SU(VAR)2-5* null mutants survive only until the late third instar larvae stage due to maternal contribution of HP1a (Lu et al., 2000).

PEV has also been studied in other model organisms. In *Schitzosaccharomyces pombe* classical PEV has been observed within the centromeres (Allshire et al., 1994), telomeres (Nimmo et al., 1994) and mating-type locus (Grewal and Klar, 1996).

The homologues of SU(VAR)3-9 and HP1 in *S. pombe* are called Clr4 and Swi6 (Ivanova et al., 1998; Lorentz et al., 1992). Both proteins were identified as modifiers of centromeric PEV in *S. pombe* (Allshire et al., 1995; Ekwall et al., 1996), suggesting of a conservation of their heterochromatin role.

Another gene that has been shown to have a suppressor of position-effect variegation phenotype is *ACF1*. ACF1 and ISWI are the subunits of ACF (ATP-utilizing chromatin assembly and remodeling factor) that catalyzes the ATP-dependent assembly of periodic nucleosome arrays *in vitro.*

2.3 ATP dependent nucleosome remodeling

Chromatin is a dynamic structure that is accessible for large transcription and replication machineries, DNA repair and other chromatin modifying complexes. This can be achieved through ATP-dependent nucleosome remodeling, which facilitates repositioning of nucleosomes to neighboring DNA segments (Becker and Horz, 2002). Nucleosome remodeling factors are multisubunit complexes containing a member of the SWI/SNF2 ATPase family (Eisen et al., 1995). SWI/SNF proteins was first identified in screens in *Saccharomyces cerevisae* for specific gene regulations (Breeden and Nasmyth, 1987; Neigeborn and Carlson, 1984; Stern et al., 1984). The SWI/SNF2 family is further divided into at least four classes according to the domain structure of the catalytic ATPases: SWI2, ISWI, CHD and Ino80 (reviewed in (Eberharter and Becker, 2004)).

ATPases of the SWI2 class feature a bromodomain (Horn and Peterson, 2001; Martens and Winston, 2003). The bromodomain can bind to acetylated lysine residues (Dhalluin et al., 1999; Jacobson et al., 2000). Acetylated histones are generally associated with transcriptionally active chromatin (Fischle et al., 2003b). Indeed, it was found that yeast SWI/SNF can function in concert with Gcn5 acetyltransferase in yeast for activation of specific genes (Pollard and Peterson, 1998). In *Drosophila* Brahma is homolog of yeast SWI/SNF (Kal et al., 2000).

The domain that characterizes the CHD class of ATPases is the chromo domain. The first DNA-helicase protein was identified in mouse (CHD1) (Delmas et al., 1993). In *Drosophila* two chromo domain containing ATPases dCHD1 and dMi-2 have been characterized (Bouazoune et al., 2002; Lusser et al., 2005). The chromo domain dMi-2 was shown to interact with nucleosomal DNA and is required for nucleosome mobilization (Bouazoune et al., 2002). CHD1 regulate nucleosome spacing and support NAP1-mediated chromatin assembly *in vitro* (Lusser et al., 2005).

Ino80 proteins have a characteristic split ATPase domain and are part of large multisubunit complexes in *Saccharomyces cerevisiae* (Ebbert et al., 1999; Krogan et al., 2003; Shen et al., 2000). Ino80 and Swr1 complexes are involved in response to double strand DNA damage during cell cycle by regulating the incorporation of different H2A variants (Papamichos-Chronakis et al., 2006).

The ISWI class of proteins contain a SANT domain and the structure comprising the HAND to SANT domain of *Drosophila* ISWI has been solved (Grune et al., 2003). Several complexes are described that contain ISWI (See table 2.1). The *Drosophila* ISWI has been purified in three complexes; NURF (Tsukiyama and Wu, 1995), ACF (Ito et al., 1997), and CHRAC (Varga-Weisz et al., 1997). These complexes differ in subunit composition and function: while NURF has been implicated in transcriptional regulation (Badenhorst et al., 2002), CHRAC/ACF are mainly involved in chromatin assembly (Fyodorov et al., 2004).

A feature common for the *Drosophila* and human ISWI complexes is the presence of subunits with ACF1 or proteins with homologous domains to ACF1 (underlined in table 2.1). *Drosophila* ACF was purified from embryos and shown to catalyze chromatin assembly (Ito et al., 1997; Ito et al., 1999). Loss of *acf1* resulted in loss of nucleosomal periodicity supporting a role in assembly of chromatin (Fyodorov et al., 2004). Mammalian ISWI homologs are SNF2H and SNF2L with distinct expression patterns during embryogenesis (Aihara et al., 1998; Lazzaro and Picketts, 2001). Human ACF1 interacts with SNF2H, and was shown to be required for DNA replication through heterochromatin in mammalian cells (Collins et al., 2002). The human NURF was the first complex purified that contained the ATPase SNF2L (Barak et al., 2003). Recently, another SNF2L complex was purified from mouse cells

comprising a bromodomain containing transcription factor CECR2 and SNF2L and CECR2 is specifically expressed in neuronal tissues (Banting et al., 2005).

Table 2.1. Summary of known ISWI-containing nucleosome remodeling complexes in *Drosophila* and human

***Drosophila* complexes**	**Complex composition**	**Human complexes**	**Complex composition**
ACF	ISWI, ACF1	ACF	SNF2H, ACF
		WICH	SNF2H, WSTF
		RSF	SNF2H, RSF
CHRAC	ISWI, ACF1, CHRAC14, CHRAC16	CHRAC	SNF2H, hACF1, CHRAC15, CHRAC17
NURF	ISWI, NURF301, p55, NURF38	NURF	SNF2L, BPTF, RbAP46, RbAP48
		NorC	SNF2H, TIP5
		CERF	SNF2L, CECR2

ACF, ATP-utilizing chromatin assembly and remodeling factor; CERF, CECR2-containing remodeling factor; CHRAC, chromatin accessibility complex; NorC, nucleolar remodeling complex; NURF, nucleosome remodeling factor; ISWI, imitation switch; SNF, sucrose nonfermenters; TIP5, TTF-I-interacting protein 5; WICH, WSTF ISWI chromatin remodeling complex; WSTF, Williams syndrome transcription factor. Underlined are the subunits containing domains homologous to ACF1.

In *Drosophila* the remodeling activity of ISWI requires and is influenced by the histone H4 tail (Clapier et al., 2001; Clapier et al., 2002; Corona et al., 2002). The interaction domain of ISWI with ACF1 has been mapped to the C-terminus of ISWI (Grune et al., 2003) and a central region (DDT-BAZ2 domain) of ACF1 (Eberharter et al., 2004). ACF1 has a functional role in ISWI nucleosome remodeling. It stimulates nucleosome mobility and the directionality of nucleosome sliding by ISWI by interacting with the core histones (Eberharter et al., 2001; Eberharter et al., 2004). The CHRAC subunits (p14-p16 in *Drosophila*/ p15-p17 in human) are histone fold proteins and facilitates nucleosome remodeling of the CHRAC complex through DNA interaction (Corona et al., 2000; Hartlepp et al., 2005; Kukimoto et al., 2004).

2.4 Histone modifications

The chromatin accessibility can also be regulated by post-translational modification of histones (for review, see (Nightingale et al., 2006)). Many proteins that interact with histone tails have been identified and characterized to have enzymatic activities that covalently modify them. Post-translational modifications such as acetylation, phosphorylation, methylation and ubiqitinylation are best studied in the tail domains of histones but modifications such as H3K79 methylation exist in the globular region (Figure 2.3) (Ng et al., 2002; van Leeuwen et al., 2002). Many more globular post-translational modifications have been identified (Cocklin et al., 2003; Freitas et al., 2004; Zhang et al., 2002a; Zhang et al., 2003a). The most characterized histone modification is acetylation and it has long been known to be connected to transcriptional regulation (Brownell and Allis, 1996; Grunstein, 1997).

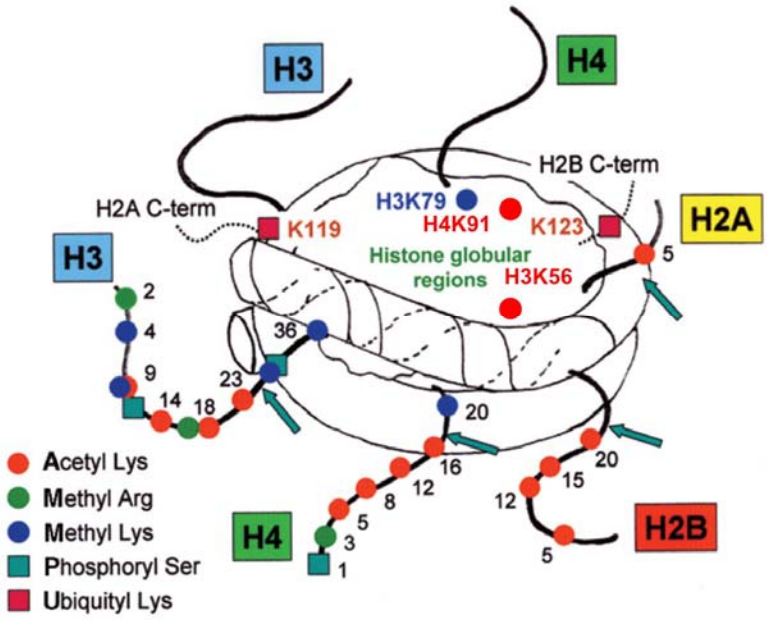

Figure 2.3 Post-translational modifications of histones within the nucleosome core particle, modified from (Turner, 2005). The arrows indicate the N-terminal domains of the four core histones.

The histone code hypothesis proposed that post-translational modifications to the histones provide specific signals that are recognized by proteins and thereby affects gene expression and other chromatin functions (Hebbes et al., 1994; Turner, 1993; Turner et al., 1992). Several studies in the past decade have proven evidential for a histone code to exist (for recent review, see (Nightingale et al., 2006)).

2.4.1 Acetylation

Acetylation of histones open chromatin to allow transcription factors to gain access (Fischle et al., 2003b). Hence, acetylation reduces the positive charge of the histone tails and reduces thereby the binding to negatively charged DNA (Hong et al., 1993; Workman and Kingston, 1998). Enzymes responsible for transfer of an acetyl group of Acetyl-CoA to histone lysines are called histone acetyltransferases (HATs) and are generally part of multiprotein complexes. The HATs can be divided into different families according to histone substrate binding and catalysis (Santos-Rosa and Caldas, 2005). The Gcn5/PCAF family and the p300/CBP family have different size of HAT domains and in addition a bromodomain. Transcriptional activators containing bromodomains recognize and bind acetylated lysines (Dhalluin et al., 1999; Jacobson et al., 2000). The MYST family features addition to the HAT domain a MYST domain and are involved in a wide range of functions including transcriptional activation and silencing, cell cycle progression and dosage compensation (Santos-Rosa and Caldas, 2005). Histone acetylation is mainly described on the histone tails of H3 and H4 (Figure 2.3). Newly synthesized H4 are acetylated at lysine 5 and 12 (Chang et al., 1997). Acetylation of H4K16 is accumulated on the hyperactive male X-chromosome in *Drosophila* (Bone et al., 1994; Smith et al., 2000; Turner et al., 1992). Recently, lysine 56 within the globular domain of H3 was shown to be acetylated (Masumoto et al., 2005; Ozdemir et al., 2005; Xu et al., 2005). Lysine 56 acetylation was shown to facilitate recruitment of the SWI/SNF remodeling complex (Xu et al., 2005), and is also involved in DNA damage response (Masumoto et al., 2005). The histone of human H2B N-terminal tail is highly charged and four of the lysines can be acetylated (K5, K12, K15 and K20) (Spencer and Davie, 1999) and has been shown to be involved in transcriptional activation in yeast (Parra et al., 2006).

Acetylation is a short-living modification. Enzymes responsible for removing acetyl groups from lysines are called histone deacetylases (HDACs). These enzymes are classified into three different groups (I, II, II) on the basis of sequence homology to the yeast HDACs and generally interacts with multiple proteins (Kouzarides, 1999). HDACs functions as corepressors and abnormal expression of HDACs are often involved in cancer (reviewed in (Santos-Rosa and Caldas, 2005)).

2.4.2 Phosphorylation

Phosphorylation is another dynamic and reversible post-translational modification of histones. Most studied are phosphorylation of H3 and H4 (Figure 2.3). However, phosphorylation of *Tetrahymena* linker histones is well known to change the charge of H1 that modulate interaction with DNA and thereby up regulate gene expression (Dou and Gorovsky, 2000; Dou and Gorovsky, 2002; Dou et al., 1999; Sweet et al., 1996). Serine 10 phosphorylation (S10P) of H3 has opposite functions during cell cycle. Firstly, S10P is correlated with pericentric heterochromatin condensation by recruiting condensins in interphase nuclei. Secondly, it is involved in chromosome compaction in transition to mitosis, and lastly in euchromatic regions that is correlated with chromatin relaxation and gene expression (for review, see (Prigent and Dimitrov, 2003). Phosphorylation of H3S10 prevents methylation of K9 by the histone methyltransferase SUV39H1 (SU(VAR)3-9 homolog 1) (Rea et al., 2000).

2.4.3 Other histone post-translational modifications

Other modifications that affect histones are ubiquitinylation, ADP-ribosylation, SUMOylation and biotinylation. Ubiquitin and the ubiquitin like SUMO are small proteins that are covalently but reversibly attached to lysines of histones (Belz et al., 2002; Shiio and Eisenman, 2003). Polyubiquitinylation of H2A and H2B is a mark for proteolysis (Pickart and Cohen, 2004). Monoubiquitinylation of histone H2B on K123 is a signal for methylation of histone H3 on K4 and leads to silencing of genes near the telomere (Dover et al., 2002). SUMOylation of yeast histones have been implicated in transcriptional repression (Nathan et al., 2006).

Biotinylated histone H1, H2A, H2B, H2B, H3 and H4 has been observed in human lymphocytes (Pickart and Cohen, 2004). Sites of biotinylation has been identified *in vitro* in human histone H4 (K8, K12) (Camporeale et al., 2004), H3 (K4, K9, K18) (Kobza et al., 2005) and H2A (K9, K13, K125, K127, K129) (Chew et al., 2006). Biotinylation of histones is a rather new discovery and the functions need to be further elucidated.

In contrast to biotinylation, ADP-ribosylation has been long known. ADP-ribosylation occurs on arginine and glutamate residues of histones, where a poly-ADP-Ribose polymerase attaches up to 250 ADP-ribose units (Hassa et al., 2006). Mono-ADP-ribosylation of histones is linked to DNA repair processes and cell proliferation (Boulikas, 1993; Kreimeyer et al., 1984).

2.5 Methylation

Histones may be methtylated on either arginine (R) or lysine (K) (Figure 2.4). The ε-amino groups of lysine residues may be mono-, di- or trimethylated, whereas the guanidion nitrogen atoms of arginine may be mono- or dimethylated (symmetrical of assymetrical) (Zhang and Reinberg, 2001). The methyl donor for most methylation reactions is S-Adenosyl methionine (SAM/AdoMet), which is converted into S-Adenosyl homocysteine (SAH/AdoHcy) (Figure 2.4).

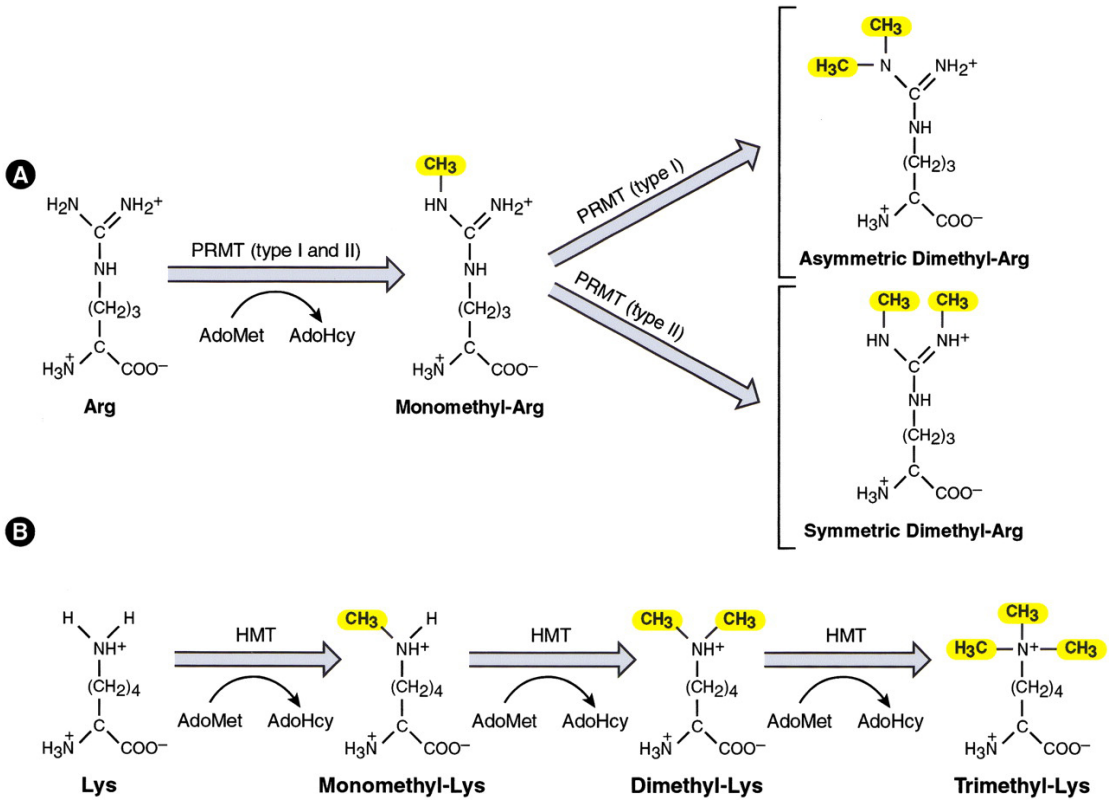

Figure 2.4 Arginine and lysine methylation, from (Zhang and Reinberg, 2001). A) The mechanism of arginine methylation. The product is mono- or dimethylated arginine. Dimethylated arginine can be assymmetric or symmetric. **B)** The mechanism of lysine methylation. The product is mono-, di- and trimethylation. AdoMet, S-Adenosyl methionine; AdoHcy, S-Adenosyl homocysteine.

Histone H3 has been shown to be methylated on lysine residues K4, K9, K27, K36 and K79 whereas in histone H4, K20 is methylated (Fischle et al., 2003b; Lachner et al., 2003). Histone arginine residues methylated in H3 are R2, R8, R17 and R26 are methylated in H3, and in H4 R3 (Zhang et al., 2003a). There may still be additional methylation sites within the histones proteins.

2.5.1 Arginine methylation

Arginine methylation is an abundant post-translational modification. There are two major types (I and II) of protein arginine methyltransferases (PRMTs) that transfer a methyl group to the guanidino group of arginines (Lee et al., 1977). PRMTI and PRMTII both monomethylate, but the catalysis of dimethylation is assymmetric and symmetric respectively (See figure 2.4). Seven mammalian PRMT genes have been reported so far: PRMT1-PRMT7 Homologs are found from yeast to plant and *Drosophila* ((Cheng et al., 2005) and references therein). Three arginine methyltransferases methylate histones (Table 2.2). Human PRMT5 interacts with SWI/SNF chromatin remodelers, and methylates H3 arginine 8 and H4 arginine 3 (Pal et al., 2004). The authors found that H3R8 methylation by PRMT5 has repressive effect on some tumour suppressor genes. On the other hand, methylation of H3 residues by PRMT4/CARM1 is involved in transcriptional activation (Koh et al., 2002). Acetylation of H3 at K18 facilitates its methylation at R17 (Bauer et al., 2002; Daujat et al., 2002). CARM1 functions as a transcriptional coactivator for E2F stimulated transcription of Cyclin E1 genes by methylating H3R17 and H3R26 (El Messaoudi et al., 2006). Similarly, CARM1 and PRMT1 act as transcriptional coactivators of tumour suppressor gene p53 (An et al., 2004).

Table 2.2 Histone arginine methyltransferases and deiminases

Specificity	Methyltransferase	Function of methylation	Deiminase
H3R2	CARM1 (Mm, Hs)		PADI4 (Hs)
H3R8	PRMT5	Repressor	PAID4 (Hs)
H3R17	CARM1 (Mm, Hs)	Activator	PAID4 (Hs)
H3R26	CARM1 (Mm, Hs)	Activator	PAID4 (Hs)
H4R3	PRMT1	Activator	
	PRMT5		

The table is modified from (Bannister and Kouzarides, 2005). Mm, Mus musculus; Hs, Homo sapiens.

Arginine methylation can be removed. The peptidyl arginine deiminase 4 (PADI4) converts histone arginine to citrulline and thereby antagonizes arginine methylation (Cuthbert et al., 2004). The authors showed that PADI4 deiminates arginine residues R2, R8, R17, and R26 in the H3 tail. The specificity is for both activating and repressing marks and a putative deiminase for the H4 tail has yet to be discovered.

2.5.2 Lysine methylation

Heterochromatin and euchromatin may be indexed according to histone methylation marks present. Lysine methylation at H3K4 and H3K36 marks transcriptionally active chromatin, whereas methylation of H3K9, H3K27 and H4K20 trimethylation defines repressed chromatin domains (Peters et al., 2003; Rice et al., 2003; Santos-Rosa et al., 2002). In *Drosophila* pericentric heterochromatin contains accumulated H3K9 mono-, di- and trimethylation, H3K27 mono-, di- and trimethylation and H4K20 methylation (Ebert et al., 2006; Ebert et al., 2004; Schotta et al., 2004a). Active chromatin states are enriched with H3K4 and H3K36 methylation (Ebert et al., 2006). Dimethylation of lysine 79 on *Drosophila* polytene chromosomes is found at some active chromatin sites (interbands and puffs) but also at some inactive sites (bands) (Shanower et al., 2005).

The functional consequences of histone lysine methylation are thought to be due to recruitment of proteins that recognize (read) specific marks (Figure 2.5). Hence, more and more readout proteins are being discovered which gives support to the histone code hypothesis described above. Repressive proteins carrying a chromo domain, HP1 and Polycomb respectively bind repressive marks such as H3K9 and H3K27 methylation (Bannister et al., 2001; Cao et al., 2002; Jacobs and Khorasanizadeh, 2002; Jacobs et al., 2001; Lachner et al., 2001; Min et al., 2003; Nielsen et al., 2002b). The chromo domain protein, chromo domain helicase DNA-binding protein (CHD1), binds the active mark H3K4Me (Pray-Grant et al., 2005). Tudor domain proteins were predicted to bind methylated lysines (Maurer-Stroh et al., 2003). A mammalian p53 binding protein (p53BP1) binds methylated H3K79, whereas in yeast the ortholog protein Cut5-Repeat-Binding protein (CRB2) recognizes H4K20Me (Huyen et al., 2004; Sanders et al., 2004). Another protein, a JMJD2a containing a double tudor domain and a JmjC domain, binds methylated H3K4 and H4 K20

(Huang et al., 2006b). Both p53BP1 and CRB2 were shown to be recruited to sites of DNA damage. Recently it was shown that a WD40 repeat and a PHD finger bind H3K4Me (Wysocka et al., 2005; Wysocka et al., 2006). WDR5 is part of a histone H3K4 methyltransferase complex containing Set1 and was postulated to mediate binding to H3K4Me chromatin (Wysocka et al., 2005). However, recent crystal structures of the WDR5 WD40 domain with methylated H3K4 peptides have given contradicting results (Couture et al., 2006; Ruthenburg et al., 2006; Schuetz et al., 2006). The first study reported that WDR5 could bind unmodified H3 peptide, but only H3K4 dimethylated peptide mediated stronger interaction (Schuetz et al., 2006). On the other hand, two other studies could find no preferred binding of WDR5 to methylated K4 (Couture et al., 2006; Ruthenburg et al., 2006). There are many challenges ahead to understand the mechanisms of proteins that are capable of specific interactions with differently methylated lysine residues within the histone tail and their biological function.

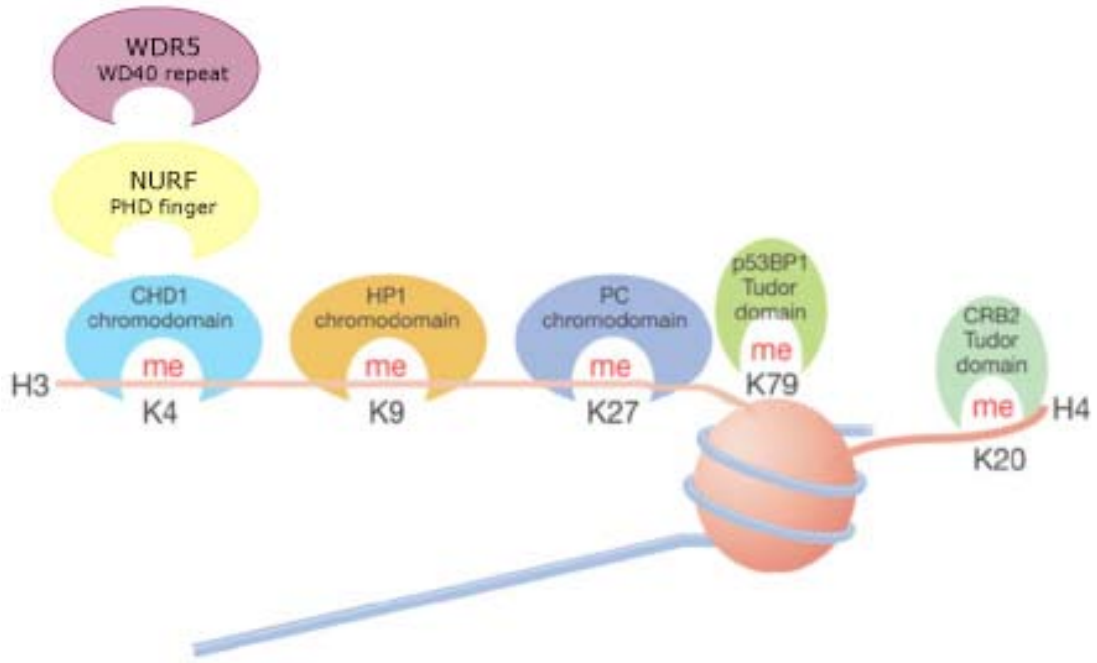

Figure 2. 5 Proteins that bind methylated histones. Modified from (Bannister and Kouzarides, 2005).

Histone methylation was long thought to be a stable mark. Replication independent assembly during active transcription of another H3.3 variant was proposed as a model for removal of (silent) histone methylations ((Henikoff et al., 2004) and references therein). In the past two years there has been a number of histone demethylases discovered. The first one was the FAD (flavin adenine dinucleotide)-dependent lysine specific demethylase 1 (LSD1) which demethylates mono- and di- but not trimethylated H3K4 (Shi et al., 2004). The activity of LSD1 can be regulated by associated proteins, such as CoREST which enables LSD1 to demethylate nucleosomes (Lee et al., 2005; Shi et al., 2005). Interaction of LSD1 with the androgen receptor results in demethylation of H3K9 mono- and dimethylation resulting in androgen-receptor-dependent gene activation (Metzger et al., 2005). Another group of demethylase were found to contain jumonji (Jmj) C domain (Trewick et al., 2005). JmjC domain containing histone demethylase 1 (JHDM1) is a Fe(II) and alpha-KG (alpha-ketoglutarate)-dependent dioxygenase that demethylates specifically dimethylated H3K36 (Tsukada et al., 2006). Jumonji genes are conserved from bacteria and fungi to plant and vertebrates (Takeuchi et al., 2006). Another jumonji protein, JHDM2A, demethylates mono- and dimethyl H3K9 (Yamane et al., 2006), whereas a third, JHDM3A is a H3K9 and H3K36 trimethyl demethylase (Klose et al., 2006). The functional significance of histone demethylation is to be unraveled, and discovery of more potential demethylases will increase understanding of this mechanism.

2.6 The SET domain

Histone methyl transferases (HMTases) responsible for lysine methylation all contain a catalytic SET domain, except for Dot1 (Ng et al., 2002). The SET domain consists of approximately 130 amino acids and it was originally identified in three *Drosophila* proteins: Suppressor of position effect variegation 3-9, SU(VAR)3-9; Enhancer of zeste, E(Z) and Trithorax, Trx (Jenuwein et al., 1998). The enzymatic activity of the SET domain was first discovered in a mammalian homolog of SU(VAR)3-9, SUV39H1 which was shown to methylate histone H3 at lysine 9 (H3K9) (Rea et al., 2000). The crystal structure of different SET domains has been solved (Figure 2.6) (Jacobs et al., 2002; Kwon et al., 2003; Min et al., 2002; Trievel et al., 2002; Wilson et al., 2002; Xiao et al., 2003a; Zhang et al., 2002b).

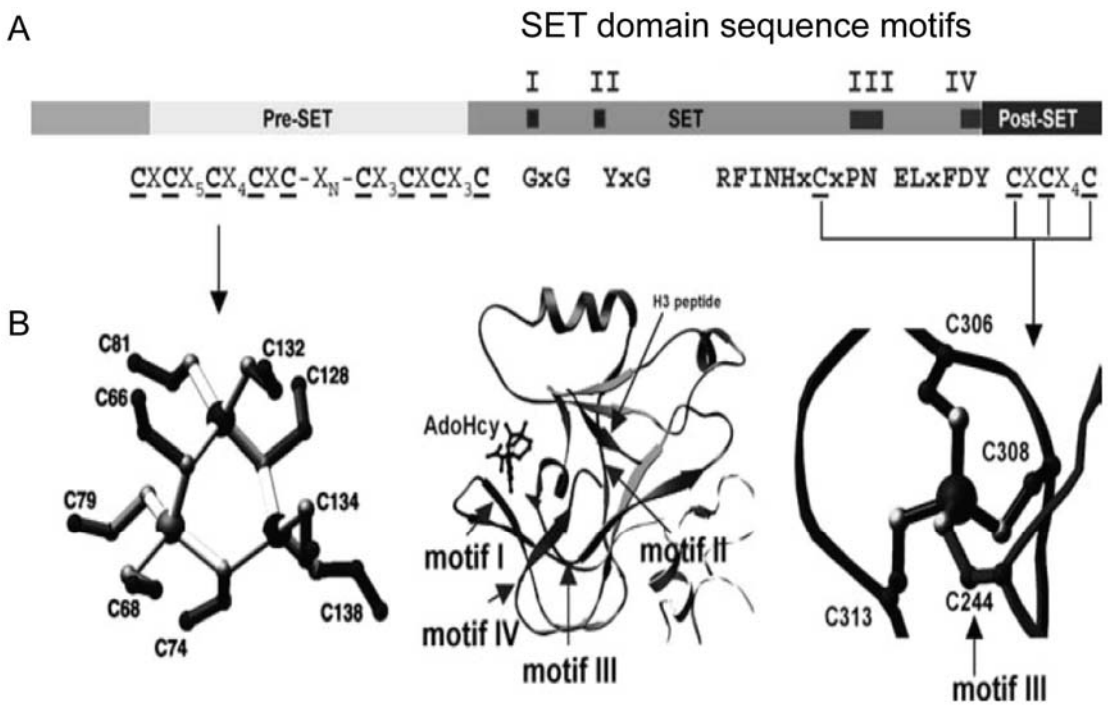

Figure 2.6 The SET domain and surrounding preSET and postSET domains. The structure of the SET domain of the SU(VAR)3-9 homolog protein DIM-5 from *Neurospora crassa*, solved by (Zhang et al., 2002b). The figure is taken from (Cheng et al., 2005). A) The preSET region of DIM-5 contains nine invariant cysteines and the postSET domain three. Both forms zink fingers (right, preSET with Zn_3Cys_9 cluster; and left, postSET with Zn_1Cys_4 (plus one cystein is from motif III)). In the middle, a ribbon diagram of the DIM-5 SET domain with the conserved motifs indicated by arrows. The binding of the H3 peptide and S-Adenosyl homocystein (AdoHcy) is indicated.

Four conserved sequence motifs, termed motif I-IV, within the SET domain were identified when different HMTase sequences were aligned (Figure 2.6.A) (Cheng et al., 2005). These four motifs cluster together and constitute the active site (Figure 2.6.B, DIM-5 SET domain in the middle) that participates in binding of SAM and targets lysines for catalysis of methyl transfer. The three cysteines in the postSET domain of DIM-5 together with a cysteine from motif III coordinate a zink ion near the active site and form a narrow channel to accommodate the target lysine binding (Figure 2.6.A and B to the right) (Zhang et al., 2003b). Indeed, the postSET domain was shown to be essential for the activity of DIM-5 (Zhang et al., 2002b; Zhang et al., 2003b). This three-cystein domain is present in SET domain proteins of the SUV, SET1 and SET2 family. On the other hand, SET domain proteins such as human SET7/9 (Kwon et al., 2003; Xiao et al., 2003a) and Rubisco MTase (Trievel et al., 2002) do not have a cysteine rich postSET domain, but rather by pack an α-helix onto the active site (Zhang et al., 2003b). The preSET domain coordinates three zink ions (Figure 2.6.A and B to the left), and has a role in stabilizing the structure of the SET domain (Xiao et al., 2003b). However, the number of cysteines in the preSET domains differs between HMTases. Both the preSET and postSET domain contributes to activity SUV39H1 (Rea et al., 2000).

Discovery of more HMTases indicated that the structure of the different SET domains confer the specificity (Table 2.3). However, the surrounding sequences of the SET domain also contribute to specificity and are conserved within major classes (Baumbusch et al., 2001; Zhang et al., 2003b). The largest class is the SUV family, in addition comes SET1, SET2, EZ and RIZ families. The histone methyltransferases SET8 and SET7/9 do not fit into any of these families (Zhang et al., 2003b).

Table 2.3 An overview of lysine specific histone methyltransferases.

Specificity	*S. Cerevisiae*	*S. Pombe*	*D. Melanogaster*	Mammals	Ref(s)
H3K4	Set1	Set1	Trithorax	Set1/MLL / ALL-1	(Milne et al., 2002; Nakamura et al., 2002; Roguev et al., 2001)
			Ash1		(Beisel et al., 2002)
				Set7/9[1]	(Nishioka et al., 2002)
H3K9	Absent	Clr4	SU(VAR)3-9	SUV39H1/ 2	(Rea et al., 2000; Schotta et al., 2002)
			Ash1		(Beisel et al., 2002)
			dG9a	G9a/ GLP	(Ogawa et al., 2002; Stabell et al., 2006; Tachibana et al., 2001)
				SETDB1 (ESET)[2]	(Schultz et al., 2002; Yang et al., 2002)
				RIZ1	(Schultz et al., 2002; Yang et al., 2002)
			E(Z)		(Czermin et al., 2002)
H3K27	Absent		E(Z)	Ezh2	(Czermin et al., 2002; Kuzmichev et al., 2002)
			dG9a	G9a	(Stabell et al., 2006; Tachibana et al., 2001)
H3K36	Set2	Set2		Set2	(Strahl et al., 2002)
				NSD1	(Huang et al., 1998b; Ra et al., 2003)
				Smyd2	(Brown et al., 2006)
H3K79	Dot1		Grappa	Dot1L	(Feng et al., 2002; Shanower et al., 2005)
H4K20	Absent	Set9	PR-Set7	PR-Set7 (SET8)	(Fang et al., 2002; Rice et al., 2002; Sanders et al., 2004)
			Ash1	NSD1	(Beisel et al., 2002; Huang et al., 1998b; Rayasam et al., 2003)
			SU(VAR)4-20	Suv4-20h1/h2	(Schotta et al., 2004b)
H4 other K?			dG9a		(Stabell et al., 2006)
H1K26				Ezh2	(Kuzmichev et al., 2004)

The table is modified from (Sims et al., 2003) including recent updates. ALL-1, acute lymphoblastic leukemia 1; Ash1, absent small or homeotic discs1; Dot1, disrupter of telomeric silencing; Dot1L, Dot1 like; ESET, SET domain bifurcated 1; E(Z), enhancer of zeste; Ezh2, E(Z) homolog 2; MLL, mixed lineage leukemia; NSD1, nuclear receptor binding SET domain protein 1; PR-Set7, PR-SET domain containing protein 7; RIZ, retinoblastoma protein-interacting zinc finger; SETDB1, SET domain bifurcated 1; Set1/2/9, SET domain containing 1, 2 or 9; Smyd2, SET and MYND 2; SU(VAR)3-9, suppressor of position effect variegation 3-9; Suv39, SU(VAR)3-9 homolog; Trx, trithorax. 1) Also called Set9; 2) ESET is the mouse homolog.

DIM-5 adds three methylgroups to H3K9 (Tamaru et al., 2003), whereas SET7/9 mainly monomethylates H3K4 (Kwon et al., 2003; Xiao et al., 2003a). By engineering different variants of DIM-5 and SET7/9 the ability to add methylgroups can drastically changed (Zhang et al., 2003b). Amino acids that lie within the lysine-binding channel cause steric hindrance that limits the methylation to the monomethyl state. Tyrosine 305 in SET7/9 was shown to cause this steric hindrance, and by mutating it with phenylalanine 281 who in the same structural position of DIM-5 to a tyrosin, DIM-5 (F281Y) was converted to a mono-MTase. The specificity as well as the number of methyl residues that is added to a lysine residue may also depend on the presence of co-factor proteins. The HMTase ERG-associated protein (ESET) dimethylates H3-K9, but is converted into a trimethylating enzyme by its association with a mouse-activating transcription-factor-associated modulator (mAM) (Wang et al., 2003). Another example is mammalian Ezh2, which requires the presence of the co-factors Suppressor of zeste-12 (SUZ12) and embryonic ectoderm development (Eed) for tri-methylation of H3-K27 (Cao and Zhang, 2004). It was also shown for the *Drosophila* homolog E(Z) that the presence of ESC (an Eed homolog) improved the enzymatic activity (Czermin et al., 2002). In human there are several Eed isoforms, and Eed1 was shown to change the HMTase specificity of Ezh2 towards histone H1 K26 (Kuzmichev et al., 2004).

Not all SET domain proteins methylate lysines within histones. Pea chloroplast Rubisco (Ribulose-1,5-bisphosphate carboxylase/oxygenase) large subunit MTase was shown to methylate K14 of Rubisco large subunit (Ying et al., 1999). SET7/9 methylates the non-histone proteins p53 and TAF10 (Chuikov et al., 2004; Kouskouti et al., 2004). Interestingly, SET7/9 was shown to methylate K372 in p53 whereas a HMTase called Smyd2 (SET and MYND 2) methylated K370 within the same protein (Huang et al., 2006a). The methylation of K372 and K370 have opposite transcriptional effects on p53 regulated genes: SET7/9 mediated K372 methylation enhance association of p53 with promoters and thereby transcription whereas Smyd2 K370 methylation results in dissociation of p53 to DNA and causes repression (Huang et al., 2006a). TFIID, a complex comprising the TATA box binding protein (TBP) and 13 TBP-associated factors (TAFs), plays a role in nucleation in the assembly of the RNA polymerase II preinitiation complexes on protein-encoding genes (for review see (Albright and Tjian, 2000)). Methylation of TBP-associated

TAF10 increases its affinity for interactions with the RNA polymerase (Kouskouti et al., 2004).

2.6.1 SU(VAR)3-9

SU(VAR)3-9 (Suppressor of position effect variegation 3-9) is the main heterochromatin H3K9 HMTase in *Drosophila* (Ebert et al., 2004). It is conserved in eukaryotes from *Schitzosaccharomyces pombe* to mammalian organisms (Table 2.3). As described above, Clr4 and SU(VAR)3-9 are both suppressors of PEV and function in heterochromatin mediated gene-silencing (Ivanova et al., 1998; Schotta et al., 2002). There are two mammalian orthologs of SU(VAR)3-9, Suv39h1 and Suv39h2 (SU(VAR)3-9 homolog 1 and 2) (human SUV39H proteins have capital letters). Mouse Suv39h1 and Suv39h2 proteins are shown to be important for heterochromatic H3K9 methylation and genome stability (Peters et al., 2001). SUV39H1 shares 42 % homology with SU(VAR)3-9 (Figure 2.7) (Aagaard et al., 1999). Human SUV39H1 and mouse Suv39h1 share 95% homology (Aagaard et al., 1999), and localize to heterochromatic foci in interphase mammalian cells with transient accumulation at centromeric positions during mitosis (Aagaard et al., 2000). On the other hand, Suv39h2 having 59% identity with Suv39h1 and is highly expressed in human testes (O'Carroll et al., 2000). Mouse Suv39h2 shares 41% identity with SU(VAR)3-9 (O'Carroll et al., 2000).

In addition to the SET domain, SU(VAR)3-9 contains a chromo domain that was first identified in Polycomb and HP1 (Paro and Hogness, 1991) (See chapter 2.7.1). The major difference between the *Drosophila* and human proteins is that SUV39H1 lacks about 155 amino acids within the N-terminus of SU(VAR)3-9. This is because *SU(VAR)3-9* forms a bi-cistronic unit with the gene *eIF2* (Krauss and Reuter, 2000) which probably originated from retrotransposition of the *SU(VAR)3-9* transcript into a conserved intron of *eIF2* (Schotta et al., 2002).

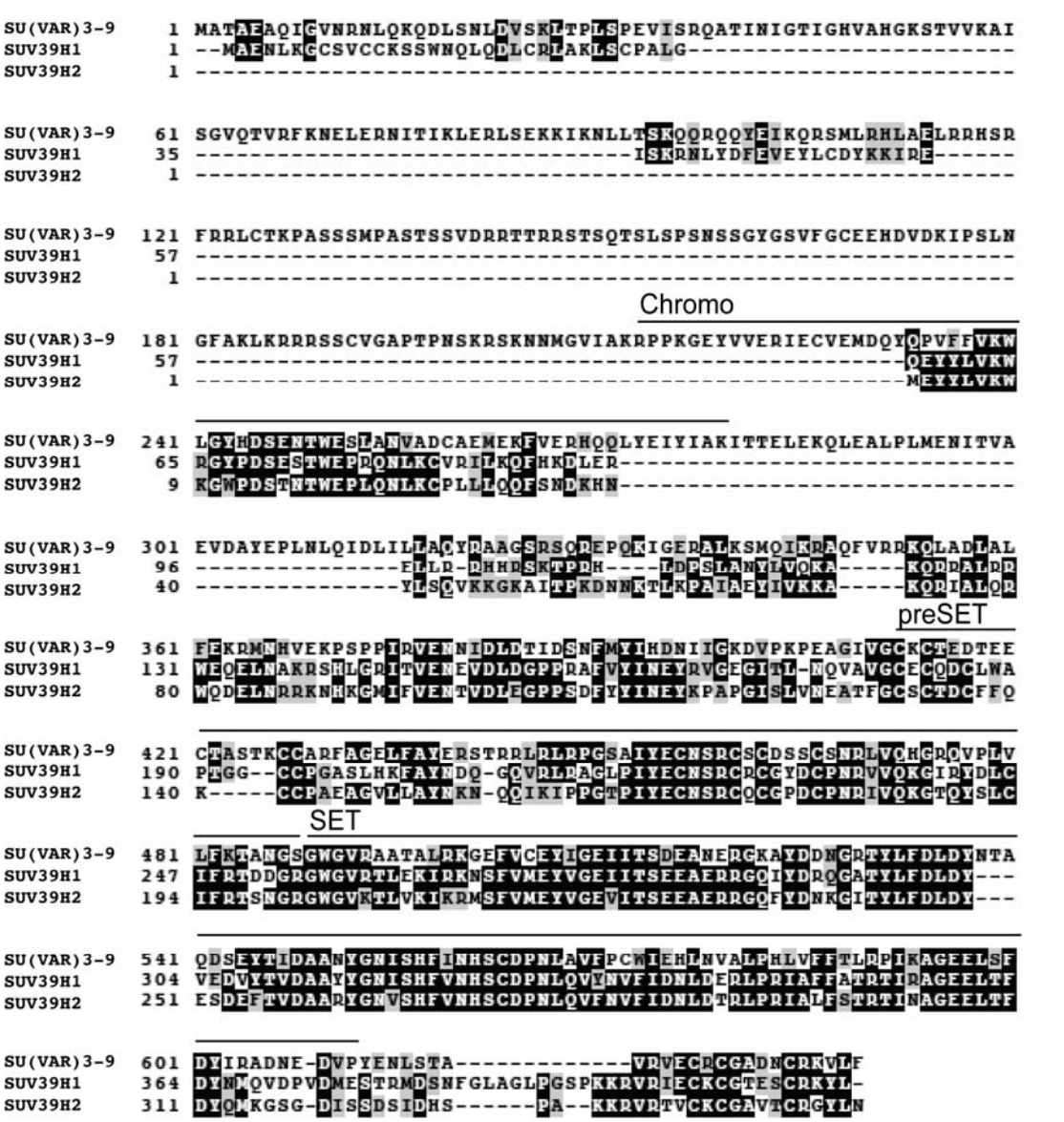

Figure 2.7 Alignment of SU(VAR)3-9 and its human orthologs. The amino acid sequences of SU(VAR)3-9, SUV39H1 and SUV39H2 were aligned using T-coffee and imported into the Boxshade program to highlight identities (dark shading) and similarities (light shading) at each position. The SU(VAR)3-9 chromo-, preSET- and SET domains are indicated.

Even though the N-terminus is moderately conserved, it is important for the interaction with silencing proteins HP1 and SU(VAR)3-7 (Schotta et al., 2002; Yamamoto and Sonoda, 2003). As described above, *Drosophila SU(VAR)3-9*, *SU(VAR)2-5* (HP1a) and *SU(VAR)3-7* also interact genetically (Schotta et al., 2002). The N-terminus was also shown to be important for targeting of SUV39H1 to heterochromatin *in vivo* (Melcher et al., 2000). In addition, mutations both in the

chromo and SET domain of Clr4 have been shown to impair silencing in *Schitzosaccharomyces pombe* (Ivanova et al., 1998).

Localization of *Drosophila* SU(VAR)3-9 was studied in salivary gland nuclei using a polyclonal antibody and heat shock inducible EGFP-tagged fusion proteins in transgenic flies (Schotta et al., 2002). Both endogenous and EGFP-proteins accumulate in heterochromatic regions such as the chromocenter and the fourth chromosome. SU(VAR)3-9 also localizes at telomeres and several euchromatic regions (Schotta et al., 2002). A study of *Suv39h1* and *Suv39h2* double null embryonic stem cells revealed a dramatic decrease in H3K9 trimethylation (Peters et al., 2003; Rice et al., 2003). The trimethylation could be restored by reintroducing *Suv39h1* or *Suv39h2* into the cells (Rice et al., 2003). Specific H3K9 activity of SU(VAR)3-9 was showed using a myc-tagged protein from *Drosophila* embryos and a truncated bacterially expressed variant (Czermin et al., 2001; Schotta et al., 2002). In *Su(var)3-9* null flies, H3K9 dimethylation at the chromocenter is completely lost (Schotta et al., 2002). Genome-wide mapping of SU(VAR)3-9 in *Drosophila* KC cells confirmed the localization observed by fluorescent microscopy (Greil et al., 2003). The authors found that one third of SU(VAR)3-9 target genes are male-specific and had a higher expression level in males than females. Another third displays elevated expression during embryogenesis whereas the last third is a heterogeneous group of genes predominantly expressed during larval stages (Greil et al., 2003). Mammalian SUV39 has also been linked to silencing of euchromatic genes. Retinoblastoma (Rb) protein recruits SUV39H1 and HP1 to promoter of S-phase genes (Nielsen et al., 2001b). Indeed, methylation by Suv39h1 was shown to terminally silence S-phase genes in differentiating, but not cycling cells (Ait-Si-Ali et al., 2004).

Methylation by the SET domain is not mandatory for silencing when SUV39H1 is tethered to DNA *in vivo* (Firestein et al., 2000). This may be due to direct interaction of SU(VAR) with silencing proteins such as histone deacetylases (HDACs) (Czermin et al., 2001; Vaute et al., 2002) and HP1 (Schotta et al., 2002; Yamamoto and Sonoda, 2003). H3K9 methylation has also been shown to be sufficient for transcriptional suppression without recruitment of HP1 through a mechanism involving histone deacetylation (Stewart et al., 2005).

In *Arabidopsis thaliana,* 10 genes encode SUV homologs (Baumbusch et al., 2001). Methylation of H3K9 by both *Arabidopsis* SUVH4 (KRYPTONITE) and *Neurospora crassa* DIM-5 (Defect In DNA Methylation) recruits DNA methylases (Jackson et al., 2002; Tamaru et al., 2003). Human SUV39H1 was also shown to directly interact with DNA methylases Dnmt1 and Dnmt3a from HELA cell extracts (Fuks et al., 2003). Studies described above show that H3K9 methylation is prerequisite for DNA methylation, however other studies indicate that H3K9 methylation occur after DNA methylation. For example it has also been described that methyl-CpG binding domain (MBD) proteins interact with a SUV39H1-HP1 complex (Fujita et al., 2003). MBD1 also recruits another H3K9 HMTase called SETDB1 (Sarraf and Stancheva, 2004). The crosstalk between H3K9 methylation and DNA methylation needs to be further elucidated. Recently it was shown that another H3K9 methyltransferase, G9a, directly interact with Dnmt1 (Esteve et al., 2006).

2.6.2 G9a

The major euchromatic histone H3K9 methyltransferase described in higher eukaryotes is G9a. This was determined by studies of *G9a*-deficient mice and embryonic stem (ES) cells (Tachibana et al., 2002). The authors found that H3K9 methylation is drastically decreased in euchromatic regions, resulting in severe growth retardation and early lethality. The loss of G9a mainly affects mono- and dimethylation of H3-K9 (Peters et al., 2003; Rice et al., 2003). However, G9a has also recently been found at heterochromatic loci (Esteve et al., 2005). Dimethylation of H3K9 by G9a is associated with the silencing of euchromatic genes (Stewart et al., 2005). G9a has a closely related homolog in mammals, called G9a related protein (GLP/Eu-HMTase1) (Ogawa et al., 2002). G9a and GLP were recently shown to be part of a multimeric E2F6 complex responsible for silencing of Myc- and E2F-responsive genes (Ogawa et al., 2002). Both enzymes have H3K9 methyltransferase activity *in vitro* (Ogawa et al., 2002; Tachibana et al., 2001), and G9a-GLP heterodimers have been shown to work cooperatively to exert their enzymatic activity *in vivo* (Tachibana et al., 2005). Indeed, G9a-GLP heterodimers have also been identified in other silencing complexes such as CtBP1 (Shi et al., 2003) and CDP/cut (Duan et al., 2005; Nishio and Walsh, 2004).

C-terminal binding proteins (CtBP) are predominantly transcriptional repressors, but have also recently been shown to act as transcriptional activators and play important roles during development (For review see (Chinnadurai, 2003)). The repression of a CtBP complex was shown to be mediated by G9a methyltransferase activity (Shi et al., 2003). Recent biochemical studies reported that the zink finger protein Wiz binds strongly to G9a-GLP heterodimer and links the histone methyltransferases to CtBP1 and 2 (Ueda et al., 2006).

The CCAAT displacement protein/cut homolog (CDP/cut), a transcription factor involved in development and cell-cycle progression, has been shown to recruit G9a and GLP to the promoter of *p21* (Nishio and Walsh, 2004). This results in repression of the *p21* gene. However, it has also recently been reported that another protein called growth factor independent 1 (Gfi1) also recruits G9a to the p21 promoter (Duan et al., 2005). Gfi1 is a transcription factor that regulates self-renewal of hematopoietic stem cells (For review see (Duan and Horwitz, 2005)). The *p21* gene is repressed due to association of Gfi-1, G9a and HDAC1 to the promoter.

G9a-/- mice are embryonic lethal (Tachibana et al., 2002). A developmental homeobox gene, *Oct-3/4*, that is expressed at high levels in early embryonic cells and is necessary for the totipotent phenotype in ES cells (Brehm et al., 1998; Nichols et al., 1998; Pikarsky et al., 1994) is regulated by G9a (Feldman et al., 2006). Retinoic acid (RA) induced differentiation of ES cells resulted in transcriptional repression of *Oct-3/4* (Ben-Shushan et al., 1995; Okamoto et al., 1990; Pikarsky et al., 1994). The repression is followed by methylation of H3K9 by G9a and *de novo* DNA methylation that prevents reactivation of *Oct-3/4* (Feldman et al., 2006). *GLP* -/- embryos were mostly identical to *G9a* -/- embryos suggesting that G9a-GLP coordinates common functions during embryonic development (Tachibana et al., 2005).

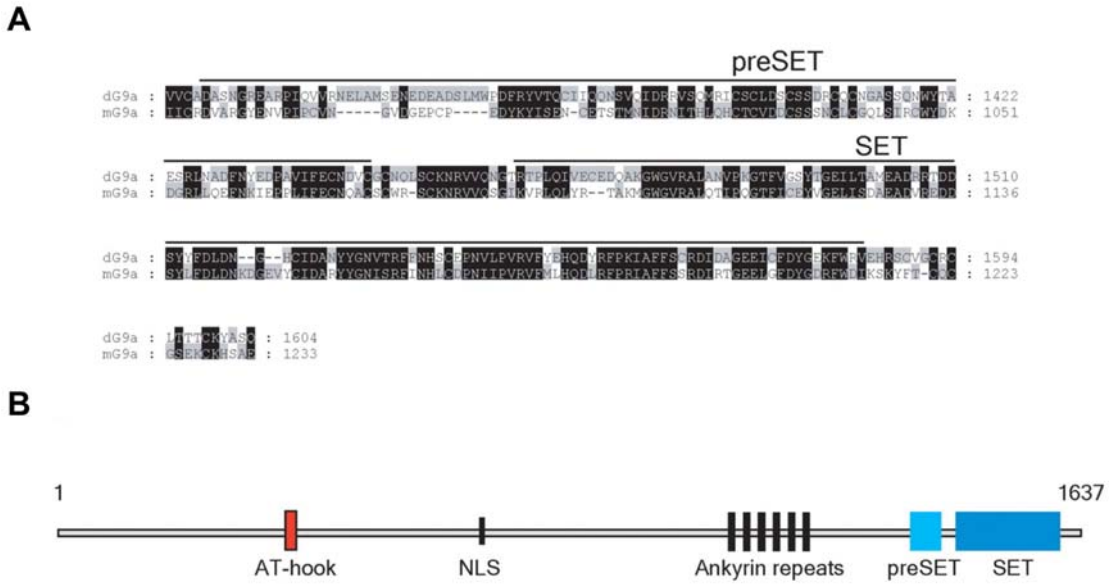

Figure 2.8 The domain organization of *Drosophila* G9a. (A) Sequence alignment of the preSET and SET domain of *Drosophila* and mouse G9a methyltransferases**.** The degree of conservation is distinguished by shade, where the darkest shade is most conserved. **(B)** Domain organization of dG9a. Modified from (Stabell et al., 2006).

Recently the *Drosophila* CG2995 was characterized as an euchromatic H3K9 HMTase (Stabell et al., 2006). *CG2995* was also shown to be a suppressor of PEV (Mis et al., 2006). Alignment of the preSET and SET domain of CG2995 and mG9a resulted in high sequence conservation (Figure 2.8). When comparing the preSET/SET/postSET domains of different *Drosophila* HMTases with mG9a, CG2995 was the closest ortholog and was named dG9a (Table 2.4). dG9a also share the same domain organization with mG9a having a N-terminal nuclear localization sequence and a C-terminal ankyrin repeat (Figure 2.8). An AT-hook was identified in the N-terminus of dG9a (Stabell et al., 2006).

Table 2.4 Comparison of preSET/SET/postSET regions of *Drosophila* HMTases with mouse G9a

HMTase	Identity	Similarity
mG9a	100%	100%
dG9a	47%	68%
SU(VAR)3-9	37%	55%
SET2	36%	50%

Data assembled from (Stabell et al., 2006).

Transcripts of *dG9a* are present in 0-3 hour embryos due to maternal contribution. Later during development (between 6 and 21 hours) *dG9a* is expressed in low amounts. In adult flies the expression of *dG9a* is restricted to the gonads both in

males and females (Stabell et al., 2006). Immunostainings revealed that the dG9a protein is found throughout oogenesis, embryogenesis and larval development whereas in the adult fly it is solely in the gonads (Stabell et al., 2006). Stabell and co-workers showed that in specific knockdowns of *dG9a* during the development, dG9a is involved in ecdysone mediated signaling. dG9a is suggested to be involved in regulation of genes involved in onset of metamorphosis and wing development because knockdown larvae fail to pupariate and removal of dG9a in the wing disc results in wing defects (Stabell et al., 2006). The data of dG9a correlates well with findings of murine G9a and GLP data. Both knockout mice were embryonic lethal and that *mG9a* was highly expressed in testes (Tachibana et al., 2002; Tachibana et al., 2005).

2.7 Heterochromatin protein 1

Heterochromatin protein 1 (HP1) was first identified when monoclonal antibodies were generated against a fraction of *Drosophila* nonhistone nuclear proteins (James and Elgin, 1986). Immunofluorescence staining of polytene chromosome showed localization to centric heterochromatin. A few years later the gene encoding HP1, *SU(VAR)2-5*, was isolated as a suppressor of position-effect variegation (PEV) (Eissenberg et al., 1990; Wustmann et al., 1989). HP1 homologues can be found in almost all eukaryotes ranging from *Schitzosaccharomyces pombe* (Ekwall et al., 1995; Klar and Bonaduce, 1991; Lorentz et al., 1992) to mammals and higher plants (Saunders et al., 1993; Singh et al., 1991). In vertebrates at least three different paralogs of HP1 (HP1α, HP1β and HP1γ) exist, whereas *D. melanogaster* has 5 paralogs (HP1a-e, Figure 2.9) (Minc et al., 1999; Smothers and Henikoff, 2001; Vermaak et al., 2005).

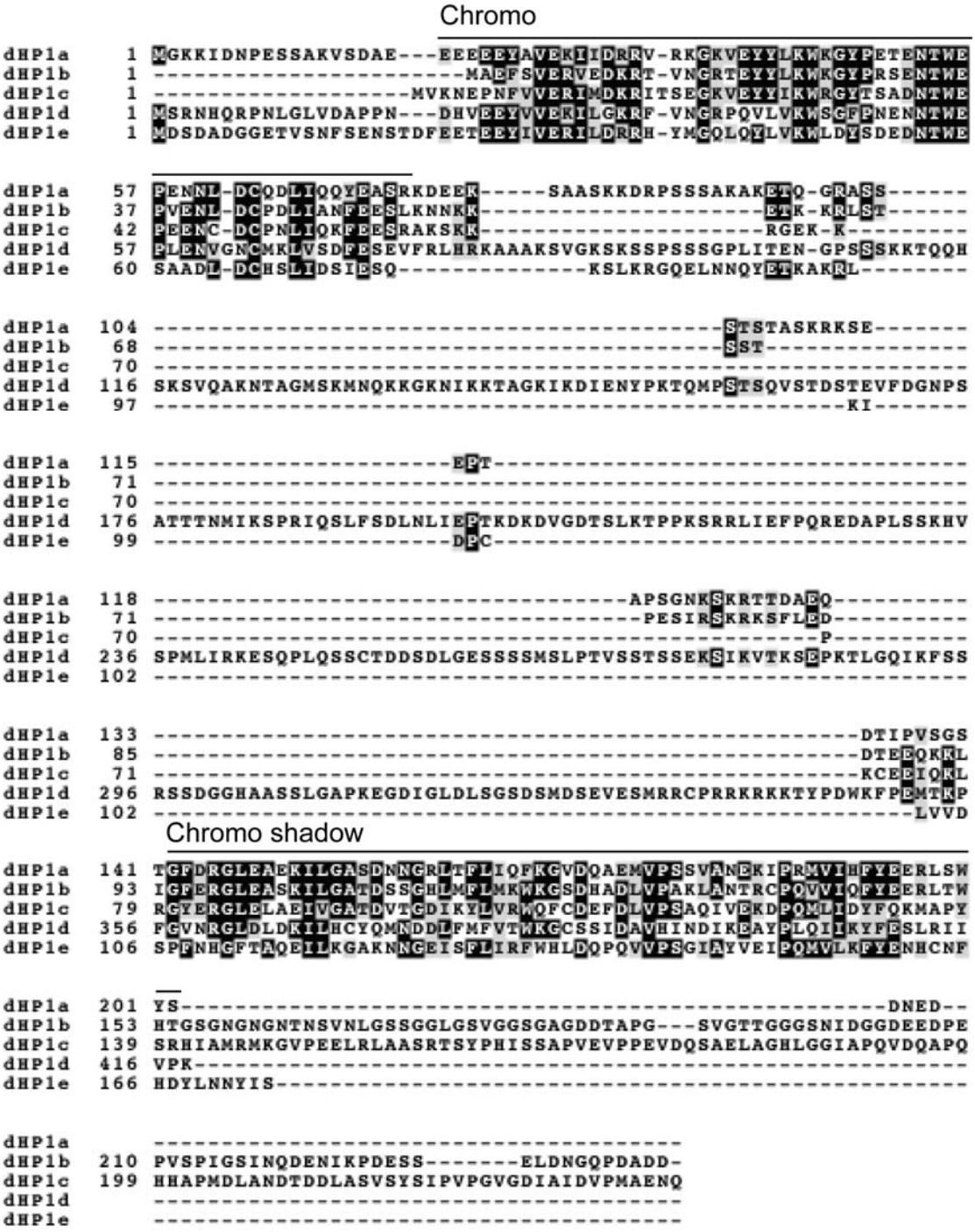

Figure 2.9 Alignment of *Drosophila melanogaster* HP1 proteins. The amino acid sequences of HP1a, HP1b, HP1c, HP1d and HP1e were aligned using T-coffee and imported into the Boxshade program to highlight identities (dark shading) and similarities (light shading) at each position. The chromo domain and the chromo shadow domain are indicated according to (Smothers and Henikoff, 2001).

The HP1 like proteins have different sub-nuclear localization; HP1α/a and HP1β/b are primarily found within centromeric heterochromatin, whereas HP1γ/c is enriched

at euchromatic sites (Greil et al., 2003; Minc et al., 1999; Minc et al., 2000; Smothers and Henikoff, 2001). On the other hand, *Drosophila* HP1d and HP1e are expressed predominantly in ovaries and testes respectively. In *Drosophila* Schneider cells (SL2), HP1d localizes to heterochromatin but with a distinct pattern from HP1a and HP1b (Vermaak et al., 2005). All HP1 like proteins share a conserved architecture consisting of a chromo domain and a chromo shadow domain separated by a flexible hinge region (Aasland and Stewart, 1995; Kellum, 2003). *D. melanogaster* HP1 like proteins are aligned in Figure 2.9. Differences between the different HP1 paralogs are readily apparent when comparing to HP1a. First, the chromo- and chromo shadow domains are conserved with HP1b sharing most identity with HP1a and HP1d the least. Second, HP1e has the shortest hinge region and HP1d the longest. Third, HP1b and HP1c both have an extended C-terminus with little significant sequence similarity. And fourth, N-termini are present in HP1a, HP1d and HP1e. *Drosophila* HP1a shares approximately total 50% identity with mammalian orthologs and only 25% with the *Schitzosaccharomyces pombe* ortholog, Swi6 (Li et al., 2002).

2.7.1 The chromo domain

Paro and Hogness found that the *Drosophila* Polycomb protein shared a homologous domain with HP1a. Since both proteins are involved in chromatin regulation they named it the chromo domain (chromatin organization modifier) (Paro and Hogness, 1991). About 20 proteins in *Drosophila* contains chromo domain(s) (Li et al., 2002) and the molecular functions of the different chromo domains are diverse (See table 2.5). The HMTase SU(VAR)3-9 and the ATP-dependent chromatin remodeling factor Mi-2 described above, both contain a chromo domain (Table 2.3) (Brehm et al., 2000; Tschiersch et al., 1994). Best studied is the chromo domain of HP1. It was shown to interact specifically with a peptide resembling the N-terminus of H3 that was di- or trimethylated at K9 (Bannister et al., 2001; Jacobs and Khorasanizadeh, 2002; Jacobs et al., 2001; Lachner et al., 2001; Nielsen et al., 2002b). This discovery supported the histone code theory which postulated that different histone modifications are recognized by chromatin proteins (Jenuwein and Allis, 2001; Turner, 1993). Supporting this idea the chromo domains of Chd1 and Polycomb were shown to bind

the H3 tail methylated at lysine 4 and 27 respectively (Cao et al., 2002; Min et al., 2003; Pray-Grant et al., 2005).

Table 2.5 Chromo domain proteins studied in *Drosophila* and their molecular function

Name	Abbreviation	Number of CD	Molecular function of the CD
Heterochromatin protein 1	HP1a, HP1b, HP1c	2[1]	H3K9me binding
Polycomb	Pc	1	H3K27me binding
Chromo-ATPase/helicase-DNA-binding	CHD1	2	H3K4me binding
Mi-2	Mi-2	2	Nucleosomal DNA binding
Males-absent on the first	MOF	1	roX RNA binding
Male-specific-lethal 3	MSL3	2	roX RNA binding
Suppressor-of-position-effect variegation 3-9	SU(VAR)3-9	1	?
Kismet	KIS-L/-S	2	?

Modified from (Brehm et al., 2004). CD, Chromo domain and 1) HP1 also contains a chromo shadow domain (see below).

The crystal structure of the HP1 chromo domain together with the methylated H3 tail revealed that the recognition of the methylated lysine involved a conserved aromatic pocket (Figure 2.10, residues are highlighted in purple) (Jacobs and Khorasanizadeh, 2002; Nielsen et al., 2002b). Four amino acids within the *Drosophila* HP1a chromo domain; Glu^{23}, Val^{26}, Asn^{60} and Asp^{62} interact with the H3 peptide to form a β-sheet (Figure 2.10; A) β-strands B0 and B4, B) residues highlighted in orange). The interaction with the H3K9 methylated tail is highly conserved among different HP1 like proteins and when a conserved Val^{26} was mutated to a methionine the binding to H3K9 methyl was abolished (Bannister et al., 2001; Lachner et al., 2001; Platero et al., 1995). The same mutation in a *SU(VAR)2-5*^{02} allele showed diminished HP1a localization to centric regions, but retained association to euchromatic and telomeric sites (Fanti et al., 1998) resulting in a loss of function allele (Platero et al., 1995).

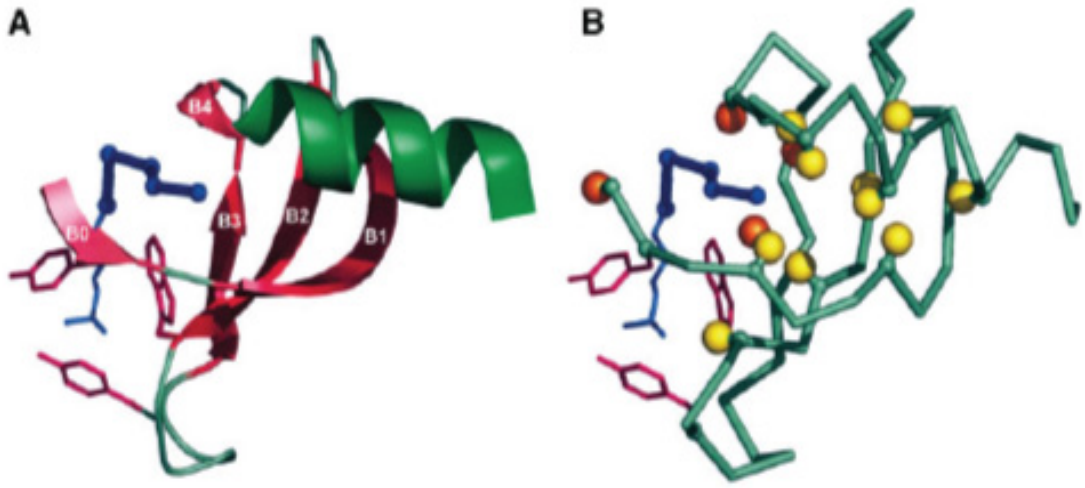

Figure 2.10 The chromo domain of *Drosophila* HP1a. Models of the chromo domain structure in complex with a histone H3 tail peptide (blue). Figure taken from (Brehm et al., 2004). The dimethylated K9 is shown in blue wireframe. **(A)** Secondary structures are shown; β-sheet (red arrows) and α-helix (green ribbon). **(B)** Residues that are structurally and functionally important are indicated with their carbon atoms shown as colored spheres. Labeled in yellow are conserved residues that form the hydrophobic core.

The affinity towards the H3K9 methylated peptide is rather weak (Table 2.6). Although it is 100-fold stronger then the affinity towards the H3K4 methylated peptide, (Table 2.4; compare rows 4 and 5 with 6). HP1a still binds H3-tail peptide containing both K4 and K9 methylation with a 2.5 fold weaker affinity than a peptide with only H3K9Me (Table 2.4; compare row 4 and 7). Isothermal titration calorimetry (ITC) measurements revealed that binding to H3K9 methylated peptide occurs in absence of significant change of the conformation of HP1a (Jacobs et al., 2001). The affinity for H3K9Me2 was improved when only the chromo domain was used compared to an N-terminal stretch including the chromo domain (Table 2.4; compare row 1 with 8 and 9), suggesting that the intact HP1 has a weaker affinity.

Table 2.6 *In vitro* HP1 binding studies

	Isoforms	Peptide	Method	kD	Reference
1.	HP1a CD (aa 17- 76)	H3 (aa 1-15) K9Me2	ITC[1]	6.9 ± 0.2 μM	(Jacobs and Khorasanizadeh, 2002)
2.	HP1a CD (aa 17-76)	H3 (aa 1-15) K9Me3	ITC[1]	2.5 ± 0.1 μM	(Jacobs and Khorasanizadeh, 2002)
3.	HP1a CD (aa 1-84)	H3 (aa 1-15) K9Me2	FA [2]	120 ± 12 μM	(Jacobs et al., 2001)
4.	HP1a CD (aa 1-84)	H3 (aa 1-15) K9Me2	FA [2]	120 ± 12 μM	(Jacobs et al., 2001)
5.	HP1a intact	H3 (aa 1-15) K9Me2	FA [2]	133 ± 11 μM	(Jacobs et al., 2001)
6.	HP1a CD (aa 1-84)	H3 (aa 1-15) K4Me2	FA [2]	1.9 ± 0.5 mM	(Jacobs et al., 2001)
7.	HP1a CD (aa 1-84)	H3 (aa 1-15) K4/K9Me2	FA[2]	268 ± 25 μM	(Jacobs et al., 2001)
8.	HP1a CD (aa 1-84)	H3 (aa 1-15) K9Me2	ITC[2]	105 ± 24 μM	(Jacobs et al., 2001)
9.	HP1a CD (aa 1-84)	H3 (aa 1-15) K9Me2	ITC[1]	59 ± 8 μM	(Jacobs et al., 2001)

Drosophila HP1a binding to premodified H3-tail peptides has been studied using different methods. Results were obtained at 15°C (1) and 25°C (2). kD, dissociation constant; ITC, isothermal titration calorimetry and FA, fluorescence anisotropy

Recently, the chromo domains of mammalian HP1α/β/γ have been shown to interact specifically with the linker histone isoform 1.4 when it is methylated at K26 (Daujat et al., 2005). The surrounding amino acids of K26 (KKARKSA) are similar to the amino acids surrounding K9 (QTARKST). H1.4 was shown to be methylated by Polycomb Repressive Complex 2 (PRC2) containing the HMTase Ezh2 and a specific EED isoform (Kuzmichev et al., 2004). This suggests that HP1 can be tethered to chromatin that lacks H3K9 methylation.

It has been reported that some proteins interact with the chromo domain of HP1 (See Table 2.7). Mouse HP1β was shown to interact with the nuclear envelope suggesting a role for HP1 in nuclear architecture (Kourmouli et al., 2000). The interaction with lamina-associated polypeptide 2β (LAP2β) and lamin B receptor (LBR) was mapped to the chromo domain. However, HP1β interaction with LBR was shown to be bridged by H3/H4 tetramers (Polioudaki et al., 2001). In addition, the chromo domain of mouse HP1α was shown to interact with the histone fold domain of bacterially expressed H3 (Nielsen et al., 2001a), suggesting that H3 may contribute to the interaction with the nuclear envelope.

The chromo domain of *Drosophila* HP1a interacts with origin recognition complexes (ORCs) (Pak et al., 1997). Another HP1/ORC associated protein (HOAP) (Shareef et al., 2001) has been described to interact with the hinge and chromo shadow domain (Badugu et al., 2003), suggesting that HP1 has a dual association with the ORC multi-protein complex. The ORC2 subunit is maternally deposited and enriched in centric heterochromatin of early embryos. In addition, *HOAP* and *ORC2* mutants suppress heterochromatin-induced silencing and display defects in HP1 localization in centric heterochromatin (Huang et al., 1998a; Pak et al., 1997). These data suggest a role for ORC and HOAP in heterochromatin silencing.

2.7.2 The chromo shadow domain

Unique for HP1 is a second C-terminal motif, the chromo shadow domain (Aasland and Stewart, 1995; Koonin et al., 1995). The chromo shadow domain bears resemblance with the chromo domain (Compare figure 2.10 and 2.11). Residues within the hydrophobic core that form an anti-parallel β- sheet and a α-helix are conserved between the different chromo shadow and chromo domains (Brasher et al., 2000). The most striking difference between the two domains are 2-3 residues in the chromo shadow central block forming a second α-helix (Cowieson et al., 2000). A proline (HP1β Pro^{156}) that lies in the turn between the two helices is conserved in the chromo shadow domain family and only present in some chromo domains (Cowieson et al., 2000). The chromo shadow domain was reported to be responsible for dimerisation of HP1 (Brasher et al., 2000; Cowieson et al., 2000; Jacobs et al., 2001; Zhao et al., 2000). Hence, the chromo domain was found to be monomeric, whereas the chromo shadow domains formed a dimer. The interface between the two dimers involves the C-terminal α-helices of each monomer (Brasher et al., 2000).

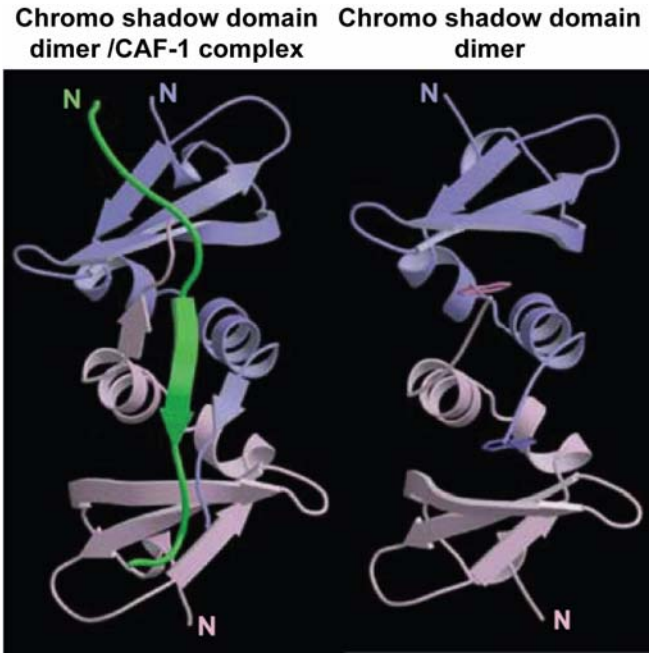

Figure 2.11 The structure of chromo shadow domain of mouse HP1β as a dimer or in a complex with CAF-1. Laue and colleagues dissolved the free chromo shadow domain structure in 2000, and the illustration is taken from (Thiru et al., 2004). The structure shows chromo shadow residues 110-172 and amino acids 214-232 of CAF-1. The side chains of Trp-170 that stabilizes the C-terminus of the chromo shadow domain.

Another interaction domain within HP1 is the chromo shadow domain, which interact with a variety of factors (see Table 2.7; reviewed in (Li et al., 2002)). In order to determine how chromo shadow domains interact with other proteins, a phage display method was used to enrich for peptides with sufficient affinity (Smothers and Henikoff, 2000). The screen resulted in a pentapeptide motif (PxVxL) that was identified in the amino acid sequence of HP1 interacting factors as well as in the chromo domain itself. Mouse HP1α was shown to interact with the large subunit of CAF1 through a PxVxL motif (Murzina et al., 1999). This interaction provided a link to the replication machinery and led to a model in which HP1 is targeted to replication foci by its interaction with CAF-1 and subsequently "handed-over" to methylated chromatin (Murzina et al., 1999). Immunofluorescence studies of replicating mouse cells revealed that a specific pool of HP1 (α and γ) coincide with CAF-1 during replication of heterochromatin domains (Quivy et al., 2004). In the structure of the chromo shadow domain with a CAF-1 peptide (Figure 2.11), the PxVxL motif forms a parallel β-sheet with the C-terminal tail of one monomer and an antiparallel β-sheet with the C-terminal tail of the other (Thiru et al., 2004). This is similar to the chromo

domain interaction with the H3 tail that also forms an intermolecular β-sheet (Jacobs and Khorasanizadeh, 2002; Nielsen et al., 2002b). The difference is that the chromo domain is monomeric and that two strands from the same domain forms an antiparallel β-sheet with the H3 peptide whereas the dimeric chromo shadow domain forms a mixed β-sheet with the PxVxL peptide (Thiru et al., 2004). The loose specificity of the chromo shadow domain allows interaction with different pentapeptide-motif proteins ranging from chromatin modifiers, transcriptional activators and transcriptional repressors (See Table 2.7).

Table 2.7 HP1 interaction and candidate partners

Protein	Organism	HP1 variant	Methodology	HP1 domain	Reference(ses)
Histones					
H1	Mouse, *Drosophila*	HP1α/a	rPD	Hinge	(Nielsen et al., 2001a)
H1-Chromatin	*Xenopus*	HP1α, HP1γ	rPDchr	Hinge	(Meehan et al., 2003)
Methylated K26 of H1.4	Human	HP1α, HP1β, HP1γ	rPD, IF	CD	(Daujat et al., 2005)
HP1-BP74 H1 like	Mouse	HP1α	Y2H, FW, rPD	Hinge	(Le Douarin et al., 1996; Nielsen et al., 2001a)
H3	Mouse	HP1α, HP1β, HP1γ	FW, rPD,exIP	CD	(Nielsen et al., 2001a; Polioudaki et al., 2001)
H3	*Drosophila*	HP1a	rPD	nd	(Nielsen et al., 2001a)
Methylated K9 of H3	*S. pombe*	Swi6	rPD, ChIP	CD	(Bannister et al., 2001; Nakayama et al., 2001)
Methylated K9 of H3	*Drosophila*	HP1a	IF, ITC, NMR	CD	(Jacobs and Khorasanizadeh, 2002; Jacobs et al., 2001)
Methylated K9 of H3	Mouse	HP1α, HP1β, HP1γ	rPD, NMR	CD	(Bannister et al., 2001; Nielsen et al., 2002b)
Methylated K9 of H3	Human	HP1α, HP1β, HP1γ	rPD,SPRA	CD	(Lachner et al., 2001)
H4	Mouse	HP1β	IF	nd	(Polioudaki et al., 2001)
H4	*Drosophila*	HP1a	*In vitro* cross-linking	CSD	(Zhao et al., 2000)
MacroH2A1.2 *	Mouse	HP1β	IF	nd	(Turner et al., 2001)
H2A.X & H4-Chromatin	Mouse	HP1α	ChIP, SED	nd	(Fan et al., 2004)
Nucleosome/ trypsinized	*Drosophila*	HP1a	NS	nd	(Zhao et al., 2000)

Protein	Organism	HP1 variant	Methodology	HP1 domain	Reference(ses)
Chromatin modifying enzymes/	*Transcript-ional regulation*				
SU(VAR)3-9	*Drosophila*	HP1a	IF, Y2H, exIP, rPD	CSD	(Eskeland et al., 2004; Schotta et al., 2002)
Suv39h1	Mouse	HP1β	IF, exIP, SED	nd	(Aagaard et al., 1999; Czvitkovich et al., 2001)
SUV39H1	Human	HP1β	IF, exIP, SED	nd	(Aagaard et al., 1999; Czvitkovich et al., 2001)
Suv39h1	Mouse	HP1α	rPD, Y2H	CSD	(Yamamoto and Sonoda, 2003)
SU(VAR)3-7	*Drosophila*	HP1a	IF, Y2H, exIP	CSD	(Cleard et al., 1997; Delattre et al., 2000)
SU(VAR)4-20	Mouse	HP1α, HP1β, HP1γ	transPD	nd	(Schotta et al., 2004b)
SuUR	*Drosophila*	HP1a	IF	nd	(Koryakov et al., 2006)
Suz12	Human	HP1α, HP1γ	IF,exIP, rPD	CSD	(Yamamoto et al., 2004)
JmjC	*S. pombe*	Swi6	IF	nd	(Zofall and Grewal, 2006)
KAP-1/TIF1β	Human	HP1α, HP1γ	IF, rPD, exIP, SPRA, GFC	CSD	(Lechner et al., 2000; Lechner et al., 2005; Nielsen et al., 2001a; Ryan et al., 1999)
KAP-1/TIF1β	Mouse	HP1α, HP1β, HP1γ	IF, rPD, exIP, GFP, Y2H	CSD	(Brasher et al., 2000; Le Douarin et al., 1996; Murzina et al., 1999; Nielsen et al., 1999; Ryan et al., 1999)
TRF1/PIN2	Mouse	HP1β	IF	nd	(Netzer et al., 2001)
$TAF_{II}130$	Human	HP1α, HP1γ	Y2H, transPD, exPD	CSD	(Vassallo and Tanese, 2002)
TIF1α	Mouse	HP1α, HP1β, HP1γ	Y2H, rPD	CSD	(Le Douarin et al., 1996; Nielsen et al., 1999)
Rb	Human	HP1α, HP1γ	Y2H, exPD, exIP, ChIP	nd	(Nielsen et al., 2001b; Williams and Grafi, 2000)
Rb	Maize	HP1γ	rPD, Y2H	nd	(Williams and Grafi, 2000)
Dnmt3a	Mouse cells	HP1α	IF	nd	(Bachman et al., 2001; Fuks et al., 2003)
Dnmt3b	Mouse cells	HP1α	IF	nd	(Bachman et al., 2001; Fuks et al., 2003)
SNF2β/BRG1	Mouse	HP1α	Y2H	CSD	(Nielsen et al., 2002a)
BRG1	Human	HP1α	exIP	CSD	(Lechner et al., 2005)
ATRX/HP1-BP38	Mouse	HP1α, M31	Y2F, IF	CSD	(Le Douarin et al., 1996; McDowell et al., 1999)

Protein	Organism	HP1 variant	Methodology	HP1 domain	Reference(ses)
NIPBL	Human	HP1α	exIP, rPD, Y2H, rPD	CSD	(Lechner et al., 2005; Murzina et al., 1999)
Pim-1	Human	HP1γ	Y2H, exIP, rPD	CSD	(Koike et al., 2000)
CKII	*Drosophila*	HP1a	*In vitro* phosphorylation	nd	(Zhao and Eissenberg, 1999)
dAF10	*Drosophila*	HP1a	transPD	CSD	(Linder et al., 2001)
MBD1	Human	HP1α	IF, exIP	nd	(Fujita et al., 2003)
EMSY	Human	HP1β	NMR, ITC, GFC	CSD	(Ekblad et al., 2005; Huang et al., 2006c)
DNA replication	*and repair*				
CAF-1 p150	Mouse	HP1α, HP1β	IF, Y2H,, rPD, GFC, NMR	CSD	(Brasher et al., 2000; Murzina et al., 1999; Thiru et al., 2004)
CAF-1 p150	Human	HP1α	rPD, exIP	CSD	(Lechner et al., 2000; Lechner et al., 2005)
Ku70	Human	HP1α, HP1γ	Y2H, rPD, exIP, IF	CSD	(Lomberk et al., 2006; Song et al., 2001)
BRCA-1*	Human	HP1α	IF	nd	(Maul et al., 1998)
ORC1, ORC2, ORC3, ORC4, ORC5, ORC6	*Drosophila*	HP1a	IF, exPD, exIP, transIP	CD, CSD	(Badugu et al., 2003; Pak et al., 1997; Shareef et al., 2003; Shareef et al., 2001)
Xorc1	*Xenopus*	HP1α, HP1γ	Y2H	nd	(Pak et al., 1997)
HOAP	*Drosophila*	HP1a	IF, exIP, transIP	CSD, Hinge	(Badugu et al., 2003; Cenci et al., 2003; Shareef et al., 2001)
Nuclear architecture					
Lamin B receptor	Human	HP1α, HP1β, HP1γ	Y2H, rPD, exPD, transPD, exIP, rPD	CSD	(Lechner et al., 2000; Lechner et al., 2005; Polioudaki et al., 2001; Ye et al., 1997; Ye and Worman, 1996)
LAP (amino peptidase)	Mouse	HP1α, HP1β	Y2H	CSD	(Le Douarin et al., 1996)
Lamin B and LAP2β	Mouse	HP1β	BA	CD	(Kourmouli et al., 2000; Polioudaki et al., 2001)
Other nuclear proteins					
Psc3	*S. pombe*	Swi6	IF, Y2H, exPD, ChIP	CD	(Nonaka et al., 2002)
Arp4/dArp6	*Drosophila*	HP1a	IF	nd	(Frankel et al., 1997; Kato et al., 2001; Ohfuchi et al., 2006)
INCENP	Human	HP1α, HP1γ	Y2H, transPD	Hinge	(Ainsztein et al., 1998)
Ki-67	Human	HP1α, HP1β, HP1γ	Y2H, exPD, IF	CSD	(Kametaka et al., 2002)

Protein	Organism	HP1 variant	Methodology	HP1 domain	Reference(ses)
SP100B	Human	HP1α, HP1β, HP1γ	IF, Y2H, rPD, transPD, exIP	CSD	(Lechner et al., 2000; Lechner et al., 2005; Lehming et al., 1998; Seeler et al., 1998)

The table is taken from (Li et al., 2002) with recent published data included. BA, binding assay; CD, chromo domain; Chip, chromatin immunoprecipitation; CSD, chromo shadow domain; exIP, co-immunoprecipitation using extract; exPD, pull-down assay using extracts; FAITC, fluorescence anistropy, isothermal titration calorimetry; FW, far Western analysis; GFC, gel filtration chromatography; IF, Immunofluorescence colocalization; nd, not detected; NS, nucleosomal shift assay; rIP, co-precipitation using recombinant proteins; rPD, pull-down assay using recombinant proteins; transIP; immunoprecipitation with *in vitro* translated protein; transPD, pull-down assay using *in vitro* translated protein; SED, sedimentation assay; SPRA, surface plasmon resonance analysis; Y2H, yeast two-hybrid assay. * Denotes cell cycle-dependent association.

2.7.3 HP1 targeting to chromatin

The HP1 family members behave as chromatin "hubs" with their two protein interaction modules. Genetic complementation assays (Powers and Eissenberg, 1993) as well as structural data (Thiru et al., 2004) showed that both globular domains are required for proper targeting of HP1. However, targeting of HP1 is not only dependent on the chromo and chromo shadow domain. Targeting of *Drosophila* HP1a to heterochromatin was shown to be dependent of both the flexible hinge and chromo shadow domain, whereas the chromo shadow domain alone can target HP1c to euchromatin (Smothers and Henikoff, 2001). A conserved portion of the mouse HP1α hinge region was reported to bind nuclear RNA *in vitro* (Muchardt et al., 2002). The authors showed that single domains of HP1α could not be targeted to pericentric heterochromatin, but that the intact chromo and hinge domain was sufficient. If mammalian tissue culture cells were treated with RNAse, HP1α was de-localized from heterochromatin (Muchardt et al., 2002) arguing for a bimodal targeting. However, in mammalian cells the Suv39h dependent H3K9 methylation decrease upon RNAse treatment (Maison et al., 2002), indicating that there are less binding sites for the HP1 chromo domain. The hinge region of mouse HP1α has also been shown to directly interact with the linker histone H1 (Nielsen et al., 2001a), and the hinge of *Xenopus* HP1α and not HP1γ was able to pull-down native H1 containing chromatin (Meehan et al., 2003). In addition, mouse HP1α was shown to interact

with the histone variant H2A.Z when incorporated into nucleosomal arrays (Fan et al., 2004). The binding of recombinant *Drosophila* HP1a to mononucleosomes required the presence of the full length protein suggesting that individual domains are not able to maintain a stable binding to a nucleosome (Zhao et al., 2000). The interaction of HP1a with chromatin could be independent of the core histone tails (Meehan et al., 2003; Zhao et al., 2000).

In vivo data suggest that binding of HP1 to chromatin is dependent on H3K9 methylation, but the results described above indicate that the targeting of HP1 is more complex: First, the chromo domain interacts with the N-terminal H3 K9Me but has also been shown to bind the globular domain of H3, H1 K26Me, and the ORC complex. Second, the hinge region mediates interaction with RNA molecules and H1. Third, the chromo shadow domain interacts with various chromatin proteins involved in chromatin assembly and transcriptional regulation arguing that these different factors are important for localization of HP1. Lastly, the interaction of HP1 with chromatin requires full-length protein or at least two domains (chromo-hinge domain, chromo shadow-hinge domain or chromo-chromo shadow domain) with the exception of *Drosophila* HP1c which localization to euchromatin depends on the chromo shadow domain.

When targeted to chromatin, it was long thought that HP1 binding was static and that HP1 behaves as a molecular glue in heterochromatin. Surprisingly, photo-bleaching experiments of living mammalian cells with green fluorescent protein-tagged HP1s (GFP-HP1) revealed that HP1 was rather dynamic (Cheutin et al., 2003; Festenstein et al., 2003; Schmiedeberg et al., 2004). The rapid exchange was observed for all three paralogs in both heterochromatin and euchromatin, although a small fraction of more static HP1 was observed in pericentric heterochromatin. A similar observation was made for Swi6 in fission yeast (Cheutin et al., 2004). The mobility of HP1 may be regulated through interaction of different factors with the chromo, chromo shadow and hinge domain. However, it is particularly interesting that HP1 interaction protein SUV39H1 that sets the H3K9 mark is less mobile than HP1 (Krouwels et al., 2005). A substantial part of SUV39H1 was immobile at pericentric heterochromatin and the binding was mediated by the SET domain, although enzymatic activity was not necessary (Krouwels et al., 2005). This suggests that the small fraction of static HP1

may be so due to interaction with SUV39H1, and the dynamic HP1 can rapidly exchange interaction partners.

2.7.4 Methyl/Phospho Switch and a subcode within the histone code

HP1 mobility can also be influenced by post-translational modifications of HP1 itself and of surrounding the H3K9Me binding site. As described above, the amino acids surrounding lysine 9 on the H3 tail can be phosphorylated (S10P) and acetylated (K14Ac). *In vitro* studies showed that S10 phosphorylation significantly reduces the binding of the chromo shadow domain to H3K9Me (Fischle et al., 2003a). Phosphorylation of S10 by Aurora B kinase in mitosis and concomitant delocalization of HP1 supported this idea (Fischle et al., 2005; Hirota et al., 2005). Unexpectedly Muchardt and colleagues reported that K9Me in combination with S10P and K14Ac delocalizes HP1α in mouse cells (Mateescu et al., 2004). The authors proposed that pericentromeric delocalization of HP1 observed at the G2/M transition (Murzina et al., 1999), coincides with a wave of S10 phosphorylation and a gradual increase of K14 acetylation (Mateescu et al., 2004). Muchardt and colleagues also reported that combination of K9MeS10P favors HP1 association with chromatin *in vivo* (Mateescu et al., 2004) which is contradictory to other studies (Fischle et al., 2005; Hirota et al., 2005).

HP1 homologs have also been reported to become phosphorylated (Eissenberg et al., 1994; Huang et al., 1998a; Minc et al., 1999; Zhao and Eissenberg, 1999). Different kinases have been shown to phosphorylate HP1, namely casein kinase II, protein kinase A and Pim-1 (Koike et al., 2000; Lomberk et al., 2006; Zhao and Eissenberg, 1999). However, specific functions of HP1 phosphorylation are diverse and need to be further investigated. Phosphorylation of HP1γ Serine 83 was demonstrated to interact with Ku70 and serve as a marker for transcription elongation (Lomberk et al., 2006). This fits well with the observation that HP1γ is recruited to actively transcribed chromatin (Vakoc et al., 2005). A recent study suggest that sumoylation may participate in heterochromatin stability (Shin et al., 2005). The authors show that the *S. pombe* HP1 homologs (Swi6 and Chp2) as well as the histone H3K9 methyltransferase Clr4 get sumoylated and that disrupted sumoylation of Swi6 or

Chp2 result in a modest silencing defect. Urrutia and colleagues proposes that post-translational modifications of HP1 provide a second regulatory layer to the histone code, and that this subcode needs to be deciphered (Lomberk et al., 2006).

2.7.5 HP1 in euchromatin

As discussed above the mammalian HP1γ and *Drosophila* HP1c localize to euchromatin (Minc et al., 2000; Smothers and Henikoff, 2001). Genome-wide mapping of HP1a in *Drosophila* KC cells revealed that it bound regions outside heterochromatin (Greil et al., 2003). Although HP1a/α action in euchromatic regions generally results in transcriptional repression (Ayyanathan et al., 2003; Hwang et al., 2001; Li et al., 2003), an increasing number of observations link HP1 to gene activation events. Gene expression analysis of *SU(VAR)2-5* mutant larvae revealed that hundreds of genes are up- and downregulated showing that HP1a have a role in euchromatic gene expression (Cryderman et al., 2005). Another study report that HP1a is essential for maintenance of active transcription of nearly one-third of genes involved in cell-cycle regulation (De Lucia et al., 2005). The heterochromatin genes *light* and *rolled* also require HP1 for active transcription (Clegg et al., 1998; Hearn et al., 1991). HP1a was also shown to be recruited to ecdysone- activated and heat-shock induced puffs when these genes are transcribed (Piacentini et al., 2003). Taken together these data suggest that HP1 can be present at sites of transcription.

2.7.6 Other functions of HP1

HP1 has also been shown to play a role in maintaining the nuclear structure. Centromeres in eukaryotes contain repetitive DNA elements. The *Schitzosaccharomyces pombe* centromeres are composed of a central core region of non-repetitive DNA containing the CENP-A H3 variant (called kinetochore) flanked by inverted repeat regions containing H3 that is methylated at K9 and the HP1 homolog Swi6 (Pidoux and Allshire, 2005). During cell division, the two sister chromatids segregate to opposite side of the cell, thereby transferring copies of chromosomes into each of the two daughter cells. The sister chromatids are pulled apart by microtubuli connected to the kinetochore. To keep the transferring of

chromosomes organized, corresponding sister chromatids are held together by a cohesin complex until cleavage of cohesin in anaphase (Nasmyth, 2002; Nasmyth, 2005). Swi6 is required for efficient cohesion (Bernard et al., 2001). The cohesion complex in fission yeast is composed of three subunits, Rad21, Psc3 and Pms1 (For nice overview of the cohesion apparatus in different organisms, see (Dorsett, 2006)). Interaction assays revealed that Swi6 interacts with Psc3 (Nonaka et al., 2002). Thus, in a *swi6* mutant strain less binding of Psc3 at centromeres and mating-type loci was observed (Nonaka et al., 2002) and loss of chromosomes occurred more frequently (Ekwall et al., 1995).

In *Drosophila,* HP1a is also required for correct chromosome segregation (Kellum and Alberts, 1995). Moreover, human Nipped-B-Like protein (NIPBL) that is required for loading of the cohesion complex, interact with HP1α through a PxVxL motif (Lechner et al., 2005). Taken together, these data suggest that HP1 is involved in loading cohesion and chromosome segregation.

In addition to HP1 involvement in mitotic cohesion, it has been demonstrated that HP1β co-localize with macroH2A1.2 in centromeric heterochromatin during male and female meiosis (Turner et al., 2001). The authors suggested that HP1β and macroH2A1.2 might have a role in kinetochore assembly. Knockout mice for *Suv39h* null mice have high frequency of non-homologous pairing in male meiosis (Peters et al., 2001). During *S. pombe* meiosis, the Rad21 subunit is replaced with a meiosis-specific cohesin subunit Rec8 whereas Rec11 replaces Psc3 at the chromosome arms but the meiotic cohesin complex in the vicinity of centromeres contain Psc3 (for review see (Watanabe, 2004)). This suggests that Psc3 at the centromeres links Swi6/HP1 to meiosis.

Immunolocalization studies on *Drosophila* polytene chromosomes showed that HP1a localizes not only to the chromocenter but also to many euchromatic bands and all telomeres (Fanti et al., 2003; Fanti et al., 1998; James et al., 1989). At the telomeres conventional polymerase machineries cannot complete their replication and therefore specific telomere complexes extend the terminal DNA. A second function essential to protect the telomeres from being degraded or fused is a capping mechanism (de

Lange, 2002). In most other organisms, a specialized reverse transcriptase termed telomerase extends the terminal DNA using a sequence specific RNA template (Nugent and Lundblad, 1998). The telomeres in *Drosophila* are maintained by transposition of three specialized retrotransposons (Abad et al., 2004; Mason and Biessmann, 1995; Pardue, 1994). Observations that mutant *SU(VAR)2-5* cells had multiple telomere-telomere fusions led to the conclusion that HP1a is required for telomere protection (Fanti et al., 1998). The chromo domain was not necessary for telomere capping (Fanti et al., 1998), rather direct binding of HP1a to telomeric DNA (Perrini et al., 2004). The authors also showed that HP1a binding to H3K9Me on telomeres was necessary for telomeric silencing (Perrini et al., 2004). Supporting HP1a`s involvement in telomere capping it was recently found that the HP1-interacting HOAP protein is required for telomere capping (Cenci et al., 2003). Taken together, these results support an important role of HP1 in capping and silencing of telomeres that involves interactions with DNA, specific proteins and H3K9Me. Whether HP1 has a role in telomere protection in higher eukaryotes remains to be seen. Cenci et al. propose that there are unexpected similarities between the capping mechanisms of *Drosophila* and human (Cenci et al., 2003). Studies in mice revealed that the three HP1 homologs are components of telomeres and that their presence depends on Suv39h dependent H3K9 methylation (Cenci et al., 2003). However, it is not known whether HP1 is a stable component of telomeres and if it interacts with the telomere machinery.

Returning to *Drosophila,* recent data suggest that HP1a has also a sex-specific role. Severe reduction of HP1a and SU(VAR)3-7 results in polytene chromosome phenotypes with a bloated X and an expanded chromocenter of males and females (Spierer et al., 2005). In addition, a genetic interaction between the HP1 interacting SU(VAR)3-7 and the DCC complex (*mle)* was also reported (Spierer et al., 2005). Genome wide mapping showed that HP1a binds along most of the X-chromosome in male but not female flies (de Wit et al., 2005). Similarly, when SU(VAR)3-7 is overexpressed, HP1a is found preferentially associated with the male X polytene chromosome (Delattre et al., 2004). Conditional depletion of HP1 in flies also resulted in preferential male-specific lethality (Liu et al., 2005). It has also been described that mutation of *Jil-1*, a histone H3S10 kinase shown to physically interact with the dosage compensation complex (Jin et al., 2000; Wang et al., 2001), resulted in

spreading of H3K9di methyl and HP1a to the chromosome arms with a pronounced increase on the X chromosomes (Zhang et al., 2006). The involvement of HP1a on the male X needs to be elucidated.

2.8 The Aim

Genetic events such as PEV have led to the understanding that the neighboring region affects gene expression. This is thought to be due to spreading of factors that affect chromatin structure. Several factors involved in gene silencing have been identified to covalently modify histone tails and their modifications act as receptors for non-histone proteins. However, it is not yet clear how these non-histone proteins specifically recognize these marks and how a modification can be accessed within a chromatin context.

The main goal of this work was to get a better understanding of specific recognition of chromatin modifications with a focus on methylation of H3K9 and binding of HP1. Therefore, recombinant, highly purified factors thought to be involved in gene silencing such as *Drosophila* histones, dG9a, SU(VAR)3-9 and HP1a were used. Bacterially expressed histone molecules completely devoid of any post-translational modification (unmodified chromatin) were used to generate chromatin carrying only the H3K9 mark. In order to retrieve highly H3K9 methylated chromatin it was necessary to characterize the recombinant HMTases SU(VAR)3-9 and dG9a. Using the highly active SU(VAR)3-9 allowed us to establish an *in vitro* system where HK9 methylated chromatin is linked to paramagnetic beads. This chromatin could be used to study binding of recombinant HP1a. We found that HP1a alone cannot bind efficiently to H3K9 methylated chromatin even if it contained more than 85% methylation. HP1a is depending on interaction with other factors that target it to chromatin and stabilize the binding to the K9 methyl. Since the factors that enhance HP1a binding to H3K9Me chromatin specifically interact with HP1a, it was of interest to identify more interaction partners. To do so, stable SL2 cell-lines expressing Flag-tagged HP1a and HP1c were used.

3. Material and Methods

3.1 Material

3.1.1 Chemicals, material and radioactive isotopes

Unless otherwise stated, all common chemicals and materials were ordered by Amersham / Pharmacia (Freiburg), E. Merck (Darmstadt), NEN / Perkin Elmer (Rodgau), Pierce (Bonn), Promega (Mannheim), Roche (Mannheim), Roth (Karlsruhe), Serva (Heidelberg) and Sigma (Deisenhofen). Radioactive S-Adenosyl-L-[methyl-^{3}H] Methionine (81 Ci/mmol) and [^{35}S] methionine/cysteine mix (7.15 mCi/ 500 µl) were purchased from Amersham.

3.1.2 Enzymes and Kits

Product	Received from
Cellfectin Reagent	Invitrogen
Effectene Transfections Kit	Qiagen
ECL™ Kit (enhanced chemoluminescence)	Amersham
Expand High Fidelity Kit	Roche
GFX PCR DNA and Gel Band Purification Kit	Amersham
Kilobase Binder	Dynal
Klenow	Roche
Maxiprep kit	Quiagen
Mnase (S7 Nuclease)	Sigma
Proteinase K	Genaxxon
Quick Change Mutagenesis Kit	Stratagene
Rabbit Reticulocyte Lysate System	Promega
Restriction endonucleases	NEB
Rnasin	Promega
Shrimp alkaline phosphatase	NEB
Taq polymerase	Genaxxon
T4 DNA ligase	NEB
TOPO TA Cloning®	Invitrogen
T7 RNA Polymerase	Promega
Trypsin (Sequencing grade)	Promega
QIAquick Gel Extraction Kit	Qiagen
Qiagen maxiprep kit	Qiagen

3.1.3 Chromatographic material

Resin/Column	Received from
Biorex 70 Resin	Bio-Rad
DEAE Sepharose	Amersham
DynaBeads M280	Dynal
Gelfiltration columns (Superose 6, Superdex 200)	Amersham
Gluthathione-Sepharose-4B	Amersham
Heparin Hi-Trap column	Amersham
Hydroxyl apatite resin	Bio-Rad
Chitin-Agarose Beads	NEB
M2-agarose (Flag-beads)	Sigma
MonoQ HR 5/5	Amersham
Protein A/G Sepharose	Amersham
Resource Q	Amersham
Sephadex G50 spin columns	Roche
SP-Sepharose FF	Amersham
Talon beads	BD Biosciences

3.1.4 Vectors

Vectors	Features	Resistance	Received
pET15b	6x his tag	Ampicillin	Novagen
pFASTBac1	Baculoexpression wo tag	Ampicillin and Gentamycin	Invitrogen
pPacFLAG	Flag tag	Ampicillin	G. Chen
pGEX4T1	GSTtag	Ampicillin	Amersham

3.1.5 Oligonucleotides

All oligonucleotides were ordered from MWG.

	Oligo name	Sequence	Description
1.	SUV39N-NdeI5	5`-TAGTGTACATATGGCCACGGCTGAA-3`	Cloning into pET15b
2.	SUV39C-XhoI3`	5`-AGTTGGCTCGAGAAAGAGGACCTTT-3	Cloning into pET15b
3.	SUV39Nchrom-SacI3`	5`-CTCCACAACGAGCTCTCCTTTGGGC-3`	Cloning into pET15b
4.	SUV39Cchrom-SacI5`	5`-ACCACTGAGCTCGAGAAGCAGCT-3`	Cloning into pET15b
5.	SUV39Cchrom-SacI3`	5`-AGCTGCTTCTCGAGCTCAGTGGT-3`	Cloning into pET15b
6.	SUV39NpreSET-SacI5`	5`-GGATTGTGAGCTCAAGTGCACTGA-3`	Cloning into pET15b
7.	Suv39Npre-SacII3`	5`-ATCCCCGCCCGCGGCTTGGGCAC-3`	Cloning into pET15b
8.	Suv39Cpre-SacII5`	5`-GATGGGGGCGGCGGGCCGCAACTG-3`	Cloning into pET15b

	Oligo name	Sequence	Description
9.	pgexHP1aNtXmaI5	5`-GTAGACCCGGGTGGCAAGAAAATCG-3`	Cloning into pGEX4T-1
10.	pgexHP1aCtXhoI3	5`-TCTCACTCGAGTTAATCTTCATTATC-3`	Cloning into pGEX4T-1
11.	pgexHP1cNtXmaI5	5`-ACACACCCGGGTGTTAAAAACGAG-3`	Cloning into pGEX4T-1
12.	pgexHP1cCtXhoI3	5`-TGCTCCTCGAGTTATTGATTTTCCG-3`	Cloning into pGEX4T-1
13.	pPacHP1aNtKpnI5	5`-CCCCAGGTACCGGCAAGAAAATCGA-3`	Cloning into pPacFLAG
14.	pPacHP1aCtXhoI3	5`-GTCTCCTCGAGTTAATCTTCATTATCA-3`	Cloning into pPacFLAG
15.	pPacHP1cNtKpnI5	5`-CCAGAAGGTACCGTTAAAAACGAGCC-3`	Cloning into pPacFLAG
16.	pPacHP1cCtSacI3	5`-CTGCTCCTCGAGTTATTGATTTTCCG-3`	Cloning into pPacFLAG
17.	HP1aW200ABstNI	5`-CGAAGAGCGCCTATCCGCGTACTCTGATAATGAAG-3`	Point mutation HP1W200A
18.	HP1aW200ABstNI rev	5`-CTTCATTATCAGAGTACGCGGATAGGCGCTCTTCG-3`	Point mutation HP1W200A
19.	Flagfwd5	5`-GACTACAAGGACGACGAT-3`	Sequencing
20.	HP1V26MNcoIfwd	5`-GAGGAGGAGTACGCCATGGAAAAGATCATCG-3`	Point mutation HP1V26M
21.	HP1V26MNcoIrew	5`-CGATGATCTTTTCCATGGCGTACTCCTCCTC-3`	Point mutation HP1V26M
22.	cg2995H1536KBstNIfwd	5`-ATGGAAATGTAACCAGGTTTTTTAACAAGTCGTGTGAGCCGAATG-3`	Point mutation dG9aH1536K
23.	cg2995H1536KBstNIrev	5`-CATTCGGCTCACACGACTTGTTAAAAAACCTGGTTACATTTCCAT-3`	Point mutation dG9aH1536K
24.	cg2995rewBamHI	5`-TGGATCCTACGCGTGTCCAAT-3`	Sequencing
25.	SUV39RNAi5	5`-GAATTAATACGACTCACTATAGGGAGACGACATAGCCGATTCCG-3`	RNAi of SU(VAR93-9
26.	SUV39RNAi3	5`-GAATTAATACGACTCACTATAGGGAGATACAAATTGGGCCCGC-3`	RNAi of SU(VAR93-9
27.	GSTRNAi5	5`-TTAATACGACTCACTATAGGGAGAATGTCCCCTATA-3`	RNAi control
28.	GSTRNAi3	5`-TTAATACGACTCACTATAGGGAGAACGCATCCAGGC-3`	RNAi control

3.1.6 Plasmids

Clone	Backbone	Description	Primers	Received	R. sites
dSU(VAR)3-9 wt	pET15b	Bacterial expression, purification over Talon beads		B. Czermin	NdeI - XhoI
dSU(VAR)3-9 mutants: Δ152, Δ213, Δ279, Δ409, Δ487, ΔSET and ΔC	pET15b	Bacterial expression, purification over Talon beads		B. Czermin	NdeI - XhoI
dSU(VAR)3-9 Δ152	pMyb2	Bacterial expression, purification over Chitin beads		B. Czermin	NdeI - XhoI
dSU(VAR)3-9 Δchromo	pET15b	Bacterial expression, purification over Talon beads	1, 2, 3, 4		NdeI - XhoI
dSU(VAR)3-9 Δ(285-412)	pET15b	Bacterial expression, purification over Talon beads	1, 2, 5, 6		NdeI - XhoI
dSU(VAR)3-9 ΔpreSET	pET15b	Bacterial expression, purification over Talon beads	1, 2, 7, 8		NdeI - XhoI
Flag dG9a	pFASTBac1	For baculovirus, purification over Flag beads		M. Stabell	SpeI - KpnI
Flag dG9a H1536K	pFASTBac1	For baculovirus, purification over Flag beads	23, 24		SpeI - KpnI
H3 K9A, K27A, K9/K27A	pET28	Bacterial expression		D. Reinberg	
H4 K20A		Bacterial expression		T. Jenuwein	
dHP1a	pET11a	Bacterial expression		J. Eissenberg	XbaI - BamHI
dHP1a (W200A)	pET11a	Bacterial expression	17, 18		XbaI - BamHI
dHP1a (V26M)	pET11a	Bacterial expression	20, 21		XbaI - BamHI
GST dHP1a	pGEX4T1	Bacterial expression, purification over	9, 10		XmaI - XhoI

Clone	Backbone	Description	Primers	Received	R. sites
		glutathione beads			
Flag dHP1a	pPacFlag	For SL2 stable transfection, purification over Flag beads	13, 14		KpnI - XhoI
dHP1c	pOT2	cDNA		BGDP EST project	EcoRI - XhoI
GST dHP1c	pGEX4T1	Bacterial expression, purification over glutathione beads	11, 12		XmaI - XhoI
Flag dHP1c	pPacFlag	For SL2 stable transfection, purification over Flag beads	15, 16		KpnI - SacI

3.1.7 *E. coli* strains

DH5α (Invitrogen)

E. coli F- Φ80d*lac*ZΔM15 Δ(*lac*ZYA-*arg*F)$_{U169}$ *deo*R *rec*A1 *end*A1 *hsd*R17 (r_k^-, m_k^+) *pho*A *sup*E44 λ$^-$ *thi*-1 *gyr*A96 *rel*A1 (Hanahan, 1983).

BL21(DE3)pLysS (Stratagene)

E. coli B F- *dcm omp*T *hsd*S(r_b^-, m_b^-) *gal*λ (DE3) (Studier et al., 1990)

3.1.8 Insect cell lines

Cell line	Origin	Phenotype	Description	Reference
Kc	*Drosophila melanogaster*	female	semi adherent cell line embryos, 6 to12 h	(Echalier and Ohanessian, 1970)
SL2	*Drosophila melanogaster*	male	adherent Oregon R embryos, 20 to 24 h	(Schneider, 1972)
SF9	*Spodoptera frugiperda*		adherent	Novagen

3.1.9 Fly lines

Drosophila embryo extracts were prepared from cultures with *Drosophila melanogaster* (Canton R).

Drosophila melanogaster yw flies are described in FlyBase (http://flybase.bio.indiana.edu)

Drosophila melanogaster Su(var)3–9^{06} (Tschiersch et al., 1994).

3.1.10 Antibodies

Antibodies	Received from	Dilutions for Western blots	Secondary antibody
α–ACF1 3B7	A. Eberharter	(1:500)	α-rat
α–flag	Sigma	(1:2000)	α-mouse
α–dG9a	M. Stabell	(1:500)	α-rabbit
α–HP1 C1A9	S. Elgin	(1:200)	α-mouse
α–HP1	S. Elgin	(1:1500)	α-rabbit
α-ISWI	J. Tamkun	(1:5000)	α-rabbit
α-Jil1	C. Regnard	(1:1000)	α-rabbit
α-myc 9E10	purified in the lab	(1:1000)	α-mouse
α–p55	J. Kardonaga	(1:10 000)	α-rabbit
α-RPD3	A. Brehm	(1:5000)	α-rabbit
α- SU(VAR)3-9 6C9	E. Kremmer	(1:5 sup) (1:250)	α-rat
α- SU(VAR)3-9 3D9	E. Kremmer	(1:5 sup) (1:1000)	α-rat
α- SU(VAR)3-9	G. Reuter	(1:1000)	α-rabbit
α- SUZ12	J. Larson	(1:1000)	α-chicken
α-rabbit-HRP	Amersham	(1:10 000)	
α-mouse-HRP	Amersham	(1:10 000)	
α-rat-HRP	Amersham	(1:5000)	
α-chicken-HRP	Amersham	(1:5000)	
α-rabbit-IRDye 800	Biomol	(1:10 000)	
α-mouse-IRDye 800	Biomol	(1:10 000)	
α-rat-IRDye 800	Biomol	(1:5000)	

3.1.11 DNA and Protein markers

Name	Received
GeneRuler 1 kb DNA ladder,	MBI Fermentas
peqGOLD Prestained Protein Marker IV	PeqLabBiotechnologie
peqGOLD Protein Marker II	PeqLabBiotechnologie
smart ladder	Eurogentec
123 bp ladder	Invitrogen

3.2 Methods

3.2.1 General molecular biology methods

3.2.1.1 Standard PCR setup

The concentration of DNA template was in general: 5-10 ng plasmid DNA. A normal PCR reaction contained 0.5 U Taq DNA plolymerase, 0.2 mM of each dNTP, 0.2 µM primers in 10 mM Tris-HCl (pH 9 at 25°C) , 50 mM KCl, 0.1 % Triton X-100 and 1.5 % $MgCl_2$. After initial denaturation of 1 minute at 94 °C, 30 amplification cycles (94 °C, 30 sec; 59-70 °C [primer dependent], 30 sec; 72 °C, [1 minute pr kb of desired PCR product]) were carried out with a final extension for 5 minutes at 72 °C.

3.2.1.2 Spectrophotometric concentration measurements of DNA and RNA

The concentration of a nucleic acid sample was measured using a DU 640 spectrophotometer (Beckman). At A_{260} an absorbance unit of dsDNA corresponds to 50µg/ml while an absorbance unit of RNA corresponds to 40 µg/ml. The purity of DNA or RNA sample was controlled by checking the ratio between absorption at 260 nm and 280 nm. A DNA sample is pure if the ratio is approximately 1.8, while RNA is pure if the ratio is approximately 2.1.

3.2.1.3 Agarose gel electrophoresis

Agarose gel electrophoresis was used to analyse the quality of DNA and to separate fragments by size (Sambrock and D.W.Russell, 2001). Depending on the size of the DNA molecules (kb) agarose solutions from 0.8 to 2% (w/v) in 1 x TBE buffer (90 mM Tris, 90 mM Boric acid, 2 mM EDTA) were used. Ethidium bromide was added to a final concentration of 0.25 µg/µl. The samples to be analysed were mixed with 1 x loading dye (5x loading dye: 50% v/v Glycerine, 10 mM EDTA, 0.05% (w/v) orange G). The voltage applied depended on the distance between the electrodes. In general the voltage applied was between 4-5 V/cm. As size standards: smart ladder, 1 kb ladder or 123 bp ladder were used. The DNA or RNA was visualized by UV light.

3.2.1.4 Isolation of DNA fragments from agarose gels

The desired DNA band was cut out from the agarose gel on a UV transilluminator and transferred into a 1.5 ml tube. For the purification QIAquick Gel Extraction Kit (Qiagen) was used.

3.2.1.5 Preparation of competent cells

Glycerol stocks of the *E. coli* bacteria were streaked on LB plates and incubated o/n at 37°C. Using one colony from this plate, a 3 ml LB pre-culture was grown o/n at 37°C. The next day 500 ml LB medium was inoculated with 1 ml of the pre-culture and grown to an OD at 600 nm of 0.6. The culture was chilled on ice for 10 min and then centrifuged (15 min, 4000 rpm, 4°C). The pelleted cells were gently resuspended in 200 ml ice cold TBPI (30 mM KAcetate, 100 mM KCl, 10 mM $CaCl_2$, 15% (v/v) Glycerol) and incubated on ice for 5 min. The centrifugation step was repeated. The cell pellet was then resuspended in 20 ml ice cold TBPII (10 mM PIPES pH 6.5, 75 mM $CaCl_2$, 10 mM KCl, 15% (v/v) Glycerol). Aliquots of 200 µl were transferred into 1.5 ml tubes, flash frozen in liquid nitrogen, and stored at -80°C. This preparation yielded an efficiency of 10^7 cfu/µg.

3.2.1.6 Transformation of competent cells

Immediately after thawing, a volume of 200 µl appropriate bacteria was added to the ligation mix/ plasmid of interest. The sample was mixed carefully and left on ice for 45 minutes. After heat shocking the cells for 1 minute at 42 °C the sample were immediately put on ice for 5 minutes. SOB medium was added (500 µl), mixed and the suspension was incubated for 45 minutes at 37 °C. Aliquots were plated out on selective LB plates with appropriate antibiotics and incubated at 37 °C over night. For cloning: 40 µg/ml X-gal and 0.5 mM IPTG was added.

3.2.1.7 Isolation of Plasmid DNA from *E. coli*

I) Plasmid miniprep

Plasmid DNA were extracted from *E.coli* with the help of alkaline lysis (Birnboim and Doly, 1979). Colonies were picked from an agar plate and used to inoculate 3 ml growth medium supplemented with the appropriate antibiotics. The cultures were incubated o/n at 37°C at 200 rpm. 1.5 ml of each o/n culture was transferred in a 1.5

ml reaction tube and centrifuged (10 min, 9000 rpm, RT) to pellet the bacteria. The cell pellet was resuspended in 250 µl P1 (50 mM Tris pH 8.0, 10 mM EDTA, 100 µg/ml RNase A), lysed by adding 250 µl P2 (200 mM NaOH, 1% (w/v) SDS) and mixed by immediately inverting the tube for 5 times. After incubation at RT for 5 min the reaction was stopped by adding 350 µl P3 (3 M KAcetate). The tube was inverted again for 5 times and then left on ice for 10 min and centrifuged (10 min, 13000 rpm, RT). The plasmid DNA in the supernatant was transferred in a new 1.5 ml tube and 600 µl of isopropanol was added. The tube was incubated on ice for 30 min and then centrifuged (20 min, 13000 rpm, 4°C) to pellet the plasmid DNA. The pellet was washed with 70% ethanol and centrifuged (5 min, 13000 rpm, 4°C). The supernatant was carefully aspirated and finally the pellet was air dried and redisolved in 25 µl TE (10 mM Tris, 1mM EDTA).

II) Plasmid maxiprep

To obtain 100 µg plasmid DNA or more, 500 ml LB medium and the appropriate antibiotics was inoculated with the bacterial glycerol stock of interest and incubated o/n at 37°C at 200 rpm. The plasmids were purified using a Qiagen maxiprep kit.

3.2.1.8 Site-directed mutagenesis

Site-directed mutagenesis was performed using the QuickChange kit (Stratagene) according to manufacturer's protocol.

3.2.2 General protein-biochemistry methods

3.2.2.1 SDS-polyacrylamide gel electrophoresis (SDS-PAGE)

Pouring and electrophoresis of SDS-polyacrylamide gels was performed using the Novex system (pre-assembled gel cassettes). Stacking gels were prepared according to standard protocols using ready-to-use polyacrylamide solutions from Roth (Rotigel, 30%, 49:1). For electrophoresis, protein samples were mixed with SDS-PAGE sample buffer, heat-denatured for 5 min at 95°C and directly loaded onto the gel. Proteins were separated at 200V until the dye front had reached the end of the gel. The molecular weight of proteins was estimated by running pre-stained or non-stained marker proteins (Peqlab, peqgold protein marker) in parallel. Following

electrophoresis, proteins were stained with either Coomassie Brilliant Blue, Silver or subjected to Western blotting.

3.2.2.2 Coomassie Blue staining of protein gels

Polyacrylamide gels were fixed for at least 30 min in fixation solution (50% methanol / 10% acetic acid) and stained for 60 min to overnight on a slowly rocking platform with Coomassie staining solution (0.025% Coomassie Blue R in 10% Acetic acid). To visualize proteins, gels were destained in 10% acetic acid. After documentation, the gels were dried onto a Whatman paper at 80°C for 1 hr on a gel dryer (BioRad).

In order to analyze proteins by Mass Spectrometry, gels were stained with a Colloidal Coomassie staining kit (Merck). Briefly, gels were fixed for at least 2 hrs in fixation solution (50% methanol /10% acetic acid) and incubated overnight in staining solution. Destaining of the gels was performed using ddH_2O. After documentation, the bands were excised with a scalpel and stored in 0.2 ml PCR tubes with 150 µl of ddH_2O at -20°C. Mass Spectrometry analysis of the proteins by MALDI-TOF or nano-spray-LC-MS/MS was carried out in a core facility (http://proteinanalytik.web.med.uni-muenchen.de/index.php/home/).
Staining solution: 10 ml Stainer A, 2.5 ml Stainer B, 10 ml Methanol and 27.5 ml ddH_2O

3.2.2.3 Silver staining of protein gels

The staining of protein gels with silver nitrate solution was carried out according to the protocol of Blum. The gel was fixed in 50% ethanol / 10% acetic acid for at least 2 hrs and washed three times in 30% ethanol (20 min each), incubated for 1 min in 0.02% $Na_2S_2O_3$ (sodium thiosulfate), washed three times with water (ddH_2O, 20 sec each) and stained with 0.2% $AgNO_3$ solution for 1 hr. Afterwards, the gel was washed with water (three times, 20 sec each) and developed using developing solution (3% Na_2CO_3, 0.05% H_2CO, 0.0004% $Na_2S_2O_3$) until the desired proteins were visible (typically, after 5 to 10 min). After a short wash in water (1 min) the reaction was stopped by incubating the gel in 0.5% glycine stop solution (more than 5 min). After a final water wash (>30 min), the gel was documented and dried onto a Whatman paper at 80°C for 1 hr on a gel dryer (BioRad).

3.2.2.4 Western Blotting

Proteins were separated by SDS-PAGE and transferred to PVDF membranes (Millipore) using the BioRad "Wet Blot system". The gel was placed onto a membrane and sandwiched between gel-sized Whatman paper soaked in transfer buffer (25 mM Tris, 192 mM glycine, 20% methanol). The proteins were then transferred onto the membrane for 1.5 hrs (400 mA constant) at room temperature. The transfer reaction was cooled by the addition of an ice block into the transfer chamber. After transfer, the PVDF membranes were incubated for 1 hr in blocking solution (PBS/0.1% Tween-20/5% dried milk) in order to reduce the non-specific background. Membranes were sealed in a plastic bag and incubated overnight on a horizontal shaker in the coldroom with an appropriate dilution of the primary antibody directed against the protein of interest. PVDF membranes were washed three times in PBS/0.1% Tween-20 (10 min each) and incubated for one additional hr with horseradish peroxidase-coupled secondary antibody at room temperature. After three washes (10 min each, in PBS/0.1% Tween-20) antigen-antibody complexes were detected using the Enhanced Chemi-Luminescence Kit (ECL, Amersham) and autoradiography according to the manufacturer´s instructions.

3.2.2.5 Li-Cor

Proteins were transferred to a PVDF memebrane (millipore) as described above. After transfer, the PVDF membranes were incubated for 1 hr in blocking solution (TBS 5% BSA) in order to reduce the non-specific background. Membranes were sealed in a plastic bag and incubated overnight on a horizontal shaker in the coldroom with an appropriate dilution of the primary antibody directed against the protein of interest (in TBS/0.05% Tween-20/5% BSA). PVDF membranes were washed three times in TBS/0.0.5% Tween-20 (10 min each) and incubated fluorescently labeled secondary antibodies (in TBS/0.05% Tween-20/3% BSA). After three washes (10 min each, in TBS/0.05% Tween-20) antigen-antibody complexes were quantified with an Odyssey system (Li-Cor). For quantification the background method was set to median, border with 1 and Top/ Bottom segment.

For quantification of HP1, both the monoclonal mouse (C1A9) and polyclonal rabbit antibodies were tested for linearity. The detection of polyclonal rabbit antibody was

linear in the range of 15-150 ng of HP1 protein and was therefore used for Li-Cor quantification (Figure3.1).

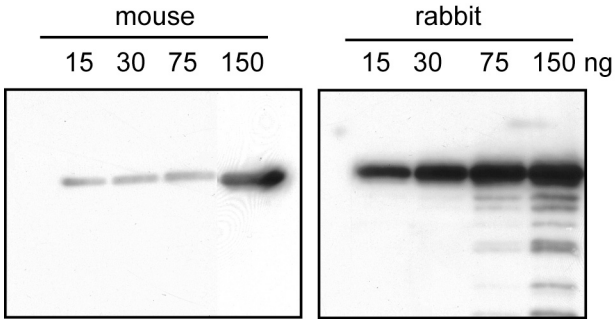

Figure 3.1 Test of HP1 antibodies on Western Blot.

3.2.2.6 Trichloroacetic acid (TCA) precipitation of proteins

TCA was added to the protein sample at a final concentration of 20%, mixed and incubated for 10 min on ice. After spinning the sample at 13000 rpm and 4°C for 10 min, the supernatant was removed and the pellet washed twice with 500 µl of cold acetone by centrifuging it at 13.000 rpm and 4°C for 5 min. The protein pellet was dried and resuspended in 1 x SDS-PAGE loading buffer and 1/40 volume of 1 M Tris pH 8.0.

3.2.2.7 Determination of protein concentration

Protein concentration was determined using the colorimetric assay Bradford. The concentration of purified proteins was also estimated according to protein standards with a known concentration (e.g. BSA) in SDS-PAGE followed by Coomassie blue staining.

3.2.2.8 *In vitro* translation

In vitro transcription and translation (IVT) reactions were performed for 2 hours at 30° with the TNT rabbit reticulocyte lysate System (Promega) using 1 µg of plasmid DNA and 10 µCi of [^{35}S] methionine in a 25 µl reaction.

3.2.3 Tissue culture methods

3.2.3.1 Cultivation of *Drosophila* cell lines

Drosophila cell lines SL2 was kept in Schneiders *Drosophila* Medium in medium sized tissue culture flasks at 26°C. SL2 cells were split in a sterile hood every 3 to 4 days in a ratio 1:3 or 1:4 then moved to a new flask and provided with fresh medium in a total volume of 30 ml. In doing so attention was paid that the cells always grew adherently to the surface. Kc and SF4 cells posses a higher doubling rate and needed to be split every 3 days in a ratio 1:6 to prevent a totally detachment of the cells. Every two month a new frozen cell stock was thawed.

3.2.3.2 Generation of SL2 stable cell-lines

The SL2 cells were split the day before transfection and seeded out (5 x 10^6) in 60 mm dish. The plasmid DNA of interest (1.8 μg) together with antibiotic selective plasmid (0.2 μg) (in general pNeo was used) was diluted in 300 μl Buffer EC (Effectene Transfection kit, Qiagen) and left at room temperature for 2-5 minutes. The mixture was shortly centrifuged down and 60 μl of Effectene (Qiagene) reagent was added. Then it was vortexed for 10 seconds and incubated for 10 min at room temperature. To the mixture 3 ml of Schneiders *Drosophila* Medium was added and then carefully pipetted onto of the SL2 cells. The transfected cells were left at 26°C for 2 days and transferred to a medium sized tissue culture flask with fresh medium and selective antibiotics (in general puromycin (1:1000). Selection of the cells lasted approximately 3 weeks.

3.2.3.3 Generation of Baculoviruses and protein expression

Protein of interest was cloned into pFastBac^{TM}1 with an N-terminal flag tag. Then it was transformed into DH10Bac (Invitrogen) and bacemids were purified according to manufacturers protocol (Invitrogen). A monolayer of Sf9 (*Spodoptera frugiperda*) (9 x10^5) was transfected with 1 μg bacemid using Cellfectin Reagent (Invitrogen) and cells were left for 7 days at 26ºC. The supernatant was amplified 2-3 times and recombinant viruses were used for test expression. Amplification was undertaken to preserve the virus stock and to gain a higher titer of virus (typical 10^7 to 10^8 plaque forming units (pfu/ml)) of the initial virus stock. A 15 cm diameter plate with 1.2x10^7 Sf9 cells (attached) was infected with 0.5 to 1 ml of virus and incubated at 26°C. The plate was sealed with parafilm (NAS) to prevent dehydration. The supernatant was collected after 7 days of cultivation (check for high level of virus infection by

comparing to mock transfected cells) and kept at 4°C in the dark. The cells stopped growing and cells lysed. For test expression: Forty-eight hours post-transfection cell extracts were checked for fusion protein expression using anti-FLAG monoclonal antibody (Sigma). For routine protein expression 10 x150 mm Petri dishes were infected and the cells kept at 26ºC.

3.2.4 Recombinant protein expression and purification

3.2.4.1 Expression and purification of recombinant *Drosophila* His-SU(VAR)3-9

Transform 1 µl peT15b-plasmid into 200 µl BL21(DE3)pLys cells and plate on amp/chloramphenicol (or suitable antibiotics) plate. Incubate at 37° overnight. The next day, inoculate several colonies from the plate in about 50 ml of LB (+ antibiotics (amp/chl)) and incubate overnight at 37°C with shaking. On day three, expand 20 - 40 ml of the preculture to 2 -4 litre of LB (+ antibiotics). Incubate bacteria at 37° C, shaking at 200 rpm and measure OD (600nm). When the culture reaches 0.8 (it will take 2 to 4 hours according to volume of pre-culture), induce cells with IPTG to a final concentration of 1 mM. The cultures were left shaking at 18° C overnight. The following day the bacteria was centrifuged down (7000 g/4 °C/ 15 –20 min) and the pellet resuspended in 25 ml to 40 ml of Lysis Buffer 1 mM Imidazole (20 mM Tris pH 8, 200 mM NaCl, 0.05% NP40 and protease inhibitors like “complete tablets”, or a mixture of leupeptin, aprotinin, pepstatine, PMSF) and transferred in a 50 ml falcon tube. The solution was quick frozen in liquid nitrogen and stored at - 80° C. For purification the solution was thawed at 37° C for 15 to 20 min. Thereafter the bacteria solution was sonicated 6 times for 30 seconds, amplitude 50% on ice. Centrifuge in Sorvall centrifuge for 30 min at 18-20 000 rpm, 4°C, SS 34 rotor. Talon beads (Clontech) were prepared: take about 4 ml of the mixture, and wash 2 times in Lysis buffer 1 mM Imidazole . Then make a 1:1 slurry of the beads in lysis buffer 1 mM Imidazole. The supernatant was transferred in a new tube, and 1 ml of Talon bead slurry per 2 l of bacterial culture (i.e. 2 ml slurry per 4 l of culture) was added. The slurry was incubated for 2 hours in the cold room rotating. After the incubation centrifuge down beads for 10 min, 4° C at 1000 rpm. Work in coldroom and take off supernatant, add 5 ml lysis buffer 1 mM Imidazole (with protease inhibitors) to the beads and transfer them into a small single-use plastic column (for example Poly-Prep from BioRad). Wash beads for 2 - 3 times with 10 ml lysis buffer 1 mM Imidazole, 1

x with 5 mM Imidazole and 2 x with 15 mM Imidazole. The protein was eluted with lysis buffer 100 mM Imidazole (+ protease inhibitors) and 0.5 ml fractions collected (collect about 10 fractions). The protein will be most concentrated in fraction 2, 3 and 4. Load 5-10 µl of each fraction onto a SDS gel for a Coomassie staining and for a western blot

For enzymatic activity would I add 10% glycerol in the Elution Buffer and add BSA to (100 ng/ul) to each fraction before freezing. After testing activity; thaw active fractions and pool them. Work in cold room and very quick. Aliquot in 50- 100 ul and flash frozen in liquid nitrogen. Store at - 80 ° C.

3.2.4.2 Expression and purification of recombinant *Drosophila* HP1

Bacterial expression of un-tagged HP1 proteins was performed as described in 3.2.4.1. Only 1 liter of culture is efficient to retrieve several mg of protein. Recombinant HP1 and point mutants were purified according to (Zhao and Eissenberg, 1999) and dialysed against BC100 (25 mM HEPES (pH 7.6), 100 mM NaCl, 1 mM $MgCl_2$, 0.5 mM EGTA, 0.1 mM EDTA, 10% (v/v) glycerol, 1 mM DTT and 0.2 mM PMSF). All HP1`s were quantified by Bradford (Bio-Rad) and Coomassie stained proteins was quantified using the ImageMaster 1D Elite v3.01 software package (Amersham) using BSA as a standard.

3.2.4.3 Purification of Flag-dG9a

The cells were harvested 48 hours post-infection and washed once with cold 1x phosphate-buffered saline. For purification of FLAG-dG9a protein, infected cells (1.2 $x10^8$) were resuspended in 4 ml of BC300 (25 mM HEPES (pH 7.6), 300 mM NaCl, 1mM $MgCl_2$, 0.5 mM EGTA, 0.1 mM EDTA, 10% (v/v) glycerol, 1 mM DTT, and protease inhibitors) containing 0.05% (v/v) NP40. The cells were sonicated on ice 2 times 15 seconds at 50% amplitude using a Branson sonifier and centrifuged at 15000 rpm for 30 minutes. 100 µl 1:1 slurry of M2 anti-FLAG agarose beads (Sigma) was added to the supernatant and incubated for 2 hours at 4ºC. After washing three times with BC300 (containing 0.05% (v/v) NP40) for 10 minutes each, and once with BC100 (0.05% (v/v) NP40) the bound protein was eluted with 0.5 mg/ml FLAG peptide BC100 (0.05 % (v/v) NP40) for 2 hours. The purity of the protein was checked by SDS-PAGE. Eluates were stored at -80ºC.

3.2.4.4 Expression and purification of GST-tagged proteins

Expression of GST-proteins were performed as described in chapter 3.2.4.1. In general 500 ml to 1 liter is sufficient for several mg of protein. Centrifuge down culture at 4000 rpm for 15 minutes at 4 degrees and redisolve pellet in ca 10ml Column buffer pr 500 ml culture (20 mM Tris pH8, 300 mM NaCl, 0.5 mM EDTA and complete protease inhibitors, 1mM DTT). Freeze in liquid nitrogen; even if you plan to continue the prep the same day or store at -70. Thaw at 37 degrees waterbath for approximately 10-15 min. Sonicate on ice 7x at 50 % on ice and add 0.5 % NP40. Then centrifuge for 30 minutes at 18000 rpm, 4 degrees. (SORVALL).After centrifugation transfer supernantant to a new Falcon tube (50 ml). During the centrifugation wash Glutathion-Sepharose 4B beads in Column buffer in 15 ml falcon. Prepare a 1:1 slurry. Add 400 ul slurry pr 500 ml LB and leave rotating in the cold room for 2 hours. Centrifuge down beads at 2000 rpm for 10 min. Remove supernantant (keep aliqote for gel to see if you have bound everything) and add 10ml Column buffer and transfer beads into column (for example Poly-Prep from BioRad). Wash 2x 10 ml Wash buffer I (20 mM Tris pH8, 1000 mM NaCl, 0.5 mM EDTA, 0.1 % NP40 and complete protease inhibitors, 1mM DTT) , 2 x 10 ml Wash buffer II (Same as Wash buffer I with 500 mM NaCl) and 1x 10 ml Wash buffer III (Same as Wash buffer I with 200 mM NaCl and without NP40) let all buffer run out by gravity. Put the yellow cap on the column. Add 200 ul Elution buffer (200 mM Tris pH 8, 40 mM reduced glutathione, 200 mM NaCl and 10% glycerol. Prepared fresh the same day) per initial 400 ul slurry (ie 1200 slurry- 600 Elution bf). Add lid and rotate for 1 hour at 4 C. If the beads are stuck in the lid a gentle short centrifugation putting the column in a 50 ml Falcon 1000 rpm 10 sec should help. Elute all in one tube and quick freeze. Usually a second elution with the same elution volume is recommended 1 hour-ON.

3.2.5 Histone purification and octamer preparation

3.2.5.1 Expression and purification of *Drosophila* histones

Recombinant histone expression and purification was undertaken according to Luger and colleagues (Luger et al., 1999). Briefly, individual recombinant histones were

expressed in BL21(DE3)pLys as described in 3.2.4.1 with a total volume of 9 litres of LB. Inclusion bodies containing the histones were prepared. The proteins were unfolded in urea buffer and the histones were purified via SP-Sepharose chromatography. The histones were dialyzed against water, lyophilized and stored at -80°C.

3.2.5.2 Purification of Native *Drosophila* histones

Native histones were purified according to (Simon and Felsenfeld, 1979). Approximately 50 g of (0-12 hour) *Drosophila* embryos were collected and dechorinated. The dried embryos were resuspended in 40 ml Glycine buffer (15 mM Hepes-KOH pH 7.6, 10 mM KCl, 5 mM $MgCl_2$, 0.05 mM EDTA, 0.25 mM EGTA, 1 mM DTT, 0.2 mM PMSF, 10% glycerol and 1 tablet complete/ 50 ml). The embryos were homogenized 6 times with a Yamamoto homogenisator at 1000 rpm, 4°C. After filtering the homogenized embryos through a miracloth, the solution was centrifugated for 10 min at 8 krpm in a HB-4 rotor at 4°C. The nuclear pellet was resuspended in a final volume of 50 ml SUC buffer (15 mM Hepes-KOH pH 7.6, 10 mM KCl, 5 mM $MgCl_2$, 0.05 mM EDTA 0.25 mM EGTA, 350 mM Sucrose,. 1 mM DTT, 0.2 mM PMSF and 1 tablet complete/ 50 ml). The nuclei solution were centrifuged again (10 min; 8 krpm; HB-4 rotor; 4°C) and the nuclei was resuspended in 30 ml SUC buffer. Then 90 ml of 1M $CaCl_2$ was added and the solution was heated up for 5 minutes at 26°C. Then add 125 ml MNase 50 u/ml and incubated for 10 min at 26°C. The reaction was stopped with 600 ml 0.5 M EDTA and centrifuged again (10 min; 8 krpm; HB-4 rotor; 4°C). The pellet was resuspended in 6 ml TE pH 7.6 including 1 mM DTT, 0.2 mM PMSF and complete protease inhibitors and rotated for 30-45 min at 4°C. Then centrifuge for 30 min at 12 krpm in a HB-4 rotor at 4°C. The pellet was the chromatin. Adjust salt to 0.63 M NaCl with the 2 M NaCl/ 100 mM K-PO4 (pH7.2) solution and centrifuge again (for 30 min at 12 krpm in a HB-4 rotor at 4°C). Afterwards the histones were loaded on a 30 ml Hydroxylapatite column (BIO RAD #130-0150 Bio gel HT) and wash column with 5 volumes of 0.63 M NaCl/ 100 mM K-PO4 (pH 7.2) and elute histones with 2 M NaCl/ 100 mM NaPO4. Histones were concentrated (Centricon 30 K; 7000 rpm, SS34 rotor (Sorvall), at 4°C successive 20 min) and 50% (vv) glycerol was added. The glycerol stock were stored at –20°C. The histones were checked on a 18% SDS PAGE

3.2.5.3 Native H1 purification

H1 was purified from *Drosophila* embryos (0-12 hrs) according to (Croston et al., 1991) and its identity was verified by MALDI TOF.

3.2.5.4 Octamer preparation

The histone octamer reconstitution was prepared according to Luger with minor modifications (Luger et al., 1999). Lyophilized recombinant histones were resuspended in unfolding buffer (7 M Guanidinium HCl, 20 mM Tris pH 7.5, 10 mM DTT) in a final concentration of about 2 mg/ml. The exact protein concentration was calculated from the UV-absorption at 275 nm using the specific absorption coefficient of each histone (Luger et al., 1999). Equal amounts of histones were mixed and a similar volume of unfolding buffer was added. This mixture was dialyzed 3 times (twice 1 hour and once o/n) against one liter of refolding buffer (2 M NaCl, 10 mM Tris pH 7.5, 1 mM EDTA, 5 mM β-mercaptoethanol). Aggregates were removed by a short centrifugation step (10 min, 15000 rpm, SS34 rotor (Sorvall)). The supernatant was concentrated to less than 2 ml by centrifugation in concentration tubes (Centricon 30 K; 7000 rpm, SS34 rotor (Sorvall), at 4°C successive 20 min). The concentrated sample was purified over a Superdex 200 gel filtration column in order to separate the refolded octamer from incomplete forms and precipitates (flow 1 ml/min, 2 ml-fractions, running in refolding buffer). Individual fractions were analyzed on a 18% SDS gel and the suitable fractions containing stochiometric histone octamers were finally concentrated by centrifugation (conditions as above) down to 1 ml. One volume of glycerol was added and the recombinant histone octamers were stored at -20°C.

3.2.5.5 Generation of H3K9 methylated octamer

120 µg of recombinant octamer was incubated in the presence of 9 µg of active recombinant *Drosophila* SU(VAR)3-9 (Eskeland et al., 2004) to retrieve 60 µg of a 70-80% H3K9 di- and tri-methylated octamer. The reaction was incubated at 30 °C for 90 minutes in the presence of 40 µM S-adenosylmethionine (New England BioLabs) as methyl donor and 40 mM NaCl. After incubation concentrations were adjusted to 100 mM NaCl, 0,2 mM PMSF and 2 mM DTT. To 1 ml total volume, 80 µl (1:1 slurry) of Biorex70 beads (Bio-Rad) were added. The reaction was rotated at 4 °C for 4 hours and washed 5 times with TEN200 (200 mM NaCl, 10 mM Tris, 1 mM

EDTA, 0.2 mM PMSF and 1 mM DTT) and 5 times with TEN400. The methylated octamer was eluted with TEN2500, and 4 µl (2 µg) was analyzed by a 15% SDS PAGE and stained by Coomassie blue.

3.2.6 Nucleosome assembly

3.2.6.1 Nucleosome assembly by salt dialysis

This protocol is adapted from (Luger et al., 1999). Salt dialysis is performed in bags/dialysis tubes (siliconised) of Spectra/membranes with a cutoff of MW 6000-8000 at 4°C. It was important to make sure the bag rotates freely during dialysis. The DNA and histones were mixed in presence of BSA and 2 M NaCl (High Salt). Low salt is pumped into the High salt buffer (while being stirred) o/n (16-20 hrs) at a speed of approx 2-3 ml pr ml. For every new batch of histone and/ or DNA a titration was performed. For example: for 60 µg DNA was titrated with following concentration of octamer to find the right ratio: 48 µg (0.8), 54 µg (0.9), 60 µg (1), 72 µg (1.2), 84 µg (1.4). In general a DNA-histone mix contains: 60 µg DNA, 50 µg BSA, Octamers (recombinant of native) for ratios: Check above, 2M NaCl final concentration and TE buffer to total volume of 500 µl.

To check the nucleosomes after dialysis, an MNase was perfomed. To 20 µl of nucleosomes 17 µl MNase mix (5 mM $CaCl_2$, 0.2 U MNase, EX100 buffer) was added by pipetting up and down constantly to mix well. After 20 seconds, 60 seconds and 120 seconds 12 µl was transferred to a tube ready prepared with 5 µl STOP buffer (4 % SDS and 100 mM EDTA). To each tube1 µl of Proteinase K (10 mg/ml) was added and the reaction incubated for 30 minutes at 37 °C. For precipitation 1 µl of glycogen, 16 µl NH_4Ac (7.5 M) and 80 µl EtOH (100%) was added. The mixture was incubated on ice for 30 min, centrifuged at max speed for 30 minutes at 4°C and washed with 70% EtOH. The pellets were very loose so care had to be taken when removing the EtOH. Dried pellet were redisolved in 10 µl 1x DNA loading dye and separated on an 1.3 % Agarose gel.

MNase Sigma: 500 U lyophilized vial was resuspended in 850 µl EX50 buffer and aliqoted in 50 µl aloqotes: Concentration is 50 U / µl (Boerhinger units).

3.2.7 Extract preparations

3.2.7.1 Preparation of chromatin assembly extract from *Drosophila* embryos

Drosophila embryo extract (DREX) assembly was performed as described (Becker and Wu, 1992).

3.2.7.2 Preparation of nuclear extract from *Drosophila* embryos

0-12 hours *Drosophila* embryos were collected over a period of 4-5 days. The embryos were washed and dechorienated. The dried embryos were weighed and resuspended in 1ml NUI buffer per gram embryos (15 mM Hepes-KOH pH 7.6, 10 mM NaCl, 5 mM $MgCl_2$, 0.1 mM EDTA, 0.5 mM EGTA, 350 mM Sucrose, 1 mM DTT, 0.2 mM PMSF). The embryos were homogenized 6 times with a Yamamoto homogenisator at 1000 rpm, 4°C. After filtering the homogenized embryos through a miracloth, the solution was centrifugated for 15 min at 8 krpm in a HB-4 rotor at 4°C. The nuclear pellet was resuspended in 1ml NUII buffer (15 mM Hepes pH 7.6, 110 mM NaCl, 5 mM $MgCl_2$, 0.1 mM EDTA pH 8)/gram embryos. To the nuclear mix, 1/10 volume of 4M $(NH_4)_2SO_4$ pH 7.9 was added and the tube inverted and rotated for 20 min at 4°C. After rotation, the sample was centrifueged for 1 hour in a Ti60 rotor at 35K, 4°C. The clear supernatant was saved, then 0.3g/g embryos of solid $(NH_4)_2SO_4$ was added during continuous stirring and then left for 10-15 min. The extract was centrifuged at 15K for 15 min in SS34, 4°C. After centrifugation the supernatant was discarded and the pellet could be stored at 4°C for 3-5 days. The pellet was resuspended by adding 190 µl of HEMG 40 (25 mM Hepes pH 7.6, 40 mM NaCl, 12.5 mM $MgCl_2$, 0.1 mM EDTA, 10% (v/v) glycerol, 1 mM DTT and 0.2 mM PMSF) per g embryo, and carefully douncing until everything was disolved. The nuclar extract was dialysed in 2 litres of HEMG 40, and followed by 3 subsequent dialysis in HEMG 100. Then the extract was centrifuged for 15 min at 15 K in SS34, 4°C, and flash frozen. Store at -70 °C.

3.2.7.3 Preparation of nuclear extract from SL2 cells

This protocol was obtained from A. Hocheimer. The stable SL2 cell lines were grown up to 1 liter (in two roller bottles) within 1 month. When harvesting the cells they were counted and the smell of the culture was checked. The cells were harvested at

2.5 K for 10 minutes in the Hearaeus centrifuge. Then the cells were collected in a 50 ml falcon and washed 3 times in cold 1x PBS (40 ml). The cell pellet got whiter. The packed cell volume (PCV) was estimated and the cells resuspended in 3x PCV ice cold Buffer A (10mM Hepes pH 7.6, 15 mM KCl, 2 mM $MgCl_2$, 0.1 mM EDTA, 1 mM DTT and freshly added complete protease inhibitors). After resuspending by pipetting (avoid air bubbles), the cells were left on ice for 30 min. Then the cells were dounced 15 times with a tight pestle, agian avoiding air bubble formation. Quickly thereafter, 1/10 of Buffer B (50 mM Hepes pH 7.6, 1 M KCl, 30 mM $MgCl_2$, 0.1 mM EDTA, 1 mM DTT and freshly added complete protease inhibitors) was added and the mixture was centrifuged for 15 min at 8 K (in SS34) at 4°C. The supernatant was removed and the packed nuclear pellet volume (PNV) estimated (approximately 1-1.5x PCV). A volume of 4x PNV Buffer A/B (9 volumes Buffer A and 1 volume Buffer B) was added and the nuclei were dounced 2 x. Afterwards 1/10 volume of 4M $(NH_4)_2SO_4$ pH 7.9 was added and the tube inverted and rotated for 20 min at 4°C. After rotation, the sample was centrifueged for 2 hours in a Ti45 rotor at 35K, 4°C. The clear supernatant was saved, then 0.3g/ml of solid $(NH_4)_2SO_4$ was added during continuous stirring and then left for 10-15 min. The extract was centrifuged at 15K for 15 min in SS34, 4°C. After centrifugation the supernatant was discarded and the pellet could be stored at 4°C for 3-5 days. For dissolving the pellet, 0.2-0.5 PCV volumes of Buffer C (25 mM Hepes pH 7.6, 150 mM KCl, 12.5 mM $MgCl_2$, 0.1 mM EDTA, 10% (v/v) glycerol, 1 mM DTT and freshly added complete protease inhibitors) was added and then dounced carefully. The nuclear extract was dialysed in 3x 1 liter (for a total of 3-4 hours) of Buffer C. Then the extract was centrifuged for 15 min at 15 K in SS34, 4°C, aliquoted in 50-100 µl aliquots, flash frozen. Store at -70 °C.

3.2.8 Histone methyltransferase assays

3.2.8.1 The "Spot and count" method

The total reaction volume was 40 µl. SU(VAR)3-9 reaction was diluted in H_2O, dG9a/mG9a in 12.5 mM Tris-HCl pH 8.8, 1 mM DTT, 50 mM NaCl, 50 ng/µl BSA, and 2.5 mM $MgCl_2$. To the reaction 1 µg H3 peptide, 2 µg histones, 4 µg octamers or 2 µg Nucleosomes were added together with 500 nCi S-Adenosyl (methyl ^3H)-L-methionin (25 µCi/ml) (Amersham). The reaction was started by addition of 100ng –

1 µg of HMTase. After incubation at 30 °C for 30 min to 2 hours, 30 µl of the reaction was spotted onto a p81 filter paper and washed 3 times 10 min in Na_2CO_3 pH 9.2. After drying the filter papers, the amount of ^{3}H-methyl groups was measured by adding Scintilization liquid and read in a Scintilator. The total amount of product that formed was measured in counts per minute (cpm)

3.2.8.2 HIM Assay measured by autoradiograph

The HIM assay was performed as described in 3.2.8.1. After incubation at 30 °C, the reaction was stopped by adding SDS PAGE loading buffer. The histones were separated on a 15% SDS PAGE and Coomassie stained. After destaining, the gel was incubated in Amplifyer (Amersham) for 30 min. The gel was dried and visualized by Autoradiography. The exposure time depended on the efficiency of the enzyme and ranged from over night till 2 weeks.

3.2.8.3 MALDI-TOF analysis of *in vitro* methylated histones

Methylation reactions were carried out as described above with 0.5 µg histone H3 or H4 and 40-250 µM S-Adenosylmethionine (New England BioLabs). Incubation ranged from 30 minutes to 2 hours. The reaction was stopped by addition of SDS PAGE loading buffer and the histones were separated by 15 % SDS PAGE. The Coomassie stained bands corresponding to H3 and H4 were excised and subjected to chemical modification (Propionylation) to derive free amino groups of lysine residues as described (Taipale et al., 2005). H3 and H4 were digested over night with 100 ng of sequencing-grade trypsin (Promega) in a total volume of 40 µl according to manufacturer`s protocol. In order to purify the methylated peptides from contaminating salts or acryl amide the peptide solution was passed over a pipette tip containing C18/SCX material (ZipTip, Millipore) and eluted 50% ACN/ 0.3 % TFA on to a target plate and 1 µl alpha-cyano4-hydroxycinnamic acid (Sigma) was added on top. The MALDI spectra were acquired and analyzed as described (Bonaldi et al., 2004). Reaction mix without enzyme was used for calibration. For quantification of the differentially methylated peptides, the corresponding peaks were monoisotoped and integrated. The total cluster area of each isoform of a single peptide was set to 100% and thereby the percentage of each peptide isoform could be calculated.

3.2.8.4 MALDI-TOF analysis of *in vitro* methylated histone H3 peptides

Methylation reactions were carried out as described above with 1 μg histone H3 peptide and 40 μM S-Adenosylmethionine (New England BioLabs). The reaction was stopped by adding 10% acetic acid. The peptides were purified from contaminating salts using C18 material and eluted as described above. The MALDI spectra were acquired and analyzed as described (Bonaldi et al., 2004).

3.2.8.5 SU(VAR)3-9 kinetics

Kinetic assays were carried out as described in 3.2.8.1 with varying the concentrations of SAM (5-60 μM) (H3 peptide 1 μg) or H3 molecules (0.82-3.1 μM) (SAM 40 μM). To avoid that the products (dimethylated peptide or S-adenosyl homocystein (SAH)) have inhibitory effects, the incubation was 1 or 5 minutes. The reaction was stopped by adding 10% acetic acid and spotted as described in 3.2.8.1.

The amount of product that formed was measured in counts per minute (cpm). The product ($^3HCH_3$) concentration (pmol) was calculated: ((cpm-Background) **x** total volume of reaction **x** S-Adenosyl (methyl ^{3}H)-L-methionin concentration (pmol) **x** dilution factor of SAM (S-Adenosyl (methyl ^{3}H)-L-methionin/ SAM) / (Spotted volume **x** total of S-Adenosyl (methyl ^{3}H)-L-methionin cpm).

To obtain values for K_m and V_{max}, a Lineweaver-Burk plot was generated. This equation was obtained by inverting the Michaelis-Menten equation:

$$V = V_{max} \mathbf{x} [S] / K_m + [S]$$

Where V is velocity, K_m is the Michaelis-Menten constant, V_{max} is the maximum reaction velocity and [S] is substrate concentration.

The y-intercept of the Lineweaver-Burk plot (Figure 3.2), is equivalent to the inverse of V_{max}. The x-intersept represent $-1/K_m$. The slope, as the equation shows, is Km/Vm.

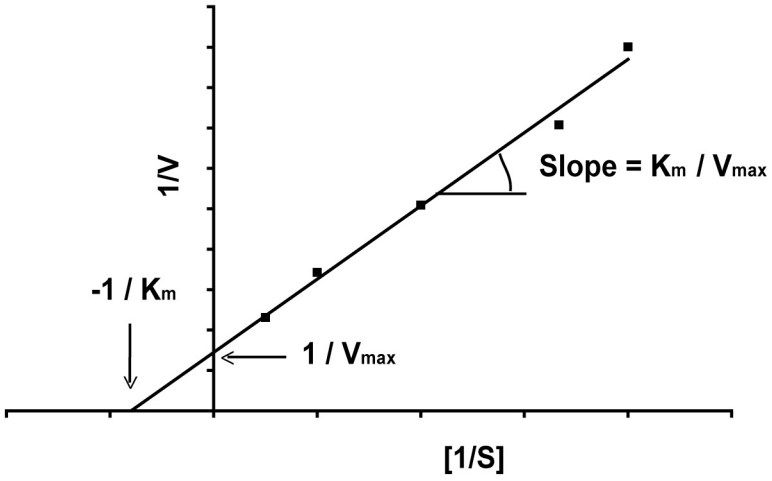

Figure 3.2 Lineveawer Burk plot

3.2.9 Pull-down assays

3.2.9.1 ACF and ACF1 pull-downs

ACF1-FLAG and ISWI were expressed in Sf9 cells as described previously (Eberharter et al., 2001) The ACF complex was generated by coexpression of ACF1-FLAG with untagged ISWI. Sf9 cells were suspended in BC500 containing 0.05% (v/v) NP40, 1 mM DTT, 0.2 mM PMSF and protease inhibitors. The cells incubated on ice were sonicated 2 times 15 seconds at 50% amplitude and centrifuged at maximum speed on a table top centrifuge for 30 minutes. A total of 500 ng of the expressed proteins were immobilized on M2 anti-FLAG agarose beads and blocked with 1 µg/µl BSA. Recombinant HP1 or HP1 mutants were added at a concentration of 1 µg of in a total volume of 200 µl BC100 containing 0.05% (v/v) NP40, 100 µg BSA and 5 µg ethidium bromide. After 30 minutes incubation at room temperature, the beads were washed 2 times in the same buffer without ethidium bromide and BSA, containing 100 mM NaCl and 4 times in a buffer containing 200 mM NaCl. The bound proteins were eluted with SDS sample buffer analyzed by SDS PAGE and transferred onto a PVDF membrane (Millipore).

3.2.9.2 Peptide pull-downs

Various H3 peptides (aa from to 1-19) were coupled to Thiolink beads (BioRad) and resuspended as 1:1 slurry in BC100. 20 µl of this slurry was incubated with 1 µg of

recombinant HP1 in a total volume of 200 µl BC100. The incubation was performed on a rotating wheel at 4 °C for 2 hrs. After washing three times with BC100 (containing 0.05% (v/v) NP40) for 10 minutes each, the bound protein was eluted with 30 µl acidic elution buffer (100 mM Glycine pH 2.5, 500 mM NaCl) for 20 min at 4 °C. The eluted proteins were analyzed by 12% SDS PAGE and Coomassie stained. 1 µg biotinylated H3 peptides: unmodified aa 1-21 (WT) and trimethylated at K9 aa 1-21 (H3K9tri) (Upstate) were mixed with 2 µg HP1 (WT or mutant proteins) and incubated for 1 hour at 4 ºC. Then 10 µl 1:1 slurry of paramagnetic beads (Dynal) (pre blocked in BSA) was added and incubated for 1 hour at 26 ºC in BC100 (containing 0.05% (v/v) NP40). The paramagnetic beads were concentrated on a Magnetic Concentrator (Dynal) and washed once with BC100 + 0.05% (v/v) NP40 and twice with BC200 + 0.05% (v/v) NP40. Bound proteins were separated on a 12% SDS PAGE and Coomassie stained.

3.2.9.3 GST pull-down

Gluthathione Sepharose 4B (Pharmasia Biothech) beads were washed in 10 ml NTEN 100 buffer (20 mM Tris HCl pH 8, 100 mM NaCl, 1mM EDTA, 0.5 % NP40, 1 mM DTT and protease inhibitors) and a 1:1 slurry prepared.

Ca 2-3 ug of GST fusion protein or GST control was added to 30 µl Gluthathione Sepharose 4B beads in a total volume of 530 µl NTEN 100. The samples were rotated at 4 °C for 45-60 minutes and washed 4 times with 1 ml NTEN100 buffer and 1 time with NTEN200 buffer. Then the beads were pre-blocked with 10 ul BSA (10 mg/ml) and 90 ul NTEN100 buffer, rotating at 4 °C for 30 min. The beads were washed 2 times 1ml NTEN100 buffer and 2- 5 µl of S^{35} labeled *in vitro* translated protein was added plus: 10 ul BSA (10 mg/ml), 0.5 ul Ethidium bromide (10 mg/ml) in a total volume 200 ul NTEN100. The reaction was rotated for 30 minutes at 20 °C. After incubation, the reaction was washed 4 times with NTEN100 and 2 times NTEN200. Then 2X loading dye buffer was added and the sample was boiled for 5 min. The reactions were separated on SDS PAGE, Comassie stained and destained. Afterwards the gel was incubated in Amplifyer (Amersham) for 30 min. The gel was dried and visualized by Autoradiography.

3.2.10 Chromatin on paramagnetic beads assays

3.2.10.1 Preparation of biotinylated DNA

This protocol was optimized for digest of 500 µg PAI61 DNA where the end product was a biotinylated insert and vector (which will not bind to paramagnetic streptavidin beads). The first digestion in a total volume of (500 µg PAI61, 75 µl BSA (1 µg/µl), 75 µl Buffer 1 (10x NEB), 10 µl SacI (NEB) and x µl ddH_2O) was incubated reaction for 3 hours in a 37 °C incubator (the one where we keep bacterial plates) to avoid too much evaporation. Each hour, the tube was vortexed shortly. Then 0.5 ul was checked on a 0.8% agarose gel, loading 300 ng of undigested vector as control. It was important that all the plasmid was linearized. For digestion 2 a total volume of 800 µl was prepared containing: (Digestion 1, 5 µl BSA (1 µg/µl), 10 µl XbaI (NEB), 5 µl Buffer 2 (10x NEB), 7.5 µl NaCl (5M) and 22.5 µl ddH_2O). The mixture was incubated for 3 hours in a 37 °C incubator as described above.1 µl was kept for agarose gel later. After the incubation, the DNA was precipitated by addition of 85 µl NaOAc (3M) pH 5.2 and 600 µl Isopropanol and then mixed and incubated on ice for 30 min. The tube was centrifuged for 30 minutes at max speed at 4 °C. The pellet was washed once with 70% Ethanol and dried. The pellet was carefully redisolved by adding 252.9 µl ddH2O.For the Biotinylation reaction the 252.9 µl DNA was mixed with 30 µl Buffer 3 (NEB), 0.8 µl dCTP (100 mM), 0.8 µl dGTP (100 mM), 3 µl biotinylated dUTP (1 mM), 7.5 µl biotinylated dATP (0.4 mM) and 5 µl Klenow (Roche 2U/µl) and incubated for 2 hours at 37 °C. To inactivate the Klenow enzyme, the reaction was incubated at 70 °C for 20 minutes. It was important to remove the biotinylated nucleotides, which was not incorporated. This was done by using 3 sepharose G50 columns (Roche). The columns were centrifuged once for 1 minute at 1000 rpm in a Beckman centrifuge for falcons. The flow through and the sample was carefully transferred to the top (in the middle) of the columns, and 100 µl of the biotinylation reaction. Then the columns were centrifuged for 2 minutes at 1000 rpm and the flow through was collected. The last digestion was performed in a total volume of 750 µl: X µl Biotinylated DNA, 45 µl Buffer 3 (NEB), 75 µl BSA (1 µg/µl), X µl ddH_2O and 10 µl PstI). It was incubated for 3 hours or ON at 37 °C. The restriction was checked on a 0.8 % agarose gel. Store Biot. DNA at -20 °C.

3.2.10.2 Chromatin assembly on immobilized DNA and micrococcal nuclease digestion

The assembly reactions for immobilized DNA were performed according to (Sandaltzopoulos et al., 1994). In short; 2 µg DNA was immobilized to 0.8 mg paramagnetic streptavidin beads (Dynal) and after extensive washing blocked for 30 minutes at 4 °C with BSA (1 µg/µl) in EX50 (10 mM HEPES pH 7.6, 50 mM NaCl, 1.5 mM $MgCl_2$, 0.5 mM EGTA, 10% (v/v) glycerol, 0.2 mM PMSF, 1 mM DTT) containing 0.05% (v/v) NP40 before assembly. Recombinant or H3K9Me histone octamers (2 µg) were mixed with the assembly extract at time point zero together with an ATP regenerating system (3 mM ATP, 30 mM creatine phosphate, 10 µg creatine kinase pr. ml, 3 mM $MgCl_2$, and 1 mM DTT). HP1 was then added at a concentration of 2 µg (8.3 ng/µl) and the reaction left rotating for 6 hours at 26 ºC. For circular DNA: 900 ng of circular DNA, 12 µl McNAP (30 mM $MgCl_2$, 10 mM DTT, 30 mM ATP, 300 mM creatine phosphate, 10 µg/ml creatine phosphate kinase) and varying amounts of *Drosophila* embryo extract (20-70 µl, depending on extract). The volume was increased with EX-80 to a final volume of 120 µl. Micrococcal nuclease (MNase) digestions was performed as described in (Sandaltzopoulos et al., 1994) with 30 Boehringer Units of MNase (Sigma). For MNase digestion of chromatin assembled onto circular DNA, 150 Boerhringer Units were used. The 123 bp ladder (Invitrogen) was used as a size marker.

3.2.10.2 Immobilization of salt assembled chromatin and HP1 binding assay

Salt assembled recombinant or H3K9Me chromatin (1 µg) was immobilized onto 0.4 mg paramagnetic streptavidin beads (Dynal) in TEN100 buffer containing 0.05% (v/v) NP40 and 250 ng/µl BSA. After 2 hours rotation at 4 °C the chromatin on paramagnetic beads was concentrated on a Magnetic concentrator (Dynal) and washed once with EX100 buffer containing 0.05% (v/v) NP40. Chromatin was immediately resuspended in total volume of 80 µl containing 60 µl Ex100 0.05% (v/v) NP40, BSA (100 ng/µl), ATP regenerating system (3 mM ATP, 30 mM creatine phosphate, 10 µg creatine kinase pr. ml, 3 mM $MgCl_2$, and 1 mM DTT) and 2 µg (25 ng/µl) HP1. Purified SU(VAR3-9) WT and Δ213 was added in a total concentration of 100 ng. FLAG eluted ACF at a total concentration of 50 ng was added in presence

of ATP or absence of ATP. *Drosophila* assembly extract was added at a concentration of 100 µg in presence of ATP or non-hydrolysable ATP-gamma-S analog.

3.2.10.3 Chromatin washes and HP1 detection

Assembled chromatin was concentrated on a Magnetic Concentrator (Dynal) and supernatant removed. The chromatin beads were washed once with 100 µl EX100 (10 mM HEPES pH 7.6, 100 mM NaCl, 1.5 mM $MgCl_2$, 0.5 mM EGTA, 10% (v/v) glycerol, 0.2 mM PMSF, 1 mM DTT) containing 0.05% (v/v) NP40 and twice with same buffer containing 200 mM NaCl. The bound proteins were eluted with 10 µl SDS loading dye and separated on a 15% SDS PAGE. The proteins on the gel smaller than 20 kDa including the histones were subjected to Coomassie staining, whereas the rest of the gel was transferred to PVDF (Millipore). Blots were probed with HP1 polyclonal rabbit antibody and incubated with fluorescently labeled secondary antibodies, and visualized using the Odyssey system (Li-Cor) as described above.

3.2.11 Bioinformatics tools

Database searches were performed using BLASTP, TBLASTN and PSI-BLAST (http://www.ncbi.nlm.nih.gov/BLAST/). Amino acid sequence alignments were created using TCoffee (http://www.ch.embnet.org/software/TCoffee.html) with default parameters. To change the output file of alignment Boxshade was used (http://www.ch.embnet.org/software/BOX_form.html). *Drosophila* gene and protein sequences were obtained from: flybase (http://flybase.bio.indiana.edu/)

3.2.12 Size exclusion column chromatography and molar mass determination

Recombinant HP1 (128 µM/ 145 µg) was loaded onto a Superdex 200 column (HR 10/30, Amersham Pharmacia). The column was run isocratically with 0.2 ml/min in BC200 buffer for 1.4 CV. 0.5 ml fractions were collected. To determine the absolute molar mass directly the eluant was monitored using a multiangle laser light scatter detector (Wyatt Technology Corporation), and a UV detector. The molar mass was determined using the Astra software supplied by Wyatt Technology Corporation.

3.2.13 Cross-linking assay

Bacterially expressed HP1 (0,17 µM) was cross-linked using 250 µM DTSSP (3,3`-Dithiobis(sulfosuccinimidylpropionate)) (Pierce) and incubated on ice for 2 hours in BC100 buffer without DTT. The reaction was stopped by adding 100 mM Tris and boiled in SDS-PAGE sample buffer with or without β- mercaptoethanol. After separation by electrophoresis, the proteins were transferred to a PVDF membrane (Millipore).

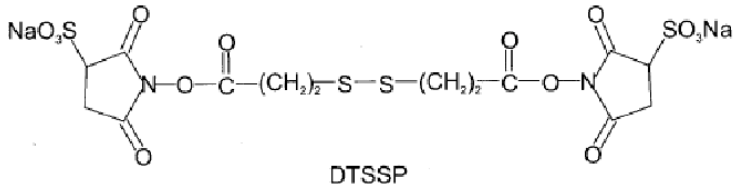

Figure 3.3 Chemical structure of DTSSP

4. Results

4.1 The N-terminus of *Drosophila* SU(VAR)3-9 mediates dimerisation and regulates its methyltransferase activity

The SET domain was initially identified as an evolutionary conserved domain in SU(VAR)3-9, Enhancer of Zeste and Trithorax (Jenuwein et al., 1998; Tschiersch et al., 1994). It was shown to be the catalytic domain responsible for histone lysine methylation in the human SU(VAR)3-9 homolog SUV39H1 (Rea et al., 2000). A myc-tagged SU(VAR)3-9, isolated from *Drosophila* embryo extracts, was shown to methylate H3K9 in our lab (Czermin et al., 2001). A recombinant N-terminally truncated SU(VAR)3-9 was shown to methylate the N-terminus of H3 (Schotta et al., 2002). The aim was to characterize a recombinant SU(VAR)3-9 and its enzymatic properties *in vitro.*

4.1.1 Purification of recombinant SU(VAR)3-9

Full length SU(VAR)3-9 was cloned into pET15b by B. Czermin modified with an N-terminal 6x his-tag. His-SU(VAR)3-9 was soluble when expressed in bacteria. It was purified over Talon beads and eluted with 100 mM imidazol. The expressed protein had the expected molar mass of 74 kDa (Figure 4.1).

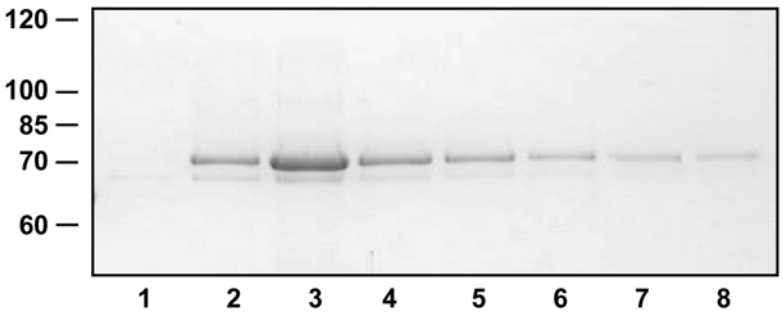

Figure 4.1 Purification of recombinant *Drosophila* SU(VAR)3-9. Elution of recombinant, His-tagged SU(VAR)3-9 eluted with 100 mM Imidazol from Talon beads. 15 µl of the first eight fractions (lanes 1-8) were loaded onto a SDS-10% polyacrylamid-gel-electrophoresis (PAGE) and stained with Comassie blue R250.

4.1.2 Full length SU(VAR)3-9 is an active histone methyltransferase

Recombinant his-SU(VAR)3-9 was incubated with histone molecules in the presence of S-Adenosyl [methyl-^{3}H] methionine (SAM) to test for histone methyltransferase activity. His-SU(VAR)3-9 methylated H3 molecules better in a mixture of free histones than in reconstituted nucleosomes (Figure 4.2.A). In order to confirm the specificity of SU(VAR)3-9 was incubated with various H3 peptides (amino acids 1-19) pre-modified at lysine 4 and 9. The methyltranferase (MTase) activity was inhibited when lysine 9 was either dimethylated or acetylated (Figure 4.2.B).

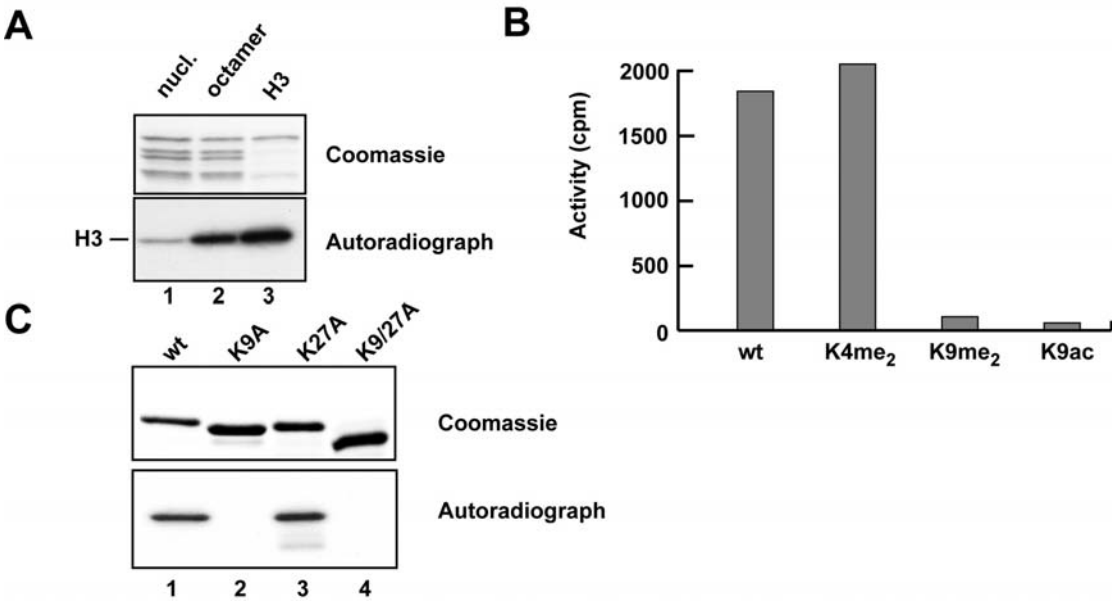

Figure 4.2 The substrate specificity of recombinant SU(VAR)3-9 (A) *In vitro* SU(VAR)3-9 methylation reactions using 600 ng potein, 0.17 μM S-Adenosyl [methyl-^{3}H] methionine and different histone substrates. Nucleosomal arrays (2 μg) (lane 1) were reconstituted on pBS(KS) (Strategene) by salt dialysis using recombinant octamers (lane 2), which were reconstituted from equimolar amounts of histones produced in *E.coli* and purified by gel-filtration chromatography. Lane 3 corresponds to 0.5 μg H3. The reaction products were then loaded onto a SDS-18% polyacrylamide (PAA) gel and the gel was stained with Coomassie blue R250, dried, and exposed to a X-ray film (autoradiograph) for 24h. **(B)** Peptides containing the first 19 amino acids of H3 (1 μg) were methylated by 600 ng of recombinant SU(VAR)3-9 in the presence of 0.17 μM S-Adenosyl [methyl-^{3}H] methionine. Unmodified peptide (wt), a peptide dimethylated at K4 (K4Me2) or at K9 (K9Me2) and a peptide acetylated at K9 (K9Ac) was used as substrates. Incorporated radioactivity was measured by a filter-binding assay. **(C)** *In vitro* methylation reaction using either wt recombinant H3 (lane 1), H3 mutated at lysine 9 (lane 2), at lysine 27 (lane 3) or at both sites (lane 4). Histones were methylated by recombinant SU(VAR)3-9 in the presence of radioactive SAM, separated by SDS-PAGE and analyzed by autoradiography.

The amino acids surrounding lysine 9 in the H3-tail (QTARKS) are similar to the amino acids surrounding lysine 27 (KAARKS). Other H3K9 HMTases have been shown to also methylate H3K27, such as mG9a (Tachibana et al., 2001; Tachibana et al., 2002) and E(Z) (Czermin et al., 2002). Therefore H3 molecules with a mutation of lysine 9 or lysine 27 to alanine or both were used for *in vitro* methylation assays. No activity toward H3 molecules mutated at K9 was detected and it could therefore be concluded that recombinant SU(VAR)3-9 was a K9 specific HMTase (Figure 4.2.C). This was in good agreement with the finding of Czermin in this lab (Czermin et al., 2002) and *in vivo* data from *SU(VAR)3-9* null mutant flies, where the H3K9 methylation at the chromocenter was strongly reduced (Schotta et al., 2002).

Lysines exist in mono-, di- or trimethylated states. Studies with specific antibodies against different H3K9 methylated states revealed that there is an enrichment of mono- and dimethylation in silent euchromatic regions, whereas trimethylation was enriched in pericentric heterochromatin within the mammalian genome (Peters et al., 2003; Rice et al., 2003). In *Drosophila melanogaster,* immunostainings of *SU(VAR)3-9* null mutant salivary glands chromosomes revealed that SU(VAR)3-9 catalyses mono- to dimethylation in the chromocenter and trimethylation in the chromocenter core (Ebert et al., 2006; Ebert et al., 2004; Schotta et al., 2002). To analyze the processivity of recombinant SU(VAR)3-9 was incubated with H3 peptides and a time course was analyzed by MALDI-TOF (Figure 4.3). Because one methyl group is 14 daltons, the mass shift for mono-, di- and trimethylation will be 14, 28, and 42 daltons respectively. For the reaction with unmodified peptide, after 5 minutes about 20% of the peptides were monomethylated and no dimethylation could be observed (Figure 4.3.A). The dimethylated peptide appears after 10 minutes when almost 50% of all the peptide was monomethylated. Almost all of the unmethylated peptides were converted into either mono- or dimethylated form after 80 minutes. No significant trimethylation could be observed under these conditions. In the time course with the monomethylated peptide as a substrate, a similar kinetic as with the unmodified peptide (Figure 4.3.B) was observed. After 5 minutes, about 20% of the monomethylated peptides were converted into dimethylated peptide. There was no significant trimethylation observed after 80 minutes, although almost all the monomethylated peptide was converted into dimethylated form.

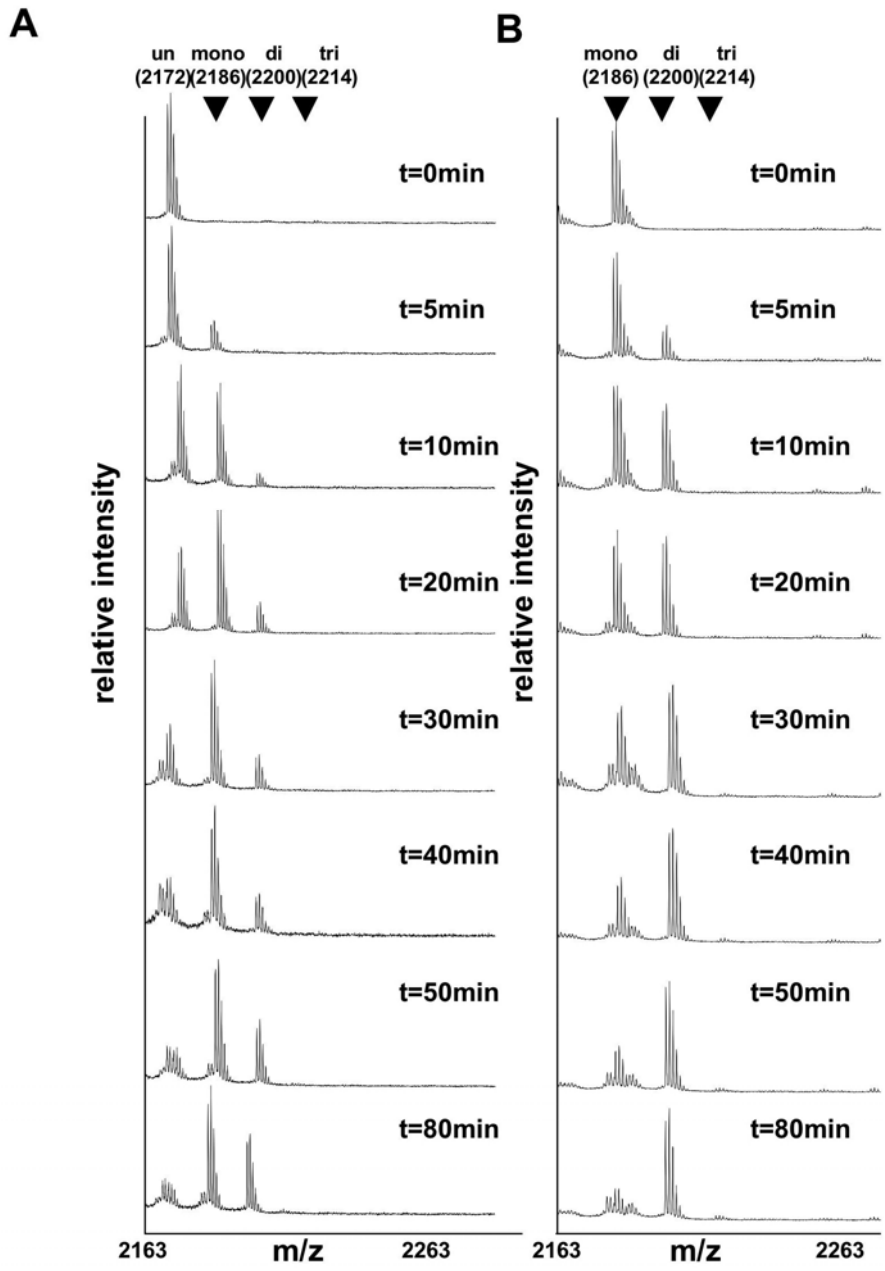

Figure 4.3 MALDI analysis of SU(VAR)3-9 reaction products. A MALDI-TOF analysis of a time-course reaction using 600 ng SU(VAR)3-9, 40 μM SAM and 1 μg of a H3 peptide, which was unmethylated **(A)**, or monomethylated **(B)** at K9. The methylation reaction was stopped at different time points and reaction products analyzed by MALDI-TOF.

To exclude the possibility that SU(VAR)3-9 needs a premodified peptide to be able to convert it into trimethylated form, a H3K9 dimethylated peptide was used as substrate (Figure 4.4). No significant trimethylation was observed, even after long incubation time.

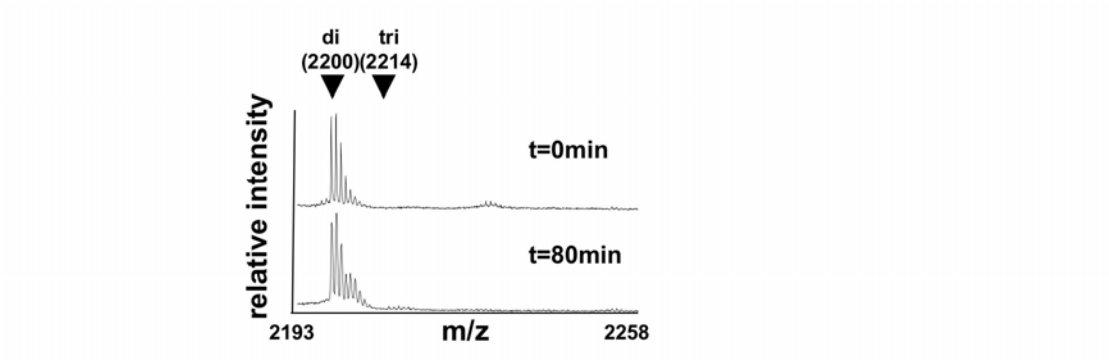

Figure 4.4 SU(VAR)3-9 has very poor activity towards a H3 peptide methylated at K9. The same methylation reaction as described in Figure 4.3, using the H3 peptide dimethylated at K9. Only 0 min and 80 min time points are shown.

The same time course as described in Figure 4.3 and 4.4 was monitored in the presence of 40 μM SAM and S-Adenosyl [methyl-^{3}H] methionine (0.4% of total SAM) to determine the linearity of product formation with time (Figure 4.5). The reactions were measured by a filter-binding assay. For unmodified (wt) and K9 monomethylated H3 peptide, the reaction remained linear for 60 minutes with a similar slope. The formation of trimethylated with K9 dimethylated peptide as substrate was not significant.

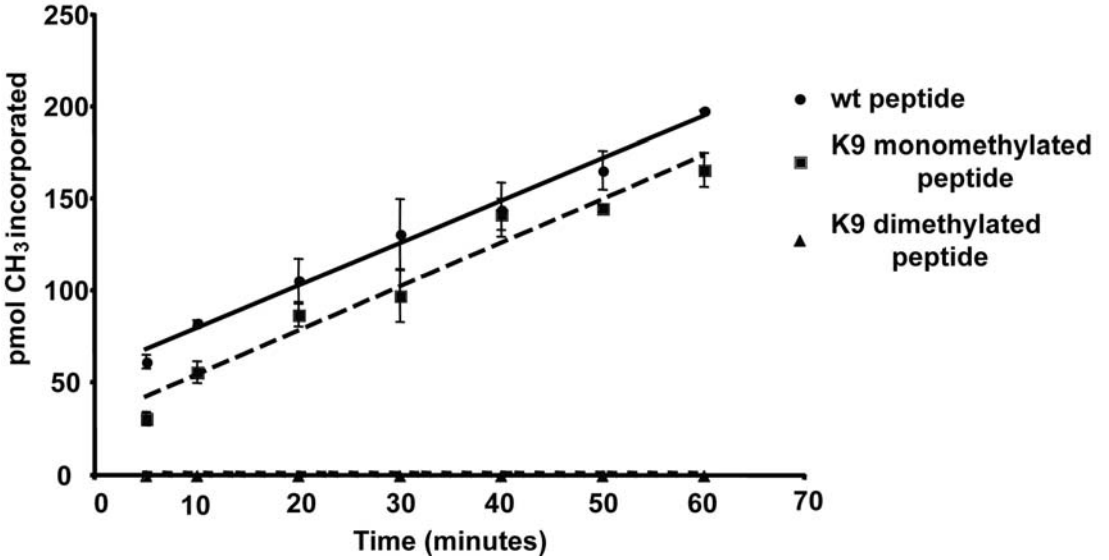

Figure 4.5 Linearity of methylation reaction by recombinant SU(VAR)3-9. A time course of a methylation reaction as described in Figure 4.3 with total 40 μM SAM (0.17 μM S-Adenosyl [methyl-^{3}H] methionine), measured by a filter-binding assay.

4.1.3 SU(VAR)3-9 adds three methyl groups onto H3 lysine 9

T. Bonaldi developed a method to analyze the modifications of full length H3 by MALDI-TOF (Bonaldi et al., 2004). To determine the methylation status on histone H3, recombinant SU(VAR)3-9 was incubated with histone octamer (Figure 4.6). Histone H3 was excised from a SDS-15% PAA gel and subjected to chemical modification of the lysines (Figure 4.6.A). The lysines that were unmodified or monomethylated, were propionylated (a shift of 56 daltons). Di- and trimethylated lysines were not chemically modified and had a lower mass than the unmodified peptide (Figure 4.6.B). Under these conditions a significant amount of di- (54 %) and trimethylation (33%) were observed.

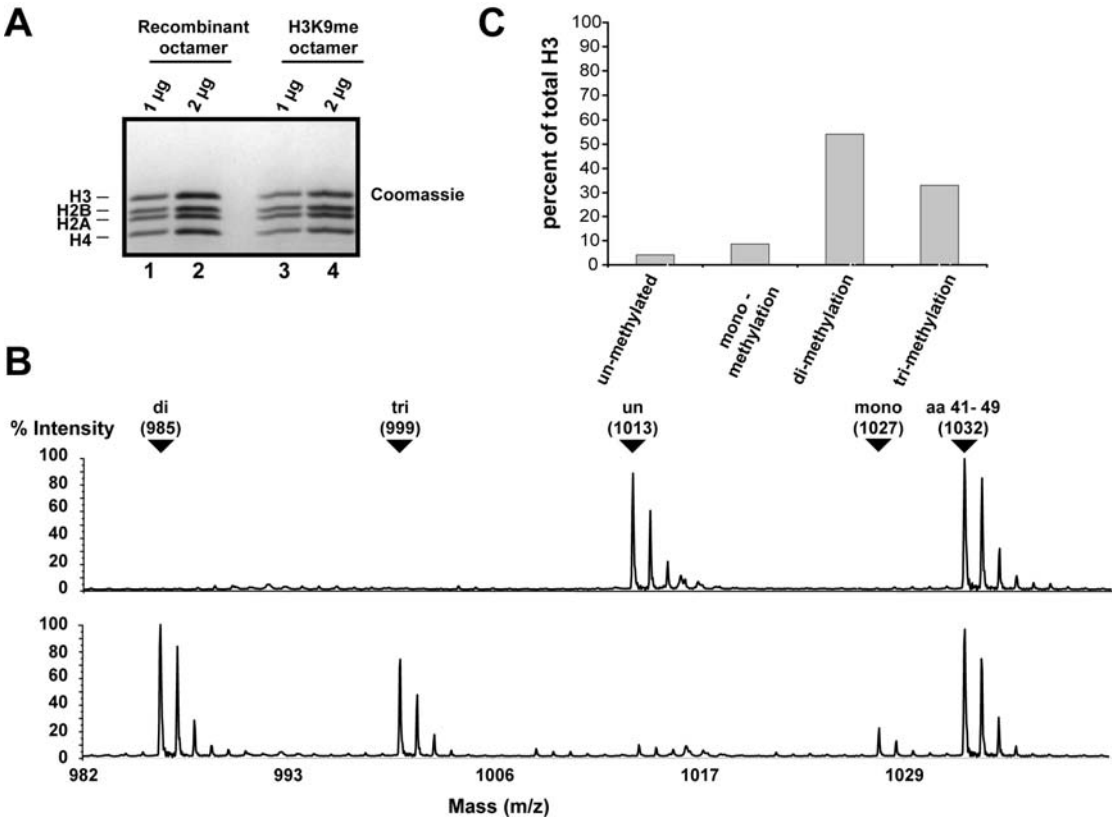

Figure 4.6. SU(VAR)3-9 adds three methyl groups onto histone 3 K9 (**A**) 300 ng SU(VAR)3-9 was incubated with 4 µg of recombinant histone octamer and 40 µM SAM for 40 minutes. SU(VAR)3-9, SAM and the reaction product S-Adenosyl homocysteine (SAH) was purified away by using a cation resin. To the left is a Coomassie blue stained SDS-15% PAA gel of reconstituted recombinant- (lane 1 and 2) and purified H3K9 methylated octamers (lane 3 and 4). **(B)** A MALDI TOF analysis of H3 peptide 9-17 from recombinant H3 (top) and H3 methylated by SU(VAR)3-9 at K9 (bottom). As an internal standard H3 peptide 41-49 is shown. Unmodified, mono-, di-, and trimethylated peptides with corresponding mass are labeled with arrows. **(C)** A quantification of the MALDI TOF analysis in (B) is shown in the upper right panel.

4.1.4 Deletion of the N-terminus of SU(VAR)3-9 impaired its activity

In order to investigate the influence of the N-terminus on the SU(VAR)3-9 enzymatic activity, various his-tagged constructs were expressed in bacteria and purified over talon beads (Figure 7.A and B).

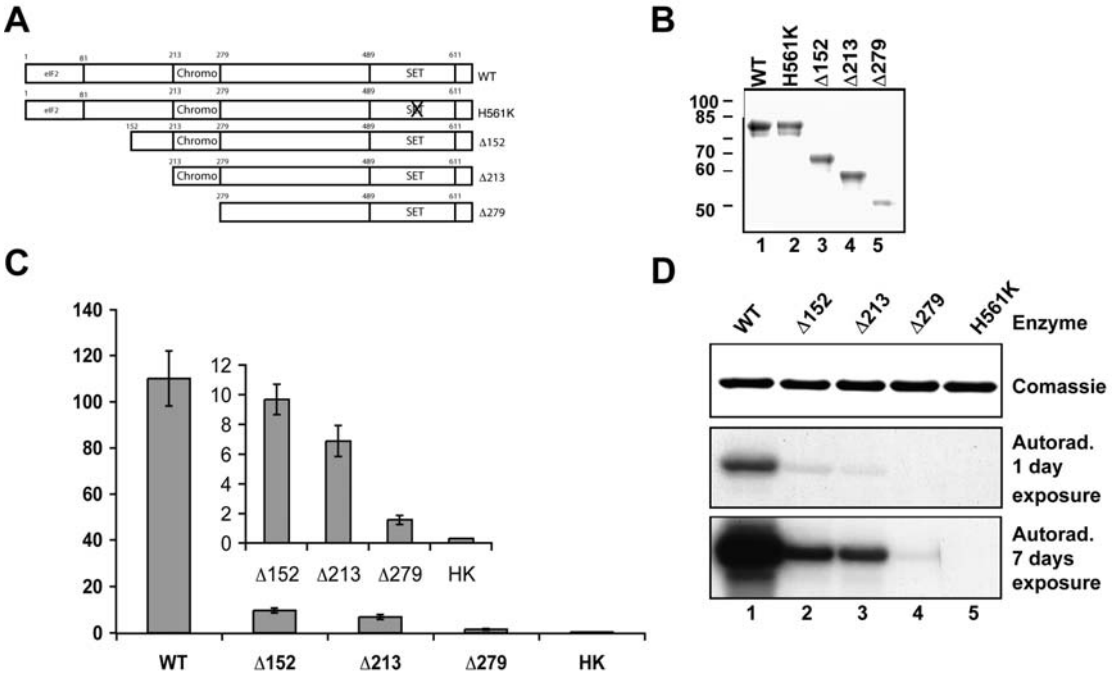

Figure 4.7 Expression and purification of SU(VAR)3-9 mutants. (A) Scheme of SU(VAR)3-9 mutants generated and expressed in bacteria. **(B)** Coomassie-stained gel of Talon purified SU(VAR)3-9 mutant proteins. **(C)** Comparison of HMT activity of SU(VAR)3-9 wild type and mutants on a H3 peptide. For a better comparison, the inset of panel C shows the activities of the N-terminal deletions and a point mutation within the SET domain. **(D)** To compare different activities on intact H3 molecules, an autoradiograph of a 1-day (mid panel) and a 7-day (bottom panel) exposure is shown. Coomassie stained H3 is shown in top panel.

In *Drosophila* SU(VAR)3-9 mRNA is generated by alternative splicing of the translation initiation factor (eIF2) RNA leading to an additional 81 amino acids at the N-terminus of the protein, which are common between eIF2 and SU(VAR)3-9. A point mutation within the conserved SET domain of SUV39H1 (H324K), abolished enzymatic activity (Rea et al., 2000). The same amino acid was mutated in SU(VAR)3-9 (H561K) and the activity abolished (Figure 4.7.C and D). The N-terminal SU(VAR)3-9 deletion mutants (Δ152 and Δ213) were still able to methylate H3 peptides and histone, but the specific methyltransferase activity was more than 10-fold lower than for the full-length SU(VAR)3-9. If the chromo domain was deleted

(Δ279), the histone methyltransferase activity declined even more despite the presence of the SET domain. The conclusion was therefore that the N-terminus and the chromo domain of SU(VAR)3-9 were utilized for catalytic activity.

4.1.5 Kinetic parameters of recombinant SU(VAR)3-9 full length and Δ213

In order to define the kinetic parameters of SU(VAR)3-9, the enzyme-catalyzed reaction at steady state was analyzed. Initial rate means the rate of product formation (in this case methylation of H3) was observed in a reaction with an enzyme (SU(VAR)3-9) and substrates. The reaction rate depends on the concentration of the substrates SAM and H3. To avoid that the products; dimethylated peptide or S-Adenosyl homocysteine (SAH) have inhibitory effects, the incubation was 1 or 5 minutes when less than 5% of product were formed (see Figure 4.3). It was verified that SAH at low concentration did not have significant inhibitory effects (data not shown and Figure 4.13). The kinetic parameters K_m and V_{max} were obtained (for calculations see Methods 3.2). K_{cat} is the number of molecules turned over in time (seconds or hours) and can be calculated from V_{max}. Recombinant SU(VAR)3-9 had a V_{max} of 95.2 nmol min^{-1} mg $protein^{-1}$, K_{cat} of 0.11 s^{-1} and a K_m[SAM] of 25.9 μM (Figure 4.8.A). The N-terminal mutant Δ213, which was shown to have 16 fold lower methyltransferase activity then full-length, had approximately the same K_m[SAM] value (24.6 μM). The substrate affinity for SAM was not reduced when deleting the N-terminus, but the K_{cat} was 22 fold reduced to 0.005 s^{-1}.

Several attempts were made to determine the K_m for histone H3 or H3 peptide. Figure 4.8.B shows the rate of methylation catalyzed by Δ213 measured over a range of histone H3 concentrations. The double reciprocal plot showed a nonlinear relationship between 1/V and 1/H3 that became nearly vertical at high concentrations. Because the plot was nonlinear, it was impossible to give a precise estimate of K_m. High concentrations of H3 have an inhibitory effect on SU(VAR)3-9, this was also shown for SUV39H1 (Chin et al., 2006). At lower concentrations of H3, the variability between assays gave a Km[H3] from 1.2 – 15.7 μM (data not shown). Histones are known to be “sticky” proteins, and at low concentrations they stick to pipette tips and

the walls of the eppendorf tube. Even if there was BSA present in the reactions, it was not enough to prevent "stickiness" of H3 and thereby variability within the assays.

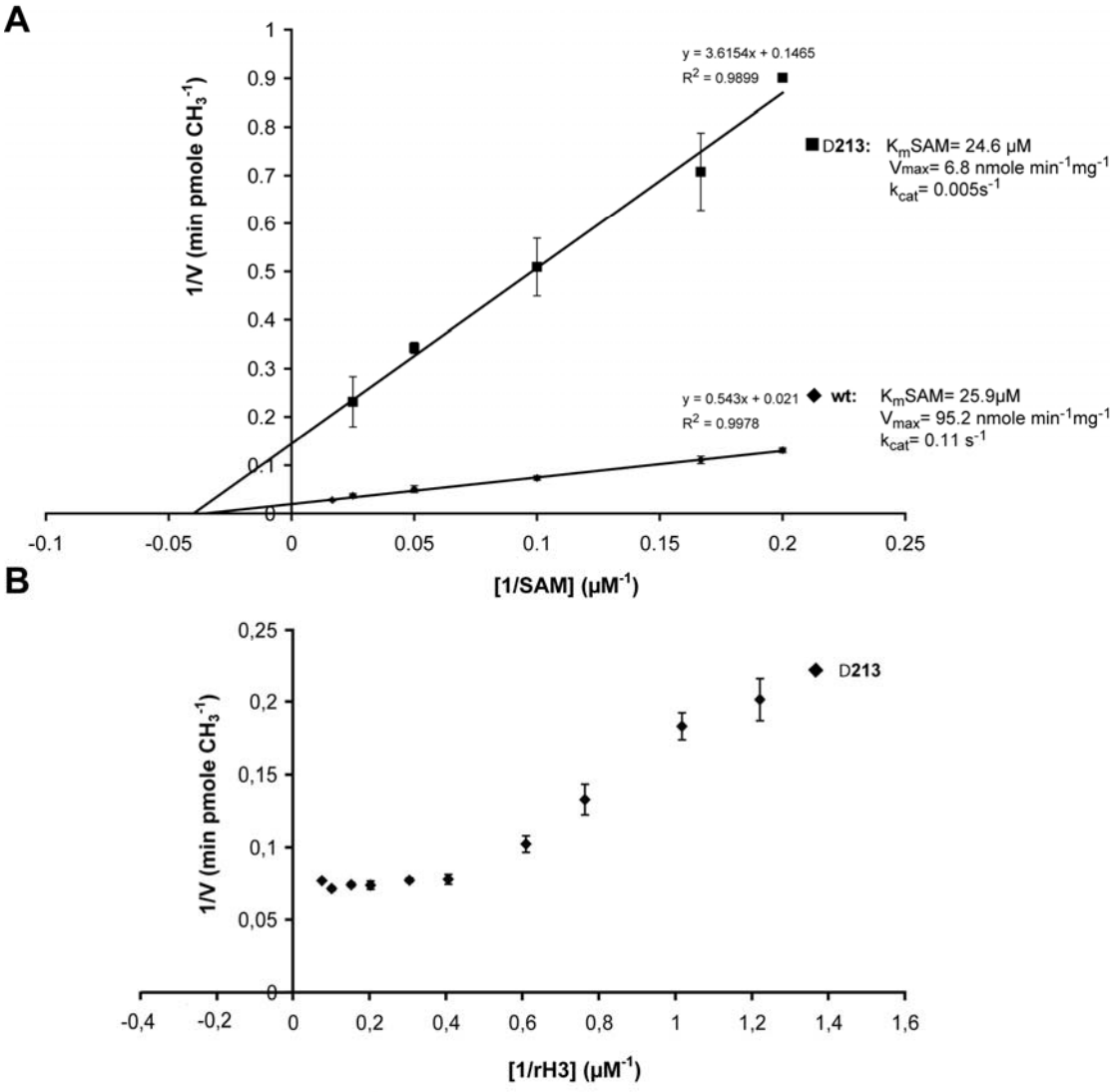

Figure 4.8 Kinetic parameters for recombinant SU(VAR)3-9 full length and Δ213. **(A)** Lineweaver- Burk plot. A comparison of *in vitro* methylation reactions with SU(VAR)3-9 wt (0.5 µg) or a N-terminally truncated protein (Δ213; 1 µg). By changing the concentrations of SAM (5, 6, 10, 20, 40 µM) and keeping H3 peptide (aa 1-19) concentrations saturating and constant (11.5 µM), K_m for SAM could be determined. Reaction time was 1 minute. Methyl group incorporation was measured by filter binding; 0.17 µM of the total SAM was S-Adenosyl [methyl-^{3}H] methionine. **(B)** A double reciprocal plot for SU(VAR)3-9 Δ213 (1 µg) with variable recombinant H3 concentrations (0.82, 0.98, 1.31, 1.64, 2.46, 3.28, 4.92, 6.55, 9.83, 13.1 µM) and SAM 40 µM (0.17 µM of the total SAM was S-Adenosyl). Reaction time was 5 minutes. A total of 800 ng of BSA was present in the reaction to block the histone H3 from sticking to the side of the tube during the incubation. Methyl group incorporation was measured by filter binding.

Full-length SU(VAR)3-9 had higher turnover numbers than other SET domain containing enzymes *in vitro* (Table 4.1). The turnover rates of mG9a and pea Rubisco large subunit methyltransferase (LSMT) was approximately 4.5 and 2.5 fold lower than SU(VAR)3-9 respectively (Patnaik et al., 2004; Trievel et al., 2002). SU(VAR)3-9 Δ213 had a similar turnover rate as wild type SUV39H1 and SET7/9 (Chin et al., 2005; Trievel et al., 2002). Both SU(VAR)3-9 and SUV39H1 had higher K_m[SAM] values than mG9a and hSET7/9, suggesting that the methylation of H3 in heterochromatin may be regulated by the local concentration of SAM *in vivo.*

Table 4.1 Comparison of steady-state kinetic parameters for SU(VAR)3-9 and other SET domain containing methyltransferases

Enzyme	Substrate	K_{cat} (h^{-1})	K_m [SAM] (μM)	Ref.
SU(VAR)3-9WT	H3 (1-19)	396	25.9	tw
SU(VAR)3-9Δ213	H3 (1-19)	18	24.6	tw
SUV39H1	H3 (1-18)	12 ± 0.5	12.3 ± 0.6	1
SUV39H1	rH3	8 ± 0.8	6 ± 0.6	1
mG9afl	H3 (1-18)	88 ± 4	1.8 ± 0.2	2
mG9afl	rH3	46 ± 1	2.65 ± 0.2	2
human SET7/9	rH3	14 ± 1	6.0 ± 1.4	3
pea LSMT[b]	rubisco	153 ± 9[a]	6.0 ± 1.3	3
Clr4	H3(1-15)	36 ± 1		4

H3 (1-19) is the first 19 aminoacids of the N-terminus of histone H3, rH3 is recombinant histone H3, (tw) is this work. The references are: (1) (Chin et al., 2006), (2) (Patnaik et al., 2004), and (3) (Trievel et al., 2002) (4) (Collazo et al., 2005). The K_{cat} is displayed in $hours^{-1}$. [a] average of K_{cat} for SAM and Rubisco. [b] pea Rubisco large subunit methyltransferase.

4.1.6 The N-terminus of SU(VAR)3-9 is important for dimerisation and activity *in vitro*

Multimeric enzymes often show an increased catalytic efficiency expressed in substrate molecules converted per molecule of enzyme (Bheemanaik et al., 2003; Salminen et al., 1999). The substantial high catalytic efficiency of full-length SU(VAR)3-9, may be due to conformational change or an association of monomeric enzymes into multimers. Therefore a relationship between the velocity of the reaction and the concentration of full-length SU(VAR)3-9 was determined (Figure 4.9).

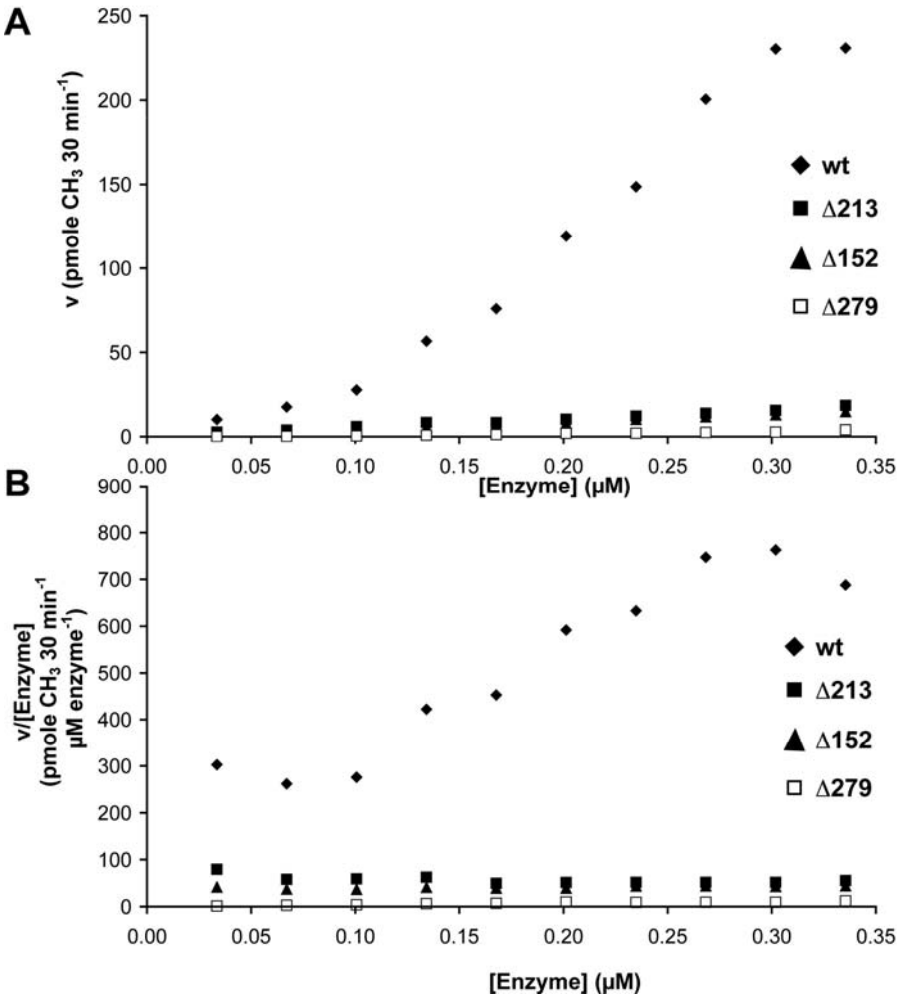

Figure 4.9 A concentration-dependent increase of SU(VAR)3-9 activity. (A) Different concentrations of wt and N-terminally truncated SU(VAR)3-9 were incubated with 1 µg H3 peptide and 20 µM SAM for 30 min. After stopping the reaction, the amount of incorporated radioactivity was measured and plotted against the concentration of enzyme. **(B)** The ratio of the incorporated radioactivity to the concentration of enzyme present was replotted against the enzyme concentration to determine the increase in specific activity.

When the rate of methyl peptide formation was plotted against corresponding enzyme concentration, a nonlinear curve was obtained. However plotting the same relation for the N-terminal deletion mutants (Δ152, Δ213 and Δ279) only showed a linear dependence of methyltransferase activity on enzyme concentration. Replotting the number of methyl groups incorporated per enzyme molecule revealed a steady increase of activity until specific activity reached a plateau at a concentration of 0.3 µM for full-length SU(VAR)3-9 (Figure 4.9.B). This increase was not observed for the N-terminal deletion mutants. It can therefore be concluded that SU(VAR)3-9 can form multimers which have a higher catalytic activity than monomers.

Formation of multimers were concentration dependent, and at 0.3 μM virtually all SU(VAR)3-9 molecules exists as multimers.

In order to test the hypothesis that SU(VAR)3-9 has a multimeric conformation, the molar mass of the recombinant protein was analyzed by gel filtration chromatography and density gradient centrifugation (Figure 4.10). Full-length SU(VAR)3-9 eluted with an apparent molar mass of 160 kDa on a Superdex 200 column (Figure 4.10.A top panel). This was indicative of a dimer. The N-terminal mutation Δ213 eluted with an apparent molar mass of 60 kDa, corresponding to monomeric form (Figure 4.10.A bottom panel). To further confirm the dimerisation of SU(VAR)3-9, the recombinant protein was loaded onto a 5-20% sucrose gradient. The full-length protein was found in fractions corresponding to higher molar mass than Δ213. However under denaturing conditions the two SU(VAR)3-9 proteins behaves identical. The BSA and Δ213 has an apparent shift of one fraction in presence of urea. From these data it can be concluded that full-length SU(VAR)3-9 was a dimer *in vitro.*

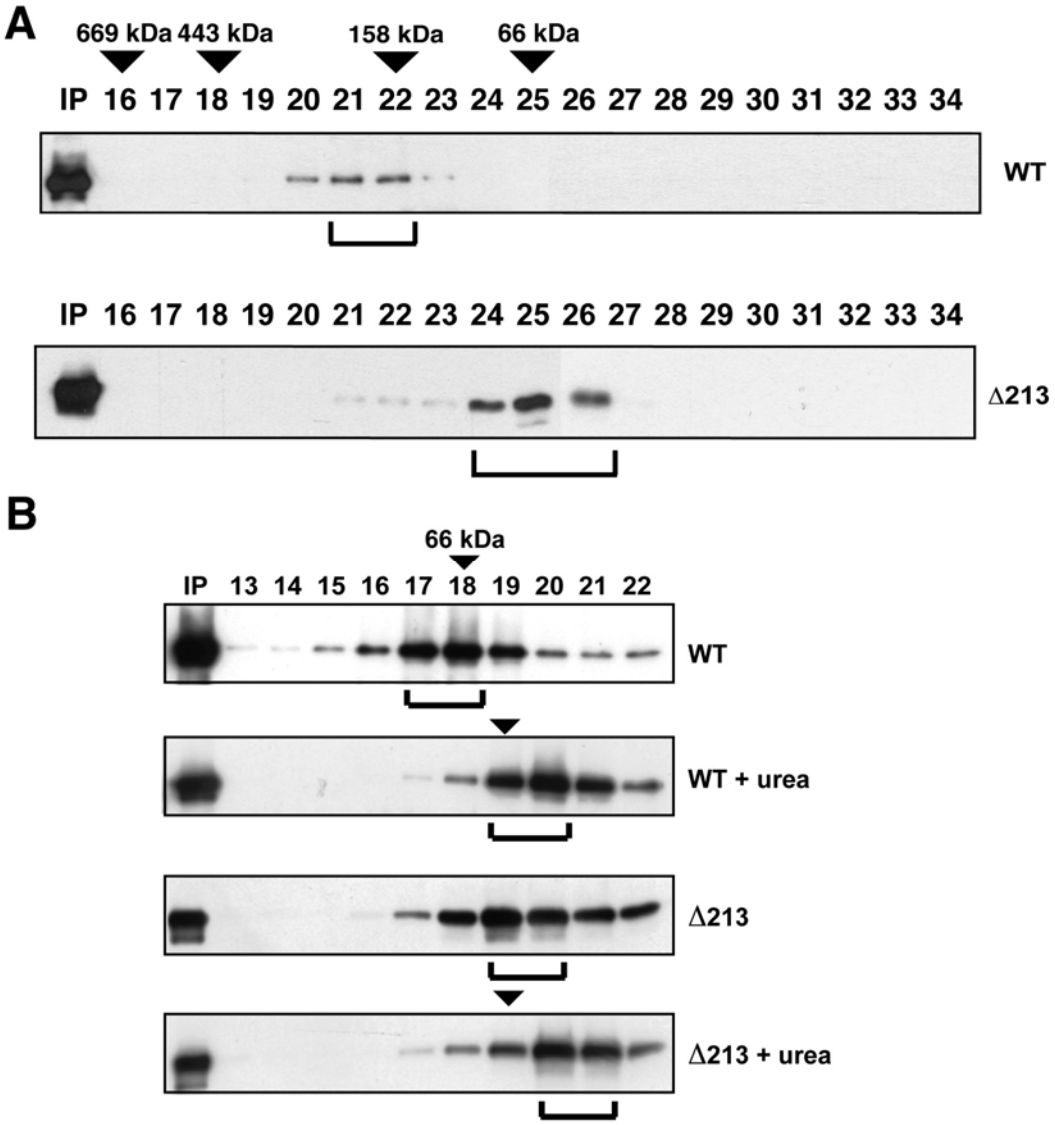

Figure 4.10 Molar mass determination of SU(VAR)3-9. **(A)** Elution profiles of wt SU(VAR)3-9 (top panels) and the N-terminal deletion construct Δ213 (bottom panels). Retention of the molar mass standards is indicated at the top. **(B)** Profile of a 5-20% sucrose gradient in the presence (panels 2 and 4) or absence of 3 M urea (panels 1 and 3). The position of the 66-kDa marker protein is indicated as a black triangle at the top of each gel. Note the slight shift (1 fraction) of the 66-kDa marker and the Δ213 protein in panel 4, which is due to the presence of urea in the buffer. In comparison there is a significant shift in case of the wt protein (>3 fractions) in panel 2.

4.1.7 Mapping of the interaction domain of SU(VAR)3-9

Deletion of the first 152 amino acids lead to a 90% loss of activity compared to full length SU(VAR)3-9 (shown in chapter 4.1.4). Therefore the first 152 amino acids were expressed as a GST fusion protein and used it for pull-down experiments. HP1 has been shown to interact with the N-terminus of SU(VAR)3-9 and SUV39H1 (Schotta et al., 2002; Yamamoto and Sonoda, 2003). This was confirmed biochemically by pull-down (Figure 4.11.B). To map the interaction responsible for SU(VAR)3-9 dimerisation, *in vitro* translated constructs (Figure 4.11.A) were incubated with the bound fusion protein. Full-length SU(VAR)3-9 interacted efficiently with the first 152 amino acids, suggesting a role for this amino acid stretch in inter- or intramolecular interaction (Figure 4.11.C). Four N-terminal deletion constructs were no longer able to interact with the first 152 amino acids (Figure 4.11.C and D). The interaction domain was mapped to amino acids 152-213. This suggests that the interaction of the first 152 amino acids with amino acids 152-213 can mediate an intra as well as intermolecular interaction.

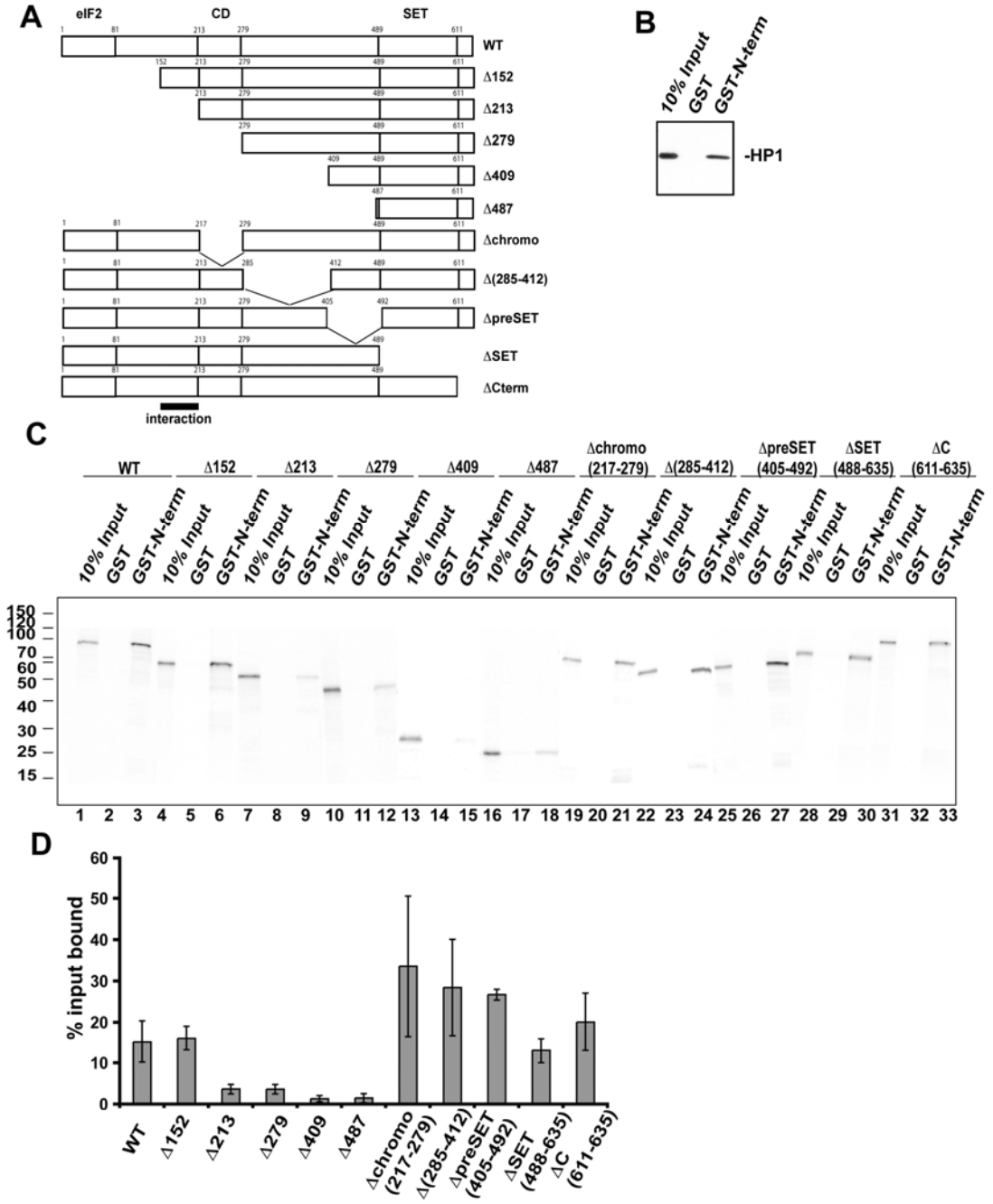

Figure 4.11 Mapping of the dimerisation domain of SU(VAR)3-9. **(A)** SU(VAR)3-9 constructs used for *in vitro* translation. **(B)** GST pull down with bacterially expressed HP1a. HP1a was detected by Western blotting using a monoclonal antibody against HP1 (C1A9). **(C)** GST and GST-SU(VAR)3-9 (1-152) pull down with *in vitro* translated SU(VAR)3-9 constructs. SU(VAR)3-9 constructs was detected by autoradiography. **(D)** Quantification of the binding affinities of the various SU(VAR)3-9 proteins. Error bars represent the variations of at least three different experiments.

To confirm the interaction domain described above, a GST fusion protein consisting of amino acids 152-213 were used to performed pull-down assays with SU(VAR)3-9 full length and N-terminal truncations. As expected, the SU(VAR)3-9 fusion protein

(aa 152-213) was able to interact with full length protein, but deletion of the first 152 amino acids weakened the interaction (Figure 4.12). SU(VAR)3-9 interacts with itself via two domains in the N-terminus.

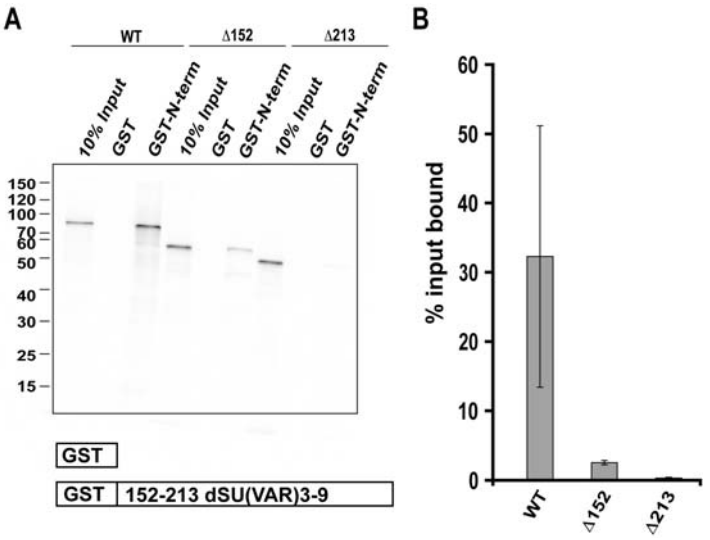

Figure 4.12 The dimerisation domain of SU(VAR3-9 lies within the first 213 amino acids (A) GST pull downs with a SU(VAR)3-9 GST fusion protein covering amino acids 152-213 and two N-terminally truncated versions of SU(VAR)3-9. **(B)** Corresponding quantification of the pull down with SU(VAR)3-9 proteins. Error bars represent the variations of at least three different experiments.

4.2 Inhibitors of SU(VAR)3-9 HMTase activity

The end product of an enzymatic reaction may inhibit the enzyme if it has enough affinity for the active site to block the binding of the substrate molecule. In both figure 4.2.B and 4.4 it was shown that the dimethylated H3K9 peptide inhibited the histone methyltransferase activity of SU(VAR)3-9. When SU(VAR)3-9 transfers a methylgroup from SAM towards H3K9 the end product formed is S-Adenosyl homocysteine (SAH). SAH was shown to be a competitive inhibitor of SAM for mG9a (Patnaik et al., 2004) and for SUV39H1 (Chin et al., 2006). Therefore it was necessary to investigate the inhibition of SAH for SU(VAR)3-9 *in vitro*. The concentration of unmodified H3 peptide and SAM was held constant with different fixed amounts of SAH added. Although SAH inhibited the histone methyltransferase activity of SU(VAR)3-9, it was not a very strong inhibitor. The half maximal inhibitory concentration, represents the concentration of an inhibitor that is required for 50% inhibition (IC_{50}) had a value for SAH around 40 μM. Adenosylornithine (AO), is a metabolite of *Streptomyces griseolus*. It was a strong competitive

inhibitor of methyltransferases which use SAM as the methyl group donor to yield methylated products such as 5-methylcytosine or N^6-methyl adenosine on DNA and RNA (Barbes et al., 1990). AO was incubated with SU(VAR)3-9 as described for SAH. AO had weaker inhibitory effect on SU(VAR)3-9 than SAH with an IC_{50} of 100 μM (Figure 4.13.A).

In order to identify specific inhibitors of SU(VAR)3-9, D. Greiner screened a small natural compound library provided by Hans-Knöll institute in Jena. One of the strongest specific inhibitors identified was a mycotoxin, called chaetocin (Greiner et al., 2005). Chaetocin inhibited SU(VAR)3-9 with an apparent IC_{50} of 0.6 μM. Chaetocin also had a strong inhibitory effect on other K9 histone methyltransferases such as SUV39H1, G9a and DIM5 (Greiner et al., 2005). In order to test the effect of chaetocin over time, a time course with Δ213 and two different concentration of chaetocin was performed (Figure 4.13.B). To avoid the possibility that chaetocin had an inhibitory effect on dimerisation of full-length SU(VAR)3-9 Δ213 was used in the assays. The time course was analyzed by MALDI-TOF, and the relative values of differentially modified H3 peptides (amino acids 1-19) were calculated according to total input concentration. The reaction of Δ213 was linear for at least 10 minutes in absence of chaetocin. After 20 minutes most peptides were dimethylated. Adding 1.5 μM chaetocin to the reaction, fewer methylgroups were transferred. After 20 minutes reaction, the amount of methylated peptides were the same as for 5 minutes incubation without chaetocin. Chaetocin at a concentration of 4.5 μM inhibited the histone methyltransferase activity of SU(VAR)3-9 after 5 minutes, and addition of methylgroups were no longer detected. Chaetocin was shown to be a competitive inhibitor of SAM (Greiner et al., 2005) and higher concentrations blocks the active site and thereby the binding of SAM for enzymatic activity.

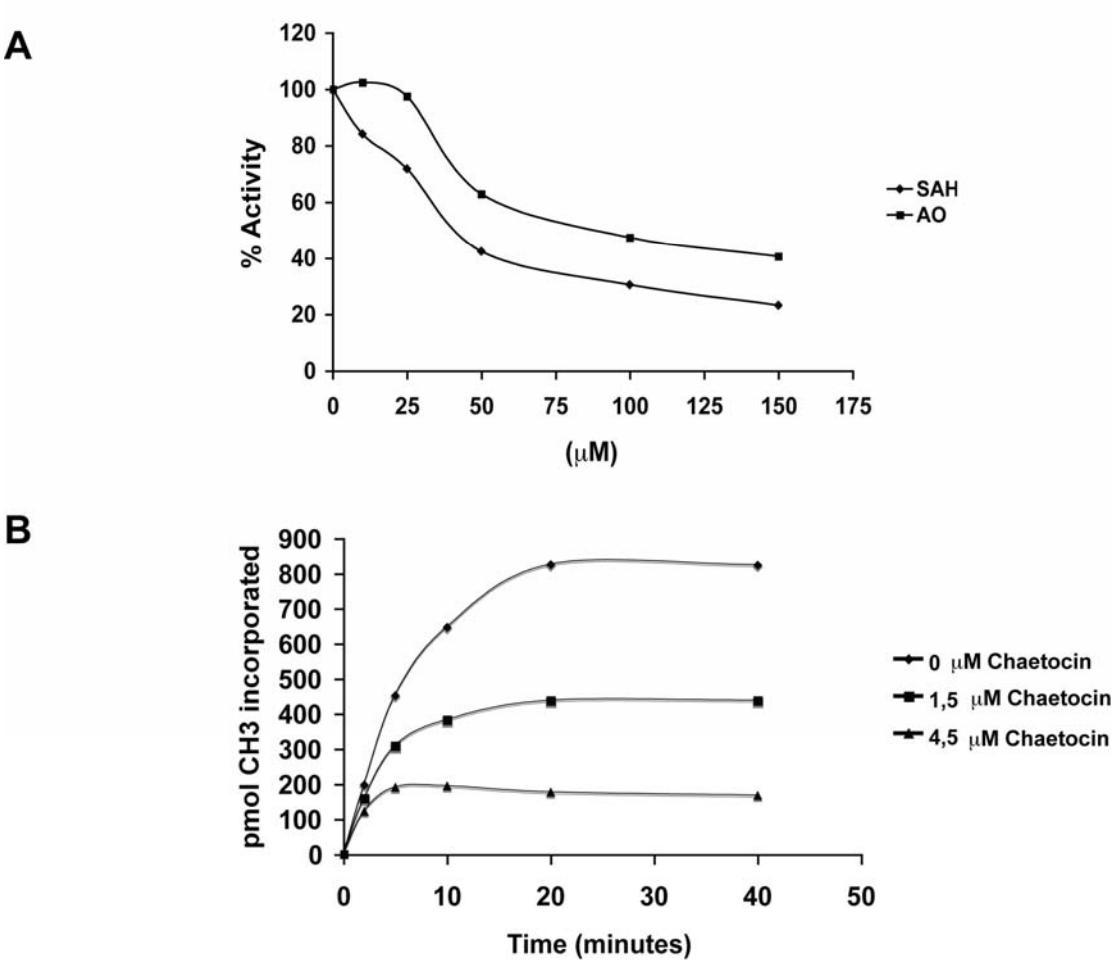

Figure 4.13 ***In vitro*** **inhibition of SU(VAR)3-9 (A)** Inhibition curves of SU(VAR)3-9 with increasing amounts of S-(5`-adenosyl)-L -homocysteine (SAH) and Adenosylornithine (AO). 250 ng of SU(VAR)3-9 was incubated with a H3 peptide monomethylated at K9 in the presence of 20 μM SAM and 0.17 μM S-Adenosyl [methyl-^{3}H] methionine for 30 minutes. The activity was measured by a filter-binding assay. The y-axis represents % activity where reaction without inhibitor set to 100%. **(B)** A time course of SU(VAR)3-9 Δ213 in the presence of the specific inhibitor chaetocin at 0, 1.5 and 4.5 μM. One μg of SU(VAR)3-9 Δ213 was incubated with a H3 peptide (1 μg, unmodified) in the presence of 40 μM SAM. The reaction was stopped by adding 10% acetic acid and analyzed by MALDI-TOF.

4.1 Characterization of monoclonal antibodies directed against SU(VAR)3-9

SU(VAR)3-9 specific rabbit antisera were generated by G. Schotta (Schotta et al., 2002). However, the rabbit antibody was not able to immunoprecipitate SU(VAR)3-9. Therefore a new attempt was made to generate monoclonal rat antibodies that recognize SU(VAR)3-9. The monoclonal antibodies were raised against his-tagged Δ213, purified over three consecutive columns as described in the thesis of B. Czermin (chapter 4.2.2) (Figure 4.14.A). E. Kremmer tested hybridoma cell supernatants in ELISA and got 9 positive. These were further analyzed by Western blotting on recombinant SU(VAR)3-9, *Drosophila* embryo nuclear extract (0-12 h) and on total cell extract from *Drosophila* SL2 cells (data not shown). All monoclonal antibodies gave a specific signal for recombinant protein, however two antibodies gave a signal in the nuclear extract with an expected size of the endogenous SU(VAR)3-9.

4.3.1 Recognition of recombinant SU(VAR)3-9 and mapping of epitopes

To map the epitopes of rat 6C9 and 3D9, recombinant expressed his-tagged proteins (Figure 4.7.A and B) and *in vitro* translated proteins (Figure 4.11.A) were used. As a control to confirm that it was not the his-tag that was recognized, Δ152 expressed with a C-terminal intein tag and purified having its intein tag cleaved off was used. Another control was a mock *in vitro* translation. The epitope of 6C9 antibody was mapped to a region within amino acids 285 and 492. This region contains a cysteine rich region also called the pre-SET domain. This domain is similar between SU(VAR)3-9 and SUV39H (See Figure 2.7) and has been shown to be important for histone methyltransferase activity. On the other hand 3D9 mapped to the SET domain. It would therefore be expected to give higher background because it may recognize other SET domain proteins.

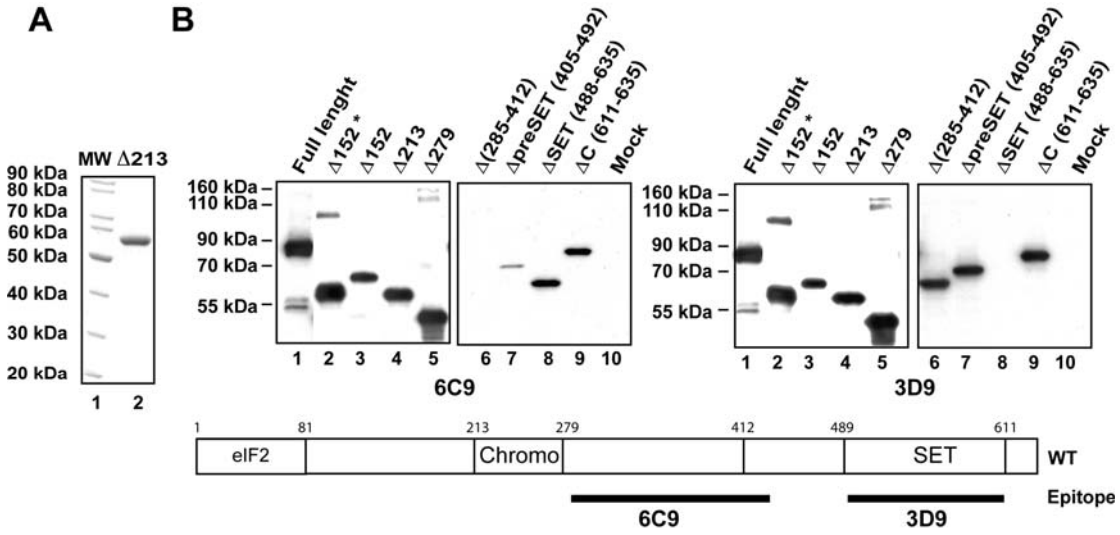

Figure 4.14 (A) A Coomassie stained SDS-12% PAA gel of his-tagged SU(VAR)3-9 Δ213 purified over 3 consecutive columns. E. Kremmer used this protein for generation of rat monoclonal antibodies. **(B)** Mapping of the epitope of the two selected monoclonal antibodies: α-6C9 (also denoted SUV4) and α-3D9 (also denoted SUV5). Lanes 1-5 is bacterially expressed SU(VAR)3-9 proteins (50 ng), his purified except Asterisks indicates Δ152 which had an intein tag cleaved off. Lanes 6-9 is cold *in vitro* translated (5 µl) SU(VAR)3-9 proteins. Lane 10 is a mock IVT.

4.3.2 Immunoprecipitation of recombinant SU(VAR)3-9

In order to test if 6C9 and 3D9 were able to immunoprecipitate SU(VAR)3-9, the supernatants were incubated with *in vitro* translated full-length protein. As a control a α-myc (9E10) antibody was used. Both antibodies were able to immunoprecipitate SU(VAR)3-9.

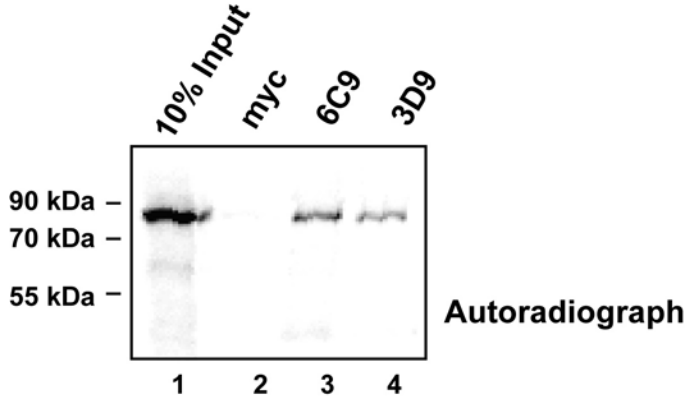

Figure 4.15 The monoclonal antibodies can immunoprecipitate SU(VAR)3-9 . Immunoprecipitation of *in vitro* translated SU(VAR)3-9 (5 µl). Monoclonal antibodies 6C9 and 3D9 were used with α-myc (9E10) as control. SU(VAR)3-9 was detected by autoradiograpy.

4.3.3 Recognition of endogenous SU(VAR)3-9

E. Kremmer purified 6C9 and 3D9 over protein A beads. Different dilutions were tested on western blots with recombinant SU(VAR)3-9 and *Drosophila* embryo nuclear extract. Purified 6C9 seemed to be very specific, but recognized the endogenous SU(VAR)3-9 protein very weakly. On the other hand, 3D9 gave a high background and detected a protein of approximately 80 kDa at much lower antibody-dilutions.

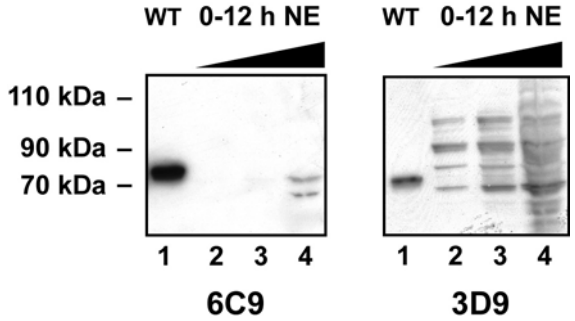

Figure 4.16 Western blots of 6C9 and 3D9. Test of monoclonal antibodies on recombinant SU(VAR)3-9 (25 ng) and 10, 20 and 100 µg of 0-12 hour *Drosophila* Nuclear Extract. The purified monoclonal antibodies and used in concentrations 1:250 for 6C9 (exposure time: 1 hour) and 1:1000 for 3D9 (exposure time: 1 minute).

The 3D9 antibody gave high background, and it was therefore necessary to confirm its specificity. A western blot of *Drosophila* SL2 cells treated with RNA interference (RNAi) against SU(VAR)3-9 showed reduced levels of SU(VAR)3-9 compared to GST RNAi treated cells when probed with polyclonal SU(VAR)3-9 antibody (Figure 4.17.A). Probing the same western blot with 3D9 antibody showed no difference between SU(VAR)3-9 and GST RNAi. To further confirm this result, embryos from *SU(VAR)3-9^{06}* null flies (Schotta et al., 2002) were blotted together with embryos from wild-type strain used, *yw (yellow "white")* (Figure 4.17.B). Although the lanes were smeary due to presence of DNA in the samples, no SU(VAR)3-9 protein could be detected in the null flies. No change in protein levels was detected for the 3D9 antibody. It was not clear whether endogenous SU(VAR)3-9 was detected, or if the signal was masked by other SET domain proteins detected by 3D9 antibody.

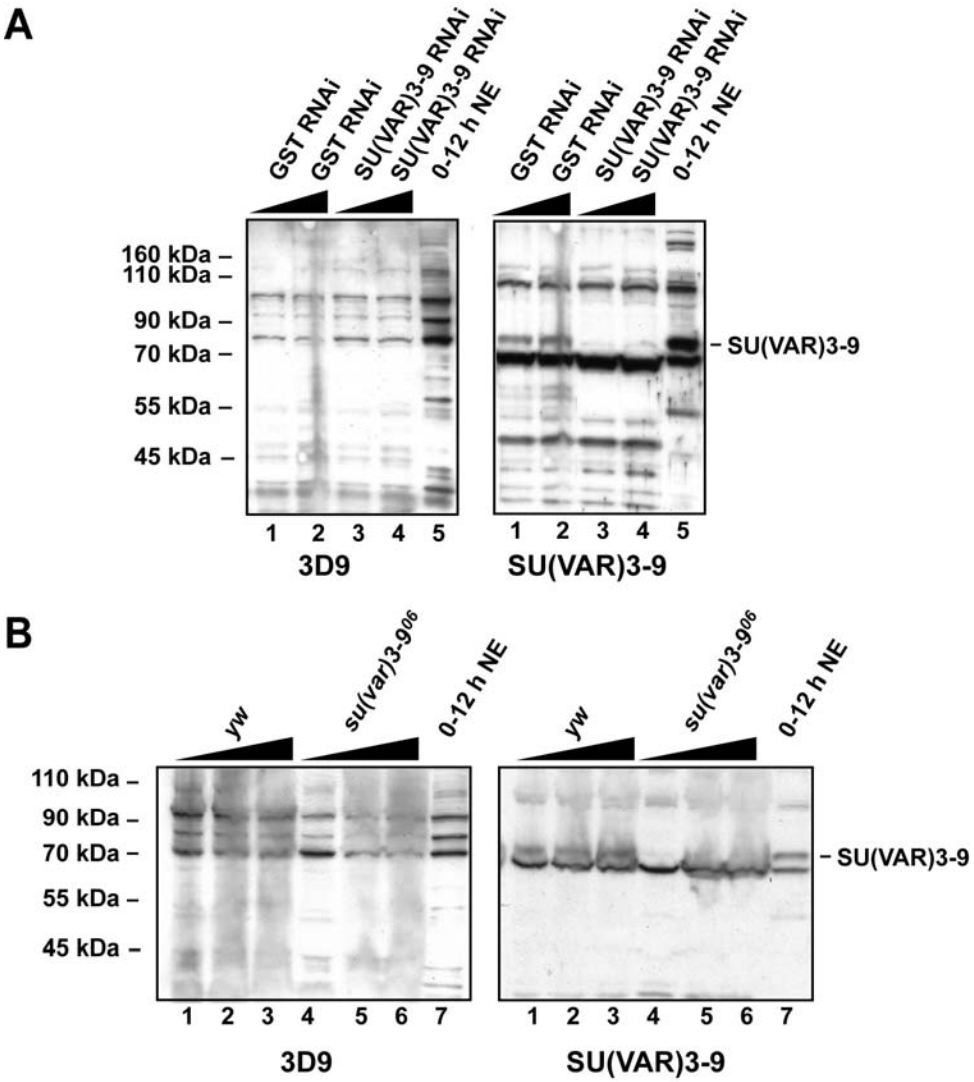

Figure 4.17 SU(VAR)3-9 monoclonal antibody 6C9 do not specifically recognize the endogenous protein. (A) Antibody α-6C9 tested on SL2 cells subjected to GST or SU(VAR)3-9 RNAi for 9 days. As a loading control 20 µg of *Drosophila* Nuclear Extract was used. The western blot was stripped and reprobed with SU(VAR)3-9 polyclonal antibody (a gift from G. Reuter) **(B)** Test of 6C9 on *Drosophila* dechorionated embryos from *yellow white* (as control) and *SU(VAR)3-9*^{06}flies (flies provided by C. Chioda). The embryos were boiled in SDS loading dye. The western blot was stripped and reprobed with the *Drosophila* SU(VAR)3-9 polyclonal antibody.

4.4 *In vitro* characterization of dG9a HMTase activity

SU(VAR)3-9 was shown to be the main H3K9 methyltransferase in *Drosophila*. Immunostaining of *Su(var)3-9*^{06} null mutant embryos there is still detectable amounts of K9 dimethyl is only slightly reduced in other regions than the chromocenter (Ebert et al., 2004; Schotta et al., 2003b). In mammalian cells mG9a was found to be a euchromatic H3K9 methyltransferase (Esteve et al., 2005; Peters et al., 2003; Rice et al., 2003) but a *Drosophila* G9a was not yet characterized. In collaboration with M. Stabell and A. Lambertson dG9a was studied *in vivo* and *in vitro* (Stabell et al., 2006).

4.4.1 Expression and purification of Flag-dG9a Sf9 cells

In order to investigate the enzymatic properties of dG9a, a Flag-tagged N-terminal fragment (aa 789 - 1637) was expressed using a baculovirus system. The purified dG9a was soluble and had the expected molar mass of 95 kDa (Figure 4.18).

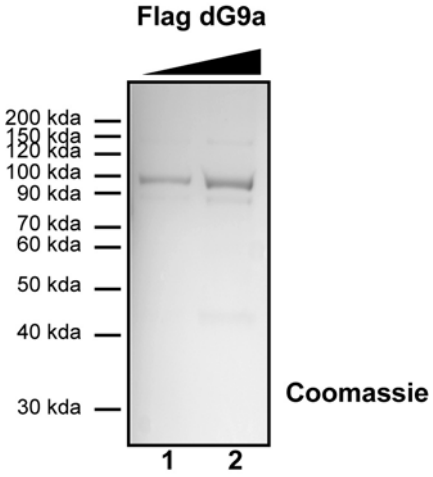

Figure 4.18 Expression and purification of recombinant dG9a. Eluted Flag-tagged dG9a (aa 789-1637) was separated by SDS -12 % PAGE and stained with Coomassie blue G250.

4.4.2 dG9a methylates histone H3K9 and K27 and H4 K8, K12 or K16

To confirm that dG9a has HMTase activity, it was incubated with H^3-S-adenosyl methionine (SAM) and different substrates (Figure 4.19). *Drosophila* G9a methylated H3 and H4 present as free histones but had no detectable activity on nucleosomal arrays.

Recombinant as well as native H3 and H4 were methylated by dG9a (Figure 4.19.A). Mouse G9a methylated H3 alone and H3 in a mixture of recombinant and native histones and had a very low activity on reconstituted nucleosomes (Figure 4.19.B).

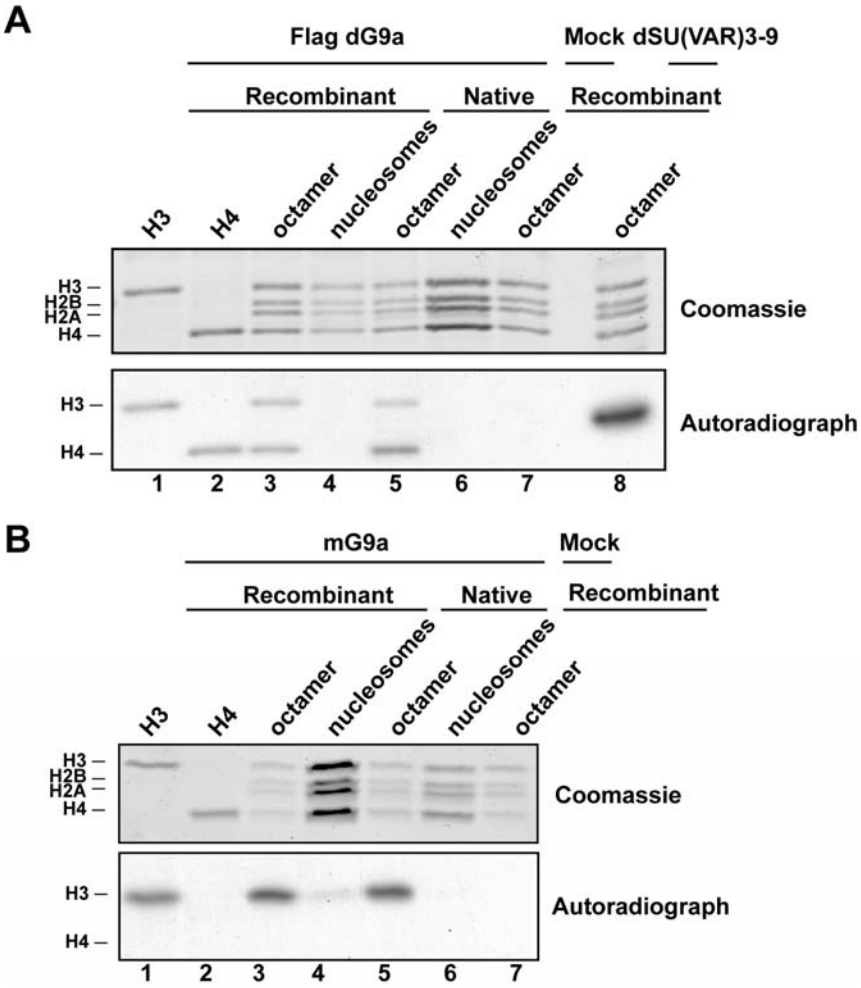

Figure 4.19 Characterization of recombinant dG9a. **(A)** *In vitro* methylation reactions using dG9a (lanes 1-6), no enzyme (lane 7) and SU(VAR)3-9 (lane 8). In the reaction 1 µg of different histones were used: recombinant histone H3 (lane 1), recombinant histone H4 (lane 2), recombinant (lane 3) and native histone octamer (lane 5) and recombinant and native nucleosomes (lane 4 and 6) reconstituted on circular pBS(KS) from equimolar amounts of histones. The upper panel shows Coomassie stained gel and the lower panel the autoradiograph. **(B)** Activity of recombinant mouse G9a expressed in baculovirus infected cells (a kind gift from S. Pradhan). HMTase activity on 1 µg of different histone substrates: recombinant histone H3 (lane 1), recombinant histone H4 (lane 2), recombinant and native histone octamers (lane 3 and 5) and recombinant and native nucleosomes (lane 4 and 6). Mock control (lane 7) is incubation of recombinant octamer without enzyme. The Coomassie gel is shown at the top and the corresponding autoradiograph at the bottom.

Mouse G9a methylated only H3 whereas dG9a methylated H3 and H4. In order to exclude that the activity towards H4 was due to a contaminating activity co-purifying with dG9a, a corresponding enzyme carrying a H1536K mutation within the conserved SET domain was expressed. The same mutation in SU(VAR)3-9 abolished its enzymatic activity (Figure 4.7). The mutated enzyme had no activity towards H3 and H4 indicating that both were methylated by dG9a (Figure 4.20). It cannot be excluded that the H4 activity may be due to the deletion of the N-terminus of dG9a.

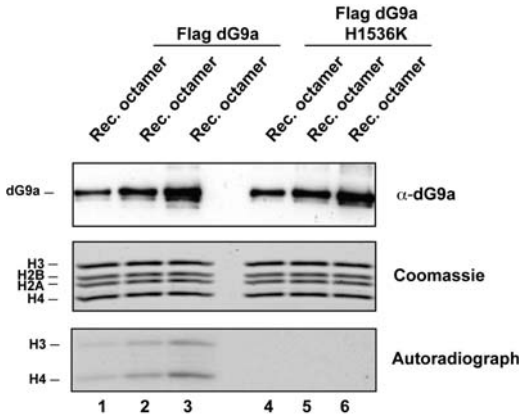

Figure 4.20. The H1536 mutation abolished the enzymatic activity of dG9a. Activity of Flag-dG9a wild type versus dG9a containing a H1536K mutation in the conserved region of the SET domain. The upper panel shows a western blot of the two proteins. Recombinant octamer (2 μg) was used as substrate for 25, 50 and 100 ng of wt (lane 1-3) and H1536K mutant (lane 4-6). The corresponding autoradiograph is shown in the lower panel.

Mouse G9a has been shown to methylate H3K9 and K27 (Tachibana et al., 2001; Tachibana et al., 2002). To define substrate specificity of dG9a, H3 molecules carrying a lysine to alanine replacement at position 9 and 27 or both were used (Figure 4.21). Decreased methylation efficiency on H3K9A and H3 K27A compared to wild type H3 was observed. In a filter binding assay a 70% reduction for the K9 mutant and a 50% reduction for the K27 mutant was observed. When both H3 lysine residues were mutated (K9A and K27A) a lower activity was observed (efficiency of 27%) indicating that in absence of K9 and K27 dG9a was also able to methylate other lysines. When a highly active full-length mG9a (Patnaik et al., 2004) was used, it methylated wild type H3 and the H3 molecules carrying a single mutation on K9 or K27 with a similar efficiency. Mouse G9a also showed a decreased activity (27%) towards the double mutant (K9A/K27A). However, it can not be excluded that K9 was methylated faster than K27, as initial rate kinetics were not performed (Collins et al., 2005; Esteve et al., 2005).

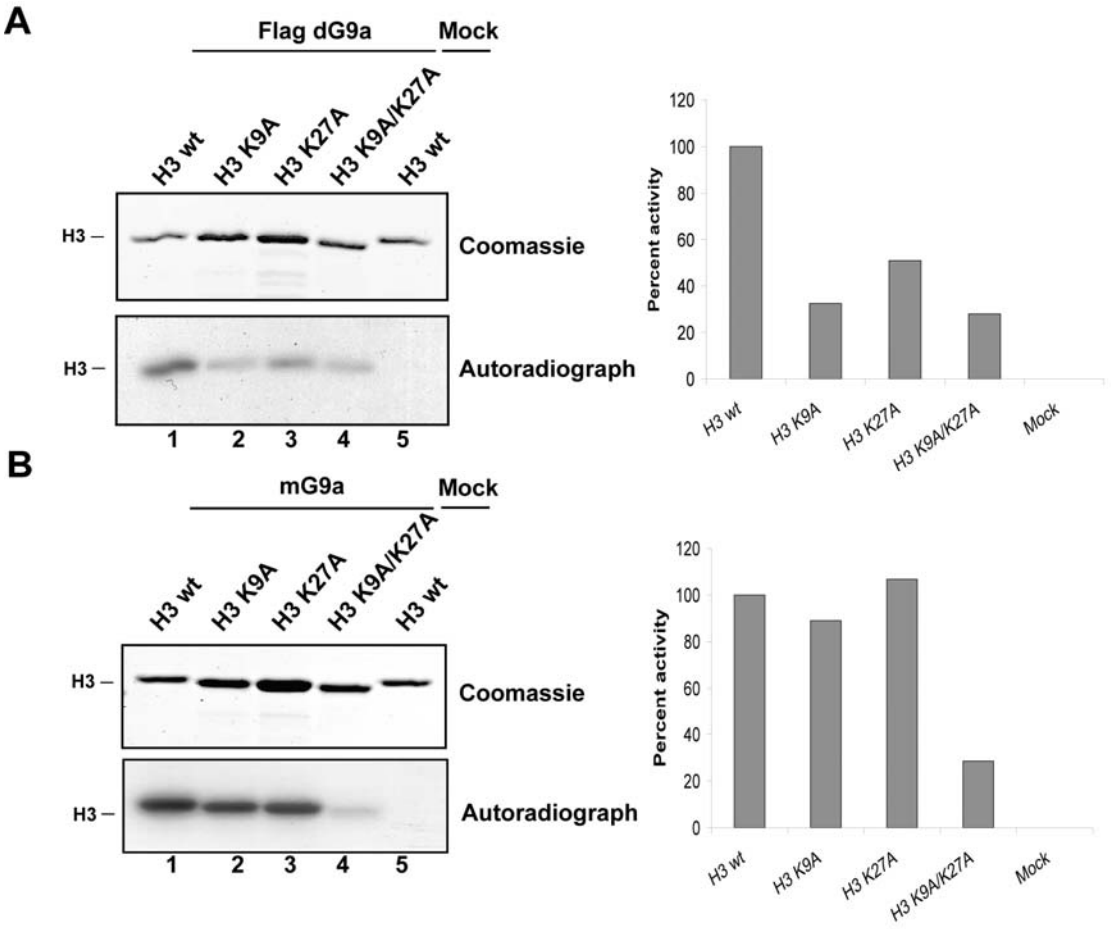

Figure 4.21 dG9a methylates H3K9 and K27. (A) *In vitro* methylation of 2 µg of recombinant H3 (lane 1), H3 mutated at lysine 9 (lane 2), H3 mutated at lysine 27 (lane 3) or both (lane 4) using dG9a and a mock purification. Coomassie stained H3 is shown in the upper panel and a corresponding autoradiography in lower panel. A corresponding filter binding assay is shown to the right. The y-axis displays the percent radioactivity incorporated on 2 µg histone H3 and H3 mutants K9A, K27A and K9/K27A with radioactivity incorporated on H3 wt set to 100 % and the background is subtracted. **(B)** HKMTase activity of mG9a on histone H3 molecules and H3K9A, H3 K27A and the double mutant K9A/K27A. A gel of Coomassie stained histones and the corresponding autoradiography is shown. On the right, a filter-binding assay showing percent radioactivity incorporated on two µg histone H3 and H3 mutants K9A, K27A and K9/K27A. The y-axis displays the percent radioactivity incorporated with activity on H3 wt set to 100 % and the background is subtracted.

Interestingly dG9a was also able to methylate histone H4 (Figure 4.19 and 4.20). This activity was not shown for mouse G9a (Figure 4.19.B) (Tachibana et al., 2001). The only lysine residue shown to be methylated in H4 is lysine 20 and the first HMTase identified with this activity was hPR-Set7/dSET8 (Fang et al., 2002; Rice et al., 2002). Other HMTases in *Drosophila* shown to methylate H4 lysine 20 are Ash1 and Suv4-20 (Beisel et al., 2002; Schotta et al., 2004).

Ash1 was in addition able to methylate lysine 4 and 9 in histone H3 (Beisel et al., 2002). Comparing the similarity within the SET domain, mouse NSD1 has closest homology to SET family member Ash1 (Huang et al., 1998) and NSD1 SET domain methylate H3K36 and H4K20 *in vitro* (Rayasam et al., 2003). The data indicated that dG9a also was a multi-catalytic histone methyltransferase with specificity for lysine 9 and 27 on H3 and possibly lysine 20 on histone H4. Surprisingly when dG9a was incubated with H4 carrying a mutation of lysine 20 to alanine no reduction of activity was observed (Figure 4.22). To further investigate the specificity, dG9a activity was tested on different N-terminal H4 mutants (Clapier et al.,2002). dG9a could methylate the H4 N-terminus when the first five amino acids were deleted, excluding K5 as a possible substrate. However, the activity was lost when a H4 Δ10 mutant was used (Figure 4.22). This suggests that the substrate was K8, but knowing that the minimal substrate specificity for mG9a surrounding K9 contains seven amino acids (TARKSTG) (Chin et al., 2005) the substrate could also be K12 or K16.

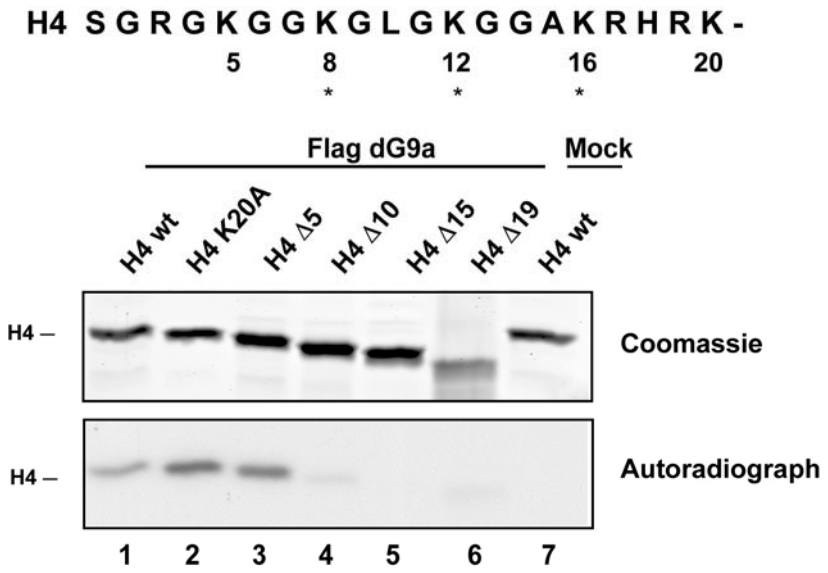

Figure 4.22 dG9a methylates H4 K8, K12 or K16. Amino acid sequence of the H4 N-terminus is shown at the top. Asterisk indicates possible substrates for dG9a *in vitro*. dG9a methylation assay with 2 µg of recombinant H4 (lane 1), H4 K20A (lane 2), H4Δ5 (lane 3), H4Δ10 (lane 4), H4Δ15 (lane 5) and globular H4 (lane 6). Mock control (lane 7) is incubation of wt H4 without enzyme.

Using MALDI-TOF analysis to measure the activity of dG9a on H3 confirmed the finding that K9 was the major substrate (Figure 4.23). Four times more activity towards K9 compared to K27 was observed. As shown for mG9a (Patnaik et al., 2004, Collins et al., 2005) dG9a was able to add three methylgroups to H3K9.

Tri-methylation of H3 peptide 27-40 was very inefficient and could only be detected when 200 ng of enzyme was used (data not shown). This was consistent with MALDI-TOF data of mouse G9a where H3 K27 methylated peptides were slowly generated (Collins et al., 2005). All visible peptides by MALDI-TOF of methylated H3 and H4 were analyzed and no other modified lysines were detected (data not shown). Peptide 4-17 on H4 methylated by dG9a, was mono-, di-, and trimethylated providing a proof of a lysine methylation (Figure 4.23). This was a novel finding that a SET domain HMTase can methylate another lysine in the H4 N-terminus than K20. There is yet no strong evidence of any of these methyl marks being present on the H4 N-terminus *in vivo*, and it remains to be seen to what level these lysines are methylated and what the function of this methylation is.

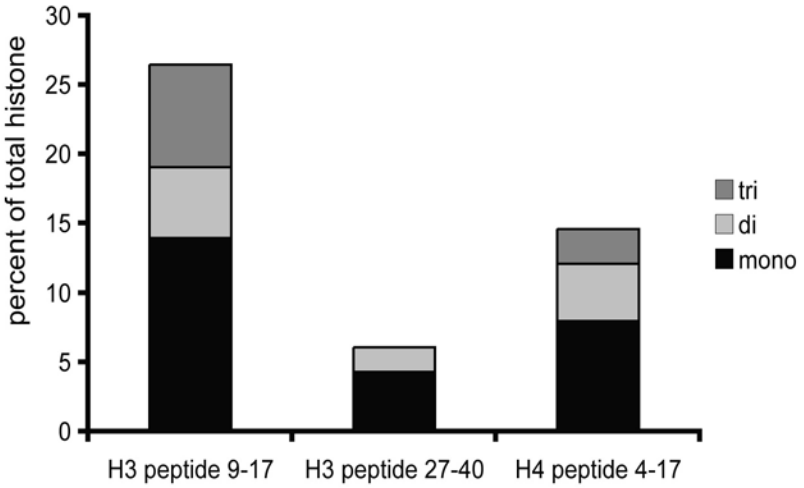

Figure 4.23 MALDI-TOF analysis of dG9a *in vitro* methylated H3 and H4. A MALDI-TOF analysis of 500 ng H3 and H4 methylated by 100 ng dG9a. Peptides spanning amino acids 9-17 and 27-40 of H3 and 4-17 of H4 is represented by graphs. Mono-, di- and trimethylation is shown as percent of total H3 or H4. This figure is representative for at least three different methyltransferase assays.

4.4.3 dG9a methylates histone H1

Mouse G9a methylates histone H1 (Tachibana et al., 2001). The histone H1 family is the most divergent class of the histones (for review see (Doenecke et al., 1997)). There is only one histone H1 protein in *Drosophila melanogaster*, which can purified from 0-12 hours embryos (Croston et al., 1991). When incubated with dG9a or mG9a *Drosophila* H1 gets methylated (Figure 4.25). This indicates that G9a methylates a more conserved lysine within the H1 family.

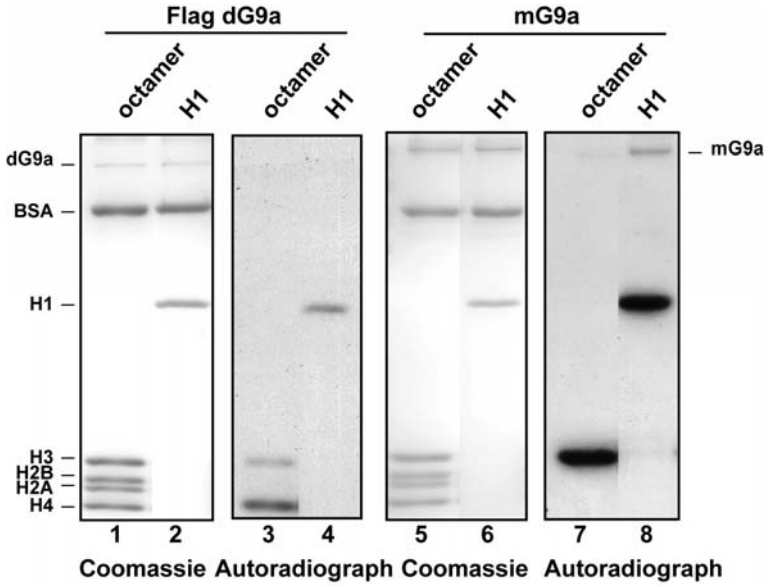

Figure 4.24 dG9a methylates histone H1. dG9a methylates *Drosophila* histone H1. *Drosophila* and mouse G9a (100 ng) was incubated for 1 hour with 500 ng H1 or two µg recombinant octamer in the presence of 0.17 µM S-Adenosyl [methyl-^{3}H] methionine.

4.5 Purification of dG9a from *Drosophila* nuclear extract

Mouse G9a has been shown to heterodimerise with a G9a related protein (GLP also known as EuHMTase1 in human) (Tachibana et al., 2005) which forms a part of a large complex called E2F6.com (Ogawa et al., 2002). G9a–GLP heterodimer was recently shown to interact with a zink finger protein called Wiz in mouse ES cells (Ueda et al., 2006).

4.5.1 Native dG9a is present in complexes of 440-670 kDa

In order to search for dG9a interaction partners, a specific polyclonal antibody generated by M. Stabell was used (Stabell et al., 2006). The dG9a antibody recognized a single band with the predicted size of approximately 180 kDa (Figure 4.25) in *Drosophila* 0-12 hours nuclear extract.

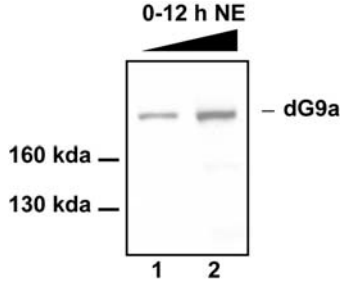

Figure 4.25 Antibody against dG9a raised in rabbit are specific and recognize a single band of approximately 180 kDa as predicted on a western blot of 1 and 2 µl *Drosophila* nuclear extract.

The Enhanzer of zeste (E(Z)) complex was purified from *Drosophila* nuclear extract, and chromatographic purification revealed that at least five distinctive HMTase activities, including SU(VAR)3-9 and E(Z), was identified in the 250 mM fraction of the Biorex 70 column (Czermin et al., 2002). Probing the fractions from the Biorex 70 column with dG9a antibody revealed that dG9a was mainly present in the 500 mM fraction (Figure 4.26.A and B).

In order to identify dG9a interaction proteins, the Biorex70 500 mM fraction was purified over another 3 successive columns (Heparin agarose, Mono Q and Superose 6 gel filtration column) (Figure 4.26.A). The presence of dG9a was followed by probing the fractions transferred to western blots with dG9a antibody and by measuring the histone methyltransferase activity (Figure 4.27A and B). dG9a and methyltransferase activity was detected in fractions 26-30 from the Superose 6 column. This indicated that dG9a was present in a complex with a size of 440 to 670 kDa. Judging from the silver-stained polyacrylamide gel of these fractions, there was more than one protein complex present in each fraction. Indeed MALDI-TOF analysis of fraction 29 revealed the presence of the ORC complex, the transcription factor TFIIH complex and other well-known proteins such as Jil-1 and SUZ12 (Figure 4.27.C). Using antibodies present in the laboratory for the proteins RPD3, SUZ12, p55 and ISWI indicated that these proteins also peak in fraction 29 (Figure 4.27.A). Another approach was necessary to identify proteins that interact with dG9a.

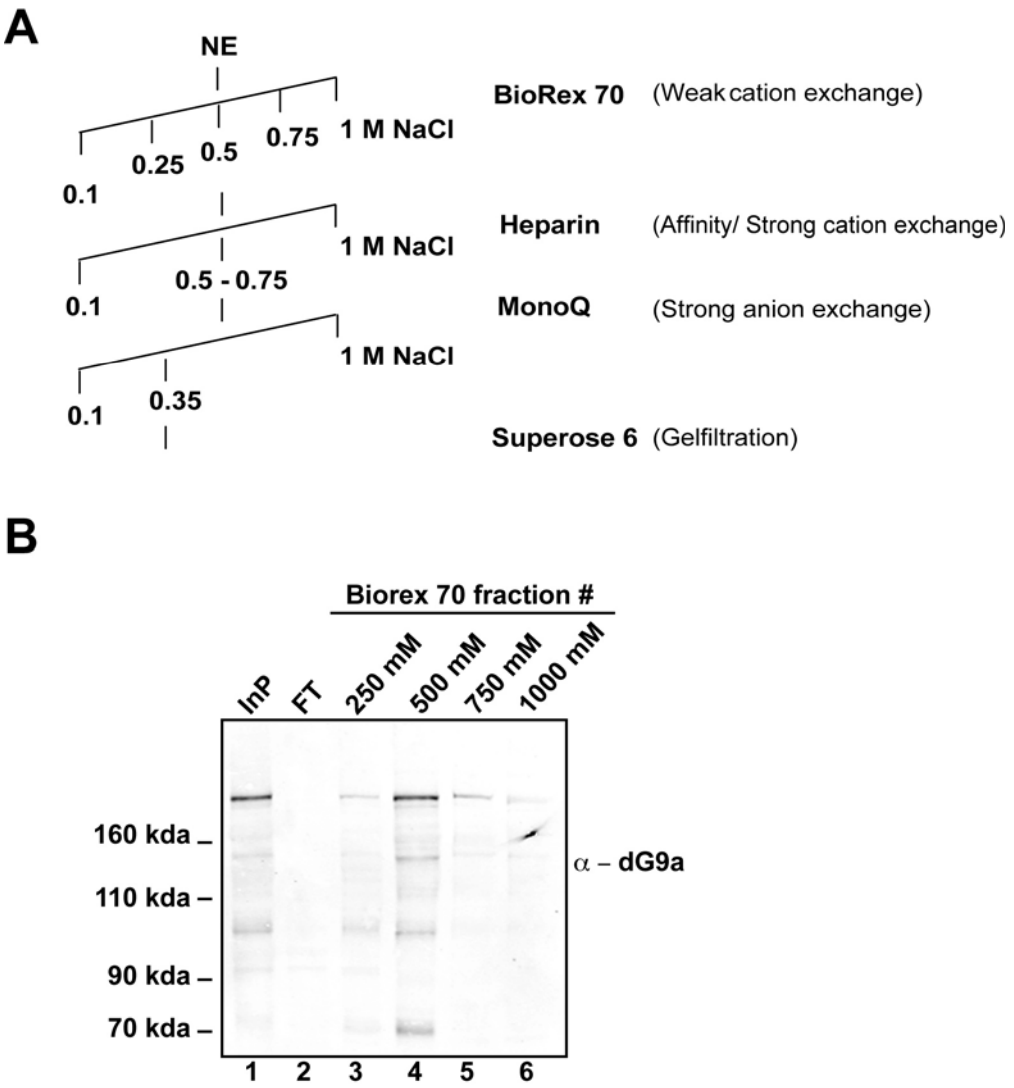

Figure 4.26 Purification of native dG9a (A) A schematic representation of the purification. **(B)** Immuno blotting of fractions from the first column. A total of 20 µg of proteins were loaded in each lane and the western blot was probed with dG9a antibody.

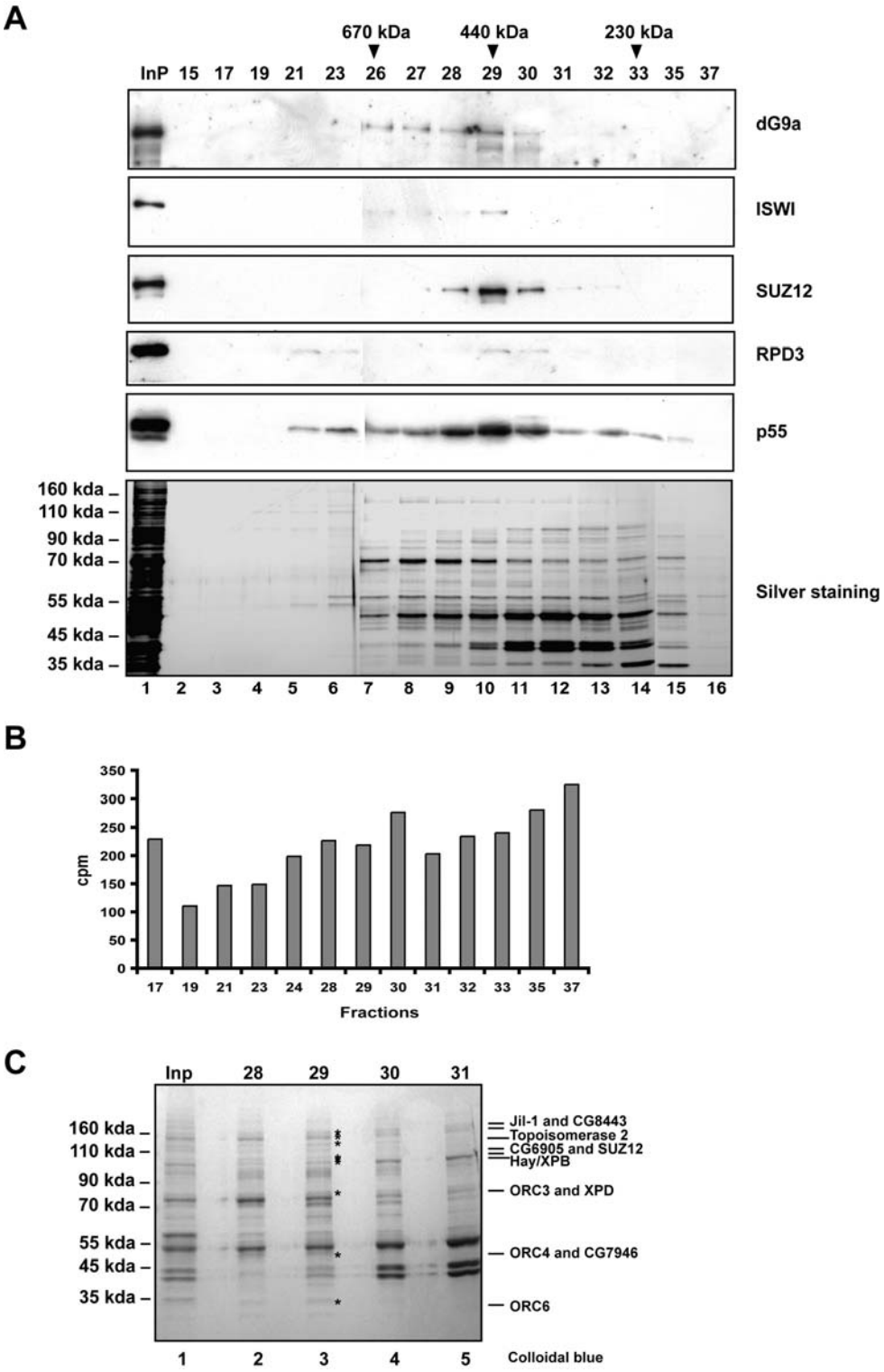

Figure 4.27 (A) 20 µl of fractions eluted from a Superose 6 gelfiltration column were analyzed by silver stain and western blot using α-dG9a, α-ISWI, α-SUZ12, α-RPD3 and α-p55 antibodies as indicated. Arrows indicate molar mass markers. **(B)** A filter binding assay where 20 µl of fractions indicated from (A) were incubated with 2 µg of recombinant histone octamer in the presence of 0.17 µM S-Adenosyl [methyl-^{3}H] methionine. The y-axis represents counts per minute, after background is subtracted. **(C)** A larger volume (100 µl) of fractions # 28-31 were precipitated and separated by SDS-8% PAGE. Bands peaking in # 29, indicated by asterisk, were analyzed by MALDI-TOF.

4.5.2 Co-immunoprecipitation of dG9a and RPD3

It was intriguing that three of the components of the E(Z) complex (Czermin et al., 2002) co-purified together with dG9a. To confirm whether dG9a was present in a similar complex a co-immunoprecipitation was performed (Figure 4.28.A). However, only RPD3 (also known as HDAC1) but not SUZ12, was pulled down by the dG9a antibody. On the other hand RPD3 pulled down SUZ12 and dG9a. This may indicate that RPD3 interacts with dG9a in the absence of SUZ12. Mammalian G9a was found to be in a complex with HDAC1 and Gfi1 responsible for repression of *p21* (Duan et al., 2005). However mG9a was shown to transcriptional repress a reporter gene in HELA cells without HDAC activity (Tachibana et al., 2002). Jil1, a histone S10 kinase that was shown to regulate H3K9 methylation (Ebert et al., 2004) did not interact with dG9a (Figure 4.28.A). The CG7946 co-purifying in fraction 29 (Figure 4.27.C) interacts with JIL1 (C. Regnard personal communication) and may therefore be excluded from interaction with dG9a.

The immunoprecipitated dG9a was also tested for histone methyltransferase activity of recombinant histone octamers and nucleosomes (Figure 4.28.B). Mainly free histone H3 but also H4 was methylated which indicate that the results obtained for recombinant dG9a is also happening *in vivo* (Results 4.4.2). On nucleosomes only histone H4 was methylated and since recombinant dG9a showed no detectable activity towards nucleosomes, one may speculate that this activity was due to a nucleosomal H4 methyltransferase co-purifying with dG9a.

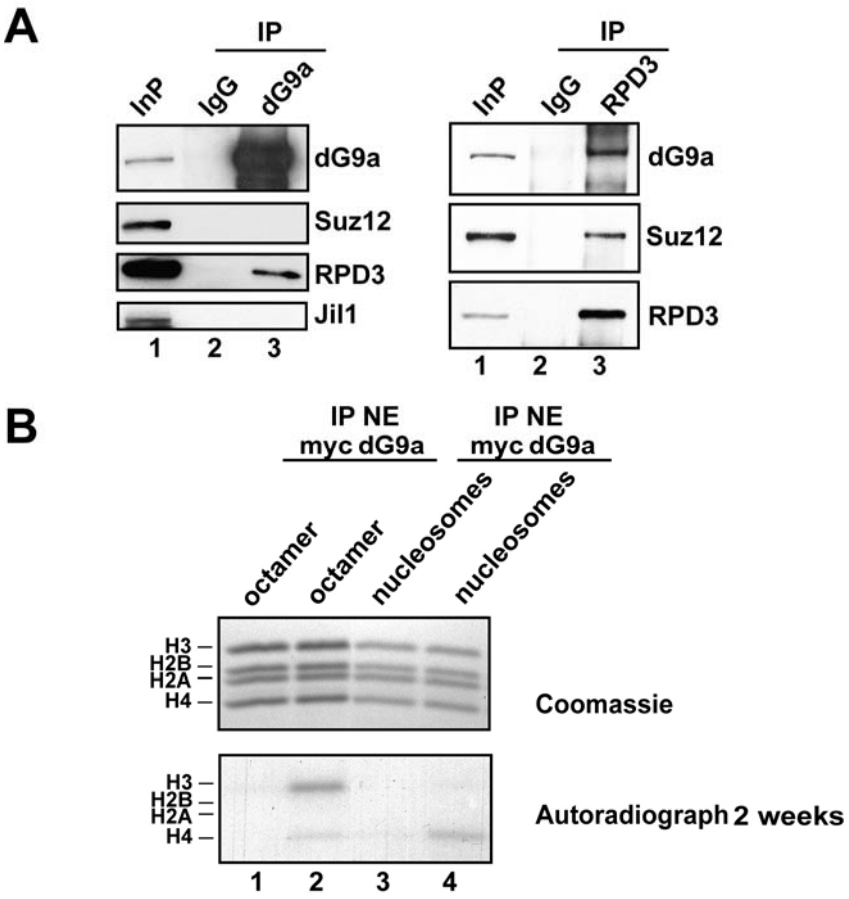

Figure 4.28 dG9a interacts with RPD3 (A) *Drosophila* nuclear extract were precipitated with antibodies directed against dG9a, RPD3 and rabbit IgG. The immunoprecipitations were transferred onto a PVDF membrane and analyzed with specific antibodies as indicated on the right. Input (Inp) is 2% nuclear extract. **(B)** Immunoprecipitations with α-dG9a and α-myc were incubated with 2 µg of recombinant histone octamer or 1 µg of nucleosomal arrays in the presence of 0.17 µM S-Adenosyl [methyl-^{3}H] methionine. The Coomassie gel is shown at the top and the corresponding autoradiograph at the bottom.

To further identify dG9a interacting proteins, immunoprecipitated dG9a was loaded onto a SDS-4-20% PAA gel and stained with colloidal blue. Bands were cut and subjected to peptide mass fingerprint. Most of the bands contained dG9a, suggesting that this protein was prone to proteolytic cleavages. The ATPase ISWI, the catalytic subunit of at least three chromatin remodeling complexes in *Drosophila*: ACF, CHRAC and NURF (for review see (Bouazoune and Brehm, 2006)), was pulled down with dG9a (Figure 4.29). ISWI was also co-eluting with dG9a from the Superose 6 column (Figure 4.27.A). Both *dG9a* and *NURF301* are involved in the ecdysone regulatory pathway (Badenhorst et al., 2005; Stabell et al., 2006).

Fibrillarin, a protein present in the nucleoli and involved in 35S RNA processing (Tollervey et al., 1991), and 40S Ribosomal protein was also identified interacting with dG9a. However, immunofluoescence analysis of mouse G9a and GLP revealed that both proteins co-localized in the nucleus but were largely excluded from the nucleoli (Ueda et al., 2006) suggesting that Fibrillarin may be a contaminant in the purification. The 40S ribosomal protein is part of the 80S ribosome responsible for translating mature mRNA in the cytoplasm (for review see (Pestova et al., 2001)). The interaction with G9a may not be excluded since immunostaining and *in situ* hybridization show that the translation apparatus was present at sites of Ecdysone-induced transcription in the nucleus (Brogna et al., 2002).

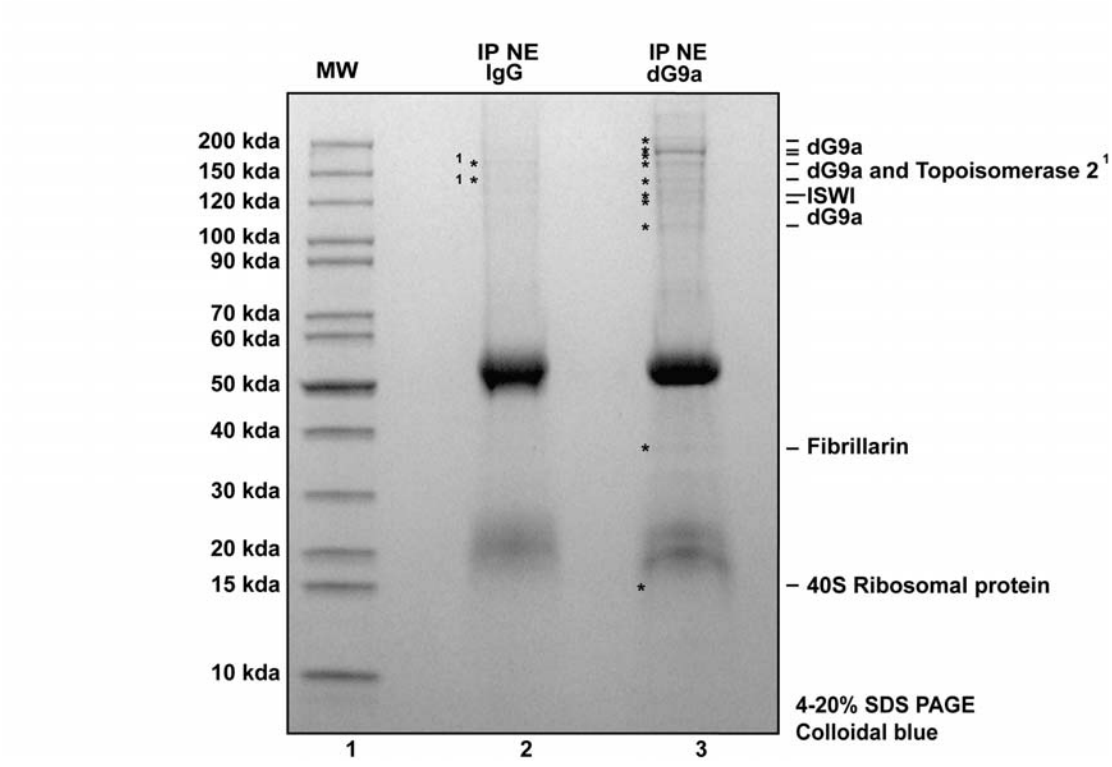

Figure 4.29 Immunoprecipitation of dG9a. Immunoprecipitation from *Drosophila* nuclear extract (NE) using the dG9a antibody was separated by SDS-4-20% PAGE and analyzed by MALDI-TOF. Bands are indicated by asterisk the identified proteins are shown on the right. MW, molecular weight markers are shown to the right. [1)] Topoisomerase was also identified in the IgG immunoprecipitation and is therefore considered a contaminant.

4.6 HP1a binding to H3K9 methylated chromatin is enhanced by auxiliary factors

Drosophila heterochromatin protein 1 (HP1) was first identified as an abundant protein localizing to pericentric heterochromatin (James et al., 1989). There are five paralogs present in *Drosophila melanogaster*, named HP1a-e (Vermaak et al., 2005). The HP1 proteins carry a N-terminal chromo domain and a C-terminal chromo shadow domain separated by a hinge region (Aasland and Stewart, 1995; Eissenberg and Elgin, 2000; Paro and Hogness, 1991; Singh et al., 1991). *In vitro* studies revealed that the chromo domain binds H3 peptides methylated at K9 (Bannister et al., 2001; Jacobs and Khorasanizadeh, 2002; Jacobs et al., 2001; Lachner et al., 2001; Nielsen et al., 2002). In addition *in vivo* reports supports these data; in a mutant background of the H3K9 HMTase SU(VAR)3-9/Clr4 methylated H3 and HP1 localization to heterochromatin was reduced (Bannister et al., 2001; Nakayama et al., 2001; Schotta et al., 2002). However, little was known about the mechanism of HP1 binding to H3K9 methylated nucleosomes.

4.6.1 Bacterially expressed HP1a dimerises

In order to generate chromatin fibers containing HP1a, bacterially expressed *Drosophila* HP1a was purified over four consecutive columns as described before to (Zhao and Eissenberg, 1999) (Figure 4.30).

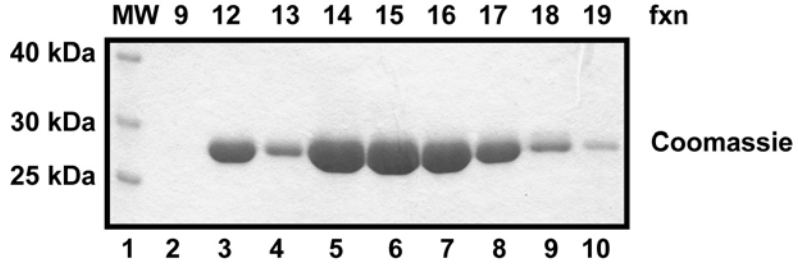

Figure 4.30 Purified recombinant HP1a. Untagged recombinant HP1a was purified over four successive columns. A Coomassie stained SDS-12% PAA gel of 5 µl of fractions 9-19 from the last column, a MonoQ, is depicted. fxn, fraction.

Structural analysis revealed that the chromo shadow domain forms dimers (Brasher et al., 2000; Cowieson et al., 2000). To confirm that the recombinant HP1a was folded properly to form dimers, the protein was analyzed on a Superdex 200 column (Figure 4.31.A). HP1a eluted with an apparent mass of a dimer.

This was confirmed by multi angle light scattering (Figure 4.31.B). To further examine the dimeric state of HP1a, the recombinant protein was cross-linked with DTSSP and separated by SDS-PAGE. Because DTSSP is cleaved in the presence of a reducing agent, cross- linked proteins would be split into their monomeric form. In the absence of reducing agent, cross-linked HP1a was detected by Western blotting as monomer and dimer. In presence of reducing agent more monomer could be detected.

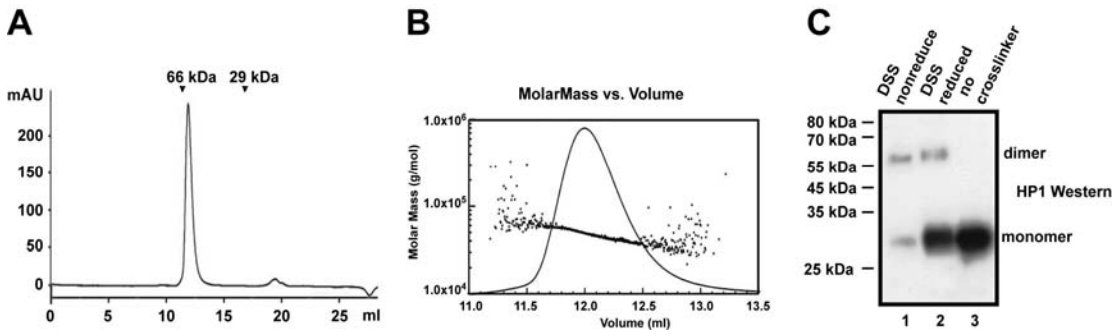

Figure 4.31 Bacterially expressed HP1a dimerises. (**A**) Purified recombinant HP1a was loaded onto a gel-filtration column (Superdex 200) and the elution profile (A_{280}) of HP1 is shown. Molar mass standards (Bovine Serum Albumin 66 kDa and Carbonic Anhydrase 29 kDa) are labeled with arrows. **(B)** A molar mass of HP1a as it elutes from the size-exclusion column in (A). The molar mass (kDa) was determined by multi angle light scatter (dots). (**C**) *In vitro* cross-linking of HP1a using DTSSP (DSS). Recombinant HP1a before (lane 3) or after (lanes 1 and 2) cross-linking was subjected to a SDS-12% PAGE, transferred to a PVDF membrane and detected with HP1 (C1A9) antibody. The DTSSP cross-linking can be partially reversed by reductive cleavage of the disulphide-containing cross-linking molecule (lane 2). The cross-linking revealed dimeric HP1.

4.6.2 Recombinant HP1a binds the H3-tail methylated at K9

HP1 specifically recognizes methylation of lysine 9 on histone H3 (Bannister et al., 2001; Lachner et al., 2001). Therefore, the binding of recombinant HP1a to H3 peptides unmodified, dimethylated at K4 or K9 were tested (Figure 4.32). HP1a bound only to the H3 peptide methylated at K9.

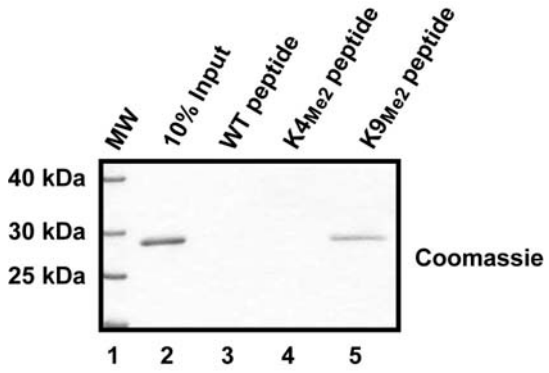

Figure 4.32 Recombinant HP1a was assayed for binding to H3 peptides containing the first 19 amino acids of H3 immobilized onto Sulfolink Sepharose. The substrates were: unmodified peptide (lane 3), peptide dimethylated at K4 ($K4_{Me2}$; lane 4) and peptide dimethylated at K9 ($K9_{Me2}$; lane 5). Bound HP1a was visualized by Coomassie staining.

4.6.3 Reconstitution of recombinant and H3K9 methylated chromatin and binding of HP1a

In order to study binding of HP1a to chromatin, recombinant *Drosophila* histones were assembled onto DNA fragments containing 11 repeats of the 5S nucleosome positioning sequence by salt dialysis (Luger et al., 1999) (Figure 4.33). The level of assembly was tested by micrococcal nuclease digestion (Figure 4.33.B). To analyze chromatin bound HP1a, the DNA fragments were biotinylated on one strand and immobilized using streptavidin coupled magnetic paramagnetic beads. Chromatin assembly was more efficient on unbound DNA; therefore the nucleosomal arrays were coupled to paramagnetic beads and washed with 100 mM salt to get rid of unbound fragments. As described in results section 4.1.3, recombinant SU(VAR)3-9 trimethylates histone H3K9. After incubation of SU(VAR)3-9 with reconstituted octamers and SAM, the histones were separated from SU(VAR)3-9, SAM and SAH by a cation-exchange resin. The histones were eluted from the resin with 2.5 M NaCl, which favors formation of octamers. The efficiency of H3K9 methylation was analyzed by MALDI-TOF and octamers with H3 molecules carrying at least 80% di-

and trimethylation (See figure 4.6) were used for salt dialysis (Figure 4.33.B lanes 2-4).

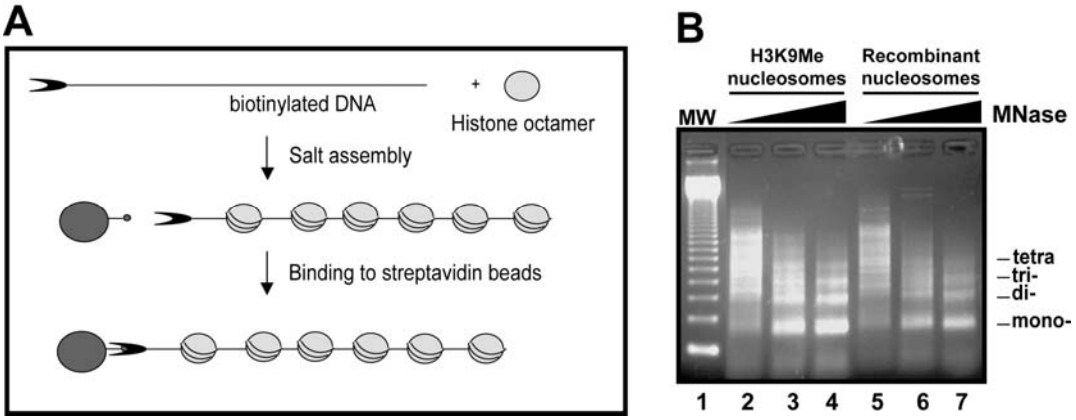

Figure 4.33 Generation of H3K9 methylated chromatin. (**A**) A scheme of the chromatin reconstitution protocol. The DNA used for chromatin reconstitution was a literalized biotinylated fragment containing 11 repeats of the 5S nucleosome positioning sequence (Tse and Hansen, 1997). **(B)** Micrococcal digestion pattern of salt-reconstituted chromatin with recombinant or *in vitro* methylated histones is shown to the right.

HP1a was incubated with either recombinant or H3K9 methylated nucleosomes at a molar ratio of 4:1. Despite the high content of methylated histone H3, HP1a showed only a weak binding that was independent of methylation and similar to the affinity to DNA (Figure 4.34.A). HP1a was reported to bind to nucleosomes, but the HP1 to nucleosome ratio was very high (500:1) (Zhao et al., 2000). The linker histone (H1) bound very efficient to chromatin fibers even at a ratio of 2:1 (Figure 4.34.B). Therefore it may be concluded that HP1a either binds to methylated histone H3 before assembly or it requires additional factors for the binding to chromatin fibers.

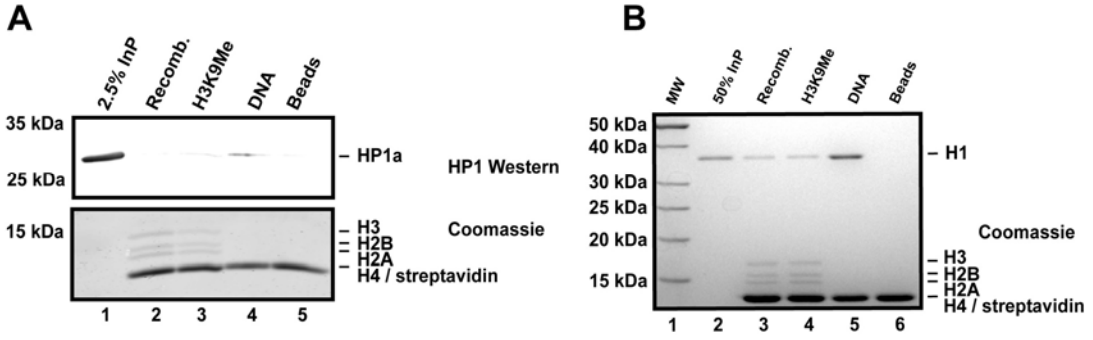

Figure 4.34 (**A**) HP1 was assayed for binding to recombinant chromatin (lane 2), H3K9Me chromatin (lane 3), DNA immobilized on paramagnetic beads (lane 4) and beads alone (lane 5). Bound HP1 was separated by SDS-15% PAGE and visualized with an HP1 polyclonal antibody. The lower the panel shows the corresponding histones are stained with Coomassie blue (**B**) The same assay as described in (C) with histone H1, visualized by Coomassie blue.

4.6.4 HP1a binds to H3K9Me during chromatin assembly

HP1 has been reported to bind to the histone fold of histone H3 (Nielsen et al., 2001) and since the histone fold domain is not easily accessed in the nucleosomal particle (Luger et al., 1997), HP1a might bind before histones were assembled into chromatin. In order to test whether HP1a binds H3 molecules before chromatin assembly, another chromatin assembly method was used since the salt assembly reaction contain high salt concentrations (2 M NaCl). A chromatin assembly extract (S150) from preblastoderm *Drosophila* embryos utilizes endogenous core histones and assembly factors to assemble cloned DNA (Becker and Wu, 1992). The S150 extract can be utilized to assemble nucleosomes on DNA immobilized to paramagnetic beads (Sandaltzopoulos et al., 1994) (Figure 4.35.A). Albeit recombinant HP1a was added at the start of the assembly reaction, only a weak association of HP1a with the assembled chromatin could be observed (Figure 4.35.C, lane 3). Histones from early *Drosophila* embryos contains less than 5% H3K9 methylation (Bonaldi et al., 2004). To increase the content of H3K9 methylated molecules, recombinant methylated octamer was added to the assembly extract before the assembly. In comparison, unmodified histones were added. Micrococcal nuclease digestions of immobilized chromatin assembled with S150 extract (Figure 4.35.B lanes 2-4) or S150 extract supplemented with unmodified (lanes 10-12) or methylated (lanes 6-8) histones revealed similar nucleosomal spacing. The chromatin with supplemented histones was slightly more sensitive to MNase. Under these conditions, HP1a showed weak binding towards chromatin supplemented with unmodified histones whereas a much stronger binding was observed to chromatin supplemented with methylated histones before the assembly reactions (Figure 4.35.C lane 4 versus 5). Using fluorescently labeled secondary antibodies for western blot detection, allowed quantification of the signals by the Odyssey system. A quantification of Figure 4.35.C is shown in (Figure 4.35.D). There was a ten-fold increase of HP1a binding to chromatin when methylated histones were present compared to unmodified histones.

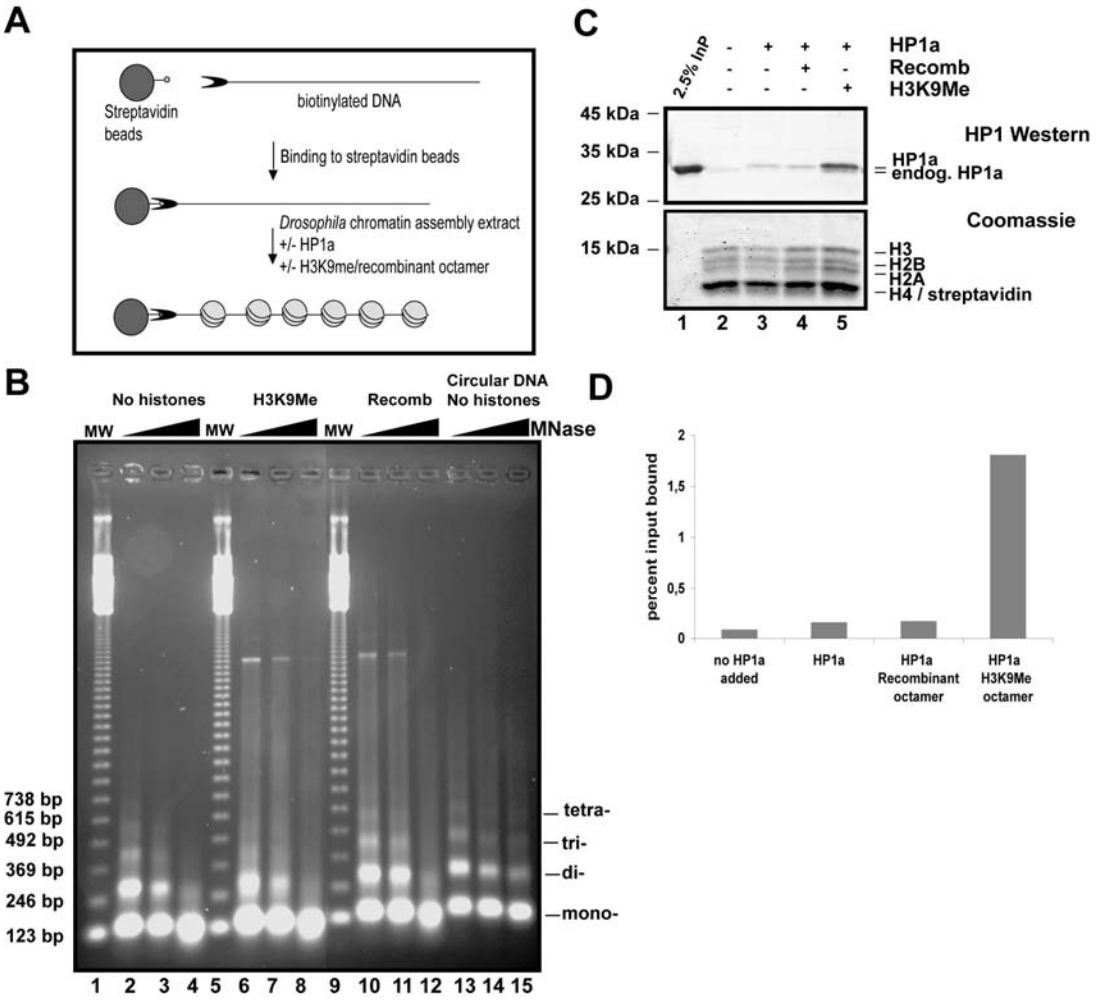

Figure 4.35 Reconstitution of methylated chromatin using a S150 *Drosophila* assembly extract and HP1a binding. (**A**) A scheme of the assay. (**B**) Micrococcal digestion pattern of chromatin assembly reactions as described in (C) without HP1a added. MNase digestions were stopped after 30-, 60-, and 300 seconds. Assembly of circular DNA was used as a control. MW indicates lanes containing the 123 bp ladder as size marker. (**C**) Chromatin was reconstituted on 2 µg linearized dsDNA bound to paramagnetic beads in the presence or absence of 2 µg of HP1a for 6 hours at 26 °C. 2 µg of recombinant octamer (lane 4) or H3K9Me octamer (lane 5) was supplemented to the extract before assembly. The paramagnetic beads were washed and proteins remaining on the beads were loaded on a SDS-15% PAGE. HP1a is visualized with an HP1a polyclonal antibody. The corresponding histones are stained by Coomassie blue. Recombinant and endogenous HP1s are labeled. **(D)** The graph corresponds to a quantification of bound HP1 in (C). Recombinant and endogenous HP1a are included in the quantification. The y- axis displays percent input bound. The graph is representative of three or more different experiments.

To test whether binding of HP1a to H3K9 enriched chromatin affects nucleosomal spacing, increasing amounts of HP1a was added to assembly reactions supplemented with methylated histones (Figure 4.36).

As a control, the highest concentration of HP1a was added to an assembly reaction with unmodified histones. No difference in nucleosomal spacing could be observed.

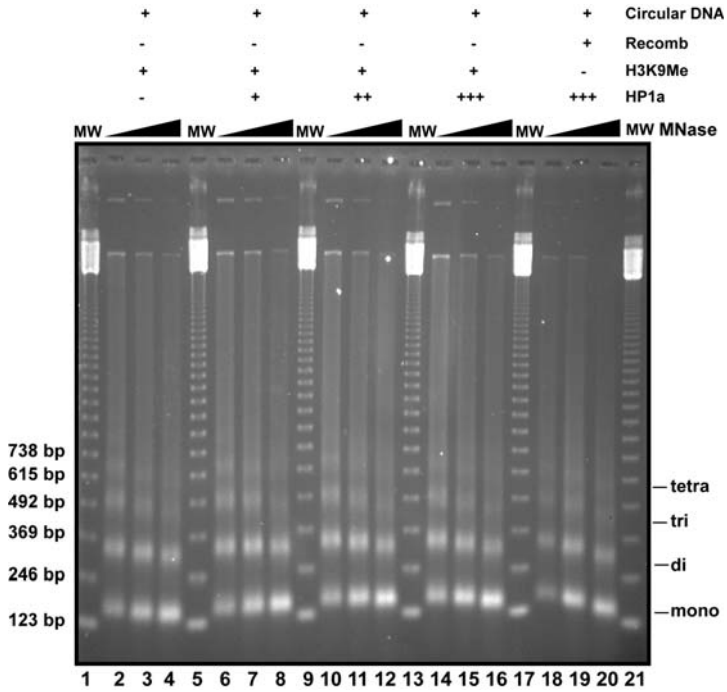

Figure 4.36 Binding of HP1 does not affect nucleosomal spacing. Chromatin was assembled of 1 µg of circular DNA in presence or absence of 2 µg HP1 for 6 hours at 26 °C. 1 µg of H3K9Me octamer (lane 4) or recombinant octamer (lane 5) was supplemented to the extract before assembly. MNase digestions were stopped after 30-, 60-, and 120 seconds. MW indicates lanes containing the 123 bp ladder as size marker.

4.6.5 HP1a binds H3K9Me chromatin in presence of auxiliary factors

HP1a bound to chromatin containing H3 molecules methylated at K9 during assembly. However, it was not clear whether HP1a bound histone H3 before assembly or if accessory factors in the S150 assembly extract facilitate HP1a binding. To distinguish between these two possibilities, recombinant HP1a and S150 extract was added to salt- assembled chromatin (Figure 4.37.A). Under these conditions HP1a bound to chromatin methylated at K9, even though the amount of assembly extract added was not sufficient to assemble chromatin *in vitro* (Figure4.37.B, lane 5). Chromatin assembly is an ATP-dependent process. To investigate whether HP1a binding to chromatin was an ATP-dependent effect ATP or the non-hydrolysable analog γS-ATP was added to the assay. ATP did not significantly stimulate HP1 binding to methylated chromatin (Figure 4.37.B, lane 5 versus 7). On the other hand

the weaker binding to unmodified chromatin was slightly enhanced by ATP (Figure 4.37.B, lane 4 versus 6). A quantification of HP1a binding is shown in (Figure 4.37.C). In the presence of assembly extract, HP1a binds more than 11 times better to H3K9 methylated chromatin compared to unmodified chromatin. The ATP dependent effect of HP1a binding to unmodified chromatin was 3 times better than for γS-ATP.

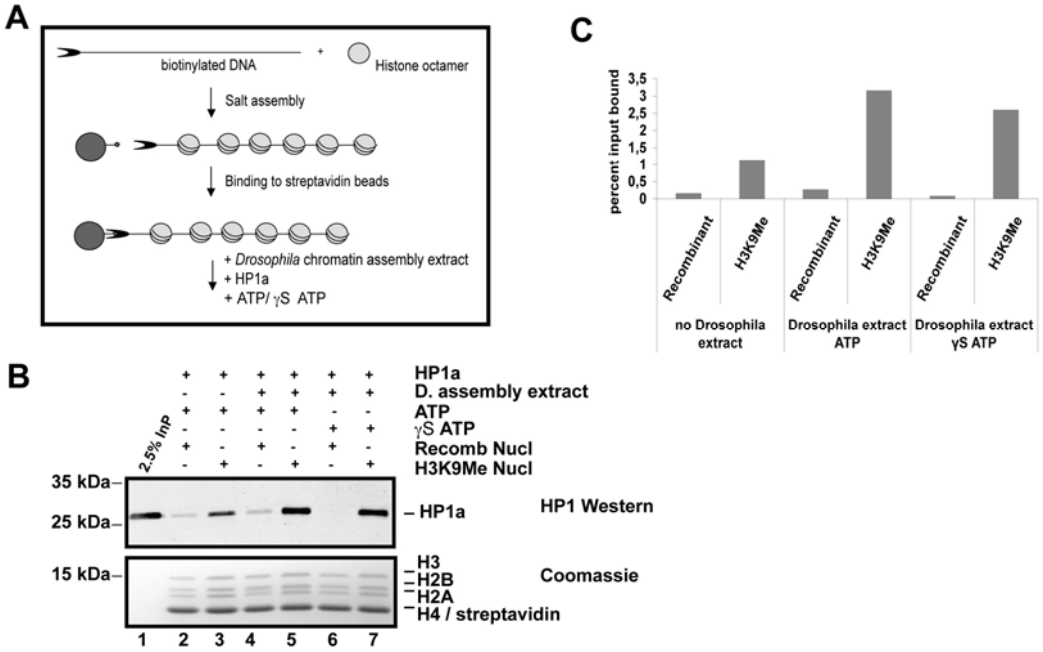

Figure 4.37 HP1a bound to salt assembled chromatin in presence of *Drosophila* assembly extract. **(A)** A scheme of the assay. **(B)** Salt assembled recombinant or H3K9Me chromatin attached to paramagnetic beads was incubated for 1 hour at 26 °C with HP1a, plus and minus *Drosophila* assembly extract. The reactions were in the presence of ATP or non-hydrolysable ATP-gamma-S analog. The assembly extract added was less than 5% of what was needed for the assembly reaction in Figure 4.35. HP1a was detected by HP1a polyclonal antibody and corresponding histones by Coomassie blue. **(C)** The graph corresponds to quantification of HP1a bound shown in Figure 3B. The y- axis displays percent input bound. The graph is representative of at least four individual experiments and displays percent input bound.

4.6.6 Characterization of the molecular mechanism of HP1a binding to H3K9Me chromatin

As shown above, HP1a binding to methylated chromatin was not dependent on chromatin assembly. The chromatin assembly extract contains factors that facilitate HP1a binding to methylated chromatin. To better understand the mechanism of HP1 binding to methylated chromatin two point mutations were generated (Figure 4.38.A). A mutation of valine 26 to methionine within the chromo domain of HP1a prevented

binding to a H3 peptide methylated at K9 (Jacobs et al., 2001). The chromo shadow domain of HP1 is the interacting module for numerous factors that contain a PxVxL motif (reviewed in (Li et al., 2002)). If the chromo shadow domain in HP1β carrying a W170A mutation (W200A in HP1a) mutation, it no longer interact with the PxVxL motif proteins such as TIF1β and CAF1 (Brasher et al., 2000). The HP1a mutants were expressed and purified as described for the wild type protein (Zhao and Eissenberg, 1999) (Figure 4.38.B). As expected HP1a (V26M) mutant no longer bound to H3K9 trimethylated peptides, whereas HP1a (W200A) did (Figure 4.38.C; compare lanes 4, 7 and 10).

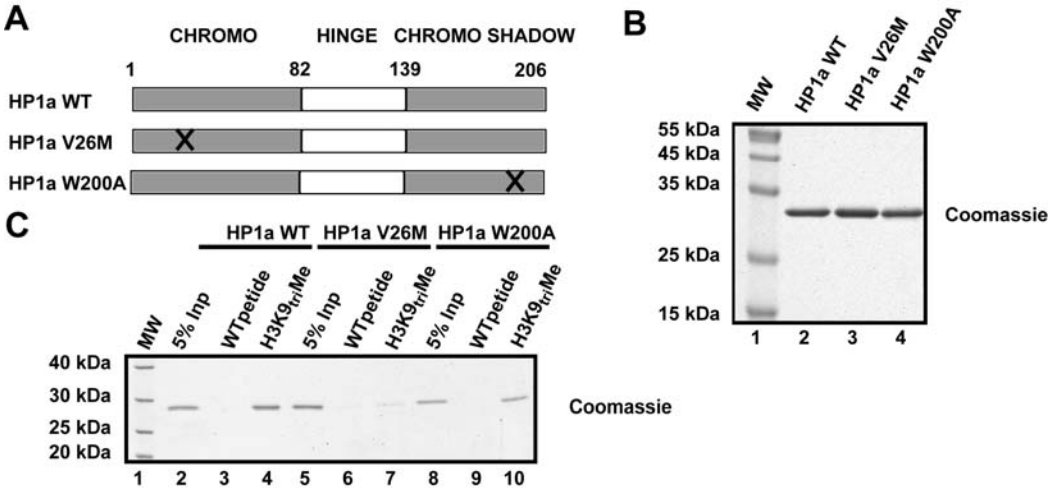

Figure 4.38 Purified recombinant HP1a mutant proteins. (**A**) A scheme of HP1a point-mutants generated. (**B**) A 15% Coomassie blue stained SDS PAA gel of the purified untagged HP1a proteins. (**C**) Peptide pull-down of the recombinant HP1 WT and mutants using H3 peptide aa 1-21, unmodified (WT) versus trimethylated at K9. Bound HP1a were visualized by Coomassie blue.

The HP1a wild type and mutant proteins (V26M and W200A) were added to S150 chromatin assembly reactions in the presence of methylated histones (Figure 4.39 A). As there was some endogenous HP1a present in the extract, a reaction without recombinant HP1a served as control (Figure 4.39.B, lane 4). The endogenous HP1a protein runs with an apparent molar mass that was slightly lower than the recombinant HP1a. HP1a (V26M) which no longer bound to H3K9 methylated peptide lost the ability to bind methylated chromatin (Figure 4.39.B; compare lanes 5 and 6). Despite the ability of HP1a (W200A) to interact with methylated peptides, the binding of methylated chromatin was also impaired. Binding of HP1a to methylated chromatin was depending on recognition of the methylated H3K9 by the chromo domain and protein-protein interactions through the chromo shadow domain. Both domains were

necessary to gain a stable interaction of HP1a to chromatin. A quantification of bound recombinant and endogenous HP1a is shown in Figure 4.39.C.

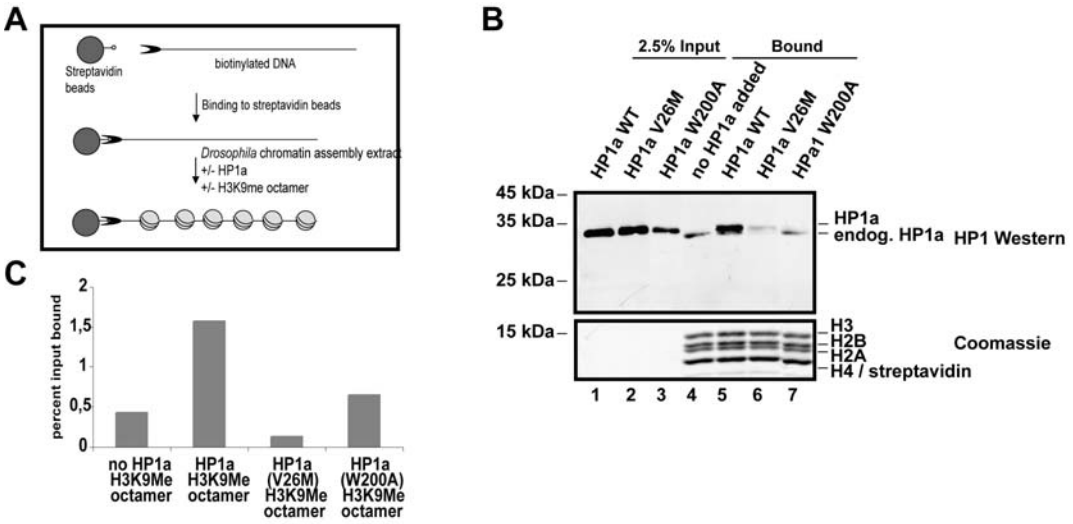

Figure 4.39 (A) A scheme of the assay (**B**) Drosophila assembly reaction with 2 μg H3K9Me octamer as described in Figure 4.35. In lane 1, 2.5% input of HP1a (WT), in lane 2, 2.5% input of HP1a (V26M), and in lane 3, 2.5% input of HP1a (W200A). Lanes 4-7 corresponds to proteins bound after 6 hours incubation. HP1a is detected by HP1 polyclonal antibody and the corresponding histones are stained with Coomassie blue. Bound exogenous and endogenous HP1a present in the *Drosophila* assembly extract are labeled. **(C)** The graph corresponds to quantification of bound HP1 in (B). Recombinant and endogenous HP1 are included in the quantification. The y- axis displays percent input bound. This quantification is representative of at least 3 different experiments.

As described above, HP1 has many interaction partners that interact through the chromo shadow domain. In search of proteins that facilitate HP1a binding to H3K9 methylated chromatin, a candidate approach for proteins involved in heterochromatin formation was chosen.

4.6.7 ACF1 interacts with HP1a and facilitates HP1a binding to chromatin

Several chromatin-associated factors have been suggested to play a role in heterochromatin formation (Reuter and Spierer, 1992; Schotta et al., 2003a). The chromatin remodeling factor ACF (ATP- utilizing chromatin assembly and remodeling factor) consisting of the ATPase ISWI and the regulatory protein ACF1 are abundant in early *Drosophila* embryos (Eberharter et al., 2001; Ito et al., 1999). Loss of ACF1 results in suppression of pericentric position effect variegation (Fyodorov et al., 2004), which places ACF1 in the same genetic pathway as HP1a

(Eissenberg et al., 1990). Mammalian ACF1 has been shown to co-localize with HP1β in mammalian cells and it is suggested to have a role in replication of heterochromatin (Collins et al., 2002). As binding of HP1a to chromatin was impaired when the chromo shadow domain was mutated, we investigated whether ACF interacts with HP1a. ACF complex and ACF1 was expressed using a baculoviral system. Flag-tagged ACF1 was expressed alone or in presence of untagged ISWI and purified over M2-Flag agarose beads (Figure 4.40.A). Immobilized ACF complex or ACF1 protein was incubated with HP1a wild type or the two mutants (V26M) and (W200A) (Figure 4.40.C and D). ACF complex as well as the ACF1 subunit interacted with HP1a wild type and (V26M). The HP1 chromo shadow mutant did not interact (Figure 4.40.A and B; compare lanes 3 and 6 with 9). This was consistent with previous findings that the chromo shadow domain of HP1 mediates most protein-protein interactions (Thiru et al., 2004).

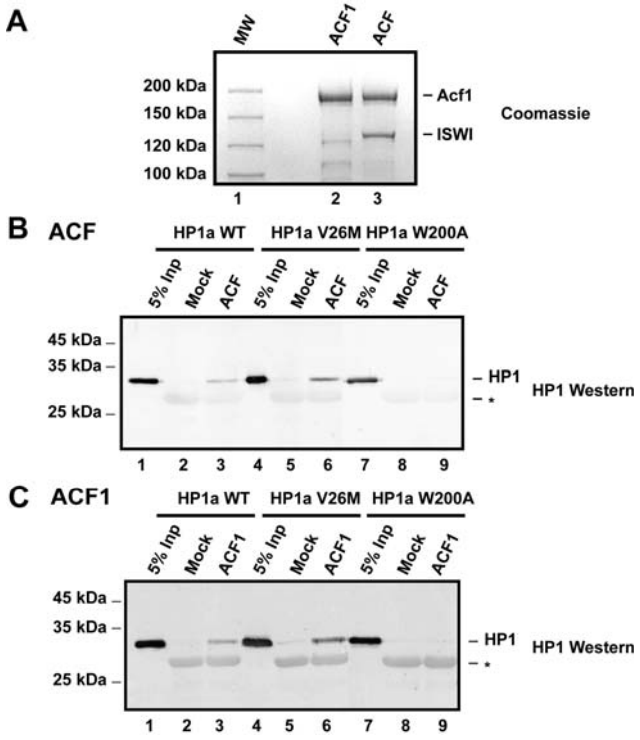

Figure 4.40 HP1 interacts with the ACF complex and ACF1. (A) Coomassie stained SDS-8% PAA gel of Flag affinity purified recombinant ACF1 and ACF complex from Sf9 cells co infected with Flag-ACF1 in presence or absence of untagged ISWI. **(B)** HP1a pull down with Flag beads incubated with mock Sf9 extract or extract-containing recombinant Flag-ACF1 and untagged ISWI. After extensive washing, the protein remaining on the beads were separated by SDS-12% PAGE, imunoblotted and detected by HP1 antibody. Asterisks indicate Flag antibody light chain. **C)** Western blot of HP1a pull down using Flag beads incubated with mock Sf9 extract or extract containing Flag- ACF1. Asterisks indicate Flag antibody light chain.

In order to map the interaction domain of ACF1, a GST-HP1a pull-down was performed. The ACF1 constructs were *in vitro* translated in presence of 35S-methionine and the pull-downs were detected by autoradiography (Figure 4.41.A and B). HP1a interacted with all ACF1 fragments that contained amino acids 202-468. This motif contains the evolutionary conserved DDT domain (Doerks et al., 2001) suggesting that it may be responsible for the interaction. The same region has been shown to be required for ISWI interaction with *Drosophila* ACF1 (Eberharter et al., 2004; Fyodorov and Kadonaga, 2002). A quantification of the pull-down experiment is shown in Figure 4.41.C.

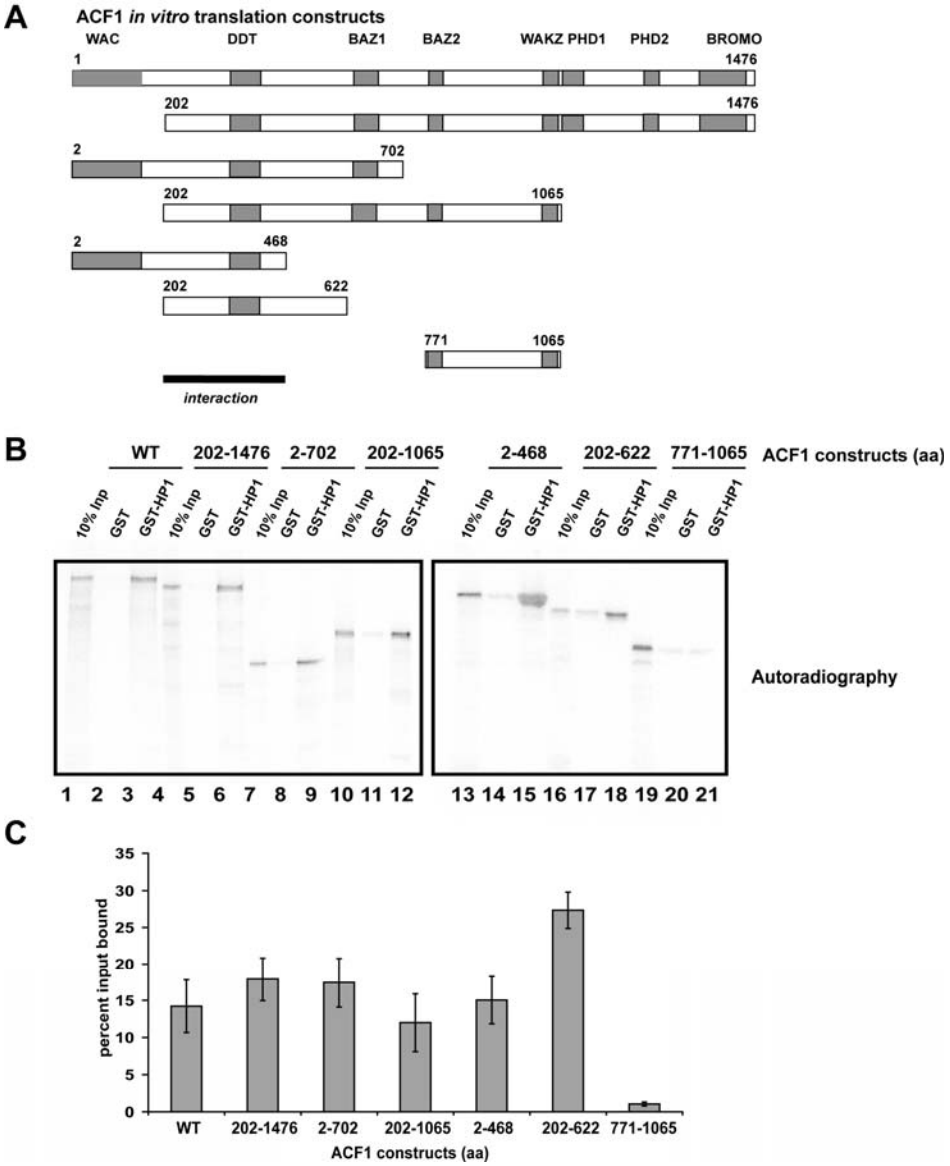

Figure 4.41 HP1a interacts with a region spanning the DDT domain (A) ACF1 constructs used for *in vitro* translation. **(B)** GST and GST-HP1a pull down with *in vitro* translated ACF1 constructs **(C)** Quantification of the binding affinities of the various ACF constructs. Error bars represent variations of three independent pull-downs.

In order to test if ACF facilitates HP1a binding to chromatin, ACF was added to unmodified or methylated salt-assembled chromatin in presence of recombinant HP1a (Figure 4.42.A). Consistent with previous observations, that HP1a needs two interaction modules for binding to chromatin, ACF complex facilitates binding of HP1a to H3K9 methylated chromatin (Figure 4.42.B; compare lanes 4 and 5). This was not due to higher affinity of ACF to methylated chromatin, as it bound equally well to unmodified chromatin. The binding of HP1a was independent of the presence of ATP (Figure 4.42.B; compare lanes 5 and 7). A quantification of the HP1a binding facilitated by ACF is shown in Figure 4.42.C.

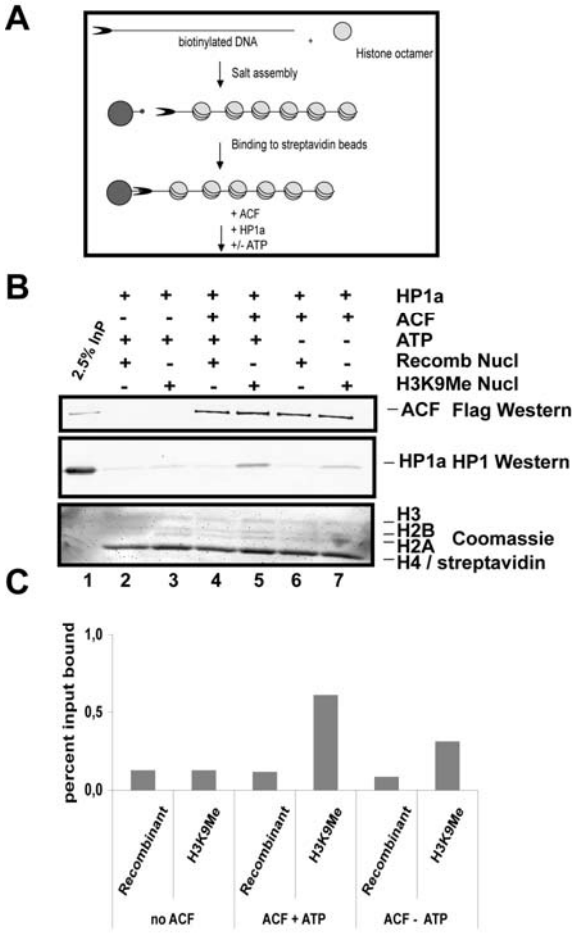

Figure 4.42 ACF facilitate HP1 binding to H3K9Me chromatin. (A) A scheme of the assay. **(B)** Salt assembled recombinant or H3K9Me chromatin bound to paramagnetic beads was incubated with HP1 in presence or absence of ACF and ATP for 1 hour at 26 ºC. After washing, the proteins remaining on the paramagnetic beads were separated by SDS-15% PAGE. ACF1 was detected with a FLAG antibody and HP1a with HP1 polyclonal antibody (upper panels). The corresponding histones are detected with Coomassie blue (lower panel). Lane 1 is corresponding to 50% ACF input and 2.5% HP1a input. **(C)** The graph displays bound HP1a as percent of input in B.

4.6.8 SU(VAR)3-9 interacts with HP1a and facilitates HP1a binding to chromatin

Another factor in *Drosophila* that is a suppressor of position effect variegation and interacts with HP1a *in vivo* is SU(VAR)3-9 (Aagaard et al., 1999; Schotta et al., 2002). SU(VAR)3-9 localizes to heterochromatin and sets the K9 methyl mark for. HP1a. The interaction between HP1a and SU(VAR)3-9 was mapped to the N-terminal region (amino acids 1-188) of SU(VAR)3-9 and to the C-terminal region of HP1a (amino acids 95-206) by yeast two-hybrid screen (Schotta et al., 2002). *In vitro* interaction between mouse SU39H1 and HP1α was mapped to the chromo shadow domain (Yamamoto and Sonoda, 2003). In order to biochemically map the interaction between recombinant SU(VAR)3-9 and HP1a, protein-protein interaction assays were performed (Figure 4.43). Full-length HP1a interacted with full-length SU(VAR)3-9. However, the interaction was lost when the N-terminus of SU(VAR)3-9 (Δ213) was removed (Figure 4.43.A). On the other hand, the interaction of HP1a with the SU(VAR)3-9 N-terminus was impaired when the chromo shadow domain was mutated (Figure 4.43.B; compare lanes 3 and 6 with 9). Hence, the chromo shadow domain of HP1a was important for protein-protein interaction (Brasher et al., 2000; Lechner et al., 2000; Yamamoto and Sonoda, 2003).

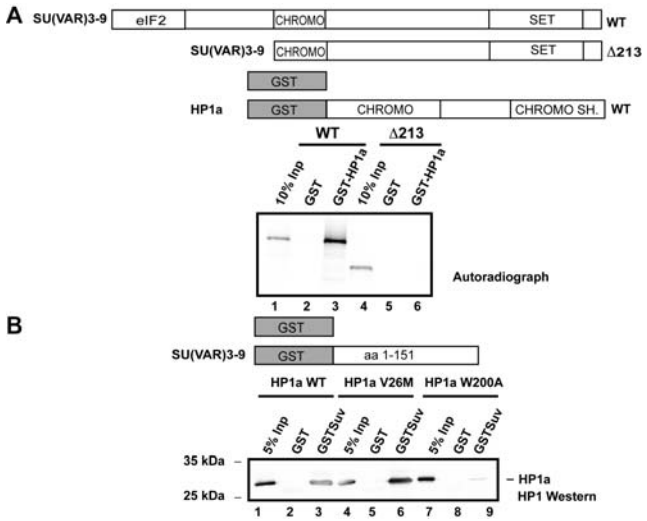

Figure 4.43 HP1a interacts with SU(VAR)3-9. (A) SU(VAR)3-9 constructs used for *in vitro* translation and GST constructs are shown at the top. The GST-pull down is shown at the bottom. SU(VAR)3-9 is detected by autoradiograph. **(B)** The upper panel shows GST constructs used for the pull down. The lower panel represents a HP1 western blot of GST pull down with recombinant HP1a WT (lane 1-3), HP1a (V26M) (lane 4-6) and HP1a (W200A) (lanes 7-9). HP1a was detected with HP1 polyclonal antibody.

Knowing that HP1a and SU(VAR)3-9 interact, it was of interest to find out whether SU(VAR)3-9 facilitates HP1 binding to chromatin. Therefore SU(VAR)3-9 and HP1a was mixed with unmodified and methylated salt-assembled chromatin (Figure 4.44.A). SU(VAR)3-9 has methyltransferase activity, and even though external SAM was not added, the specific inhibitor chaetocin (Greiner et al., 2005) (Results 4.2), was used as a control. SU(VAR)3-9 could couple HP1a to methylated chromatin, and the HMTase activity was not required for binding (Figure 4.44.B; compare lanes 4 and 5 with 6 and 7). The binding of HP1a to methylated chromatin was dependent on interaction with SU(VAR)3-9, as addition of the N-terminal deletion had no effect (Figure 4.44.B; compare lanes 5 and 7 with 9). Hence, this again confirms the importance of protein-protein interaction through the chromo shadow domain to stabilize the interaction of HP1a with methylated chromatin. A quantification of the SU(VAR)3-9 facilitated binding of HP1a to chromatin is shown in Figure 4.44.C. The binding of HP1a to methylated chromatin was about two times stronger in presence of SU(VAR)3-9.

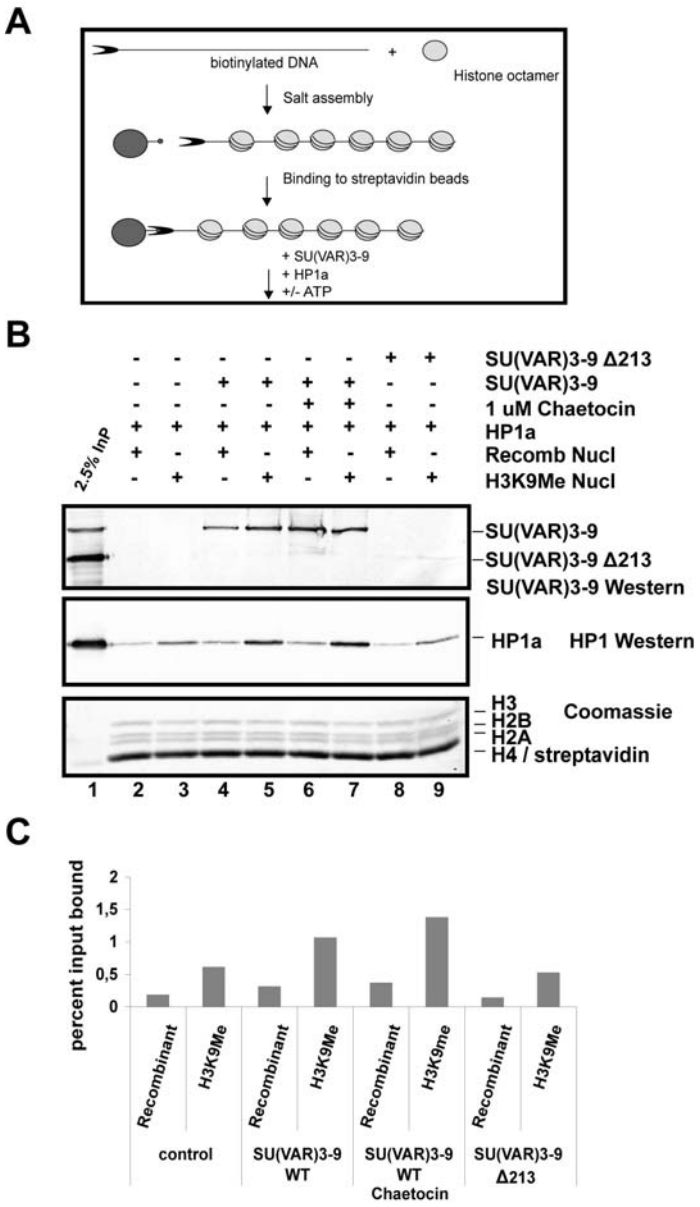

Figure 4.44 SU(VAR)3-9 facilitate HP1 binding to H3K9Me chromatin. (A) SU(VAR)3-9 couples HP1a to chromatin. HP1 was incubated with recombinant or H3K9Me chromatin in the presence of recombinant SU(VAR)3-9 WT (lanes 4-7) or Δ213 (lanes 8 and 9). The SU(VAR)3-9 specific HMTase inhibitor Chaetocin was added to 1 µM (lanes 6 and 7). The remaining SU(VAR)3-9 and HP1a on paramagnetic beads was detected by Western analysis and the histones by Coomassie blue**.** Lane 1 is corresponding to 100% SU(VAR)3-9 input and 2.5% HP1 input. (**B)** A quantification of HP1 bound in Figure D. The y- axis corresponds to percent input bound.

As shown above, interaction of SU(VAR)3-9 with HP1a was important to stabilize the binding to methylated chromatin. To further analyze the effect of stabilization, the same assay as described in Figure 4.44.A was performed with HP1a mutants (Figure 4.45). Under these conditions, the interaction with SU(VAR)3-9 had a greater impact on chromatin binding than H3K9 methylation. In other words, the HP1a (W200A)

binding to chromatin was more severely interrupted than for HP1a (V26M) (Figure 4.45.A; compare lane 3 with 6 and 9). It was also noticeable that HP1a (V26M) bound slightly stronger to unmodified chromatin, compared with wild type HP1a (Figure 4.45.A; compare lane 2 with 5). The quantification of the experiment is shown in Figure 4.45.B.

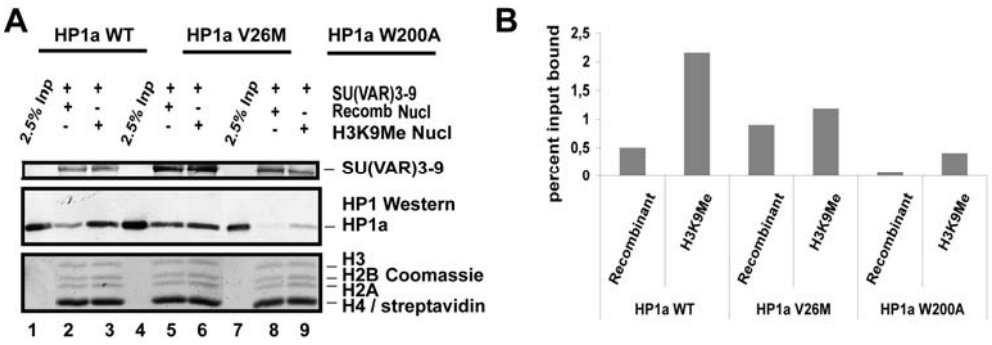

Figure 4.45 HP1a binding to H3K9Me chromatin was dependent on the chromo- and chromo shadow domain (A) SU(VAR)3-9 was added in the presence of HP1a WT (lanes 1-3), HP1a (V26M) (lanes 4-6) and HP1a (W200A) (lanes 7-9) to recombinant and H3K9Me chromatin. Bound SU(VAR)3-9 and HP1a were detected by Western analysis and histones were detected by Coomassie blue. **(B)** The graph corresponds to total HP1 binding in Figure F. The y- axis displays percent input bound.

4.7 HP1a and HP1c have distinct interaction factors

Drosophila HP1a and HP1c exhibit spatial distinct localization in the nucleus (Smothers and Henikoff, 2001). HP1a localizes to heterochromatin, whereas HP1c localizes exclusively to euchromatin. As discussed above, binding of HP1a to methylated chromatin was enhanced with interaction of auxiliary factors that are involved in heterochromatin formation. Hence, HP1c-interaction partners should be distinct from HP1a and confer to euchromatin.

4.7.1 Identification of HP1a interacting proteins

In order to examine the interaction partners of HP1a *in vivo,* an immunopurification strategy from transfected SL2 cells were used. Nuclear extract was prepared from Flag-HP1a stable cell lines (Figure 4.46.A), and pulled down Flag-HP1a complexes were analyzed by Western blotting and MALDI-TOF. To confirm an *in vivo* interaction between HP1a and ACF1, a pull down from a stable Purified Flag-HP1a from SL2 cells were probed with specific ACF1 antibody. As a control, nuclear

extract from un-transfected cells were used. ACF1 was found to interact weakly with Flag-HP1a (Figure 4.46.B). This interaction was stable in up to 500 mM NaCl (data not shown). Also SU(VAR)3-9 interacted specifically with HP1a in SL2 cells. The Flag-HP1a complex was analyzed by mass spectrometry (Figure 4.46.C). For several associated polypeptides, the apparent molar mass was corresponding to proteins previously shown to interact with HP1. Nipped-B is required for sister chromatid cohesion, and is therefore a functional adherin (Rollins et al., 1999). The human homolog NIPBL has been shown to interact with HP1α in transfected human embryonic kidney 293 (HEK293) cells (Lechner et al., 2005). In addition fission yeast Swi6/HP1 was required for cohesion at centromeres (Bernard et al., 2001). XNP is a homolog of human ATR-X, a nuclear SNF2 ATPase involved in mental retardation (Inlow and Restifo, 2004). HP1α interacted with mouse ATR-X in a yeast two-hybrid screen (Le Douarin et al., 1996). In addition, ATR-X co localize with HP1β at pericentromeric heterochromatin in Hela cells (McDowell et al., 1999), and *Caenohabditis elegans* XNP-1 has been found to act with HP1 during development (Cardoso et al., 2005). Dis3 was a novel HP1a-interacting protein. A cold-sensitive mutation of *dis3* in *Schitzosaccharomyces Pombe* is implicated in sister chromatid separation (Ohkura et al., 1988), linking HP1a and Dis3 with Nipped-B.

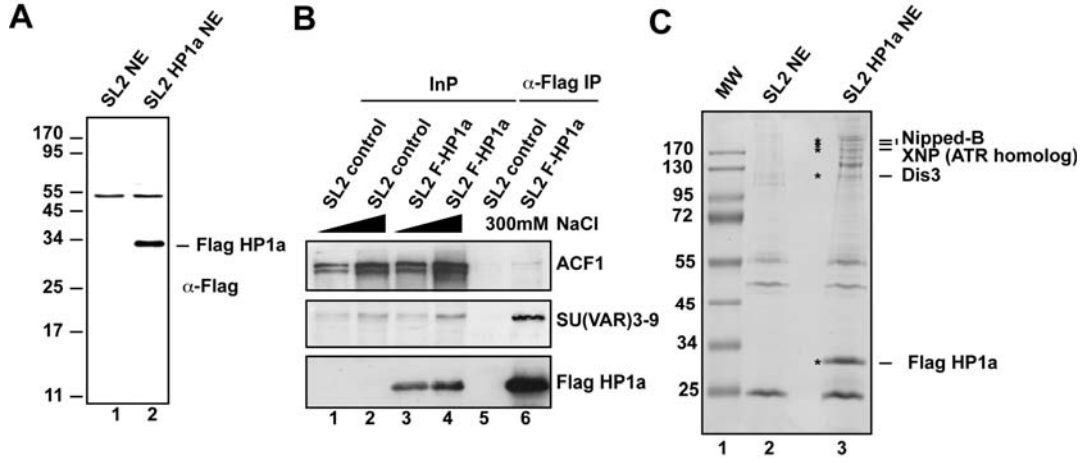

Figure 4.46 Identification of HP1a interacting proteins by MALDI-TOF. (A) Nuclear extracts derived from SL2 cells or SL2 line stably expressing Flag-HP1a were separated on a SDS-15% PAGE, immunoblotted and detected with a α-Flag antibody**. (B)** ACF1 co-purifies weakly with stably transfected Flag-HP1a. Nuclear extracts derived from SL2 cells or SL2 line stably expressing Flag-HP1a were subjected to immunoprecipitation with α-Flag antibody. Input (Inp) is two and four percent. 300 mM indicate concentrations of three NaCl washes. **(C)** A colloidal blue stained SDS-10% PAA gel with α-Flag immunoprecipitations as described in Figure B. MW indicates molecular weight markers. Co-purifying proteins identified by MALDI-TOF analysis are indicated by asterisk and named (left).

4.7.2 Identification of HP1c interacting proteins

In order to examine the interaction partners of HP1c *in vivo,* an immunopurification strategy from transfected SL2 cells as described in Results 4.7.1 were used. Nuclear extract was prepared from Flag-HP1c stable cell lines (Figure 4.47.A), and pulled down Flag-HP1c complexes were analyzed by mass spectrometry (Figure 4.47.B). Two distinct proteins, compared with the HP1a complex were identified. *Without children (woc)* was shown to be a transcription factor involved in ecdysone synthesis (Wismar et al., 2000), but has also recently been implicated in prevention of telomeric fusions (Raffa et al., 2005). CG8092 is a novel zink finger protein.

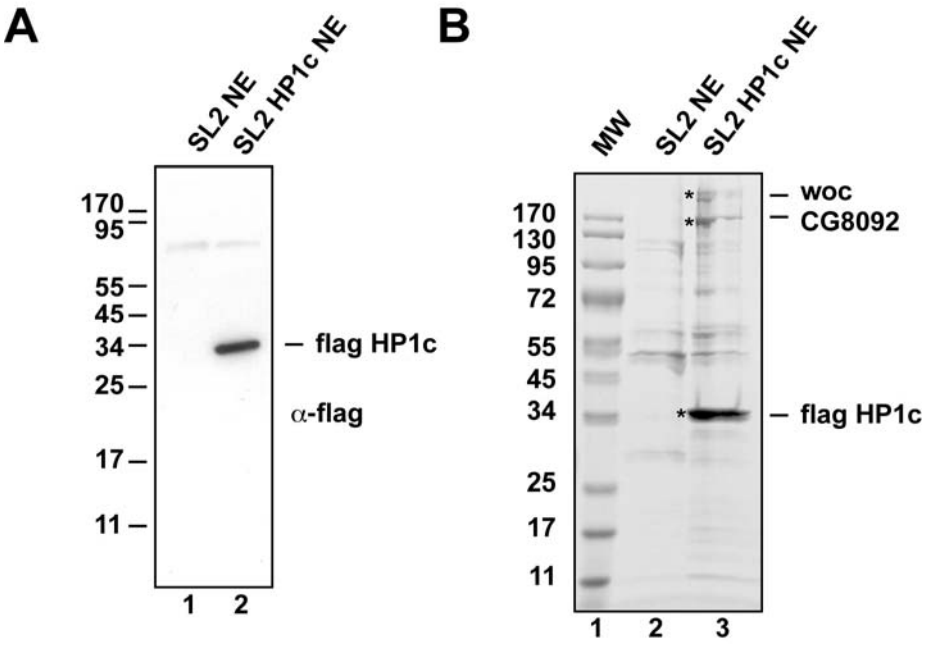

Figure 4.47 Identification of HP1c interacting proteins by MALDI-TOF. Nuclear extracts derived from SL2 cells or a SL2 cell-line stably expressing Flag-HP1c were subjected to immunoprecipitation with α-Flag antibody. **(A) I**mmunoprecipitations were separated by SDS-15% PAGE, immunoblotted and detected with a α-Flag antibody. **(B)** A colloidal blue stained SDS-4-20% PAA gel with α-Flag immunoprecipitations as described in Figure A. MW indicates molecular weight markers. Co-purifying proteins identified by MALDI-TOF analysis are indicated by asterisk and its identity to the left.

4.7.3 *In vitro* GST-HP1a and HP1c pull down experiment

As discussed above, HP1a and c have distinct interacting complexes. To further support the theory that distinct proteins are involved in coupling of HP1a and c to chromatin, a pull down was performed. GST-HP1a or c was incubated with *in vitro* translated ACF1 and SU(VAR)3-9. HP1c did not interact with ACF-1 nor SU(VAR)3-9, hence supporting the theory that these two proteins couples HP1a to heterochromatin. It may be that HP1c is coupled to by other factors to H3K9 methylated
euchromatin.

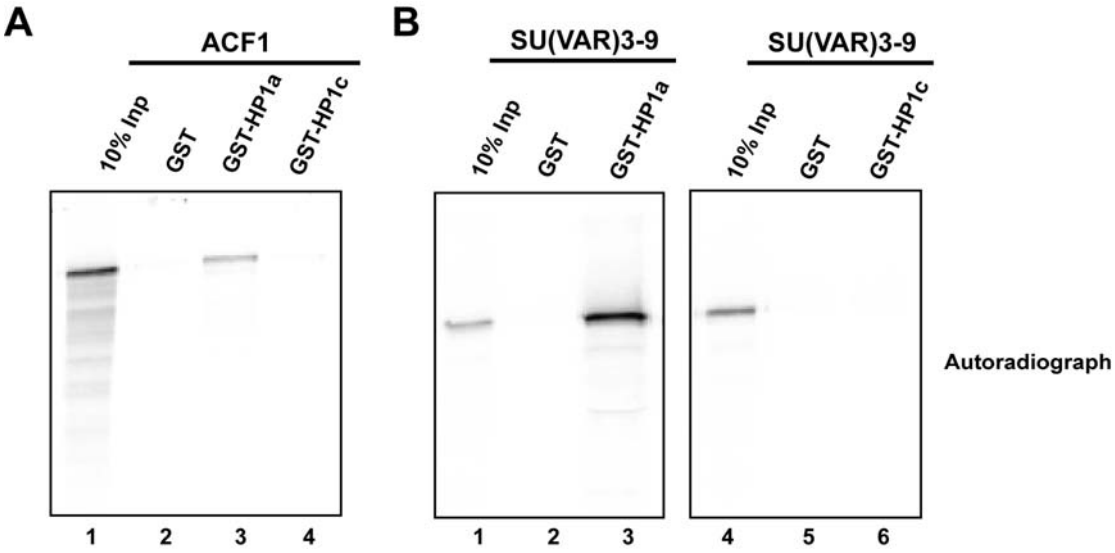

Figure 4.48 HP1c does not interact with SU(VAR)3-9 or ACF1. **(A)** A GST pull-down is shown with *in vitro* translated ACF1 full length and GST-HP1a and GST-HP1c. ACF1 is detected with autoradiography. **(B)** A GST pull-down as described in (A) with *in vitro* translated SU(VAR)3-9 . SU(VAR)3-9 is detected by autoradiography.

5. Discussion

This work focuses on histone H3 lysine 9 methylation which is associated to transcriptional silencing *in vivo* (Peters et al., 2003; Rice et al., 2003; Schotta et al., 2004). Here the well known *Drosophila* H3K9 HMTase SU(VAR)3-9 and a new HMTase homologous to G9a were characterized *in vitro.* H3 lysine 9 was identified as their sole or at least main substrate. Supporting the histone code hypothesis, the chromo domain of HP1 recognizes and binds H3K9 methyl. However, the binding of *Drosophila* HP1a to methylated H3K9 within a nucleosomal context requires a bimodal interaction of the chromo domain with H3K9Me and interaction of the chromo shadow domain with an auxiliary factors (SU(VAR)3-9 and ACF).

5.1 SU(VAR)3-9

In summary, full-length recombinant SU(VAR)3-9 adds three methylgroups to full-length H3 and only two methylgroups to an H3-tail peptide. The transfer of two methylgroups to the H3-tail peptide is achieved in a nonprocessive manner. SU(VAR)3-9 requires the N-terminus for homodimerization to retrieve full activity *in vitro.* The interaction occurs within two parts of the N-terminus.

5.1.1 Recombinant SU(VAR)3-9 is a nonprocessive enzyme

It has been described that *Drosophila* SU(VAR)3-9 methylates H3 lysine 9 (Czermin et al., 2001; Schotta et al., 2002). Recombinant SU(VAR)3-9 methylates H3K9 and preferred free H3 molecules to reconstituted nucleosomes. This indicates that SU(VAR)3-9 has a higher activity towards non-nucleosomal histones. However, immunostainings of polytene chromosomes of *SU(VAR)3-9* null mutant salivary glands revealed that SU(VAR)3-9 is required for mono- to dimethylation in the chromocenter and trimethylation in the chromocenter core (Ebert et al., 2006; Ebert et al., 2004; Schotta et al., 2002). In addition it has been shown that only a small proportion of histones in mammalian cells are non-nucleosomal and a significant fraction of these carry H3K9 monomethylation (Loyola et al., 2006). This rather suggest that *in vivo* SU(VAR)3-9 methylates H3 within nucleosomes. Interestingly, SU(VAR)3-9 has similar affinity toward unmodified and monomethylated H3-tail

peptide. Although has been shown that SU(VAR)3-9 mainly di- and trimethylates H3K9 *in vivo* (Ebert et al., 2006; Schotta et al., 2002), it can also add methylgroups to unmodified H3. Supporting our finding, is the interaction of SU(VAR)3-9 with histone deacetylase HDAC1 (Czermin et al., 2001). SU(VAR)3-9 may directly methylate H3K9 after removal of an acetyl group by HDAC1. *In vitro* trimethylation of full-length H3 by SU(VAR)3-9 is less efficient than dimethylation (33% versus 54% respectively; Figure 4.6). It remains puzzling to observe a poor trimethylation of H3-tail peptide by SU(VAR)3-9 *in vitro*. However, a steric hindrance in the peptide binding channel of the SET domain as observed for the monomethylase SET7/9 (Zhang et al., 2003b) can be excluded because SU(VAR)3-9 trimethylates the H3 molecule. Supporting this result is the finding that K9 dimethylated H3-tail peptide is also a poor substrate for the human SUV39H1 *in vitro* (Chin et al., 2006; Czermin et al., 2001; Rea et al., 2000) despite the fact that *Suv39h1* and *Suv39h2* double null embryonic stem cells display a dramatic decrease in H3K9 trimethylation (Peters et al., 2003; Rice et al., 2003). The discrepancy between *in vitro* and *in vivo* observations could be due to interactions with additional factors (Czermin et al., 2001; Firestein et al., 2000; Zhang et al., 2006) or post-translational modification of SU(VAR)3-9 (Aagaard et al., 2000; Firestein et al., 2000) regulating the trimethylation of nucleosomal H3 *in vivo*. In addition there are uncharacterized SET domain proteins that may add a third methylgroup to dimethylated H3K9 (Schotta et al., 2004). Several studies describe the mechanism of methyl transfer by different HMTases revealing differences in their ability to transfer methyl groups. Human SET7/9 for example, mainly monomethylates H3K4 albeit having a low efficiency for dimethylation (Kwon et al., 2003; Xiao et al., 2003; Zhang et al., 2003b). On the other hand, *Neurospora crassa* DIM-5 and murine G9a both trimethylate H3K9, in a processive manner (Patnaik et al., 2004; Zhang et al., 2002; Zhang et al., 2003b). This work shows that SU(VAR)3-9 adds two methylgroups to the H3 peptide in a non-processive manner. Recently, it was shown that the mammalian homolog, SUV39H1, also is a non-processive enzyme (Chin et al., 2006). The processivity of an HMTase depends on the exchange of S-Adenosyl methionine (SAM) and the reaction product S-Adenosyl homocysteine (SAH) within the SET domain. For example, DIM-5 is a processive enzyme because it can exchange SAM and the reaction product S-Adenosyl homocysteine (SAH) without releasing the peptide (Zhang et al., 2003b). Zhang and colleagues solved the crystal structure of the trimethylase DIM-5 and

argue that its SAM-binding pocket is larger than necessary due to the highly conserved residues (R155, W161, Y204 and R238) within the SET domain facilitating exchange of the SAH and SAM (See Figure 5.1.A). Indeed, a DIM-5 R238H mutant has impaired catalytic activity, with substantial amounts of unmodified, mono and dimethylated peptide even after extended incubation (Zhang et al., 2003b). The comparison of SU(VAR)3-9, SUV39H1 and SET7/9 with DIM-5 ^{238}RΦΦNHS^{243} motif (where Φ indicates a hydrophobic residue) reveal that all have a histidine residue instead of an arginine at this position (HΦΦNHS). However, the yeast SU(VAR)3-9 homolog Clr4 has arginine at this position (^{406}RΦΦNHS^{411}) arguing for it being a trimethylase (Min et al., 2002). Sedimentation transfer difference NMR measurements of SU(VAR)3-9 indicate that SAM binds in a similar manner as shown by a crystal structure of SET7/9 (Seeger et al., 2005). Indeed, it has been shown that if the corresponding histidine is mutated to arginine (H320R) in SUV39H1 the activity is strongly increased *in vitro* (Rea et al., 2000). To test this hypothesis, we generated a SU(VAR)3-9 (H557R) mutant (Figure 5.1.B). After incubation with unmodified H3 peptide (upper panel) and SAM for one hour the reaction products were analyzed by MALDI-TOF. All unmodified peptide were converted into di- and trimethylated peptides supporting the notion that the arginine makes the SAM-binding pocket larger (Compare with figure 4.3.A). Hence, a reason for the H3 peptide to be a poor trimethylation substrate for SU(VAR)3-9 may be that binding of the full-length H3 molecule by SU(VAR)3-9 facilitate a conformational change of the SAM binding pocket changing the affinity for the methylated substrate. Although, it is worth noticing that the (H557R) mutation did not make SU(VAR)3-9 a processive enzyme.

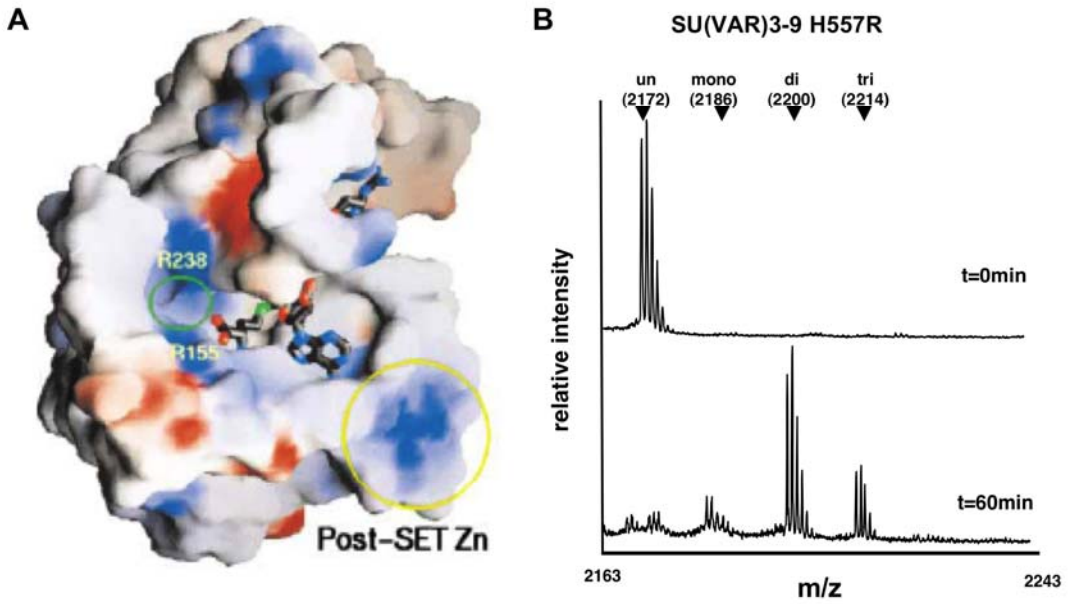

Figure 5.1 Processivity of SET domain enzymes. (A) A part of the SET domain structure of DIM-5 (Zhang et al., 2002). SAM is bound in a large surface pocket of DIM-5, allowing for processive methylation. The green circle indicates the location where SAM and SAH bind. The yellow circle indicates the postSET domain. The surface is displayed with charge distribution (blue for positive, red for negative and white for neutral). SAM is displayed as a stick model. The figure is taken from (Zhang et al., 2003b). **(B)** A methylation reaction SU(VAR)3-9 H557R with H3 peptide (aa 1-19) and SAM analyzed by MALDI-TOF. The point mutation H557R within the SU(VAR)3-9 SET domain corresponds to DIM-5 R238, and results in a larger surface pocket for SAM binding and higher trimethylase activity. Upper panel, time point zero (t = 0 min); lower panel, after one-hour incubation (t = 60 min).

5.1.2 Initial kinetics of SU(VAR)3-9

Full-length SU(VAR)3-9 transfers two methyl groups to the H3 peptide with a high turnover number. Indeed, the turnover rate is 4.5 fold higher than for murine G9a (Patnaik et al., 2004) and 33 fold higher than for human SUV39H1 (Chin et al., 2006), suggesting that SU(VAR)3-9 methylates a H3 peptide better than mG9a and SUV39H1 *in vitro*. Deletion of the N-terminus of SU(VAR)3-9 results in a more than 20 fold reduction of the turnover number. Actually, SU(VAR)3-9 Δ213 has a similar turnover rate as full-length human SUV39H1 and SET9 (Chin et al., 2005; Trievel et al., 2002). However, both SU(VAR)3-9 and SUV39H1 have significantly higher K_m[SAM] values than mG9a and hSET7/9, suggesting that the concentration of SAM may regulate their catalytic activity *in vivo*. In a cell, the SAM concentration varies

between 20 and 40 μM depending on cell type (Hoffman et al., 1980). With a K_m[SAM] of 26 μM, SU(VAR)3-9 arguing that *in vivo* the rate of methylation is optimal the higher SAM concentration. In *D. melanogaster* SU(Z)5 is involved in the biosynthesis of SAM (Larsson and Rasmuson-Lestander, 1994). SU(Z)5 suppresses position effect variegation in *Drosophila,* enhances the phenotype of *Polycomb* mutation (Larsson et al., 1996) and is embryonically lethal (Larsson and Rasmuson-Lestander, 1998). In other words, SU(Z)5 regulates chromatin structure through production of SAM, which is necessary for the activity of histone and DNA methyltransferases. It would be interesting to see whether SU(Z)5 directly interacts with SU(VAR)3-9 as a regulator of heterochromatin formation.

Higher concentrations of H3 molecules had an inhibitory effect on SU(VAR)3-9, which was also shown for SUV39H1 (Chin et al., 2006). Several attempts were made to determine the K_m of SU(VAR)3-9 for histone H3 molecules without success. The double reciprocal plots showed a nonlinear relationship between 1/Velocity and 1/H3 that became nearly vertical at high concentrations. The inhibitory effect of H3 observed was above 2.5 μM, which was higher than the values for SUV39H1 (0.55 μM) (Chin et al., 2006). This might be due to the much higher catalytic activity of SU(VAR)3-9. Methylation of H3 in a mixture of all four histones turned out to be very efficient (more than 85% methylation). Perhaps the histone octamer would be a better substrate to determine the K_m for H3.

5.1.3 SU(VAR)3-9 requires the N-terminus for its full enzymatic activity

Interestingly, deletion of the N-terminal portion of SU(VAR)3-9 results in a > 90% loss of activity. A major finding was that the N-terminus allows the formation of homodimers that are necessary for full activity of SU(VAR)3-9 *in vitro.* This was observed by a concentration-dependent increase in specific methylation activity expressed as the number of SAM molecules converted per molecule of enzyme. In addition, SU(VAR)3-9 migrated with a molecular weight predicted for a dimer on gel filtration columns and density gradients. Crystallization of SET domain proteins such as *Schitzosaccharomyces pombe* Clr4, human SET7/9 and *Neurospora crassa* DIM-5

revealed they exist as monomers *in vitro* (Min et al., 2002; Wilson et al., 2002; Xiao et al., 2003; Zhang et al., 2002). However, structural analysis of a viral H3K27 HMTase showed a butterfly-shaped head to head symmetric dimer (Manzur et al., 2003). In addition, pea Rubisco LSMT SET domain methyltransferase has been shown to form trimers under crystallization conditions through domain swapping (Trievel et al., 2002). The mammalian HMTase G9a heterodimerise with GLP (G9a like protein) of which it shares share 63% sequence similarity (Ogawa et al., 2002; Tachibana et al., 2005). G9a-GLP heterodimerise to exert their enzymatic activity *in vivo* (Ogawa et al., 2002; Tachibana et al., 2005). Hence, dimerisation of HMTases may regulate the activity *in vivo* through by modulating the levels of catalytic activity. The dimerisation motifs were mapped by GST pull down to two regions within the N-terminus of SU(VAR)3-9. More precisely, amino acids 1-152 and 152-213 can interact intra- or intermolecularly. This suggest a formation of a dimer by domain swapping (Liu and Eisenberg, 2002). 3D domain swapping is a mechanism for two or more proteins to create bonds through the exchange of their identical domains (Liu and Eisenberg, 2002) as has been observed for the LSMT trimer (Trievel et al., 2002) and other proteins. RNAse A, for example forms dimers *in vivo* (Park and Raines, 2000), formed by domain swapping and thereby display higher enzymatic activity on double-strand RNA than the monomer *in vitro* (Gotte et al., 1999). Perhaps by domain swapping SU(VAR)3-9 displays higher activity because one SET domain can “hand over” the monomethylated H3K9 tail to the other SET domain. Supporting this idea is the result that the full-length SU(VAR)3-9 has 20 times higher catalytic capacity than the N-terminal truncated protein. High concentration of protein favors 3D domain swapping and oligomers may form (Liu and Eisenberg, 2002).

Although *in vitro* under these conditions, SU(VAR)3-9 only dimerises, it can not be excluded that *in vivo* it can oligomerise. It is well accepted that SU(VAR)3-9 has a dosage-dependent effect on PEV (Locke et al., 1988; Wustmann et al., 1989). In analogy to SU(VAR)3-9, the over expression of SUV39H1 in mammalian cells results in accumulation and formation of nuclear bodies (Firestein et al., 2000). The fact that the N-terminus is responsible for dimerisation of SU(VAR)3-9 therefore may indicate a role for this domain in the dosage-dependent effect on PEV.

Further deletion from the N-terminus including the chromo domain of SU(VAR)3-9 results in a catalytically inactive protein. Following this observation, Chin and coworkers showed that the deletion of the chromo domain of SUV39H1 has the same effect on activity (Chin et al., 2006). The chromo domain of HP1 binds H3K9Me peptides (Bannister et al., 2001; Jacobs and Khorasanizadeh, 2002; Jacobs et al., 2001; Lachner et al., 2001; Nielsen et al., 2002). Two point mutations within the chromo domain of SUV39H1 that are conserved among most chromo domain proteins also resulted in loss of enzymatic activity (Chin et al., 2006). However, the work done in this thesis showed that full-length SU(VAR)3-9 did not bind preferentially to H3K9Me chromatin *in vitro* (Figure 4.44). Actually the N-terminal truncation Δ213 which carries the chromo domain intact, bound very poorly to unmodified and H3K9Me chromatin. The *in vivo* localization of human SUV39H1 depends on the N-terminus and chromo domain. This was shown in mammalian cells where a transfected truncated SUV39H1 protein consisting of only the N-terminus and the chromo domain bound efficiently to heterochromatin (Melcher et al., 2000). Whether the chromo domain binds H3K9Me, or is necessary for correct folding of SU(VAR)3-9 and thereby modulating the enzymatic activity needs to be further elucidated.

5.1.4 Inhibitors of SU(VAR)3-9

Inhibitors of histone deacetylases (HDACs) and DNA methyltransferases are used for cancer drug therapy (for recent review, see (Santos-Rosa and Caldas, 2005)). However, histone methylation can also be linked to cancer (Santos-Rosa and Caldas, 2005). The SET1 family protein MLL is named after its involvement in leukemia: mixed lineage leukemia (Hess, 2004). Most of the chromosomal rearrangements involve the N-terminal part of MLL (Hess, 2004), which does not contain the SET domain, but it is suggested that its HMTase activity may also play a role. Furthermore, Polycomb repressive complex 2 (PRC2) HMTase EZH2 is highly expressed in metastatic prostate cancer, lymphomas and breast cancer (Kleer et al., 2003; Varambally et al., 2002). It has been proposed that the PRC2 complex is central to proliferation control acting downstream of the pRB-E2F pathway and therefore misexpression of EZH2 seems likely to contribute to cancer (Bracken et al., 2003). In addition the H3K9 HMTase RIZ1 has been shown to be a tumour suppressor (Du et al., 2001; Kim et al., 2003). HMTases utilizes S-Adenosyl methionine with

S-Adenosyl homocysteine (SAH) as the end product formed after methylation. It was observed that H3K9 and not H3K4 methylation in U2OS cells were sensitive to higher level of SAH (Kim et al., 2003). The authors showed that *in vitro* the HMTase activity RIZ1 was 100% inhibited with 5 μM SAH (Kim et al., 2003). However, SU(VAR)3-9 was not that sensitive to SAH with 50% inhibition (IC_{50}) at 40 μM. Adenosylornithine (AO), is another strong competitive inhibitor of methyltransferases that form 5-methylcytosine or N^6-methyl adenosine on DNA and RNA (Barbes et al., 1990). However, AO had an even weaker inhibitory effect on SU(VAR)3-9 than SAH with an IC_{50} of 100 μM.

The finding of specific inhibitor of a histone methyltransferase such as SU(VAR)3-9 may increase our understanding on transcriptional regulation and disease control. Therefore a screen was performed for specific inhibitors of SU(VAR)3-9 by D. Greiner in our lab (Greiner et al., 2005). One of the strongest specific inhibitors identified was a mycotoxin, called chaetocin. Chaetocin inhibited SU(VAR)3-9 with an apparent IC_{50} of 0.6 μM but also had a strong inhibitory effect on other K9 histone methyltransferases such as SUV39H1, G9a and DIM5 (Greiner et al., 2005). Chaetocin was shown to be a competitive inhibitor of SAM (Greiner et al., 2005) as has been shown for SAH for mG9a (Patnaik et al., 2004) and for SUV39H1 (Chin et al., 2006). When testing the effect of different concentration of chaetocin on SU(VAR)3-9 methylation over time, an inhibition by chaetocin could be observed after 2.5 minutes (1.5-4.5 μM). Chaetocin at these concentrations blocks the SU(VAR)3-9 active site and thereby the binding of SAM for enzymatic activity. On the other hand chaetocin did not prevent binding of SU(VAR)3-9 to chromatin. The effect on K9 methylation was also observed in *Drosophila* SL2 cells although chaetocin at a concentration of 0.5 μM caused growth retardation of 24-48 hours (Greiner et al., 2005). Synthesis of chaetocin derivatives with less toxicity may have experimental and therapeutic applications in the future.

5.1.5 SU(VAR)3-9 monoclonal antibodies

Two monoclonal antibodies against SU(VAR)3-9 were developed by E. Kremmer. They antibodies recognized recombinant SU(VAR)3-9 and the epitopes were mapped to a region between the chromo and preSET domain (amino acids 285 -492) for clone

6C9 and to the SET domain for clone 3D9. Both antibodies were working in immunoprecipitation with *in vitro* translated SU(VAR)3-9. As described above, the SET domain is very conserved. Therefore, as expected the 3D9 antibody recognized many more bands than the 6C9 antibody in a western blot of nuclear extract from 0-12 hour embryos. The 6C9 antibody recognized only two bands corresponding to the size of endogenous SU(VAR)3-9, but it was not very sensitive. In order to confirm the specificity of the 3D9 antibody, proteins were extracted from *Drosophila* Schneider cells treated with RNA interference against SU(VAR)3-9 and from embryos of *SU(VAR)3-9*^{06} null flies (Schotta et al., 2002). However, even if the 3D9 antibody recognized recombinant SU(VAR)3-9 there was no specific recognition of endogenous SU(VAR)3-9 on western blots derived from such extracts. It was not clear whether other SET domain proteins detected by 3D9 antibody masked the SU(VAR)3-9 signal or if 3D9 was less sensitive toward endogenous SU(VAR)3-9. These antibodies detects recombinant SU(VAR)3-9 well and can therefore be used for this. E. Kremmer has very good experience with GST-tagged proteins, and therefore it would be an idea to generate monoclonal antibodies against the N-terminus of SU(VAR)3-9 (GST 152-213) since this region is not so conserved.

5.2 dG9a

In mammalian cells, G9a was found to be an euchromatic H3K9 methyltransferase (Esteve et al., 2005; Peters et al., 2003; Rice et al., 2003). This work presents the characterization of the enzymatic activity of *Drosophila* G9a (Stabell et al., 2006). dG9a adds three methylgroups toward H3K9 and K27, with a preference for K9. Surprisingly, dG9a also methylated H4 with specificity for K8, K12 or K16. While this work was carried out, another group showed that *in vitro* dG9a is a H3 methyltransferase and suppresses PEV *in vivo* (Mis et al., 2006).

5.2.1 Substrate specificity of dG9a *in vitro*

Mis and colleagues performed *in vitro* methylation assays with a truncated GST-dG9a (amino acids 1261 – 1637). They observed methylation of H3 and an H3 peptide (amino acids 1-20) (Mis et al., 2006). Here we show the *in vitro* HMTase activity of N-terminal Flag-tagged truncated version of dG9a (amino acids 789 – 1637) expressed in Sf9 cells using the baculovirus system. In contrast to Mis et al. (2006),

Flag-tagged dG9a methylates recombinant and native H3 and H4 molecules. A mutation within the conserved SET domain (H1536K) of dG9a confirms the specificity toward H3 and H4. However, it cannot be excluded that the H3K27 and H4 activity may be due to the deletion of the N-terminus of dG9a. Although, dG9a immunoprecipitated from (0-12 h) embryos methylated both histone H3 and H4 supporting the *in vitro* data. Furthermore, recombinant dG9a had no detectable activity toward nucleosomal arrays. The activity on nucleosomal arrays using immunoprecipitated dG9a was only toward histone H4. This argues for a nucleosomal H4 methyltransferase co-purifying with dG9a or that specific interaction proteins changes the specificity of dG9a to H4 in a nucleosomal environment.

The analysis of dG9a distribution on polytene chromosomes from salivary glands of third instar larvae reveals that dG9a localize to euchromatic regions with no staining in the chromocenter (Stabell et al., 2006). Therefore, it may be concluded that dG9a methylates H3 and H4 within euchromatin.

Mouse G9a has been shown to methylate H3K9 and K27 (Tachibana et al., 2001; Tachibana et al., 2002). The specific activity of dG9a on H3 is mapped to K9 and K27 using H3 molecules carrying a lysine to alanine replacement at position 9 and 27 and subsequent MALDI-TOF analysis. Based on these *in vitro* observations, it can be concluded that dG9a specifically methylates K9 and K27 on H3 with a preference toward K9. In addition, dG9a can add three methyl groups. Although dG9a can trimethylate, the majority is mono- and dimethylation. From the MALDI-TOF analysis 72% of total methylated K9 is mono- and dimethylated. This was not the case for a processive enzyme like DIM-5 where the majority of H3 peptides were trimethylated after 30 minutes (Zhang et al., 2003b). *In vitro* mammalian G9a was also able to transfer three methyl groups in a processive manner, but the turnover rate was seven times slower on a H3K9 dimethyl substrate (Patnaik et al., 2004). In mG9a knockout embryonic stem cells, euchromatic H3K9 mono- and dimethylation was severely reduced (Peters et al., 2003; Rice et al., 2003). Hence, dG9a may also be responsible for mono- and dimethylation of K9 within euchromatic regions in *Drosophila*. Methylation of H3K9 and K27 is mainly correlated with silencing (Martin and Zhang, 2005), suggesting an involvement of dG9a in transcriptional repression *in vivo*. This needs to be further elucidated.

In contrast to mG9a (Tachibana et al., 2001), dG9a also methylates histone H4. So far the only lysine residue shown to be methylated in H4 is lysine 20 and the HMTases identified with this activity were hPR-Set7/dSET8 (Fang et al., 2002; Rice et al., 2002), hNSD1/dAsh1 (Beisel et al., 2002; Rayasam et al., 2003) and human/*Drosophila* Suv4-20 (Schotta et al., 2004). It is surprising that dG9a can methylate H4 carrying a mutation of lysine 20 to alanine. The MALDI-TOF analysis confirms that dG9a trimethylates a lysine residue within amino acid 4 to 17 of the H4 tail. When using H4 N-terminal deletion mutants in the methylation assay with dG9a, dG9a methylates H4 in which the first five amino acids of the N-terminus are deleted. However, the activity is lost when the N-terminal 10 amino acids are deleted. This suggests that the substrate is K8, but considering that the minimal substrate specificity for mG9a surrounding K9 contains seven amino acids (TARKSTG) (Chin et al., 2005) the substrate could also be K12 or K16. These three residues have been shown to be acetylated *in vivo* (Santos-Rosa and Caldas, 2005), and a methylation of any of these lysines remains to be identified. A MALDI-TOF approach identified a mass shift of a calf H4 peptide (amino acid 11-15) containing K12 (Zhang et al., 2003a) indicating this may be the methylation site of dG9a. The specific dG9a-methylation site on H4 needs to be further characterized. Generating H4 K8, K12 and K16 point mutants and testing in vitro activity of dG9a can give an answer to the specificity. When knowing the specific H4 lysine that dG9a methylates, an antibody can be raised to test on native *Drosophila* histones *in vitro* and existence and possible localization of this H4 mark *in vivo.*

Mouse G9a was also shown to methylate histone H1 (Tachibana et al., 2001). In this study both mouse and *Drosophila* G9a could methylate the single *Drosophila* H1 variant. As the histone H1 family is the most divergent class of the histones (for review see (Doenecke et al., 1997)), it remains to be seen if a more conserved lysine residue is methylated.

5.2.2 dG9a exists in protein complexes

Mouse G9a has been shown to be part of silencing complexes such as the E2F6 complex (Ogawa et al., 2002), CtBP1 (Shi et al., 2003) and CDP/cut (Duan et al., 2005; Nishio and Walsh, 2004). This work shows that *Drosophila* dG9a is present in

complexes of 440-670 kDa. The molecular mass of dG9a is 180 kDa; therefore a limited number of proteins could be present in these complexes. In contrast to SU(VAR)3-9, E(Z) and other HMTase activities purified from the Biorex 70 250 mM fraction (Czermin et al., 2001), the dG9a complexes binds more strongly to the cation exchange resin and eluted with 500 mM NaCl. The histone deacetylase RPD3 (HDAC1), which is also present in the E(Z) complex (Czermin et al., 2002), was found to specifically interact with G9a. In contrast, SUZ12 another component of the E(Z) complex does not, indicating that RPD3 interacts with dG9a in the absence of SUZ12. Mammalian G9a was found to be part of a repression complex with HDAC1 and Gfi1 (Growth independent factor 1) (Duan et al., 2005). However, mG9a could repress a reporter gene in Hela cells without requiring HDAC activity (Tachibana et al., 2002). This suggests that Rpd3 may contribute to the repression of dG9a at euchromatic target genes in *Drosophila.*

Another protein that was co-precipitating with dG9a was the ATPase ISWI, which is the catalytic subunit of at least three chromatin remodeling complexes in *Drosophila*: ACF, CHRAC and NURF (for review see (Bouazoune and Brehm, 2006)). ISWI was also co-eluting with dG9a on a gelfiltration column. Interestingly, both *dG9a* and *NURF301* are involved in the ecdysone regulatory pathway (Badenhorst et al., 2005; Stabell et al., 2006). Ecdysone (20-hydroxyecdysone) is a steroid hormone that is synthesized from dietary cholesterol, and pulses of ecdysone influence *Drosophila* metamorphosis and differentiation through its life-cycle (Figure 5.2) (Thummel, 1995).

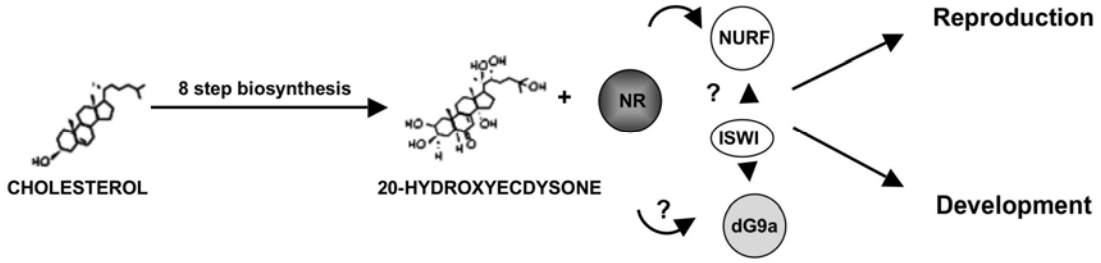

Figure 5.2 A theoretical scheme of the ecdysone biosynthesis and the function in *Drosophila* life-cycle. NR; ecdysone nuclear receptor, NURF, nucleosome remodeling factor and ISWI, imitation switch.

Binding of the nuclear ecdysone receptor to the ecdysone hormone results in activation of ecdysone-responsive genes (Thummel, 1995). The NURF complex was

shown to be a coactivator of the ecdysone receptor steroid hormone-dependent transcription, and the interaction with the ecdysone receptor was dependent on ecdysone (Badenhorst et al., 2005). On the contrary, the dG9a RNAi mutants are not rescued by feeding ecdysone arguing for a downstream effect of the ecdysone biosynthesis and metabolism (Stabell et al., 2006). Another element supporting the involvement in ecdysone induced transcription of dG9a is an interaction with 40S Ribosomal protein which in immunostainings and *in situ* hybridization was present at sites of ecdysone-induced transcription in the nucleus (Brogna et al., 2002). Mammalian G9a was shown to be a coactivator of nuclear androgen receptor target genes through cooperation with other coactivators (Lee et al., 2006). Another study showed that mammalian SHP (small heterodimer partner), an atypical orphan nuclear receptor interacts with high affinity with G9a and HDAC1 (Boulias and Talianidis, 2004). Repression of certain but not other SHP regulated genes were dependent on deacetylation and H3K9 methylation (Boulias et al., 2005; Boulias and Talianidis, 2004). Whether dG9a interacts with the ecdysone receptor directly or possibly through ISWI and NURF, and whether dG9a act as a co-activator or repressor needs to be further investigated.

dG9a was also shown to be a suppressor of PEV (Mis et al., 2006). Mis and co-workers studied a hypomorphic mutation and not a null mutation of *dG9a* (*dG9a*^{13414}/ *dG9a*^{13414}) and suggested an overlapping function with SU(VAR)3-9 and may be member of the same silencing complexes in heterochromatin (Mis et al., 2006). In contrast it was shown that dG9a co-localize to euchromatin (Stabell et al., 2006) and SU(VAR)3-9 was not identified as an interacting protein in dG9a immunoprecipitation.

5.3 HP1

In the present study, the mechanism for HP1a binding to H3K9Me chromatin has been investigated. Specific interaction with another factor through the chromo shadow domain stabilizes the binding of the chromo domain with H3K9Me within nucleosomal arrays. Since the factors that enhance HP1a binding to H3K9Me chromatin should specifically interact with HP1a, new interaction partners were identified. The two HP1 paralogs HP1a and HP1c binds to distinct chromatin

structures (Smothers and Henikoff, 2001) and this is mirrored in their interaction partners.

5.3.1 HP1a binding to H3K9Me chromatin is stabilized by interacting factors

HP1a is predominantly associated with centromeric heterochromatin in *Drosophila* (Smothers and Henikoff, 2001), but it is also found at many sites in euchromatin and telomeres (de Wit et al., 2005; Fanti et al., 2003; Fanti et al., 1998; Greil et al., 2003; James et al., 1989). The HP1 chromo domain binds H3 peptides methylated at lysine 9 (Bannister et al., 2001; Jacobs and Khorasanizadeh, 2002; Jacobs et al., 2001; Lachner et al., 2001; Nielsen et al., 2002) but little is known how HP1 binds to this mark within chromatin.

This work shows *in vitro* reconstituted HP1a containing chromatin fibers containing recombinant histones with H3 highly methylated at K9 and two known recombinant SU(VAR)s. Both ACF and SU(VAR)3-9 bind chromatin irrespective of its methylation state and interact with the chromo shadow domain of HP1a. HP1a did not bind efficiently to H3K9Me chromatin alone, but the presence of interacting partners anchor HP1 stably to chromatin.

Analysis of recombinant mutant HP1a proteins carrying either a mutation in the chromo domain or in the chromo shadow domain, showed that both are necessary for HP1a binding to chromatin. The fact that the chromo shadow domain mutant fails to bind H3K9Me suggests that HP1a is assisted by a factor within the *Drosophila* S-150 chromatin assembly extract. This supports the observation that HP1 molecules carrying mutations within the chromo domain and the chromo shadow domain have weaker affinity to heterochromatin *in vivo* (Thiru et al., 2004). Detailed studies of single point mutations within HP1β showed that localization and stable association with heterochromatin of HP1β needs to form a dimer and interact with other PxVxL motif proteins (Thiru et al., 2004). Two candidate factors were tested for their ability to stabilize HP1a binding to H3K9 chromatin both having a SU(VAR) phenotype *Drosophila melanogaster* (Fyodorov et al., 2004; Tschiersch et al., 1994).

Drosophila ACF was purified from embryos and shown to be a major chromatin assembly factor (Fyodorov et al., 2004; Ito et al., 1997; Ito et al., 1999). *Acf1-/-* flies had lower nucleosomal periodicity, supporting a role in assembly of chromatin (Fyodorov et al., 2004). Immunostainings of mouse cells revealed that ACF1 co-localize with HP1β (Collins et al., 2002). Recombinant *Drosophila* ACF1 interacts with the chromo shadow domain of HP1a through a region spanning the DDT motif. This region is also interacting with ISWI (Eberharter et al., 2004). The DDT motif was identified through homology-based sequence analyses in several PHD finger transcription factors and BAZ family chromatin remodelers (Doerks et al., 2001). Interaction of HP1a with ACF increased the affinity for HP1a to H3K9Me chromatin in an ATP independent manner. It remains to be solved where ACF targets HP1a *in vivo.*

SU(VAR)3-9 methylates H3 at K9 (Schotta et al., 2002) thereby generating a potential binding site for HP1a within heterochromatin. SU(VAR)3-9 interacts with HP1a via the N-terminus and this interaction has been suggested to serve as a part of an autoregulatory loop, which helps maintaining the methylated state of heterochromatin (Schotta et al., 2002). The interaction is mapped to the chromo shadow domain of HP1a and the N-terminus of SU(VAR)3-9. As observed for ACF, SU(VAR)3-9 facilitated the binding of HP1a to H3K9Me chromatin independent of its methyltransferase activity. However, binding of HP1a to H3K9Me chromatin weakened when the interaction between SU(VAR)3-9 and HP1a was impaired either due to a mutation in HP1a or in SU(VAR)3-9. This additional function of SU(VAR)3-9 in stabilizing HP1a binding could contribute to explain the strong dose dependent effect of SU(VAR)3-9 gene duplication which is rather unusual for an enzymatic activity.

The weak but specific binding of HP1a to H3K9Me peptide with a dissociation constant in the micro molar (µM) range *in vitro* (Jacobs and Khorasanizadeh, 2002; Nielsen et al., 2002) is so low that the physiological relevance *in vivo* can be questioned. In agreement, the binding of HP1a to H3K9Me chromatin was weak and only interaction with additional factors can push the affinity toward H3K9Me chromatin into a more physiological range. The dynamic nature of HP1 in the nuclei

of eukaryotic cells (Cheutin et al., 2003; Festenstein et al., 2003) also indicates that the interaction of HP1 with chromatin is not very stable.

Targeting of *Drosophila* HP1s *in vivo* is dependent on the chromo shadow domain (or hinge for HP1a) (Smothers and Henikoff, 2001). When comparing the chromo shadow domain of HP1a with the other paralogs (Figure 2.9), the tryptophan 200 (W200) important for interaction with SU(VAR)3-9 and ACF1 can only be found in HP1b. Indeed HP1b localizes both to heterochromatin and euchromatin (Smothers and Henikoff, 2001). HP1c does not interact with ACF1 and SU(VAR)3-9, which suggests that the euchromatic localization is due to binding of distinct factors than the interaction partners of HP1a. However, the hinge domain of HP1a can also target it to heterochromatin (Smothers and Henikoff, 2001). The chromo shadow domains of mammalian HP1s are nearly identical and they still feature a spatially distinct localization (Minc et al., 1999; Minc et al., 2000). However, the hinge domain among mammalian paralogs differs in their length and composition and might function to determine their localization *in vivo*. Indeed, the hinge domain of the mouse HP1α was reported to bind nuclear RNA *in vitro* (Muchardt et al., 2002) and in mouse and *Xenopus* it has also been reported to bind the linker histone H1 (Meehan et al., 2003; Nielsen et al., 2001). This work shows that both the chromo domain and the chromo shadow domain are necessary to stabilize HP1a binding to H3K9Me chromatin. A model for targeting of HP1 proteins to H3K9Me chromatin is that a bimodal interaction of the chromo domain and either the chromo shadow or hinge domain is necessary for binding and stabilization of HP1. Albeit the evident co-localization of SU(VAR)3-9 and HP1a at centromeric heterochromatin, HP1a was shown to bind distinct chromatin regions independently of SU(VAR)3-9 (Greil et al., 2003) supporting the idea that different interaction partners of HP1a contribute to its specific localization *in vivo*.

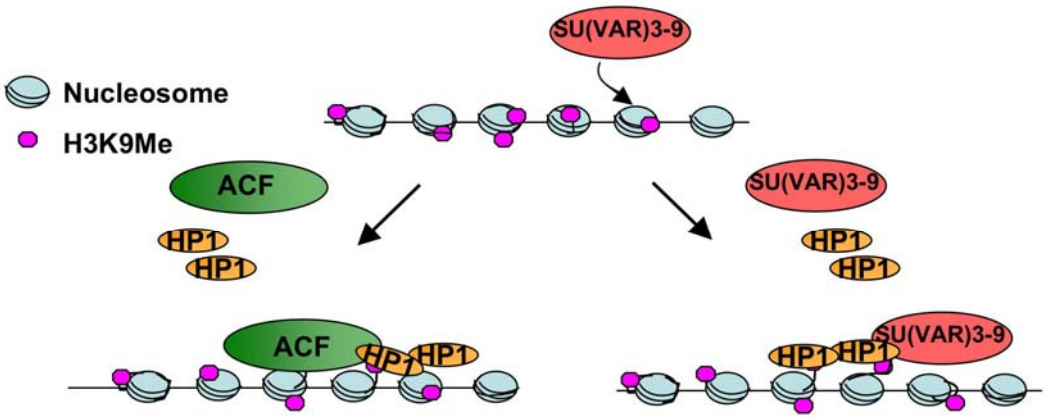

Figure 5.3 HP1a binding to chromatin is stabilized by auxiliary factors as for example SU(VAR)3-9 and ACF. SU(VAR)3-9 methylates H3K9 and both SU(VAR)3-9 and ACF contribute to stable anchoring of HP1a to H3K9Me chromatin.

A recent study showed that a truncated version of HP1α/β lacking the chromo domain and fused to a lac repressor is sufficient for heterochromatinization of the region surrounding a *lac* operator-containing gene including H3K9 methylation and endogenous HP1 (Brink et al., 2006). This argues for a targeting by the chromo shadow and the hinge region. Knowing that HP1 dimerises it might be that the truncated HP1 brings endogenous HP1 to the *lac* operator gene and the chromo domain of the endogenous HP1 binds H3K9Me. Another study could show that mutation of a single serine within the hinge domain of HP1a that mimic phosphorylation resulted in stronger affinity of the protein for H3K9Me and enhanced homodimerization (Badugu et al., 2005). This is an interesting observation that post-translational modifications of the hinge domain can impact both the chromo and the chromo shadow domain.

Several studies have shown that H3 serine 10 phosphorylation has a negative (Fischle et al., 2005; Hirota et al., 2005; Zhang et al., 2006) or positive (Mateescu et al., 2004) effect on HP1 binding to chromatin. Using this recombinant system and introducing a S10 phosphorylation with the Aurora Kinase to the H3K9Me chromatin could give a detailed analysis of a combinatorial histone code effect on HP1 binding.

It will be interesting to see whether the different targeting factors have distinctive contribution to the localization of HP1 at different stages of the cell cycle, during different stages of development or in different cell types. This *in vitro* system can be used to identify new interaction partners anchoring HP1 to methylated chromatin. Another interesting feature that needs to be further investigated is the effect of post-translational modifications of HP1 and H3 that affects HP1 interaction with H3K9Me chromatin. However, this *in vitro* system can also be used to study the binding to chromatin by other chromatin factors. The limitation of such a system is the efficiency of the histone-modifying enzyme that sets the mark of interest. As an alternative, native histones can be used since MALDI-TOF analysis allows detailed information of the modifications present on the different histones.

5.3.2 HP1a and HP1c have distinct interaction partners

The different HP1 homologues interact with a myriad of interaction partners (See table 2.7). To identify new interaction partners of HP1a and c in stable *Drosophila* SL2 cell lines were generated expressing N-terminal Flag tagged HP1a/c. The proteins identified in this work are listed in table 5.1.

Table 5.1 *Drosophila* HP1 interaction partners

Protein	HP1 variant	Methodology	HP1 domain
Nucleosome Methylated K9	HP1a	rPD	CD/CSD
ATR-X	HP1a	exIP	nd
Nipped-B	HP1a	exIP	nd
Dis3	HP1a	exIP	nd
ACF1	HP1a	rPD, transPD, exIP	CSD
woc	HP1c	exIP	nd
CG8092	HP1c	exIP	nd

CD, chromo domain; CSD, chromo shadow domain; exIP, co-immunoprecipitation using extract; exPD, pull-down assay using *in vitro* translated extracts; rPD, pull-down assay using recombinant proteins; transPD, pull-down assay using *in vitro* translated protein.

Supporting the finding that ACF stabilizes binding of HP1a to H3K9Me chromatin, ACF1 was found to interact weakly with Flag-HP1a. SU(VAR)3-9 interacted specifically with HP1a in SL2 cells. The weak interaction of ACF1 with Flag-HP1a may reflect the number of binding sites where HP1a is targeted by ACF *in vivo*.

In contrast SU(VAR)3-9 and HP1a are both found at high concentrations on the chromocenter of *Drosophila* chromosomes (Schotta et al., 2002).

HP1 has also been shown to play a role in maintaining the nuclear structure. It was previously shown that HP1a is required for correct chromosome segregation (Kellum and Alberts, 1995). In *Schitzosaccharomyces Pombe*, *dis3* has been implicated in sister chromatid separation (Ohkura et al., 1988) whereas *Drosophila* Nipped-B is required for sister chromatid cohesion (Rollins et al., 1999). The novel finding of Nipped-B and Dis3 interacting with HP1a in *Drosophila,* provide a biochemical link HP1a to chromatin cohesion. This is supported by the finding that Swi6 is required for efficient cohesion in *Schitzosaccharomyces Pombe* (Bernard et al., 2001; Ekwall et al., 1995; Nonaka et al., 2002) and that human Nipped-B-Like protein (NIPBL) interacts with HP1α (Lechner et al., 2005). How HP1a proteins participate in sister chromatid cohesion remains to be elucidated. However the direct interaction of Swi6 with the cohesin complex in yeast has been suggested to be responsible for the high concentration of cohesin complex around the centromere and retention of cohesin at metaphase (Dorsett, 2006). Perhaps Nipped-B links HP1 to the cohesion complex in *Drosophila.*

The interaction with the SNF2 ATPase ATR-X, shown to be involved in mental retardation human (Inlow and Restifo, 2004) is also supported by interaction and co-localization of mammalian HP1α and HP1β (Le Douarin et al., 1996; McDowell et al., 1999). In *C. elegans* the ATR-X homolog XNP-1 has been found to act with HP1 during development (Cardoso et al., 2005). Therefore it would be of interest to see if the interaction of HP1 with ATR-X affects developmental gene expression in *Drosophila.*

Flag-HP1c had different interaction partners than HP1a. To our knowledge there have not been any *Drosophila* HP1c interaction proteins identified previously. Two distinct proteins, novel protein interactors were identified. *Without children (woc)* was shown to be a transcription factor involved in ecdysone synthesis (Wismar et al., 2000), but has also recently been implicated in prevention of telomeric fusions (Raffa et al., 2005) and CG8092 is a novel zink finger protein. The zink finger protein woc is believed to activate expression of a 7,8- dehydrogenase, which is important in the first

step of ecdysteriodogenesis (Warren et al., 2001; Wismar et al., 2000). A more potent function of a HP1c and woc interaction is in telomeric protection, since woc functions in telomeric capping independent of HP1a (Raffa et al., 2005).

5.4 Concluding remarks

Some evidences for a histone code has been unraveled (for review, see (Nightingale et al., 2006)). New histone modifications are being discovered and identification of enzyme families that add or remove these marks is expanding. The data presented in this thesis adds a new *Drosophila* HMTase to this list and discusses a new potential methylation site within histone H4. Except for methylating H4, dG9a behaves very similar to the mammalian G9a (Stabell et al., 2006; Tachibana et al., 2001; Tachibana et al., 2002). Furthermore, the detailed *in vitro* characterization of *Drosophila* SU(VAR)3-9 may provide a better understanding for the mechanism of heterochromatin formation *in vivo.*

Specific histone modifications, in particular methylation marks, are recognized by a growing number of proteins (Martin and Zhang, 2005). The best studied interaction is between H3 lysine 9 methylation and HP1 (Bannister et al., 2001; Cao et al., 2002; Jacobs and Khorasanizadeh, 2002; Jacobs et al., 2001; Lachner et al., 2001; Min et al., 2003; Nielsen et al., 2002). The key finding in this work is that HP1 is depending on multiple binding sites that contribute to a stable binding of H3K9Me chromatin. This mechanism may be similar for other proteins that recognize histone modifications, adding another level to the histone code. It would be intriguing to examine whether local concentration of specific interaction proteins affect targeting of HP1 to chromatin sites *in vivo.*

Histone marks are shown to have functional readouts such as the silencing or activation of transcription and DNA repair. For example H3K9 and H4K20 trimethylation has been described as characteristic of transcriptionally silent chromatin (Peters et al., 2003; Rice et al., 2003; Schotta et al., 2004). However, the combinatorial aspect of modification marks and effect of a histone code on transcriptional activation and silencing is not fully understood, in addition the heritability of the histone code remains to be demonstrated.

6. References

Aagaard, L., Laible, G., Selenko, P., Schmid, M., Dorn, R., Schotta, G., Kuhfittig, S., Wolf, A., Lebersorger, A., Singh, P. B., Reuter, G., and Jenuwein, T. (1999). Functional mammalian homologues of the Drosophila PEV-modifier Su(var)3-9 encode centromere-associated proteins which complex with the heterochromatin component M31. *Embo J* **18,** 1923-38.

Aagaard, L., Schmid, M., Warburton, P., and Jenuwein, T. (2000). Mitotic phosphorylation of SUV39H1, a novel component of active centromeres, coincides with transient accumulation at mammalian centromeres. *J Cell Sci* **113 (Pt 5),** 817-29.

Aasland, R., and Stewart, A. F. (1995). The chromo shadow domain, a second chromo domain in heterochromatin-binding protein 1, HP1. *Nucleic Acids Res* **23,** 3168-73.

Abad, J. P., De Pablos, B., Osoegawa, K., De Jong, P. J., Martin-Gallardo, A., and Villasante, A. (2004). TAHRE, a novel telomeric retrotransposon from Drosophila melanogaster, reveals the origin of Drosophila telomeres. *Mol Biol Evol* **21,** 1620-4.

Aihara, T., Miyoshi, Y., Koyama, K., Suzuki, M., Takahashi, E., Monden, M., and Nakamura, Y. (1998). Cloning and mapping of SMARCA5 encoding hSNF2H, a novel human homologue of Drosophila ISWI. *Cytogenet Cell Genet* **81,** 191-3.

Ainsztein, A. M., Kandels-Lewis, S. E., Mackay, A. M., and Earnshaw, W. C. (1998). INCENP centromere and spindle targeting: identification of essential conserved motifs and involvement of heterochromatin protein HP1. *J Cell Biol* **143,** 1763-74.

Ait-Si-Ali, S., Guasconi, V., Fritsch, L., Yahi, H., Sekhri, R., Naguibneva, I., Robin, P., Cabon, F., Polesskaya, A., and Harel-Bellan, A. (2004). A Suv39h-dependent mechanism for silencing S-phase genes in differentiating but not in cycling cells. *Embo J* **23,** 605-15.

Akhmanova, A., Miedema, K., and Hennig, W. (1996). Identification and characterization of the Drosophila histone H4 replacement gene. *FEBS Lett* **388,** 219-22.

Albiez, H., Cremer, M., Tiberi, C., Vecchio, L., Schermelleh, L., Dittrich, S., Kupper, K., Joffe, B., Thormeyer, T., von Hase, J., Yang, S., Rohr, K., Leonhardt, H., Solovei, I., Cremer, C., Fakan, S., and Cremer, T. (2006). Chromatin domains and the interchromatin compartment form structurally defined and functionally interacting nuclear networks. *Chromosome Res* **14,** 707-733.

Albright, S. R., and Tjian, R. (2000). TAFs revisited: more data reveal new twists and confirm old ideas. *Gene* **242,** 1-13.

Allshire, R. C., Javerzat, J. P., Redhead, N. J., and Cranston, G. (1994). Position effect variegation at fission yeast centromeres. *Cell* **76,** 157-69.

Allshire, R. C., Nimmo, E. R., Ekwall, K., Javerzat, J. P., and Cranston, G. (1995). Mutations derepressing silent centromeric domains in fission yeast disrupt chromosome segregation. *Genes Dev* **9,** 218-33.

An, W., Kim, J., and Roeder, R. G. (2004). Ordered cooperative functions of PRMT1, p300, and CARM1 in transcriptional activation by p53. *Cell* **117,** 735-48.

Ayyanathan, K., Lechner, M. S., Bell, P., Maul, G. G., Schultz, D. C., Yamada, Y., Tanaka, K., Torigoe, K., and Rauscher, F. J., 3rd. (2003). Regulated

recruitment of HP1 to a euchromatic gene induces mitotically heritable, epigenetic gene silencing: a mammalian cell culture model of gene variegation. *Genes Dev* **17,** 1855-69.

Bachman, K. E., Rountree, M. R., and Baylin, S. B. (2001). Dnmt3a and Dnmt3b are transcriptional repressors that exhibit unique localization properties to heterochromatin. *J Biol Chem* **276,** 32282-7.

Badenhorst, P., Voas, M., Rebay, I., and Wu, C. (2002). Biological functions of the ISWI chromatin remodeling complex NURF. *Genes Dev* **16,** 3186-98.

Badenhorst, P., Xiao, H., Cherbas, L., Kwon, S. Y., Voas, M., Rebay, I., Cherbas, P., and Wu, C. (2005). The Drosophila nucleosome remodeling factor NURF is required for Ecdysteroid signaling and metamorphosis. *Genes Dev* **19,** 2540-5.

Badugu, R., Shareef, M. M., and Kellum, R. (2003). Novel Drosophila heterochromatin protein 1 (HP1)/origin recognition complex-associated protein (HOAP) repeat motif in HP1/HOAP interactions and chromocenter associations. *J Biol Chem* **278,** 34491-8.

Badugu, R., Yoo, Y., Singh, P. B., and Kellum, R. (2005). Mutations in the heterochromatin protein 1 (HP1) hinge domain affect HP1 protein interactions and chromosomal distribution. *Chromosoma* **113,** 370-84.

Bannister, A. J., and Kouzarides, T. (2005). Reversing histone methylation. *Nature* **436,** 1103-6.

Bannister, A. J., Zegerman, P., Partridge, J. F., Miska, E. A., Thomas, J. O., Allshire, R. C., and Kouzarides, T. (2001). Selective recognition of methylated lysine 9 on histone H3 by the HP1 chromo domain. *Nature* **410,** 120-4.

Banting, G. S., Barak, O., Ames, T. M., Burnham, A. C., Kardel, M. D., Cooch, N. S., Davidson, C. E., Godbout, R., McDermid, H. E., and Shiekhattar, R. (2005). CECR2, a protein involved in neurulation, forms a novel chromatin remodeling complex with SNF2L. *Hum Mol Genet* **14,** 513-24.

Barak, O., Lazzaro, M. A., Lane, W. S., Speicher, D. W., Picketts, D. J., and Shiekhattar, R. (2003). Isolation of human NURF: a regulator of Engrailed gene expression. *Embo J* **22,** 6089-100.

Barbes, C., Sanchez, J., Yebra, M. J., Robert-Gero, M., and Hardisson, C. (1990). Effects of sinefungin and S-adenosylhomocysteine on DNA and protein methyltransferases from Streptomyces and other bacteria. *FEMS Microbiol Lett* **57,** 239-43.

Bauer, U. M., Daujat, S., Nielsen, S. J., Nightingale, K., and Kouzarides, T. (2002). Methylation at arginine 17 of histone H3 is linked to gene activation. *EMBO Rep* **3,** 39-44.

Baumbusch, L. O., Thorstensen, T., Krauss, V., Fischer, A., Naumann, K., Assalkhou, R., Schulz, I., Reuter, G., and Aalen, R. B. (2001). The Arabidopsis thaliana genome contains at least 29 active genes encoding SET domain proteins that can be assigned to four evolutionarily conserved classes. *Nucleic Acids Res* **29,** 4319-33.

Becker, H. J. (1957). [Roentgen mosaic spots & defective mutations at the eye of Drosophila & the evolutive physiology of the eye.]. *Z Indukt Abstamm Vererbungsl* **88,** 333-73.

Becker, P. B., and Horz, W. (2002). ATP-dependent nucleosome remodeling. *Annu Rev Biochem* **71,** 247-73.

Becker, P. B., and Wu, C. (1992). Cell-free system for assembly of transcriptionally repressed chromatin from Drosophila embryos. *Mol Cell Biol* **12,** 2241-9.

Beisel, C., Imhof, A., Greene, J., Kremmer, E., and Sauer, F. (2002). Histone methylation by the Drosophila epigenetic transcriptional regulator Ash1. *Nature* **419,** 857-62.

Belz, T., Pham, A. D., Beisel, C., Anders, N., Bogin, J., Kwozynski, S., and Sauer, F. (2002). In vitro assays to study protein ubiquitination in transcription. *Methods* **26,** 233-44.

Ben-Shushan, E., Sharir, H., Pikarsky, E., and Bergman, Y. (1995). A dynamic balance between ARP-1/COUP-TFII, EAR-3/COUP-TFI, and retinoic acid receptor:retinoid X receptor heterodimers regulates Oct-3/4 expression in embryonal carcinoma cells. *Mol Cell Biol* **15,** 1034-48.

Bernard, P., Maure, J. F., Partridge, J. F., Genier, S., Javerzat, J. P., and Allshire, R. C. (2001). Requirement of heterochromatin for cohesion at centromeres. *Science* **294,** 2539-42.

Bheemanaik, S., Chandrashekaran, S., Nagaraja, V., and Rao, D. N. (2003). Kinetic and catalytic properties of dimeric KpnI DNA methyltransferase. *J Biol Chem* **278,** 7863-74.

Bonaldi, T., Imhof, A., and Regula, J. T. (2004). A combination of different mass spectroscopic techniques for the analysis of dynamic changes of histone modifications. *Proteomics* **4,** 1382-96.

Bone, J. R., Lavender, J., Richman, R., Palmer, M. J., Turner, B. M., and Kuroda, M. I. (1994). Acetylated histone H4 on the male X chromosome is associated with dosage compensation in Drosophila. *Genes Dev* **8,** 96-104.

Bouazoune, K., and Brehm, A. (2006). ATP-dependent chromatin remodeling complexes in Drosophila. *Chromosome Res* **14,** 433-49.

Bouazoune, K., Mitterweger, A., Langst, G., Imhof, A., Akhtar, A., Becker, P. B., and Brehm, A. (2002). The dMi-2 chromodomains are DNA binding modules important for ATP-dependent nucleosome mobilization. *Embo J* **21,** 2430-40.

Boulias, K., Katrakili, N., Bamberg, K., Underhill, P., Greenfield, A., and Talianidis, I. (2005). Regulation of hepatic metabolic pathways by the orphan nuclear receptor SHP. *Embo J* **24,** 2624-33.

Boulias, K., and Talianidis, I. (2004). Functional role of G9a-induced histone methylation in small heterodimer partner-mediated transcriptional repression. *Nucleic Acids Res* **32,** 6096-103.

Boulikas, T. (1993). Poly(ADP-ribosyl)ation, DNA strand breaks, chromatin and cancer. *Toxicol Lett* **67,** 129-50.

Bracken, A. P., Pasini, D., Capra, M., Prosperini, E., Colli, E., and Helin, K. (2003). EZH2 is downstream of the pRB-E2F pathway, essential for proliferation and amplified in cancer. *Embo J* **22,** 5323-35.

Brasher, S. V., Smith, B. O., Fogh, R. H., Nietlispach, D., Thiru, A., Nielsen, P. R., Broadhurst, R. W., Ball, L. J., Murzina, N. V., and Laue, E. D. (2000). The structure of mouse HP1 suggests a unique mode of single peptide recognition by the shadow chromo domain dimer. *Embo J* **19,** 1587-97.

Breeden, L., and Nasmyth, K. (1987). Cell cycle control of the yeast HO gene: cis- and trans-acting regulators. *Cell* **48,** 389-97.

Brehm, A., Langst, G., Kehle, J., Clapier, C. R., Imhof, A., Eberharter, A., Muller, J., and Becker, P. B. (2000). dMi-2 and ISWI chromatin remodelling factors have distinct nucleosome binding and mobilization properties. *Embo J* **19,** 4332-41.

Brehm, A., Ovitt, C. E., and Scholer, H. R. (1998). Oct-4: more than just a POUerful marker of the mammalian germline? *Apmis* **106,** 114-24; discussion 124-6.

Brehm, A., Tufteland, K. R., Aasland, R., and Becker, P. B. (2004). The many colours of chromodomains. *Bioessays* **26,** 133-40.

Brink, M. C., van der Velden, Y., de Leeuw, W., Mateos-Langerak, J., Belmont, A. S., van Driel, R., and Verschure, P. J. (2006). Truncated HP1 lacking a functional chromodomain induces heterochromatinization upon in vivo targeting. *Histochem Cell Biol* **125,** 53-61.

Brogna, S., Sato, T. A., and Rosbash, M. (2002). Ribosome components are associated with sites of transcription. *Mol Cell* **10,** 93-104.

Brown, M. A., Sims, R. J., 3rd, Gottlieb, P. D., and Tucker, P. W. (2006). Identification and characterization of Smyd2: a split SET/MYND domain-containing histone H3 lysine 36-specific methyltransferase that interacts with the Sin3 histone deacetylase complex. *Mol Cancer* **5,** 26.

Brownell, J. E., and Allis, C. D. (1996). Special HATs for special occasions: linking histone acetylation to chromatin assembly and gene activation. *Curr Opin Genet Dev* **6,** 176-84.

Camporeale, G., Shubert, E. E., Sarath, G., Cerny, R., and Zempleni, J. (2004). K8 and K12 are biotinylated in human histone H4. *Eur J Biochem* **271,** 2257-63.

Cao, R., Wang, L., Wang, H., Xia, L., Erdjument-Bromage, H., Tempst, P., Jones, R. S., and Zhang, Y. (2002). Role of histone H3 lysine 27 methylation in Polycomb-group silencing. *Science* **298,** 1039-43.

Cardoso, C., Couillault, C., Mignon-Ravix, C., Millet, A., Ewbank, J. J., Fontes, M., and Pujol, N. (2005). XNP-1/ATR-X acts with RB, HP1 and the NuRD complex during larval development in C. elegans. *Dev Biol* **278,** 49-59.

Cenci, G., Siriaco, G., Raffa, G. D., Kellum, R., and Gatti, M. (2003). The Drosophila HOAP protein is required for telomere capping. *Nat Cell Biol* **5,** 82-4.

Chadwick, B. P., and Willard, H. F. (2002). Cell cycle-dependent localization of macroH2A in chromatin of the inactive X chromosome. *J Cell Biol* **157,** 1113-23.

Chang, L., Loranger, S. S., Mizzen, C., Ernst, S. G., Allis, C. D., and Annunziato, A. T. (1997). Histones in transit: cytosolic histone complexes and diacetylation of H4 during nucleosome assembly in human cells. *Biochemistry* **36,** 469-80.

Cheng, X., Collins, R. E., and Zhang, X. (2005). Structural and sequence motifs of protein (histone) methylation enzymes. *Annu Rev Biophys Biomol Struct* **34,** 267-94.

Cheutin, T., Gorski, S. A., May, K. M., Singh, P. B., and Misteli, T. (2004). In vivo dynamics of Swi6 in yeast: evidence for a stochastic model of heterochromatin. *Mol Cell Biol* **24,** 3157-67.

Cheutin, T., McNairn, A. J., Jenuwein, T., Gilbert, D. M., Singh, P. B., and Misteli, T. (2003). Maintenance of stable heterochromatin domains by dynamic HP1 binding. *Science* **299,** 721-5.

Chew, Y. C., Camporeale, G., Kothapalli, N., Sarath, G., and Zempleni, J. (2006). Lysine residues in N-terminal and C-terminal regions of human histone H2A are targets for biotinylation by biotinidase. *J Nutr Biochem* **17,** 225-33.

Chin, H. G., Patnaik, D., Esteve, P. O., Jacobsen, S. E., and Pradhan, S. (2006). Catalytic properties and kinetic mechanism of human recombinant Lys-9 histone H3 methyltransferase SUV39H1: participation of the chromodomain in enzymatic catalysis. *Biochemistry* **45,** 3272-84.

Chin, H. G., Pradhan, M., Esteve, P. O., Patnaik, D., Evans, T. C., Jr., and Pradhan, S. (2005). Sequence specificity and role of proximal amino acids of the histone

H3 tail on catalysis of murine G9A lysine 9 histone H3 methyltransferase. *Biochemistry* **44,** 12998-3006.

Chinnadurai, G. (2003). CtBP family proteins: more than transcriptional corepressors. *Bioessays* **25,** 9-12.

Chuikov, S., Kurash, J. K., Wilson, J. R., Xiao, B., Justin, N., Ivanov, G. S., McKinney, K., Tempst, P., Prives, C., Gamblin, S. J., Barlev, N. A., and Reinberg, D. (2004). Regulation of p53 activity through lysine methylation. *Nature* **432,** 353-60.

Clapier, C. R., Langst, G., Corona, D. F., Becker, P. B., and Nightingale, K. P. (2001). Critical role for the histone H4 N terminus in nucleosome remodeling by ISWI. *Mol Cell Biol* **21,** 875-83.

Clapier, C. R., Nightingale, K. P., and Becker, P. B. (2002). A critical epitope for substrate recognition by the nucleosome remodeling ATPase ISWI. *Nucleic Acids Res* **30,** 649-55.

Cleard, F., Delattre, M., and Spierer, P. (1997). SU(VAR)3-7, a Drosophila heterochromatin-associated protein and companion of HP1 in the genomic silencing of position-effect variegation. *Embo J* **16,** 5280-8.

Clegg, N. J., Honda, B. M., Whitehead, I. P., Grigliatti, T. A., Wakimoto, B., Brock, H. W., Lloyd, V. K., and Sinclair, D. A. (1998). Suppressors of position-effect variegation in Drosophila melanogaster affect expression of the heterochromatic gene light in the absence of a chromosome rearrangement. *Genome* **41,** 495-503.

Cocklin, R. R., Zhang, Y., O'Neill, K. D., Chen, N. X., Moe, S. M., Bidasee, K. R., and Wang, M. (2003). Identity and localization of advanced glycation end products on human beta2-microglobulin using matrix-assisted laser desorption/ionization time-of-flight mass spectrometry. *Anal Biochem* **314,** 322-5.

Collazo, E., Couture, J. F., Bulfer, S., and Trievel, R. C. (2005). A coupled fluorescent assay for histone methyltransferases. *Anal Biochem* **342,** 86-92.

Collins, N., Poot, R. A., Kukimoto, I., Garcia-Jimenez, C., Dellaire, G., and Varga-Weisz, P. D. (2002). An ACF1-ISWI chromatin-remodeling complex is required for DNA replication through heterochromatin. *Nat Genet* **32,** 627-32.

Collins, R. E., Tachibana, M., Tamaru, H., Smith, K. M., Jia, D., Zhang, X., Selker, E. U., Shinkai, Y., and Cheng, X. (2005). In vitro and in vivo analyses of a Phe/Tyr switch controlling product specificity of histone lysine methyltransferases. *J Biol Chem* **280,** 5563-70.

Corona, D. F., Clapier, C. R., Becker, P. B., and Tamkun, J. W. (2002). Modulation of ISWI function by site-specific histone acetylation. *EMBO Rep* **3,** 242-7.

Corona, D. F., Eberharter, A., Budde, A., Deuring, R., Ferrari, S., Varga-Weisz, P., Wilm, M., Tamkun, J., and Becker, P. B. (2000). Two histone fold proteins, CHRAC-14 and CHRAC-16, are developmentally regulated subunits of chromatin accessibility complex (CHRAC). *Embo J* **19,** 3049-59.

Couture, J. F., Collazo, E., and Trievel, R. C. (2006). Molecular recognition of histone H3 by the WD40 protein WDR5. *Nat Struct Mol Biol* **13,** 698-703.

Cowieson, N. P., Partridge, J. F., Allshire, R. C., and McLaughlin, P. J. (2000). Dimerisation of a chromo shadow domain and distinctions from the chromodomain as revealed by structural analysis. *Curr Biol* **10,** 517-25.

Cremer, T., and Cremer, C. (2001). Chromosome territories, nuclear architecture and gene regulation in mammalian cells. *Nat Rev Genet* **2,** 292-301.

Cremer, T., Cremer, M., Dietzel, S., Muller, S., Solovei, I., and Fakan, S. (2006). Chromosome territories--a functional nuclear landscape. *Curr Opin Cell Biol* **18,** 307-16.

Croston, G. E., Lira, L. M., and Kadonaga, J. T. (1991). A general method for purification of H1 histones that are active for repression of basal RNA polymerase II transcription. *Protein Expr Purif* **2,** 162-9.

Cryderman, D. E., Grade, S. K., Li, Y., Fanti, L., Pimpinelli, S., and Wallrath, L. L. (2005). Role of Drosophila HP1 in euchromatic gene expression. *Dev Dyn* **232,** 767-74.

Cuthbert, G. L., Daujat, S., Snowden, A. W., Erdjument-Bromage, H., Hagiwara, T., Yamada, M., Schneider, R., Gregory, P. D., Tempst, P., Bannister, A. J., and Kouzarides, T. (2004). Histone deimination antagonizes arginine methylation. *Cell* **118,** 545-53.

Czermin, B., Melfi, R., McCabe, D., Seitz, V., Imhof, A., and Pirrotta, V. (2002). Drosophila enhancer of Zeste/ESC complexes have a histone H3 methyltransferase activity that marks chromosomal Polycomb sites. *Cell* **111,** 185-96.

Czermin, B., Schotta, G., Hulsmann, B. B., Brehm, A., Becker, P. B., Reuter, G., and Imhof, A. (2001). Physical and functional association of SU(VAR)3-9 and HDAC1 in Drosophila. *EMBO Rep* **2,** 915-9.

Czvitkovich, S., Sauer, S., Peters, A. H., Deiner, E., Wolf, A., Laible, G., Opravil, S., Beug, H., and Jenuwein, T. (2001). Over-expression of the SUV39H1 histone methyltransferase induces altered proliferation and differentiation in transgenic mice. *Mech Dev* **107,** 141-53.

Daujat, S., Bauer, U. M., Shah, V., Turner, B., Berger, S., and Kouzarides, T. (2002). Crosstalk between CARM1 methylation and CBP acetylation on histone H3. *Curr Biol* **12,** 2090-7.

Daujat, S., Zeissler, U., Waldmann, T., Happel, N., and Schneider, R. (2005). HP1 binds specifically to Lys26-methylated histone H1.4, whereas simultaneous Ser27 phosphorylation blocks HP1 binding. *J Biol Chem* **280,** 38090-5.

de Lange, T. (2002). Protection of mammalian telomeres. *Oncogene* **21,** 532-40.

De Lucia, F., Ni, J. Q., Vaillant, C., and Sun, F. L. (2005). HP1 modulates the transcription of cell-cycle regulators in Drosophila melanogaster. *Nucleic Acids Res* **33,** 2852-8.

de Wit, E., Greil, F., and van Steensel, B. (2005). Genome-wide HP1 binding in Drosophila: developmental plasticity and genomic targeting signals. *Genome Res* **15,** 1265-73.

Delattre, M., Spierer, A., Jaquet, Y., and Spierer, P. (2004). Increased expression of Drosophila Su(var)3-7 triggers Su(var)3-9-dependent heterochromatin formation. *J Cell Sci* **117,** 6239-47.

Delattre, M., Spierer, A., Tonka, C. H., and Spierer, P. (2000). The genomic silencing of position-effect variegation in Drosophila melanogaster: interaction between the heterochromatin-associated proteins Su(var)3-7 and HP1. *J Cell Sci* **113 Pt 23,** 4253-61.

Delmas, V., Stokes, D. G., and Perry, R. P. (1993). A mammalian DNA-binding protein that contains a chromodomain and an SNF2/SWI2-like helicase domain. *Proc Natl Acad Sci U S A* **90,** 2414-8.

Dhalluin, C., Carlson, J. E., Zeng, L., He, C., Aggarwal, A. K., and Zhou, M. M. (1999). Structure and ligand of a histone acetyltransferase bromodomain. *Nature* **399,** 491-6.

Doenecke, D., Albig, W., Bode, C., Drabent, B., Franke, K., Gavenis, K., and Witt, O. (1997). Histones: genetic diversity and tissue-specific gene expression. *Histochem Cell Biol* **107,** 1-10.

Doerks, T., Copley, R., and Bork, P. (2001). DDT -- a novel domain in different transcription and chromosome remodeling factors. *Trends Biochem Sci* **26,** 145-6.

Dorsett, D. (2006). Roles of the sister chromatid cohesion apparatus in gene expression, development, and human syndromes. *Chromosoma*.

Du, Y., Carling, T., Fang, W., Piao, Z., Sheu, J. C., and Huang, S. (2001). Hypermethylation in human cancers of the RIZ1 tumor suppressor gene, a member of a histone/protein methyltransferase superfamily. *Cancer Res* **61,** 8094-9.

Duan, Z., and Horwitz, M. (2005). Gfi-1 takes center stage in hematopoietic stem cells. *Trends Mol Med* **11,** 49-52.

Duan, Z., Zarebski, A., Montoya-Durango, D., Grimes, H. L., and Horwitz, M. (2005). Gfi1 coordinates epigenetic repression of p21Cip/WAF1 by recruitment of histone lysine methyltransferase G9a and histone deacetylase 1. *Mol Cell Biol* **25,** 10338-51.

Ebbert, R., Birkmann, A., and Schuller, H. J. (1999). The product of the SNF2/SWI2 paralogue INO80 of Saccharomyces cerevisiae required for efficient expression of various yeast structural genes is part of a high-molecular-weight protein complex. *Mol Microbiol* **32,** 741-51.

Eberharter, A., and Becker, P. B. (2004). ATP-dependent nucleosome remodelling: factors and functions. *J Cell Sci* **117,** 3707-11.

Eberharter, A., Ferrari, S., Langst, G., Straub, T., Imhof, A., Varga-Weisz, P., Wilm, M., and Becker, P. B. (2001). Acf1, the largest subunit of CHRAC, regulates ISWI-induced nucleosome remodelling. *Embo J* **20,** 3781-8.

Eberharter, A., Vetter, I., Ferreira, R., and Becker, P. B. (2004). ACF1 improves the effectiveness of nucleosome mobilization by ISWI through PHD-histone contacts. *Embo J* **23,** 4029-39.

Ebert, A., Lein, S., Schotta, G., and Reuter, G. (2006). Histone modification and the control of heterochromatic gene silencing in Drosophila. *Chromosome Res* **14,** 377-92.

Ebert, A., Schotta, G., Lein, S., Kubicek, S., Krauss, V., Jenuwein, T., and Reuter, G. (2004). Su(var) genes regulate the balance between euchromatin and heterochromatin in Drosophila. *Genes Dev* **18,** 2973-83.

Eisen, J. A., Sweder, K. S., and Hanawalt, P. C. (1995). Evolution of the SNF2 family of proteins: subfamilies with distinct sequences and functions. *Nucleic Acids Res* **23,** 2715-23.

Eissenberg, J. C., and Elgin, S. C. (2000). The HP1 protein family: getting a grip on chromatin. *Curr Opin Genet Dev* **10,** 204-10.

Eissenberg, J. C., Ge, Y. W., and Hartnett, T. (1994). Increased phosphorylation of HP1, a heterochromatin-associated protein of Drosophila, is correlated with heterochromatin assembly. *J Biol Chem* **269,** 21315-21.

Eissenberg, J. C., James, T. C., Foster-Hartnett, D. M., Hartnett, T., Ngan, V., and Elgin, S. C. (1990). Mutation in a heterochromatin-specific chromosomal protein is associated with suppression of position-effect variegation in Drosophila melanogaster. *Proc Natl Acad Sci U S A* **87,** 9923-7.

Ekblad, C. M., Chavali, G. B., Basu, B. P., Freund, S. M., Veprintsev, D., Hughes-Davies, L., Kouzarides, T., Doherty, A. J., and Itzhaki, L. S. (2005). Binding

of EMSY to HP1beta: implications for recruitment of HP1beta and BS69. *EMBO Rep* **6,** 675-80.

Ekwall, K., Javerzat, J. P., Lorentz, A., Schmidt, H., Cranston, G., and Allshire, R. (1995). The chromodomain protein Swi6: a key component at fission yeast centromeres. *Science* **269,** 1429-31.

Ekwall, K., Nimmo, E. R., Javerzat, J. P., Borgstrom, B., Egel, R., Cranston, G., and Allshire, R. (1996). Mutations in the fission yeast silencing factors clr4+ and rik1+ disrupt the localisation of the chromo domain protein Swi6p and impair centromere function. *J Cell Sci* **109 (Pt 11),** 2637-48.

El Messaoudi, S., Fabbrizio, E., Rodriguez, C., Chuchana, P., Fauquier, L., Cheng, D., Theillet, C., Vandel, L., Bedford, M. T., and Sardet, C. (2006). Coactivator-associated arginine methyltransferase 1 (CARM1) is a positive regulator of the Cyclin E1 gene. *Proc Natl Acad Sci U S A* **103,** 13351-6.

Eskeland, R., Czermin, B., Boeke, J., Bonaldi, T., Regula, J. T., and Imhof, A. (2004). The N-terminus of Drosophila SU(VAR)3-9 mediates dimerization and regulates its methyltransferase activity. *Biochemistry* **43,** 3740-9.

Esteve, P. O., Chin, H. G., Smallwood, A., Feehery, G. R., Gangisetty, O., Karpf, A. R., Carey, M. F., and Pradhan, S. (2006). Direct interaction between DNMT1and G9a coordinates DNA and histone methylation during replication. *Genes Dev*.

Esteve, P. O., Patnaik, D., Chin, H. G., Benner, J., Teitell, M. A., and Pradhan, S. (2005). Functional analysis of the N- and C-terminus of mammalian G9a histone H3 methyltransferase. *Nucleic Acids Res* **33,** 3211-23.

Fan, J. Y., Rangasamy, D., Luger, K., and Tremethick, D. J. (2004). H2A.Z alters the nucleosome surface to promote HP1alpha-mediated chromatin fiber folding. *Mol Cell* **16,** 655-61.

Fang, J., Feng, Q., Ketel, C. S., Wang, H., Cao, R., Xia, L., Erdjument-Bromage, H., Tempst, P., Simon, J. A., and Zhang, Y. (2002). Purification and functional characterization of SET8, a nucleosomal histone H4-lysine 20-specific methyltransferase. *Curr Biol* **12,** 1086-99.

Fanti, L., Berloco, M., Piacentini, L., and Pimpinelli, S. (2003). Chromosomal distribution of heterochromatin protein 1 (HP1) in Drosophila: a cytological map of euchromatic HP1 binding sites. *Genetica* **117,** 135-47.

Fanti, L., Giovinazzo, G., Berloco, M., and Pimpinelli, S. (1998). The heterochromatin protein 1 prevents telomere fusions in Drosophila. *Mol Cell* **2,** 527-38.

Feldman, N., Gerson, A., Fang, J., Li, E., Zhang, Y., Shinkai, Y., Cedar, H., and Bergman, Y. (2006). G9a-mediated irreversible epigenetic inactivation of Oct-3/4 during early embryogenesis. *Nat Cell Biol* **8,** 188-94.

Felsenfeld, G., and Groudine, M. (2003). Controlling the double helix. *Nature* **421,** 448-53.

Feng, Q., Wang, H., Ng, H. H., Erdjument-Bromage, H., Tempst, P., Struhl, K., and Zhang, Y. (2002). Methylation of H3-lysine 79 is mediated by a new family of HMTases without a SET domain. *Curr Biol* **12,** 1052-8.

Festenstein, R., Pagakis, S. N., Hiragami, K., Lyon, D., Verreault, A., Sekkali, B., and Kioussis, D. (2003). Modulation of heterochromatin protein 1 dynamics in primary Mammalian cells. *Science* **299,** 719-21.

Firestein, R., Cui, X., Huie, P., and Cleary, M. L. (2000). Set domain-dependent regulation of transcriptional silencing and growth control by SUV39H1, a mammalian ortholog of Drosophila Su(var)3-9. *Mol Cell Biol* **20,** 4900-9.

Fischle, W., Tseng, B. S., Dormann, H. L., Ueberheide, B. M., Garcia, B. A., Shabanowitz, J., Hunt, D. F., Funabiki, H., and Allis, C. D. (2005). Regulation of HP1-chromatin binding by histone H3 methylation and phosphorylation. *Nature* **438,** 1116-22.

Fischle, W., Wang, Y., and Allis, C. D. (2003a). Binary switches and modification cassettes in histone biology and beyond. *Nature* **425,** 475-9.

Fischle, W., Wang, Y., and Allis, C. D. (2003b). Histone and chromatin cross-talk. *Curr Opin Cell Biol* **15,** 172-83.

Fourel, G., Magdinier, F., and Gilson, E. (2004). Insulator dynamics and the setting of chromatin domains. *Bioessays* **26,** 523-32.

Frankel, S., Sigel, E. A., Craig, C., Elgin, S. C., Mooseker, M. S., and Artavanis-Tsakonas, S. (1997). An actin-related protein in Drosophila colocalizes with heterochromatin protein 1 in pericentric heterochromatin. *J Cell Sci* **110 (Pt 17),** 1999-2012.

Freitas, M. A., Sklenar, A. R., and Parthun, M. R. (2004). Application of mass spectrometry to the identification and quantification of histone post-translational modifications. *J Cell Biochem* **92,** 691-700.

Fujita, N., Watanabe, S., Ichimura, T., Tsuruzoe, S., Shinkai, Y., Tachibana, M., Chiba, T., and Nakao, M. (2003). Methyl-CpG binding domain 1 (MBD1) interacts with the Suv39h1-HP1 heterochromatic complex for DNA methylation-based transcriptional repression. *J Biol Chem* **278,** 24132-8.

Fuks, F., Hurd, P. J., Deplus, R., and Kouzarides, T. (2003). The DNA methyltransferases associate with HP1 and the SUV39H1 histone methyltransferase. *Nucleic Acids Res* **31,** 2305-12.

Fyodorov, D. V., Blower, M. D., Karpen, G. H., and Kadonaga, J. T. (2004). Acf1 confers unique activities to ACF/CHRAC and promotes the formation rather than disruption of chromatin in vivo. *Genes Dev* **18,** 170-83.

Fyodorov, D. V., and Kadonaga, J. T. (2002). Binding of Acf1 to DNA involves a WAC motif and is important for ACF-mediated chromatin assembly. *Mol Cell Biol* **22,** 6344-53.

Gerasimova, T. I., Byrd, K., and Corces, V. G. (2000). A chromatin insulator determines the nuclear localization of DNA. *Mol Cell* **6,** 1025-35.

Gotte, G., Bertoldi, M., and Libonati, M. (1999). Structural versatility of bovine ribonuclease A. Distinct conformers of trimeric and tetrameric aggregates of the enzyme. *Eur J Biochem* **265,** 680-7.

Greil, F., van der Kraan, I., Delrow, J., Smothers, J. F., de Wit, E., Bussemaker, H. J., van Driel, R., Henikoff, S., and van Steensel, B. (2003). Distinct HP1 and Su(var)3-9 complexes bind to sets of developmentally coexpressed genes depending on chromosomal location. *Genes Dev* **17,** 2825-38.

Greiner, D., Bonaldi, T., Eskeland, R., Roemer, E., and Imhof, A. (2005). Identification of a specific inhibitor of the histone methyltransferase SU(VAR)3-9. *Nat Chem Biol* **1,** 143-5.

Grewal, S. I., and Elgin, S. C. (2002). Heterochromatin: new possibilities for the inheritance of structure. *Curr Opin Genet Dev* **12,** 178-87.

Grewal, S. I., and Klar, A. J. (1996). Chromosomal inheritance of epigenetic states in fission yeast during mitosis and meiosis. *Cell* **86,** 95-101.

Grune, T., Brzeski, J., Eberharter, A., Clapier, C. R., Corona, D. F., Becker, P. B., and Muller, C. W. (2003). Crystal structure and functional analysis of a nucleosome recognition module of the remodeling factor ISWI. *Mol Cell* **12,** 449-60.

Grunstein, M. (1997). Histone acetylation in chromatin structure and transcription. *Nature* **389,** 349-52.

Hartlepp, K. F., Fernandez-Tornero, C., Eberharter, A., Grune, T., Muller, C. W., and Becker, P. B. (2005). The histone fold subunits of Drosophila CHRAC facilitate nucleosome sliding through dynamic DNA interactions. *Mol Cell Biol* **25,** 9886-96.

Hassa, P. O., Haenni, S. S., Elser, M., and Hottiger, M. O. (2006). Nuclear ADP-ribosylation reactions in mammalian cells: where are we today and where are we going? *Microbiol Mol Biol Rev* **70,** 789-829.

Hearn, M. G., Hedrick, A., Grigliatti, T. A., and Wakimoto, B. T. (1991). The effect of modifiers of position-effect variegation on the variegation of heterochromatic genes of Drosophila melanogaster. *Genetics* **128,** 785-97.

Hebbes, T. R., Clayton, A. L., Thorne, A. W., and Crane-Robinson, C. (1994). Core histone hyperacetylation co-maps with generalized DNase I sensitivity in the chicken beta-globin chromosomal domain. *Embo J* **13,** 1823-30.

Henikoff, S., Furuyama, T., and Ahmad, K. (2004). Histone variants, nucleosome assembly and epigenetic inheritance. *Trends Genet* **20,** 320-6.

Hess, J. L. (2004). MLL: a histone methyltransferase disrupted in leukemia. *Trends Mol Med* **10,** 500-7.

Hirota, T., Lipp, J. J., Toh, B. H., and Peters, J. M. (2005). Histone H3 serine 10 phosphorylation by Aurora B causes HP1 dissociation from heterochromatin. *Nature* **438,** 1176-80.

Hoffman, D. R., Marion, D. W., Cornatzer, W. E., and Duerre, J. A. (1980). S-Adenosylmethionine and S-adenosylhomocystein metabolism in isolated rat liver. Effects of L-methionine, L-homocystein, and adenosine. *J Biol Chem* **255,** 10822-7.

Hong, L., Schroth, G. P., Matthews, H. R., Yau, P., and Bradbury, E. M. (1993). Studies of the DNA binding properties of histone H4 amino terminus. Thermal denaturation studies reveal that acetylation markedly reduces the binding constant of the H4 "tail" to DNA. *J Biol Chem* **268,** 305-14.

Horn, P. J., and Peterson, C. L. (2001). The bromodomain: a regulator of ATP-dependent chromatin remodeling? *Front Biosci* **6,** D1019-23.

Huang, D. W., Fanti, L., Pak, D. T., Botchan, M. R., Pimpinelli, S., and Kellum, R. (1998a). Distinct cytoplasmic and nuclear fractions of Drosophila heterochromatin protein 1: their phosphorylation levels and associations with origin recognition complex proteins. *J Cell Biol* **142,** 307-18.

Huang, J., Perez-Burgos, L., Placek, B. J., Sengupta, R., Richter, M., Dorsey, J. A., Kubicek, S., Opravil, S., Jenuwein, T., and Berger, S. L. (2006a). Repression of p53 activity by Smyd2-mediated methylation. *Nature* **444,** 629-32.

Huang, N., vom Baur, E., Garnier, J. M., Lerouge, T., Vonesch, J. L., Lutz, Y., Chambon, P., and Losson, R. (1998b). Two distinct nuclear receptor interaction domains in NSD1, a novel SET protein that exhibits characteristics of both corepressors and coactivators. *Embo J* **17,** 3398-412.

Huang, Y., Fang, J., Bedford, M. T., Zhang, Y., and Xu, R. M. (2006b). Recognition of histone H3 lysine-4 methylation by the double tudor domain of JMJD2A. *Science* **312,** 748-51.

Huang, Y., Myers, M. P., and Xu, R. M. (2006c). Crystal structure of the HP1-EMSY complex reveals an unusual mode of HP1 binding. *Structure* **14,** 703-12.

Huyen, Y., Zgheib, O., Ditullio, R. A., Jr., Gorgoulis, V. G., Zacharatos, P., Petty, T. J., Sheston, E. A., Mellert, H. S., Stavridi, E. S., and Halazonetis, T. D.

(2004). Methylated lysine 79 of histone H3 targets 53BP1 to DNA double-strand breaks. *Nature* **432,** 406-11.

Hwang, K. K., Eissenberg, J. C., and Worman, H. J. (2001). Transcriptional repression of euchromatic genes by Drosophila heterochromatin protein 1 and histone modifiers. *Proc Natl Acad Sci U S A* **98,** 11423-7.

Inlow, J. K., and Restifo, L. L. (2004). Molecular and comparative genetics of mental retardation. *Genetics* **166,** 835-81.

Ito, T., Bulger, M., Pazin, M. J., Kobayashi, R., and Kadonaga, J. T. (1997). ACF, an ISWI-containing and ATP-utilizing chromatin assembly and remodeling factor. *Cell* **90,** 145-55.

Ito, T., Levenstein, M. E., Fyodorov, D. V., Kutach, A. K., Kobayashi, R., and Kadonaga, J. T. (1999). ACF consists of two subunits, Acf1 and ISWI, that function cooperatively in the ATP-dependent catalysis of chromatin assembly. *Genes Dev* **13,** 1529-39.

Ivanova, A. V., Bonaduce, M. J., Ivanov, S. V., and Klar, A. J. (1998). The chromo and SET domains of the Clr4 protein are essential for silencing in fission yeast. *Nat Genet* **19,** 192-5.

Jackson, J. P., Lindroth, A. M., Cao, X., and Jacobsen, S. E. (2002). Control of CpNpG DNA methylation by the KRYPTONITE histone H3 methyltransferase. *Nature* **416,** 556-60.

Jacobs, S. A., Harp, J. M., Devarakonda, S., Kim, Y., Rastinejad, F., and Khorasanizadeh, S. (2002). The active site of the SET domain is constructed on a knot. *Nat Struct Biol* **9,** 833-8.

Jacobs, S. A., and Khorasanizadeh, S. (2002). Structure of HP1 chromodomain bound to a lysine 9-methylated histone H3 tail. *Science* **295,** 2080-3.

Jacobs, S. A., Taverna, S. D., Zhang, Y., Briggs, S. D., Li, J., Eissenberg, J. C., Allis, C. D., and Khorasanizadeh, S. (2001). Specificity of the HP1 chromo domain for the methylated N-terminus of histone H3. *Embo J* **20,** 5232-41.

Jacobson, R. H., Ladurner, A. G., King, D. S., and Tjian, R. (2000). Structure and function of a human TAFII250 double bromodomain module. *Science* **288,** 1422-5.

James, T. C., Eissenberg, J. C., Craig, C., Dietrich, V., Hobson, A., and Elgin, S. C. (1989). Distribution patterns of HP1, a heterochromatin-associated nonhistone chromosomal protein of Drosophila. *Eur J Cell Biol* **50,** 170-80.

James, T. C., and Elgin, S. C. (1986). Identification of a nonhistone chromosomal protein associated with heterochromatin in Drosophila melanogaster and its gene. *Mol Cell Biol* **6,** 3862-72.

Jenuwein, T., and Allis, C. D. (2001). Translating the histone code. *Science* **293,** 1074-80.

Jenuwein, T., Laible, G., Dorn, R., and Reuter, G. (1998). SET domain proteins modulate chromatin domains in eu- and heterochromatin. *Cell Mol Life Sci* **54,** 80-93.

Jin, Y., Wang, Y., Johansen, J., and Johansen, K. M. (2000). JIL-1, a chromosomal kinase implicated in regulation of chromatin structure, associates with the male specific lethal (MSL) dosage compensation complex. *J Cell Biol* **149,** 1005-10.

Kal, A. J., Mahmoudi, T., Zak, N. B., and Verrijzer, C. P. (2000). The Drosophila brahma complex is an essential coactivator for the trithorax group protein zeste. *Genes Dev* **14,** 1058-71.

Kamakaka, R. T., and Biggins, S. (2005). Histone variants: deviants? *Genes Dev* **19,** 295-310.

Kametaka, A., Takagi, M., Hayakawa, T., Haraguchi, T., Hiraoka, Y., and Yoneda, Y. (2002). Interaction of the chromatin compaction-inducing domain (LR domain) of Ki-67 antigen with HP1 proteins. *Genes Cells* **7,** 1231-42.

Kato, M., Sasaki, M., Mizuno, S., and Harata, M. (2001). Novel actin-related proteins in vertebrates: similarities of structure and expression pattern to Arp6 localized on Drosophila heterochromatin. *Gene* **268,** 133-40.

Kellum, R. (2003). Is HP1 an RNA detector that functions both in repression and activation? *J Cell Biol* **161,** 671-2.

Kellum, R., and Alberts, B. M. (1995). Heterochromatin protein 1 is required for correct chromosome segregation in Drosophila embryos. *J Cell Sci* **108 (Pt 4),** 1419-31.

Kim, K. C., Geng, L., and Huang, S. (2003). Inactivation of a histone methyltransferase by mutations in human cancers. *Cancer Res* **63,** 7619-23.

Kleer, C. G., Cao, Q., Varambally, S., Shen, R., Ota, I., Tomlins, S. A., Ghosh, D., Sewalt, R. G., Otte, A. P., Hayes, D. F., Sabel, M. S., Livant, D., Weiss, S. J., Rubin, M. A., and Chinnaiyan, A. M. (2003). EZH2 is a marker of aggressive breast cancer and promotes neoplastic transformation of breast epithelial cells. *Proc Natl Acad Sci U S A* **100,** 11606-11.

Klose, R. J., Yamane, K., Bae, Y., Zhang, D., Erdjument-Bromage, H., Tempst, P., Wong, J., and Zhang, Y. (2006). The transcriptional repressor JHDM3A demethylates trimethyl histone H3 lysine 9 and lysine 36. *Nature* **442,** 312-6.

Kobza, K., Camporeale, G., Rueckert, B., Kueh, A., Griffin, J. B., Sarath, G., and Zempleni, J. (2005). K4, K9 and K18 in human histone H3 are targets for biotinylation by biotinidase. *Febs J* **272,** 4249-59.

Koh, S. S., Li, H., Lee, Y. H., Widelitz, R. B., Chuong, C. M., and Stallcup, M. R. (2002). Synergistic coactivator function by coactivator-associated arginine methyltransferase (CARM) 1 and beta-catenin with two different classes of DNA-binding transcriptional activators. *J Biol Chem* **277,** 26031-5.

Koike, N., Maita, H., Taira, T., Ariga, H., and Iguchi-Ariga, S. M. (2000). Identification of heterochromatin protein 1 (HP1) as a phosphorylation target by Pim-1 kinase and the effect of phosphorylation on the transcriptional repression function of HP1(1). *FEBS Lett* **467,** 17-21.

Koonin, E. V., Zhou, S., and Lucchesi, J. C. (1995). The chromo superfamily: new members, duplication of the chromo domain and possible role in delivering transcription regulators to chromatin. *Nucleic Acids Res* **23,** 4229-33.

Kornberg, R. D. (1974). Chromatin structure: a repeating unit of histones and DNA. *Science* **184,** 868-71.

Koryakov, D. E., Reuter, G., Dimitri, P., and Zhimulev, I. F. (2006). The SuUR gene influences the distribution of heterochromatic proteins HP1 and SU(VAR)3-9 on nurse cell polytene chromosomes of Drosophila melanogaster. *Chromosoma* **115,** 296-310.

Kourmouli, N., Theodoropoulos, P. A., Dialynas, G., Bakou, A., Politou, A. S., Cowell, I. G., Singh, P. B., and Georgatos, S. D. (2000). Dynamic associations of heterochromatin protein 1 with the nuclear envelope. *Embo J* **19,** 6558-68.

Kouskouti, A., Scheer, E., Staub, A., Tora, L., and Talianidis, I. (2004). Gene-specific modulation of TAF10 function by SET9-mediated methylation. *Mol Cell* **14,** 175-82.

Kouzarides, T. (1999). Histone acetylases and deacetylases in cell proliferation. *Curr Opin Genet Dev* **9,** 40-8.

Krauss, V., and Reuter, G. (2000). Two genes become one: the genes encoding heterochromatin protein Su(var)3-9 and translation initiation factor subunit eIF-2gamma are joined to a dicistronic unit in holometabolic insects. *Genetics* **156,** 1157-67.

Kreimeyer, A., Wielckens, K., Adamietz, P., and Hilz, H. (1984). DNA repair-associated ADP-ribosylation in vivo. Modification of histone H1 differs from that of the principal acceptor proteins. *J Biol Chem* **259,** 890-6.

Krogan, N. J., Keogh, M. C., Datta, N., Sawa, C., Ryan, O. W., Ding, H., Haw, R. A., Pootoolal, J., Tong, A., Canadien, V., Richards, D. P., Wu, X., Emili, A., Hughes, T. R., Buratowski, S., and Greenblatt, J. F. (2003). A Snf2 family ATPase complex required for recruitment of the histone H2A variant Htz1. *Mol Cell* **12,** 1565-76.

Krouwels, I. M., Wiesmeijer, K., Abraham, T. E., Molenaar, C., Verwoerd, N. P., Tanke, H. J., and Dirks, R. W. (2005). A glue for heterochromatin maintenance: stable SUV39H1 binding to heterochromatin is reinforced by the SET domain. *J Cell Biol* **170,** 537-49.

Kukimoto, I., Elderkin, S., Grimaldi, M., Oelgeschlager, T., and Varga-Weisz, P. D. (2004). The histone-fold protein complex CHRAC-15/17 enhances nucleosome sliding and assembly mediated by ACF. *Mol Cell* **13,** 265-77.

Kuzmichev, A., Jenuwein, T., Tempst, P., and Reinberg, D. (2004). Different EZH2-containing complexes target methylation of histone H1 or nucleosomal histone H3. *Mol Cell* **14,** 183-93.

Kuzmichev, A., Nishioka, K., Erdjument-Bromage, H., Tempst, P., and Reinberg, D. (2002). Histone methyltransferase activity associated with a human multiprotein complex containing the Enhancer of Zeste protein. *Genes Dev* **16,** 2893-905.

Kwon, T., Chang, J. H., Kwak, E., Lee, C. W., Joachimiak, A., Kim, Y. C., Lee, J., and Cho, Y. (2003). Mechanism of histone lysine methyl transfer revealed by the structure of SET7/9-AdoMet. *Embo J* **22,** 292-303.

Lachner, M., O'Carroll, D., Rea, S., Mechtler, K., and Jenuwein, T. (2001). Methylation of histone H3 lysine 9 creates a binding site for HP1 proteins. *Nature* **410,** 116-20.

Larsson, J., and Rasmuson-Lestander, A. (1994). Molecular cloning of the S-adenosylmethionine synthetase gene in Drosophila melanogaster. *FEBS Lett* **342,** 329-33.

Larsson, J., and Rasmuson-Lestander, A. (1998). Somatic and germline clone analysis in mutants of the S-adenosylmethionine synthetase encoding gene in Drosophila melanogaster. *FEBS Lett* **427,** 119-23.

Larsson, J., Zhang, J., and Rasmuson-Lestander, A. (1996). Mutations in the Drosophila melanogaster gene encoding S-adenosylmethionine synthetase [corrected] suppress position-effect variegation. *Genetics* **143,** 887-96.

Lazzaro, M. A., and Picketts, D. J. (2001). Cloning and characterization of the murine Imitation Switch (ISWI) genes: differential expression patterns suggest distinct developmental roles for Snf2h and Snf2l. *J Neurochem* **77,** 1145-56.

Le Douarin, B., Nielsen, A. L., Garnier, J. M., Ichinose, H., Jeanmougin, F., Losson, R., and Chambon, P. (1996). A possible involvement of TIF1 alpha and TIF1 beta in the epigenetic control of transcription by nuclear receptors. *Embo J* **15,** 6701-15.

Lechner, M. S., Begg, G. E., Speicher, D. W., and Rauscher, F. J., 3rd. (2000). Molecular determinants for targeting heterochromatin protein 1-mediated gene silencing: direct chromoshadow domain-KAP-1 corepressor interaction is essential. *Mol Cell Biol* **20,** 6449-65.

Lechner, M. S., Schultz, D. C., Negorev, D., Maul, G. G., and Rauscher, F. J., 3rd. (2005). The mammalian heterochromatin protein 1 binds diverse nuclear proteins through a common motif that targets the chromoshadow domain. *Biochem Biophys Res Commun* **331,** 929-37.

Lee, D. Y., Northrop, J. P., Kuo, M. H., and Stallcup, M. R. (2006). Histone H3 lysine 9 methyltransferase G9a is a transcriptional coactivator for nuclear receptors. *J Biol Chem* **281,** 8476-85.

Lee, H. W., Kim, S., and Paik, W. K. (1977). S-adenosylmethionine: protein-arginine methyltransferase. Purification and mechanism of the enzyme. *Biochemistry* **16,** 78-85.

Lee, M. G., Wynder, C., Cooch, N., and Shiekhattar, R. (2005). An essential role for CoREST in nucleosomal histone 3 lysine 4 demethylation. *Nature* **437,** 432-5.

Lehming, N., Le Saux, A., Schuller, J., and Ptashne, M. (1998). Chromatin components as part of a putative transcriptional repressing complex. *Proc Natl Acad Sci U S A* **95,** 7322-6.

Li, Y., Danzer, J. R., Alvarez, P., Belmont, A. S., and Wallrath, L. L. (2003). Effects of tethering HP1 to euchromatic regions of the Drosophila genome. *Development* **130,** 1817-24.

Li, Y., Kirschmann, D. A., and Wallrath, L. L. (2002). Does heterochromatin protein 1 always follow code? *Proc Natl Acad Sci U S A* **99 Suppl 4,** 16462-9.

Linder, B., Gerlach, N., and Jackle, H. (2001). The Drosophila homolog of the human AF10 is an HP1-interacting suppressor of position effect variegation. *EMBO Rep* **2,** 211-6.

Liu, L. P., Ni, J. Q., Shi, Y. D., Oakeley, E. J., and Sun, F. L. (2005). Sex-specific role of Drosophila melanogaster HP1 in regulating chromatin structure and gene transcription. *Nat Genet* **37,** 1361-6.

Liu, Y., and Eisenberg, D. (2002). 3D domain swapping: as domains continue to swap. *Protein Sci* **11,** 1285-99.

Locke, J., Kotarski, M. A., and Tartof, K. D. (1988). Dosage-dependent modifiers of position effect variegation in Drosophila and a mass action model that explains their effect. *Genetics* **120,** 181-98.

Lomberk, G., Bensi, D., Fernandez-Zapico, M. E., and Urrutia, R. (2006). Evidence for the existence of an HP1-mediated subcode within the histone code. *Nat Cell Biol* **8,** 407-15.

Lorentz, A., Heim, L., and Schmidt, H. (1992). The switching gene swi6 affects recombination and gene expression in the mating-type region of Schizosaccharomyces pombe. *Mol Gen Genet* **233,** 436-42.

Loyola, A., Bonaldi, T., Roche, D., Imhof, A., and Almouzni, G. (2006). PTMs on H3 variants before chromatin assembly potentiate their final epigenetic state. *Mol Cell* **24,** 309-16.

Lu, B. Y., Emtage, P. C., Duyf, B. J., Hilliker, A. J., and Eissenberg, J. C. (2000). Heterochromatin protein 1 is required for the normal expression of two heterochromatin genes in Drosophila. *Genetics* **155,** 699-708.

Luger, K., Mader, A. W., Richmond, R. K., Sargent, D. F., and Richmond, T. J. (1997). Crystal structure of the nucleosome core particle at 2.8 A resolution. *Nature* **389,** 251-60.

Luger, K., Rechsteiner, T. J., and Richmond, T. J. (1999). Expression and purification of recombinant histones and nucleosome reconstitution. *Methods Mol Biol* **119,** 1-16.

Lusser, A., Urwin, D. L., and Kadonaga, J. T. (2005). Distinct activities of CHD1 and ACF in ATP-dependent chromatin assembly. *Nat Struct Mol Biol* **12,** 160-6.

Mahy, N. L., Perry, P. E., and Bickmore, W. A. (2002). Gene density and transcription influence the localization of chromatin outside of chromosome territories detectable by FISH. *J Cell Biol* **159,** 753-63.

Maison, C., Bailly, D., Peters, A. H., Quivy, J. P., Roche, D., Taddei, A., Lachner, M., Jenuwein, T., and Almouzni, G. (2002). Higher-order structure in pericentric heterochromatin involves a distinct pattern of histone modification and an RNA component. *Nat Genet* **30,** 329-34.

Malik, H. S., and Henikoff, S. (2003). Phylogenomics of the nucleosome. *Nat Struct Biol* **10,** 882-91.

Manzur, K. L., Farooq, A., Zeng, L., Plotnikova, O., Koch, A. W., Sachchidanand, and Zhou, M. M. (2003). A dimeric viral SET domain methyltransferase specific to Lys27 of histone H3. *Nat Struct Biol* **10,** 187-96.

Martens, J. A., and Winston, F. (2003). Recent advances in understanding chromatin remodeling by Swi/Snf complexes. *Curr Opin Genet Dev* **13,** 136-42.

Martin, C., and Zhang, Y. (2005). The diverse functions of histone lysine methylation. *Nat Rev Mol Cell Biol* **6,** 838-49.

Mason, J. M., and Biessmann, H. (1995). The unusual telomeres of Drosophila. *Trends Genet* **11,** 58-62.

Masumoto, H., Hawke, D., Kobayashi, R., and Verreault, A. (2005). A role for cell-cycle-regulated histone H3 lysine 56 acetylation in the DNA damage response. *Nature* **436,** 294-8.

Mateescu, B., England, P., Halgand, F., Yaniv, M., and Muchardt, C. (2004). Tethering of HP1 proteins to chromatin is relieved by phosphoacetylation of histone H3. *EMBO Rep* **5,** 490-6.

Maul, G. G., Jensen, D. E., Ishov, A. M., Herlyn, M., and Rauscher, F. J., 3rd. (1998). Nuclear redistribution of BRCA1 during viral infection. *Cell Growth Differ* **9,** 743-55.

Maurer-Stroh, S., Dickens, N. J., Hughes-Davies, L., Kouzarides, T., Eisenhaber, F., and Ponting, C. P. (2003). The Tudor domain 'Royal Family': Tudor, plant Agenet, Chromo, PWWP and MBT domains. *Trends Biochem Sci* **28,** 69-74.

McDowell, T. L., Gibbons, R. J., Sutherland, H., O'Rourke, D. M., Bickmore, W. A., Pombo, A., Turley, H., Gatter, K., Picketts, D. J., Buckle, V. J., Chapman, L., Rhodes, D., and Higgs, D. R. (1999). Localization of a putative transcriptional regulator (ATRX) at pericentromeric heterochromatin and the short arms of acrocentric chromosomes. *Proc Natl Acad Sci U S A* **96,** 13983-8.

Meehan, R. R., Kao, C. F., and Pennings, S. (2003). HP1 binding to native chromatin in vitro is determined by the hinge region and not by the chromodomain. *Embo J* **22,** 3164-74.

Melcher, M., Schmid, M., Aagaard, L., Selenko, P., Laible, G., and Jenuwein, T. (2000). Structure-function analysis of SUV39H1 reveals a dominant role in heterochromatin organization, chromosome segregation, and mitotic progression. *Mol Cell Biol* **20,** 3728-41.

Metzger, E., Wissmann, M., Yin, N., Muller, J. M., Schneider, R., Peters, A. H., Gunther, T., Buettner, R., and Schule, R. (2005). LSD1 demethylates

repressive histone marks to promote androgen-receptor-dependent transcription. *Nature* **437,** 436-9.

Milne, T. A., Briggs, S. D., Brock, H. W., Martin, M. E., Gibbs, D., Allis, C. D., and Hess, J. L. (2002). MLL targets SET domain methyltransferase activity to Hox gene promoters. *Mol Cell* **10,** 1107-17.

Min, J., Zhang, X., Cheng, X., Grewal, S. I., and Xu, R. M. (2002). Structure of the SET domain histone lysine methyltransferase Clr4. *Nat Struct Biol* **9,** 828-32.

Min, J., Zhang, Y., and Xu, R. M. (2003). Structural basis for specific binding of Polycomb chromodomain to histone H3 methylated at Lys 27. *Genes Dev* **17,** 1823-8.

Minc, E., Allory, Y., Worman, H. J., Courvalin, J. C., and Buendia, B. (1999). Localization and phosphorylation of HP1 proteins during the cell cycle in mammalian cells. *Chromosoma* **108,** 220-34.

Minc, E., Courvalin, J. C., and Buendia, B. (2000). HP1gamma associates with euchromatin and heterochromatin in mammalian nuclei and chromosomes. *Cytogenet Cell Genet* **90,** 279-84.

Mis, J., Ner, S. S., and Grigliatti, T. A. (2006). Identification of three histone methyltransferases in Drosophila: dG9a is a suppressor of PEV and is required for gene silencing. *Mol Genet Genomics* **275,** 513-26.

Muchardt, C., Guilleme, M., Seeler, J. S., Trouche, D., Dejean, A., and Yaniv, M. (2002). Coordinated methyl and RNA binding is required for heterochromatin localization of mammalian HP1alpha. *EMBO Rep* **3,** 975-81.

Mukhopadhyay, R., Yu, W., Whitehead, J., Xu, J., Lezcano, M., Pack, S., Kanduri, C., Kanduri, M., Ginjala, V., Vostrov, A., Quitschke, W., Chernukhin, I., Klenova, E., Lobanenkov, V., and Ohlsson, R. (2004). The binding sites for the chromatin insulator protein CTCF map to DNA methylation-free domains genome-wide. *Genome Res* **14,** 1594-602.

Muller, H. (1930). Types of visible variations induced by X-rays in Drosophila. *J Genetics* **1930,** 299-334.

Murzina, N., Verreault, A., Laue, E., and Stillman, B. (1999). Heterochromatin dynamics in mouse cells: interaction between chromatin assembly factor 1 and HP1 proteins. *Mol Cell* **4,** 529-40.

Nakamura, T., Mori, T., Tada, S., Krajewski, W., Rozovskaia, T., Wassell, R., Dubois, G., Mazo, A., Croce, C. M., and Canaani, E. (2002). ALL-1 is a histone methyltransferase that assembles a supercomplex of proteins involved in transcriptional regulation. *Mol Cell* **10,** 1119-28.

Nakayama, J., Rice, J. C., Strahl, B. D., Allis, C. D., and Grewal, S. I. (2001). Role of histone H3 lysine 9 methylation in epigenetic control of heterochromatin assembly. *Science* **292,** 110-3.

Nasmyth, K. (2002). Segregating sister genomes: the molecular biology of chromosome separation. *Science* **297,** 559-65.

Nasmyth, K. (2005). How might cohesin hold sister chromatids together? *Philos Trans R Soc Lond B Biol Sci* **360,** 483-96.

Nathan, D., Ingvarsdottir, K., Sterner, D. E., Bylebyl, G. R., Dokmanovic, M., Dorsey, J. A., Whelan, K. A., Krsmanovic, M., Lane, W. S., Meluh, P. B., Johnson, E. S., and Berger, S. L. (2006). Histone sumoylation is a negative regulator in Saccharomyces cerevisiae and shows dynamic interplay with positive-acting histone modifications. *Genes Dev* **20,** 966-76.

Neigeborn, L., and Carlson, M. (1984). Genes affecting the regulation of SUC2 gene expression by glucose repression in Saccharomyces cerevisiae. *Genetics* **108,** 845-58.

Netzer, C., Rieger, L., Brero, A., Zhang, C. D., Hinzke, M., Kohlhase, J., and Bohlander, S. K. (2001). SALL1, the gene mutated in Townes-Brocks syndrome, encodes a transcriptional repressor which interacts with TRF1/PIN2 and localizes to pericentromeric heterochromatin. *Hum Mol Genet* **10,** 3017-24.

Ng, H. H., Feng, Q., Wang, H., Erdjument-Bromage, H., Tempst, P., Zhang, Y., and Struhl, K. (2002). Lysine methylation within the globular domain of histone H3 by Dot1 is important for telomeric silencing and Sir protein association. *Genes Dev* **16,** 1518-27.

Nichols, J., Zevnik, B., Anastassiadis, K., Niwa, H., Klewe-Nebenius, D., Chambers, I., Scholer, H., and Smith, A. (1998). Formation of pluripotent stem cells in the mammalian embryo depends on the POU transcription factor Oct4. *Cell* **95,** 379-91.

Nielsen, A. L., Ortiz, J. A., You, J., Oulad-Abdelghani, M., Khechumian, R., Gansmuller, A., Chambon, P., and Losson, R. (1999). Interaction with members of the heterochromatin protein 1 (HP1) family and histone deacetylation are differentially involved in transcriptional silencing by members of the TIF1 family. *Embo J* **18,** 6385-95.

Nielsen, A. L., Oulad-Abdelghani, M., Ortiz, J. A., Remboutsika, E., Chambon, P., and Losson, R. (2001a). Heterochromatin formation in mammalian cells: interaction between histones and HP1 proteins. *Mol Cell* **7,** 729-39.

Nielsen, A. L., Sanchez, C., Ichinose, H., Cervino, M., Lerouge, T., Chambon, P., and Losson, R. (2002a). Selective interaction between the chromatin-remodeling factor BRG1 and the heterochromatin-associated protein HP1alpha. *Embo J* **21,** 5797-806.

Nielsen, P. R., Nietlispach, D., Mott, H. R., Callaghan, J., Bannister, A., Kouzarides, T., Murzin, A. G., Murzina, N. V., and Laue, E. D. (2002b). Structure of the HP1 chromodomain bound to histone H3 methylated at lysine 9. *Nature* **416,** 103-7.

Nielsen, S. J., Schneider, R., Bauer, U. M., Bannister, A. J., Morrison, A., O'Carroll, D., Firestein, R., Cleary, M., Jenuwein, T., Herrera, R. E., and Kouzarides, T. (2001b). Rb targets histone H3 methylation and HP1 to promoters. *Nature* **412,** 561-5.

Nightingale, K. P., O'Neill, L. P., and Turner, B. M. (2006). Histone modifications: signalling receptors and potential elements of a heritable epigenetic code. *Curr Opin Genet Dev* **16,** 125-36.

Nimmo, E. R., Cranston, G., and Allshire, R. C. (1994). Telomere-associated chromosome breakage in fission yeast results in variegated expression of adjacent genes. *Embo J* **13,** 3801-11.

Nishio, H., and Walsh, M. J. (2004). CCAAT displacement protein/cut homolog recruits G9a histone lysine methyltransferase to repress transcription. *Proc Natl Acad Sci U S A* **101,** 11257-62.

Nishioka, K., Chuikov, S., Sarma, K., Erdjument-Bromage, H., Allis, C. D., Tempst, P., and Reinberg, D. (2002). Set9, a novel histone H3 methyltransferase that facilitates transcription by precluding histone tail modifications required for heterochromatin formation. *Genes Dev* **16,** 479-89.

Nonaka, N., Kitajima, T., Yokobayashi, S., Xiao, G., Yamamoto, M., Grewal, S. I., and Watanabe, Y. (2002). Recruitment of cohesin to heterochromatic regions by Swi6/HP1 in fission yeast. *Nat Cell Biol* **4,** 89-93.

Nugent, C. I., and Lundblad, V. (1998). The telomerase reverse transcriptase: components and regulation. *Genes Dev* **12,** 1073-85.

O'Carroll, D., Scherthan, H., Peters, A. H., Opravil, S., Haynes, A. R., Laible, G., Rea, S., Schmid, M., Lebersorger, A., Jerratsch, M., Sattler, L., Mattei, M. G., Denny, P., Brown, S. D., Schweizer, D., and Jenuwein, T. (2000). Isolation and characterization of Suv39h2, a second histone H3 methyltransferase gene that displays testis-specific expression. *Mol Cell Biol* **20,** 9423-33.

Ogawa, H., Ishiguro, K., Gaubatz, S., Livingston, D. M., and Nakatani, Y. (2002). A complex with chromatin modifiers that occupies E2F- and Myc-responsive genes in G0 cells. *Science* **296,** 1132-6.

Ohfuchi, E., Kato, M., Sasaki, M., Sugimoto, K., Oma, Y., and Harata, M. (2006). Vertebrate Arp6, a novel nuclear actin-related protein, interacts with heterochromatin protein 1. *Eur J Cell Biol* **85,** 411-21.

Ohkura, H., Adachi, Y., Kinoshita, N., Niwa, O., Toda, T., and Yanagida, M. (1988). Cold-sensitive and caffeine-supersensitive mutants of the Schizosaccharomyces pombe dis genes implicated in sister chromatid separation during mitosis. *Embo J* **7,** 1465-73.

Okamoto, K., Okazawa, H., Okuda, A., Sakai, M., Muramatsu, M., and Hamada, H. (1990). A novel octamer binding transcription factor is differentially expressed in mouse embryonic cells. *Cell* **60,** 461-72.

Ozdemir, A., Spicuglia, S., Lasonder, E., Vermeulen, M., Campsteijn, C., Stunnenberg, H. G., and Logie, C. (2005). Characterization of lysine 56 of histone H3 as an acetylation site in Saccharomyces cerevisiae. *J Biol Chem* **280,** 25949-52.

Pak, D. T., Pflumm, M., Chesnokov, I., Huang, D. W., Kellum, R., Marr, J., Romanowski, P., and Botchan, M. R. (1997). Association of the origin recognition complex with heterochromatin and HP1 in higher eukaryotes. *Cell* **91,** 311-23.

Pal, S., Vishwanath, S. N., Erdjument-Bromage, H., Tempst, P., and Sif, S. (2004). Human SWI/SNF-associated PRMT5 methylates histone H3 arginine 8 and negatively regulates expression of ST7 and NM23 tumor suppressor genes. *Mol Cell Biol* **24,** 9630-45.

Palmer, D. K., O'Day, K., Trong, H. L., Charbonneau, H., and Margolis, R. L. (1991). Purification of the centromere-specific protein CENP-A and demonstration that it is a distinctive histone. *Proc Natl Acad Sci U S A* **88,** 3734-8.

Pant, V., Kurukuti, S., Pugacheva, E., Shamsuddin, S., Mariano, P., Renkawitz, R., Klenova, E., Lobanenkov, V., and Ohlsson, R. (2004). Mutation of a single CTCF target site within the H19 imprinting control region leads to loss of Igf2 imprinting and complex patterns of de novo methylation upon maternal inheritance. *Mol Cell Biol* **24,** 3497-504.

Papamichos-Chronakis, M., Krebs, J. E., and Peterson, C. L. (2006). Interplay between Ino80 and Swr1 chromatin remodeling enzymes regulates cell cycle checkpoint adaptation in response to DNA damage. *Genes Dev* **20,** 2437-49.

Pardue, M. L. (1994). The ends and the middle: putting chromosomes together. *Curr Opin Genet Dev* **4,** 845-50.

Park, C., and Raines, R. T. (2000). Dimer formation by a "monomeric" protein. *Protein Sci* **9,** 2026-33.

Paro, R., and Hogness, D. S. (1991). The Polycomb protein shares a homologous domain with a heterochromatin-associated protein of Drosophila. *Proc Natl Acad Sci U S A* **88,** 263-7.

Parra, M. A., Kerr, D., Fahy, D., Pouchnik, D. J., and Wyrick, J. J. (2006). Deciphering the roles of the histone H2B N-terminal domain in genome-wide transcription. *Mol Cell Biol* **26,** 3842-52.

Patnaik, D., Chin, H. G., Esteve, P. O., Benner, J., Jacobsen, S. E., and Pradhan, S. (2004). Substrate specificity and kinetic mechanism of mammalian G9a histone H3 methyltransferase. *J Biol Chem* **279,** 53248-58.

Perrini, B., Piacentini, L., Fanti, L., Altieri, F., Chichiarelli, S., Berloco, M., Turano, C., Ferraro, A., and Pimpinelli, S. (2004). HP1 controls telomere capping, telomere elongation, and telomere silencing by two different mechanisms in Drosophila. *Mol Cell* **15,** 467-76.

Pestova, T. V., Kolupaeva, V. G., Lomakin, I. B., Pilipenko, E. V., Shatsky, I. N., Agol, V. I., and Hellen, C. U. (2001). Molecular mechanisms of translation initiation in eukaryotes. *Proc Natl Acad Sci U S A* **98,** 7029-36.

Peters, A. H., Kubicek, S., Mechtler, K., O'Sullivan, R. J., Derijck, A. A., Perez-Burgos, L., Kohlmaier, A., Opravil, S., Tachibana, M., Shinkai, Y., Martens, J. H., and Jenuwein, T. (2003). Partitioning and plasticity of repressive histone methylation states in mammalian chromatin. *Mol Cell* **12,** 1577-89.

Peters, A. H., O'Carroll, D., Scherthan, H., Mechtler, K., Sauer, S., Schofer, C., Weipoltshammer, K., Pagani, M., Lachner, M., Kohlmaier, A., Opravil, S., Doyle, M., Sibilia, M., and Jenuwein, T. (2001). Loss of the Suv39h histone methyltransferases impairs mammalian heterochromatin and genome stability. *Cell* **107,** 323-37.

Piacentini, L., Fanti, L., Berloco, M., Perrini, B., and Pimpinelli, S. (2003). Heterochromatin protein 1 (HP1) is associated with induced gene expression in Drosophila euchromatin. *J Cell Biol* **161,** 707-14.

Pickart, C. M., and Cohen, R. E. (2004). Proteasomes and their kin: proteases in the machine age. *Nat Rev Mol Cell Biol* **5,** 177-87.

Pidoux, A. L., and Allshire, R. C. (2005). The role of heterochromatin in centromere function. *Philos Trans R Soc Lond B Biol Sci* **360,** 569-79.

Pikarsky, E., Sharir, H., Ben-Shushan, E., and Bergman, Y. (1994). Retinoic acid represses Oct-3/4 gene expression through several retinoic acid-responsive elements located in the promoter-enhancer region. *Mol Cell Biol* **14,** 1026-38.

Platero, J. S., Hartnett, T., and Eissenberg, J. C. (1995). Functional analysis of the chromo domain of HP1. *Embo J* **14,** 3977-86.

Polioudaki, H., Kourmouli, N., Drosou, V., Bakou, A., Theodoropoulos, P. A., Singh, P. B., Giannakouros, T., and Georgatos, S. D. (2001). Histones H3/H4 form a tight complex with the inner nuclear membrane protein LBR and heterochromatin protein 1. *EMBO Rep* **2,** 920-5.

Pollard, K. J., and Peterson, C. L. (1998). Chromatin remodeling: a marriage between two families? *Bioessays* **20,** 771-80.

Powers, J. A., and Eissenberg, J. C. (1993). Overlapping domains of the heterochromatin-associated protein HP1 mediate nuclear localization and heterochromatin binding. *J Cell Biol* **120,** 291-9.

Pray-Grant, M. G., Daniel, J. A., Schieltz, D., Yates, J. R., 3rd, and Grant, P. A. (2005). Chd1 chromodomain links histone H3 methylation with SAGA- and SLIK-dependent acetylation. *Nature* **433,** 434-8.

Prigent, C., and Dimitrov, S. (2003). Phosphorylation of serine 10 in histone H3, what for? *J Cell Sci* **116,** 3677-85.

Quivy, J. P., Roche, D., Kirschner, D., Tagami, H., Nakatani, Y., and Almouzni, G. (2004). A CAF-1 dependent pool of HP1 during heterochromatin duplication. *Embo J* **23,** 3516-26.

Raffa, G. D., Cenci, G., Siriaco, G., Goldberg, M. L., and Gatti, M. (2005). The putative Drosophila transcription factor woc is required to prevent telomeric fusions. *Mol Cell* **20,** 821-31.

Ramakrishnan, V. (1997). Histone H1 and chromatin higher-order structure. *Crit Rev Eukaryot Gene Expr* **7,** 215-30.

Rayasam, G. V., Wendling, O., Angrand, P. O., Mark, M., Niederreither, K., Song, L., Lerouge, T., Hager, G. L., Chambon, P., and Losson, R. (2003). NSD1 is essential for early post-implantation development and has a catalytically active SET domain. *Embo J* **22,** 3153-63.

Rea, S., Eisenhaber, F., O'Carroll, D., Strahl, B. D., Sun, Z. W., Schmid, M., Opravil, S., Mechtler, K., Ponting, C. P., Allis, C. D., and Jenuwein, T. (2000). Regulation of chromatin structure by site-specific histone H3 methyltransferases. *Nature* **406,** 593-9.

Reuter, G., Giarre, M., Farah, J., Gausz, J., Spierer, A., and Spierer, P. (1990). Dependence of position-effect variegation in Drosophila on dose of a gene encoding an unusual zinc-finger protein. *Nature* **344,** 219-23.

Reuter, G., and Spierer, P. (1992). Position effect variegation and chromatin proteins. *Bioessays* **14,** 605-12.

Rice, J. C., Briggs, S. D., Ueberheide, B., Barber, C. M., Shabanowitz, J., Hunt, D. F., Shinkai, Y., and Allis, C. D. (2003). Histone methyltransferases direct different degrees of methylation to define distinct chromatin domains. *Mol Cell* **12,** 1591-8.

Rice, J. C., Nishioka, K., Sarma, K., Steward, R., Reinberg, D., and Allis, C. D. (2002). Mitotic-specific methylation of histone H4 Lys 20 follows increased PR-Set7 expression and its localization to mitotic chromosomes. *Genes Dev* **16,** 2225-30.

Roguev, A., Schaft, D., Shevchenko, A., Pijnappel, W. W., Wilm, M., Aasland, R., and Stewart, A. F. (2001). The Saccharomyces cerevisiae Set1 complex includes an Ash2 homologue and methylates histone 3 lysine 4. *Embo J* **20,** 7137-48.

Rollins, R. A., Morcillo, P., and Dorsett, D. (1999). Nipped-B, a Drosophila homologue of chromosomal adherins, participates in activation by remote enhancers in the cut and Ultrabithorax genes. *Genetics* **152,** 577-93.

Ruthenburg, A. J., Wang, W., Graybosch, D. M., Li, H., Allis, C. D., Patel, D. J., and Verdine, G. L. (2006). Histone H3 recognition and presentation by the WDR5 module of the MLL1 complex. *Nat Struct Mol Biol* **13,** 704-12.

Ryan, R. F., Schultz, D. C., Ayyanathan, K., Singh, P. B., Friedman, J. R., Fredericks, W. J., and Rauscher, F. J., 3rd. (1999). KAP-1 corepressor protein interacts and colocalizes with heterochromatic and euchromatic HP1 proteins: a potential role for Kruppel-associated box-zinc finger proteins in heterochromatin-mediated gene silencing. *Mol Cell Biol* **19,** 4366-78.

Salminen, A., Efimova, I. S., Parfenyev, A. N., Magretova, N. N., Mikalahti, K., Goldman, A., Baykov, A. A., and Lahti, R. (1999). Reciprocal effects of substitutions at the subunit interfaces in hexameric pyrophosphatase of

Escherichia coli. Dimeric and monomeric forms of the enzyme. *J Biol Chem* **274,** 33898-904.

Sandaltzopoulos, R., Blank, T., and Becker, P. B. (1994). Transcriptional repression by nucleosomes but not H1 in reconstituted preblastoderm Drosophila chromatin. *Embo J* **13,** 373-9.

Sanders, S. L., Portoso, M., Mata, J., Bahler, J., Allshire, R. C., and Kouzarides, T. (2004). Methylation of histone H4 lysine 20 controls recruitment of Crb2 to sites of DNA damage. *Cell* **119,** 603-14.

Santos-Rosa, H., and Caldas, C. (2005). Chromatin modifier enzymes, the histone code and cancer. *Eur J Cancer* **41,** 2381-402.

Santos-Rosa, H., Schneider, R., Bannister, A. J., Sherriff, J., Bernstein, B. E., Emre, N. C., Schreiber, S. L., Mellor, J., and Kouzarides, T. (2002). Active genes are tri-methylated at K4 of histone H3. *Nature* **419,** 407-11.

Sarraf, S. A., and Stancheva, I. (2004). Methyl-CpG binding protein MBD1 couples histone H3 methylation at lysine 9 by SETDB1 to DNA replication and chromatin assembly. *Mol Cell* **15,** 595-605.

Schmiedeberg, L., Weisshart, K., Diekmann, S., Meyer Zu Hoerste, G., and Hemmerich, P. (2004). High- and low-mobility populations of HP1 in heterochromatin of mammalian cells. *Mol Biol Cell* **15,** 2819-33.

Schotta, G., Ebert, A., Dorn, R., and Reuter, G. (2003a). Position-effect variegation and the genetic dissection of chromatin regulation in Drosophila. *Semin Cell Dev Biol* **14,** 67-75.

Schotta, G., Ebert, A., Krauss, V., Fischer, A., Hoffmann, J., Rea, S., Jenuwein, T., Dorn, R., and Reuter, G. (2002). Central role of Drosophila SU(VAR)3-9 in histone H3-K9 methylation and heterochromatic gene silencing. *Embo J* **21,** 1121-31.

Schotta, G., Ebert, A., and Reuter, G. (2003b). SU(VAR)3-9 is a conserved key function in heterochromatic gene silencing. *Genetica* **117,** 149-58.

Schotta, G., Lachner, M., Peters, A. H., and Jenuwein, T. (2004a). The indexing potential of histone lysine methylation. *Novartis Found Symp* **259,** 22-37; discussion 37-47, 163-9.

Schotta, G., Lachner, M., Sarma, K., Ebert, A., Sengupta, R., Reuter, G., Reinberg, D., and Jenuwein, T. (2004b). A silencing pathway to induce H3-K9 and H4-K20 trimethylation at constitutive heterochromatin. *Genes Dev* **18,** 1251-62.

Schuetz, A., Allali-Hassani, A., Martin, F., Loppnau, P., Vedadi, M., Bochkarev, A., Plotnikov, A. N., Arrowsmith, C. H., and Min, J. (2006). Structural basis for molecular recognition and presentation of histone H3 by WDR5. *Embo J* **25,** 4245-52.

Schultz, D. C., Ayyanathan, K., Negorev, D., Maul, G. G., and Rauscher, F. J., 3rd. (2002). SETDB1: a novel KAP-1-associated histone H3, lysine 9-specific methyltransferase that contributes to HP1-mediated silencing of euchromatic genes by KRAB zinc-finger proteins. *Genes Dev* **16,** 919-32.

Scott, K. C., Taubman, A. D., and Geyer, P. K. (1999). Enhancer blocking by the Drosophila gypsy insulator depends upon insulator anatomy and enhancer strength. *Genetics* **153,** 787-98.

Seeger, K., Lein, S., Reuter, G., and Berger, S. (2005). Saturation transfer difference measurements with SU(VAR)3-9 and S-adenosyl-L-methionine. *Biochemistry* **44,** 6208-13.

Seeler, J. S., Marchio, A., Sitterlin, D., Transy, C., and Dejean, A. (1998). Interaction of SP100 with HP1 proteins: a link between the promyelocytic leukemia-

associated nuclear bodies and the chromatin compartment. *Proc Natl Acad Sci U S A* **95,** 7316-21.

Shanower, G. A., Muller, M., Blanton, J. L., Honti, V., Gyurkovics, H., and Schedl, P. (2005). Characterization of the grappa gene, the Drosophila histone H3 lysine 79 methyltransferase. *Genetics* **169,** 173-84.

Shareef, M. M., Badugu, R., and Kellum, R. (2003). HP1/ORC complex and heterochromatin assembly. *Genetica* **117,** 127-34.

Shareef, M. M., King, C., Damaj, M., Badagu, R., Huang, D. W., and Kellum, R. (2001). Drosophila heterochromatin protein 1 (HP1)/origin recognition complex (ORC) protein is associated with HP1 and ORC and functions in heterochromatin-induced silencing. *Mol Biol Cell* **12,** 1671-85.

Shen, X., Mizuguchi, G., Hamiche, A., and Wu, C. (2000). A chromatin remodelling complex involved in transcription and DNA processing. *Nature* **406,** 541-4.

Shi, Y., Lan, F., Matson, C., Mulligan, P., Whetstine, J. R., Cole, P. A., Casero, R. A., and Shi, Y. (2004). Histone demethylation mediated by the nuclear amine oxidase homolog LSD1. *Cell* **119,** 941-53.

Shi, Y., Sawada, J., Sui, G., Affar el, B., Whetstine, J. R., Lan, F., Ogawa, H., Luke, M. P., Nakatani, Y., and Shi, Y. (2003). Coordinated histone modifications mediated by a CtBP co-repressor complex. *Nature* **422,** 735-8.

Shi, Y. J., Matson, C., Lan, F., Iwase, S., Baba, T., and Shi, Y. (2005). Regulation of LSD1 histone demethylase activity by its associated factors. *Mol Cell* **19,** 857-64.

Shiio, Y., and Eisenman, R. N. (2003). Histone sumoylation is associated with transcriptional repression. *Proc Natl Acad Sci U S A* **100,** 13225-30.

Shin, J. A., Choi, E. S., Kim, H. S., Ho, J. C., Watts, F. Z., Park, S. D., and Jang, Y. K. (2005). SUMO modification is involved in the maintenance of heterochromatin stability in fission yeast. *Mol Cell* **19,** 817-28.

Simon, R. H., and Felsenfeld, G. (1979). A new procedure for purifying histone pairs H2A + H2B and H3 + H4 from chromatin using hydroxylapatite. *Nucleic Acids Res* **6,** 689-96.

Sims, R. J., 3rd, Nishioka, K., and Reinberg, D. (2003). Histone lysine methylation: a signature for chromatin function. *Trends Genet* **19,** 629-39.

Singh, P. B., Miller, J. R., Pearce, J., Kothary, R., Burton, R. D., Paro, R., James, T. C., and Gaunt, S. J. (1991). A sequence motif found in a Drosophila heterochromatin protein is conserved in animals and plants. *Nucleic Acids Res* **19,** 789-94.

Smith, E. R., Pannuti, A., Gu, W., Steurnagel, A., Cook, R. G., Allis, C. D., and Lucchesi, J. C. (2000). The drosophila MSL complex acetylates histone H4 at lysine 16, a chromatin modification linked to dosage compensation. *Mol Cell Biol* **20,** 312-8.

Smothers, J. F., and Henikoff, S. (2000). The HP1 chromo shadow domain binds a consensus peptide pentamer. *Curr Biol* **10,** 27-30.

Smothers, J. F., and Henikoff, S. (2001). The hinge and chromo shadow domain impart distinct targeting of HP1-like proteins. *Mol Cell Biol* **21,** 2555-69.

Song, K., Jung, Y., Jung, D., and Lee, I. (2001). Human Ku70 interacts with heterochromatin protein 1alpha. *J Biol Chem* **276,** 8321-7.

Spencer, V. A., and Davie, J. R. (1999). Role of covalent modifications of histones in regulating gene expression. *Gene* **240,** 1-12.

Spierer, A., Seum, C., Delattre, M., and Spierer, P. (2005). Loss of the modifiers of variegation Su(var)3-7 or HP1 impacts male X polytene chromosome morphology and dosage compensation. *J Cell Sci* **118,** 5047-57.

Stabell, M., Eskeland, R., Bjorkmo, M., Larsson, J., Aalen, R. B., Imhof, A., and Lambertsson, A. (2006). The Drosophila G9a gene encodes a multi-catalytic histone methyltransferase required for normal development. *Nucleic Acids Res* **34,** 4609-21.

Stern, M., Jensen, R., and Herskowitz, I. (1984). Five SWI genes are required for expression of the HO gene in yeast. *J Mol Biol* **178,** 853-68.

Stewart, M. D., Li, J., and Wong, J. (2005). Relationship between histone H3 lysine 9 methylation, transcription repression, and heterochromatin protein 1 recruitment. *Mol Cell Biol* **25,** 2525-38.

Strahl, B. D., Grant, P. A., Briggs, S. D., Sun, Z. W., Bone, J. R., Caldwell, J. A., Mollah, S., Cook, R. G., Shabanowitz, J., Hunt, D. F., and Allis, C. D. (2002). Set2 is a nucleosomal histone H3-selective methyltransferase that mediates transcriptional repression. *Mol Cell Biol* **22,** 1298-306.

Tachibana, M., Sugimoto, K., Fukushima, T., and Shinkai, Y. (2001). Set domain-containing protein, G9a, is a novel lysine-preferring mammalian histone methyltransferase with hyperactivity and specific selectivity to lysines 9 and 27 of histone H3. *J Biol Chem* **276,** 25309-17.

Tachibana, M., Sugimoto, K., Nozaki, M., Ueda, J., Ohta, T., Ohki, M., Fukuda, M., Takeda, N., Niida, H., Kato, H., and Shinkai, Y. (2002). G9a histone methyltransferase plays a dominant role in euchromatic histone H3 lysine 9 methylation and is essential for early embryogenesis. *Genes Dev* **16,** 1779-91.

Tachibana, M., Ueda, J., Fukuda, M., Takeda, N., Ohta, T., Iwanari, H., Sakihama, T., Kodama, T., Hamakubo, T., and Shinkai, Y. (2005). Histone methyltransferases G9a and GLP form heteromeric complexes and are both crucial for methylation of euchromatin at H3-K9. *Genes Dev* **19,** 815-26.

Taipale, M., Rea, S., Richter, K., Vilar, A., Lichter, P., Imhof, A., and Akhtar, A. (2005). hMOF histone acetyltransferase is required for histone H4 lysine 16 acetylation in mammalian cells. *Mol Cell Biol* **25,** 6798-810.

Takeuchi, T., Watanabe, Y., Takano-Shimizu, T., and Kondo, S. (2006). Roles of jumonji and jumonji family genes in chromatin regulation and development. *Dev Dyn* **235,** 2449-59.

Tamaru, H., Zhang, X., McMillen, D., Singh, P. B., Nakayama, J., Grewal, S. I., Allis, C. D., Cheng, X., and Selker, E. U. (2003). Trimethylated lysine 9 of histone H3 is a mark for DNA methylation in Neurospora crassa. *Nat Genet* **34,** 75-9.

Tartof, K. D., Hobbs, C., and Jones, M. (1984). A structural basis for variegating position effects. *Cell* **37,** 869-78.

Thiru, A., Nietlispach, D., Mott, H. R., Okuwaki, M., Lyon, D., Nielsen, P. R., Hirshberg, M., Verreault, A., Murzina, N. V., and Laue, E. D. (2004). Structural basis of HP1/PXVXL motif peptide interactions and HP1 localisation to heterochromatin. *Embo J* **23,** 489-99.

Thomas, J. O. (1999). Histone H1: location and role. *Curr Opin Cell Biol* **11,** 312-7.

Thummel, C. S. (1995). From embryogenesis to metamorphosis: the regulation and function of Drosophila nuclear receptor superfamily members. *Cell* **83,** 871-7.

Tollervey, D., Lehtonen, H., Carmo-Fonseca, M., and Hurt, E. C. (1991). The small nucleolar RNP protein NOP1 (fibrillarin) is required for pre-rRNA processing in yeast. *Embo J* **10,** 573-83.

Trewick, S. C., McLaughlin, P. J., and Allshire, R. C. (2005). Methylation: lost in hydroxylation? *EMBO Rep* **6,** 315-20.

Trievel, R. C., Beach, B. M., Dirk, L. M., Houtz, R. L., and Hurley, J. H. (2002). Structure and catalytic mechanism of a SET domain protein methyltransferase. *Cell* **111,** 91-103.

Tschiersch, B., Hofmann, A., Krauss, V., Dorn, R., Korge, G., and Reuter, G. (1994). The protein encoded by the Drosophila position-effect variegation suppressor gene Su(var)3-9 combines domains of antagonistic regulators of homeotic gene complexes. *Embo J* **13,** 3822-31.

Tse, C., and Hansen, J. C. (1997). Hybrid trypsinized nucleosomal arrays: identification of multiple functional roles of the H2A/H2B and H3/H4 N-termini in chromatin fiber compaction. *Biochemistry* **36,** 11381-8.

Tsukada, Y., Fang, J., Erdjument-Bromage, H., Warren, M. E., Borchers, C. H., Tempst, P., and Zhang, Y. (2006). Histone demethylation by a family of JmjC domain-containing proteins. *Nature* **439,** 811-6.

Tsukiyama, T., and Wu, C. (1995). Purification and properties of an ATP-dependent nucleosome remodeling factor. *Cell* **83,** 1011-20.

Turner, B. M. (1993). Decoding the nucleosome. *Cell* **75,** 5-8.

Turner, B. M. (2005). Reading signals on the nucleosome with a new nomenclature for modified histones. *Nat Struct Mol Biol* **12,** 110-2.

Turner, B. M., Birley, A. J., and Lavender, J. (1992). Histone H4 isoforms acetylated at specific lysine residues define individual chromosomes and chromatin domains in Drosophila polytene nuclei. *Cell* **69,** 375-84.

Turner, J. M., Burgoyne, P. S., and Singh, P. B. (2001). M31 and macroH2A1.2 colocalise at the pseudoautosomal region during mouse meiosis. *J Cell Sci* **114,** 3367-75.

Ueda, J., Tachibana, M., Ikura, T., and Shinkai, Y. (2006). Zinc finger protein Wiz links G9a/GLP histone methyltransferases to the co-repressor molecule CtBP. *J Biol Chem* **281,** 20120-8.

Vakoc, C. R., Mandat, S. A., Olenchock, B. A., and Blobel, G. A. (2005). Histone H3 lysine 9 methylation and HP1gamma are associated with transcription elongation through mammalian chromatin. *Mol Cell* **19,** 381-91.

van Leeuwen, F., Gafken, P. R., and Gottschling, D. E. (2002). Dot1p modulates silencing in yeast by methylation of the nucleosome core. *Cell* **109,** 745-56.

Varambally, S., Dhanasekaran, S. M., Zhou, M., Barrette, T. R., Kumar-Sinha, C., Sanda, M. G., Ghosh, D., Pienta, K. J., Sewalt, R. G., Otte, A. P., Rubin, M. A., and Chinnaiyan, A. M. (2002). The polycomb group protein EZH2 is involved in progression of prostate cancer. *Nature* **419,** 624-9.

Varga-Weisz, P. D., Wilm, M., Bonte, E., Dumas, K., Mann, M., and Becker, P. B. (1997). Chromatin-remodelling factor CHRAC contains the ATPases ISWI and topoisomerase II. *Nature* **388,** 598-602.

Vassallo, M. F., and Tanese, N. (2002). Isoform-specific interaction of HP1 with human TAFII130. *Proc Natl Acad Sci U S A* **99,** 5919-24.

Vaute, O., Nicolas, E., Vandel, L., and Trouche, D. (2002). Functional and physical interaction between the histone methyl transferase Suv39H1 and histone deacetylases. *Nucleic Acids Res* **30,** 475-81.

Vermaak, D., Henikoff, S., and Malik, H. S. (2005). Positive selection drives the evolution of rhino, a member of the heterochromatin protein 1 family in Drosophila. *PLoS Genet* **1,** 96-108.

Wang, Y., Zhang, W., Jin, Y., Johansen, J., and Johansen, K. M. (2001). The JIL-1 tandem kinase mediates histone H3 phosphorylation and is required for maintenance of chromatin structure in Drosophila. *Cell* **105,** 433-43.

Warren, J. T., Wismar, J., Subrahmanyam, B., and Gilbert, L. I. (2001). Woc (without children) gene control of ecdysone biosynthesis in Drosophila melanogaster. *Mol Cell Endocrinol* **181,** 1-14.

Watanabe, Y. (2004). Modifying sister chromatid cohesion for meiosis. *J Cell Sci* **117,** 4017-23.

West, A. G., Gaszner, M., and Felsenfeld, G. (2002). Insulators: many functions, many mechanisms. *Genes Dev* **16,** 271-88.

Williams, L., and Grafi, G. (2000). The retinoblastoma protein - a bridge to heterochromatin. *Trends Plant Sci* **5,** 239-40.

Wilson, J. R., Jing, C., Walker, P. A., Martin, S. R., Howell, S. A., Blackburn, G. M., Gamblin, S. J., and Xiao, B. (2002). Crystal structure and functional analysis of the histone methyltransferase SET7/9. *Cell* **111,** 105-15.

Wismar, J., Habtemichael, N., Warren, J. T., Dai, J. D., Gilbert, L. I., and Gateff, E. (2000). The mutation without children(rgl) causes ecdysteroid deficiency in third-instar larvae of Drosophila melanogaster. *Dev Biol* **226,** 1-17.

Workman, J. L. (2006). Nucleosome displacement in transcription. *Genes Dev* **20,** 2009-17.

Workman, J. L., and Kingston, R. E. (1998). Alteration of nucleosome structure as a mechanism of transcriptional regulation. *Annu Rev Biochem* **67,** 545-79.

Wustmann, G., Szidonya, J., Taubert, H., and Reuter, G. (1989). The genetics of position-effect variegation modifying loci in Drosophila melanogaster. *Mol Gen Genet* **217,** 520-7.

Wysocka, J., Swigut, T., Milne, T. A., Dou, Y., Zhang, X., Burlingame, A. L., Roeder, R. G., Brivanlou, A. H., and Allis, C. D. (2005). WDR5 associates with histone H3 methylated at K4 and is essential for H3 K4 methylation and vertebrate development. *Cell* **121,** 859-72.

Wysocka, J., Swigut, T., Xiao, H., Milne, T. A., Kwon, S. Y., Landry, J., Kauer, M., Tackett, A. J., Chait, B. T., Badenhorst, P., Wu, C., and Allis, C. D. (2006). A PHD finger of NURF couples histone H3 lysine 4 trimethylation with chromatin remodelling. *Nature* **442,** 86-90.

Xiao, B., Jing, C., Wilson, J. R., Walker, P. A., Vasisht, N., Kelly, G., Howell, S., Taylor, I. A., Blackburn, G. M., and Gamblin, S. J. (2003a). Structure and catalytic mechanism of the human histone methyltransferase SET7/9. *Nature* **421,** 652-6.

Xiao, B., Wilson, J. R., and Gamblin, S. J. (2003b). SET domains and histone methylation. *Curr Opin Struct Biol* **13,** 699-705.

Xu, F., Zhang, K., and Grunstein, M. (2005). Acetylation in histone H3 globular domain regulates gene expression in yeast. *Cell* **121,** 375-85.

Yamamoto, K., and Sonoda, M. (2003). Self-interaction of heterochromatin protein 1 is required for direct binding to histone methyltransferase, SUV39H1. *Biochem Biophys Res Commun* **301,** 287-92.

Yamamoto, K., Sonoda, M., Inokuchi, J., Shirasawa, S., and Sasazuki, T. (2004). Polycomb group suppressor of zeste 12 links heterochromatin protein 1alpha and enhancer of zeste 2. *J Biol Chem* **279,** 401-6.

Yamane, K., Toumazou, C., Tsukada, Y., Erdjument-Bromage, H., Tempst, P., Wong, J., and Zhang, Y. (2006). JHDM2A, a JmjC-containing H3K9 demethylase, facilitates transcription activation by androgen receptor. *Cell* **125,** 483-95.

Yang, L., Xia, L., Wu, D. Y., Wang, H., Chansky, H. A., Schubach, W. H., Hickstein, D. D., and Zhang, Y. (2002). Molecular cloning of ESET, a novel histone H3-specific methyltransferase that interacts with ERG transcription factor. *Oncogene* **21,** 148-52.

Ye, Q., Callebaut, I., Pezhman, A., Courvalin, J. C., and Worman, H. J. (1997). Domain-specific interactions of human HP1-type chromodomain proteins and inner nuclear membrane protein LBR. *J Biol Chem* **272,** 14983-9.

Ye, Q., and Worman, H. J. (1996). Interaction between an integral protein of the nuclear envelope inner membrane and human chromodomain proteins homologous to Drosophila HP1. *J Biol Chem* **271,** 14653-6.

Ying, Z., Mulligan, R. M., Janney, N., and Houtz, R. L. (1999). Rubisco small and large subunit N-methyltransferases. Bi- and mono-functional methyltransferases that methylate the small and large subunits of Rubisco. *J Biol Chem* **274,** 36750-6.

Zhang, K., Tang, H., Huang, L., Blankenship, J. W., Jones, P. R., Xiang, F., Yau, P. M., and Burlingame, A. L. (2002a). Identification of acetylation and methylation sites of histone H3 from chicken erythrocytes by high-accuracy matrix-assisted laser desorption ionization-time-of-flight, matrix-assisted laser desorption ionization-postsource decay, and nanoelectrospray ionization tandem mass spectrometry. *Anal Biochem* **306,** 259-69.

Zhang, L., Eugeni, E. E., Parthun, M. R., and Freitas, M. A. (2003a). Identification of novel histone post-translational modifications by peptide mass fingerprinting. *Chromosoma* **112,** 77-86.

Zhang, W., Deng, H., Bao, X., Lerach, S., Girton, J., Johansen, J., and Johansen, K. M. (2006). The JIL-1 histone H3S10 kinase regulates dimethyl H3K9 modifications and heterochromatic spreading in Drosophila. *Development* **133,** 229-35.

Zhang, X., Tamaru, H., Khan, S. I., Horton, J. R., Keefe, L. J., Selker, E. U., and Cheng, X. (2002b). Structure of the Neurospora SET domain protein DIM-5, a histone H3 lysine methyltransferase. *Cell* **111,** 117-27.

Zhang, X., Yang, Z., Khan, S. I., Horton, J. R., Tamaru, H., Selker, E. U., and Cheng, X. (2003b). Structural basis for the product specificity of histone lysine methyltransferases. *Mol Cell* **12,** 177-85.

Zhang, Y., and Reinberg, D. (2001). Transcription regulation by histone methylation: interplay between different covalent modifications of the core histone tails. *Genes Dev* **15,** 2343-60.

Zhao, T., and Eissenberg, J. C. (1999). Phosphorylation of heterochromatin protein 1 by casein kinase II is required for efficient heterochromatin binding in Drosophila. *J Biol Chem* **274,** 15095-100.

Zhao, T., Heyduk, T., Allis, C. D., and Eissenberg, J. C. (2000). Heterochromatin protein 1 binds to nucleosomes and DNA in vitro. *J Biol Chem* **275,** 28332-8.

Zofall, M., and Grewal, S. I. (2006). Swi6/HP1 recruits a JmjC domain protein to facilitate transcription of heterochromatic repeats. *Mol Cell* **22,** 681-92.

7. Appendix

7.1 Curriculum Vitae

Personal data

Family name:	Eskeland
First name:	Ragnhild
Nationality:	Norwegian
Date of birth:	22nd of February 1977
Place of birth:	Bergen, Norway

Education

November 2002- December 2006	PhD Adolf-Butenandt Institute, Ludwig-Maximillians University of Munich, Germany Group head: Prof. Dr. Axel Imhof "Histone H3 lysine 9 methylation: A signature for chromatin function" Member of the International Graduate Program 'Protein Dynamics in Health and Disease'
September 2000- December 2002	Master Degree (Candidatus Scientiarum), Sars International Centre for Marine Molecular Biology and University of Bergen, Norway Group head: Dr. Eric Thompson UIB supervisor Prof. Dr. Rein Aasland. "Characterization of linker and core histones in the Urochordate *Oikopleura dioica*"
October 1999 - January 2000	Chemistry and Physiology, ERASMUS Exchange Program University of Aberdeen, Scotland
August 1997 - December 2000	Cand. Mag. Molecular Biology and Chemistry, Faculty of Natural Sciences, University of Bergen, Norway

Training, Courses and Meetings

December 2006	Chromatin Structure & Function, Dominican Republic Poster: "HP1 binding to chromatin methylated at H3K9 is enhanced by auxiliary factors"
June 2006	Organizer of Mini Symposia: "Hopes and Concerns in Science", Munich, Germany.
October 2005	Second Course on Epigenetics, Curie Institute, Paris.
May 2005	Chromatin and Epigenetics, Alan Wolffe EMBO Conference, EMBL Heidelberg, Germany. Poster: "Characterization of HP1 binding *in vitro*"
June 2004	10th Regional Drosophila Meeting, Regensburg, Germany. Oral presentation: "The N-terminus of Drosophila SU(VAR)3-9 mediates oligomerisation and regulates its methyltranferase activity"
January 2004	Chromatin structure and gene expression mechanisms as therapeutic targets, Luxembourg. Oral presentation: "The N-terminus of Drosophila SU(VAR)3-9 mediates oligomerisation and regulates its methyltranferase activity"
October 2003	Chromatin Assembly and Inheritance of functional States, Munich, Germany. Poster: "The N-terminus of Drosophila SU(VAR)3-9 mediates oligomerisation and regulates its methyltranferase activity"

7.2 Abbreviations

aa	Amino acid
ACF	ATP-utilizing chromatin assembly and remodeling factor
ACF1	large subunit of ACF and CHRAC
AdoHcy	S-Adenosyl homocysteine
AdoMet	S-Adenosyl methionine
ALL-1	acute lymphoblastic leukemia 1
Ash1	absent small or homeotic discs1
ATP	Adenosine-5'-triphosphate
BAZ	Bromodomain Adjacent to Zinc finger domain
bp	Base pairs
BSA	Bovine serum albumine
CD	chromo domain
CERF	CECR2-containing remodeling factor
CHIP	Chromatin Immunoprecipitation
CHRAC	Chromatin accessibility complex
Ci	Curie
Cpm	counts per minute
CSD	chromo shadow domain
C-terminal	Carboxy-terminal
CtBP	C-terminal binding proteins
CV	Column volume
DEAE	Diethylaminoethyl
DIM-5	Defect In DNA Methylation 5
DNA	Deoxyribonucleic acid
DNase I	Deoxyribonucleosidase I
DNMT 1/ 3a / 3b	DNA methyl transferase
dNTP	Deoxyribonucleoside triphosphate
Dot1	disrupter of telomeric silencing
Dot1L	Dot1 like
DREX	*Drosophila* embryo extract
DTT	Dithiothreitol
E. coli	*Escherichia coli*
EDTA	Ethylenediaminetetraacetic acid
EGTA	Ethylene glycol-bis(β-aminoethyl ether)-N,N,N',N'-tetraacetic acid
ESET	SET domain bifurcated 1
E(Z)	enhancer of zeste
Ezh2	E(Z) homolog 2
FA	fluorescence anisotropy
FCS	Foetal calf serum
g	gram or relative centrifugal force
GST	Glutathione-S-transferase
H1 / H2A / H2B / H3 / H4	histone proteins
H3K9Me	histone H3 lysine 9 methylation
HAT	Histone acetyltransferase
HDAC	Histone deacetylase
HMTase	histone methyl transferase
HP1	heterochromatin protein 1
HRP	Horse radish peroxidase
h	hour
Ig	Immunoglobulin
IGS	Intergenic spacer
IP	Immunoprecipitation
ISWI	Imitation of switch
ITC	isothermal titration calorimetry and
kDa	Kilo daltons
M	Molar
MBD	methyl binding domain

min	minute(s)
MLL	mixed lineage leukemia
MNase	Micrococcus Nuclease
MW	Molecular weight
NoRC	Nucleolar remodeling complex
NP-40	Nonidet P-40
NSD1	nuclear receptor binding SET domain protein 1
N-terminal	Amino-terminal
NURF	Nucleosome-remodeling factor
PAA	Polyacrylamide
PAGE	Polyacrylamide gelelectrophoresis
PBS	Phosphate-buffered saline
PCR	Polymerase chain reaction
PEV	Position effect variegation
Pol I, II, III	RNA polymerase I, II, III
pre-rRNA	precursor of ribosomal RNA
PRMT	protein arginine methyltransferase
PR-Set7	PR-SET domain containing protein 7
PTRF	Polymerase I transcript release factor
rDNA	Ribosomal DNA
RIZ	retinoblastoma protein-interacting zinc finger
RNA	Ribonucleic acid
RNAi	RNA interference
rpm	Rounds pro minute
RT	Room temperature
SDS	Sodium Dodecyl Sulphate
sec	second
SET	Suppressor of position effect variegation 3-9, SU(VAR)3-9; Enhancer of zeste, E(Z) and Trithorax, Trx
Set1/2/9	SET domain containing 1, 2 or 9
SETDB1	SET domain bifurcated 1
Sf9	*Spodoptera frugiperda* 9 cells
Smyd2	SET and MYND 2
Snf	Sucrose non-fermenter
Snf2h	Snf2 homolog protein
SU(VAR)3-9	suppressor of position effect variegation 3-9
Suv39	SU(VAR)3-9 homolog
SUZ12	Suppressor of zeste-12
SWI	Mating type switching
TAF	TBP-associated factor
TBE	Tris borate EDTA buffer
TBP	TATA-binding protein
Tip5	TTF-I interacting protein 5
Tris	Tris(hydroxymethyl)-amino-methane
Trx	trithorax
TSA	Trichostatin A
TTF-I	Transcription termination factor for RNA polymerase I
Tween-20	Polyoxyethylene-sorbitan monolaurate
UV	Ultraviolet light
V	Volts
Vol	Volume(s)
WICH	WSTF ISWI chromatin remodeling complex
WSTF	Williams syndrome transcription factor
WT	wild type

7.3 Publications

The following publications are to be found in the Appendix:

Eskeland, R.*, Czermin, B.*, Boeke, J., Bonaldi, T., Regula, J. T., and Imhof, A. (2004). The N-terminus of Drosophila SU(VAR)3-9 mediates dimerization and regulates its methyltransferase activity. *Biochemistry* **43,** 3740-9.

Eskeland, R., Eberharter, A., and Imhof, A. (2007). HP1 binding to chromatin methylated at H3K9 is enhanced by auxiliary factors. Mol Cell Biol 27, 453-465.

Greiner, D., Bonaldi, T., Eskeland, R., Roemer, E., and Imhof, A. (2005). Identification of a specific inhibitor of the histone methyltransferase SU(VAR)3-9. *Nat Chem Biol* **1,** 143-5.

Stabell, M., Eskeland, R., Bjorkmo, M., Larsson, J., Aalen, R. B., Imhof, A., and Lambertsson, A. (2006). The Drosophila G9a gene encodes a multi-catalytic histone methyltransferase required for normal development. *Nucleic Acids Res* **34,** 4609-21.

*Co-first author.

The N-Terminus of Drosophila SU(VAR)3−9 Mediates Dimerization and Regulates Its Methyltransferase Activity†

Ragnhild Eskeland,[§,#] Birgit Czermin,[§,#] Jörn Boeke,[#] Tiziana Bonaldi,[#] Jörg T. Regula,[‡] and Axel Imhof*[,#]

Adolf-Butenandt Institute, Department of Molecular Biology, Histone Modifications Group and Protein Analysis Unit, Ludwig-Maximillians University of Munich, Schillerstrasse 44, 80336 Munich, Germany

Received November 4, 2003; Revised Manuscript Received January 17, 2004

ABSTRACT: In most eukaryotes, the histone methyltransferase SU(VAR)3−9 and its orthologues play a major role in the function of centromeric heterochromatin. Although the methyltransferase domain is required for the formation of a fully functional centromere, mutations within other regions of the gene such as the N-terminus also have a strong impact on its in vivo function. To analyze the contribution of the N-terminus on the methyltransferase activity, we have expressed the full-length *Drosophila* SU(VAR)3−9 (dSU(VAR)3−9) together with various N-terminal deletions in *Escherichia coli* and analyzed the structural and enzymatic properties of the purified recombinant enzymes. Full-length dSU(VAR)3−9 specifically methylates lysine 9 within histone H3 on peptides, on intact histones, and, to a lesser extent, on nucleosomes. A detailed analysis of the reaction products shows that dSU(VAR)3−9 adds two methyl groups to an unmethylated H3 tail peptide in a nonprocessive manner. The full-length enzyme elutes with an apparent molecular weight of 160 kDa from a gel filtration column, which indicates the formation of a dimer. This property is dependent on an intact N-terminus. In contrast to the full-length enzymes, proteins lacking the N-terminus fail to dimerize, and show a 10-fold lower specific activity and a linear dependence of methyltransferase activity on enzyme concentration. A N-terminal peptide containing amino acids 1−152 of dSU(VAR)3−9 is sufficient to mediate this interaction in vitro. The dimerization of dSU(VAR)3−9 and the subsequent increase of its methyltransferase activity provide a starting point to understand the molecular details of the formation of heterochromatic structures in vivo.

Centromeres are conserved structures of eukaryotic chromosomes, which ensure their proper segregation during mitotic divisions (*1*, *2*). Most centromers are formed by association of the centromeric DNA with specific proteins such as CENP-A, -B, and -C (*3*, *4*) and have been shown to form clusters within interphase chromatin (*5*, *6*). Although centromeres as well as pericentromeric regions are typically rich in repetitive DNA, the main determinant of centromers seems to be of an epigenetic nature as they can also form ectopically within euchromatic arms (*7*, *8*). Centromeric regions of chromosomes are generally transcriptionally quiescent, a property that can "spread" into neighboring regions (*2*, *9*). The variable transcriptional activity of normally active genes, after their translocation close to heterochromatin, has been termed position effect variegation (PEV)[1] (*10*, *11*) (*9*).

Histones within centromeric regions are usually hypoacteylated (*12*, *13*) and methylated at lysine 9 within the H3 tail (*14*). The enzyme that is critical for this modification is the histone methyltransferase SU(VAR)3−9 (*15*). *Drosophila* SU(VAR)3−9 (dSU(VAR)3−9) has been initially identified in a genetic screen for suppressors of PEV (for a review see ref *16*). SU(VAR)3−9 or its orthologue CLR4 are required for heterochromatin-mediated gene silencing in *Drosophila* and *Schizosaccharomyces pombe* (*17*). Mouse SUV39 enzyme is important to maintain genome stability (*18*). Furthermore, it acts as a transcriptional repressor in transient as well as in stable transfection experiments in tissue culture cells (*19*, *20*).

Drosophila SU(VAR)3−9 belongs to a large class of proteins containing a SET domain. The SET domain confers methyltransferase activity and is crucial for the in vivo function of most SET-containing proteins. Although the SET domain is relatively well conserved, SET-methyltransferases show a remarkable structural and functional variability. SET domain proteins can exist as monomers (*21*−*25*) or dimers (*26*). In addition, some need auxiliary factors (*27*−*30*) or require nucleic acids for full activity (*31*, *32*).

In addition to the well-characterized SET domain, dSU(VAR)3−9 contains a chromo domain (*17*, *19*, *33*), a

† Funding for this work has been provided by a grant (IM23/4-1) from the Deutsche Forschungsgemeinschaft (DFG).

* Correspondence should be sent to Axel Imhof, Adolf-Butenandt Institute, Ludwig-Maximillians University of Munich, Schillerstr. 44, 80336 Muenchen, Germany. Tel.: - -49 89 5996 435 Fax: - -49 89 5996 425. E-mail: axel.imhof@mol-bio.med.uni-muenchen.de.

§ Both authors contributed equally to this work.

Department of Molecular Biology.

‡ Histone Modifications Group and Protein Analysis Unit.

[1] PEV, position effect variegation; PCR, polymerase chain reaction; PMSF, phenylmethanesulfonyl fluoride; HEPES, *N*-(2-hydroxyethyl)-piperazine-*N*′-(2-ethanesulfonic acid); BSA, bovine serum albumin; EGTA, ethylene glycol-bis(2-aminoethyl ether)-*N*,*N*,*N*′,*N*′-tetraacetic acid; EDTA, ethylenediaminetetraacetic acid; DTT, DL-dithiothreitol; MTase, methyltransferase; HMT, histone methyltransferase; ACN, acetonitrile; TFA, trifluoroacetic acid; MALDI-TOF, matrix assisted laser desorption ionization-time-of-flight mass spectrometry; SAM, *S*-adenosyl methionine; SAH, *S*-adenosyl homocystein.

10.1021/bi035964s CCC: $27.50
Published on Web 03/06/2004

GTPase domain that is derived from a common exon used by dSU(VAR)3−9 and the eukaryotic translation initiation factor 2 and a relatively ill-defined N-terminal domain (*15*). The N-terminus is moderately conserved in humans, mice, and flies and interacts with at least two additional suppressors of PEV, HP1, and SU(VAR) 3−7 (*14*, *34*). A Structure−function analysis of the human SUV39H1 indicated that a deletion of the N-terminus leads to a failure of SUV39 to bind chromatin in vivo (*33*). A fragment of SUV39H1 containing just the N-terminus and the chromo domain binds efficiently to heterochromatin when expressed in tissue culture cells. This binding is thought to be mediated by HP1 and has been suggested to be a main component in the maintenance mechanism of histone methylation as the chromo domain of HP1 binds strongly to a H3 tail, which is methylated at lysine 9. In the absence of HP1, SU(VAR)3−9 is found at multiple sites along the chromosome arms, suggesting a role for HP1 in restricting SU(VAR)3−9 to centromeric heterochromatin. However, the HP1 interacting region is not sufficient to confer chromatin binding to an overexpressed fusion protein (*33*), suggesting an additional structural component in addition to HP1 binding, which is important for heterochromatin association. This hypothetical structural component may well be the conformation of dSU(VAR)3−9 itself. SUV39H1 forms distinct nuclear domains when overexpressed in vivo (*19*), a phenomenon that has already been described for certain ring finger proteins which form higher order aggregates in vivo and in vitro (*35*, *36*). In flies, overexpression of dSU(VAR)3−9 or other suppressors of PEV leads to a strong dosage-dependent enhancement of PEV independent of the dosage of the other partners. This strong dosage dependence argues against a single limiting factor regulating PEV but rather favors a model in which several factors participate in the assembly of a specific heterochromatin scaffold (*16*, *37*).

In this report, we show that full-length dSU(VAR)3−9 is a very active methyltransferase when expressed in bacteria. It adds two methyl groups to lysine 9 within the H3 tail in a nonprocessive manner. Moreover, the N-terminus of dSU(VAR)3−9 mediates an interaction between two SU(VAR)3−9 molecules, thereby increasing its ability to methylate H3. The N-terminus of dSU(VAR)3−9 has a bipartite interaction domain, which allows the formation of multimers of SU(VAR)3−9 proteins. This interaction between dSU(VAR)3−9 molecules may contribute to the clustering of centromers within living cells and the formation of nuclear substructures in vivo after expressing the N-terminus of SU(VAR)3−9 alone and may therefore explain the strong dosage dependence of the dSU(VAR)3−9 mediated enhancement of PEV.

MATERIALS AND METHODS

Cloning of dSU(VAR)3−9. Full-length dSU(VAR)3−9, deletion mutants, and point mutants were cloned into pET15b (Novagen) via NdeI and XhoI. The pET15b plasmid adds a 6× his-tag on the N-terminus. All inserts were created by PCR from a plasmid carrying the dSU(VAR)3−9 cDNA (kind gift of G. Reuter, Halle, Germany) and verified by DNA sequencing. GST fusion proteins were cloned by inserting a PCR generated EcoRI-XhoI fragment into a pGEX 4T-2 vector (Amersham).

Protein Purification. His-tagged dSU(VAR)3−9 and dSU(VAR)3−9 mutant polypeptides were expressed in *E. coli* BL21(DE3)pLys, and purified with Talon (Clontech) resin according to the manufacturer's instructions. For the molecular weight analysis, the Talon-purified proteins were loaded on a Superdex 200 column (HR 10/30, Amersham) or on a 5−20% sucrose gradient. The column was run isocratically in BC100 buffer (25 mM HEPES/KOH (pH 7.3), 100 mM NaCl, 1 mM $MgCl_2$, 0.5 mM EGTA, 0.1 mM EDTA, 10% glycerol (v/v), 1 mM DTT, and 0.2 mM PMSF) for 1.4 CV. 0.5 mL fractions were collected and 15 μL of each fraction were analyzed on a 10% SDS PAA gel. 5−20% (w/v) sucrose gradients were prepared in BC100 buffer with or without 3 M urea. The gradient was prepared using a Gradient Master 105/106 (BioComp) set at 2.40 min/81.5 deg/15 rpm. A 500 μL sample containing 10 μg of dSU(VAR)3−9 wild type or Δ213 or 20 μg of BSA was loaded on top of the gradient. Centrifugation was performed using a SW41 rotor (Beckman) at 41 000 rpm for 28 h at 4 °C. 0.5 mL fractions were collected and analyzed by 10% SDS−PAGE.

For activity assays, the enzyme was stabilized by addition of BSA to a final concentration of 100 ng/μL followed by dialysis against BC100 buffer. All recombinant dSU(VAR)3−9 were quantified by Coomassie staining with the ImageMaster 1D Elite v3.01 software package (Amersham) using BSA as a standard. Bacterially expressed HP1 was purified according to ref *38* and dialyzed against BC100.

Methyltransferase Activity. H3 peptides used contained amino acid 1−19 plus a C-terminal cysteine (ARTKQTARKSTGGKAPRKQC) and were either unmodified, dimethylated at K4, monomethylated at K9, acetylated at K9, or dimethylated at K9 (Peptide Speciality Laboratories, Heidelberg). Recombinant Drosophila histones were expressed and purified from *E. coli*, and reconstituted into octamers as described previously (*39*). Nucleosomes were reconstituted by salt dialysis. Recombinant histone H3 carrying the mutations K9A, K27A, or both, were expressed in bacteria from plasmids kindly provided by D. Reinberg. HMT assays were done in ddH_2O using H3-peptide, histone H3, octamer, or nucleosomes as substrates and *S*-adenosyl-[methyl-^{3}H]-L-methionine (25 μCi/mL) and/or *S*-adenosylmethionine (New England BioLabs) as methyl donor. Reactions were performed at 30 °C for 1−80 min. To stop the reaction, acetic acid was added to a final concentration of 5−10% (v/v). Kinetic assays were carried out in triplicates by varying the concentration of the H3 peptide (1−16 μM) or SAM (5−60 μM) at saturating amounts of SAM/peptide and analyzed by double reciprocal plots.

GST Pulldown. dSU(VAR)3−9 and mutants were translated in vitro from pET15b vectors, [^{35}S]methionine-labeled. GST-pulldowns were carried out as described earlier (*40*). In vitro translated proteins and HP1 (1 μg) were incubated in a total volume of 200 μL containing $NTEN_{100}$ (20 mM TrisHCl (pH 8), 100 mM NaCl, 1 mM EDTA, 0.5% (v/v) Nonidet P-40), 100 μg of BSA, and 5 μg of ethidium bromide. Washes were performed two times in $NTEN_{100}$ and four times in the $NTEN_{200}$. The bound proteins were eluted with SDS sample buffer and analyzed using a phosphoimager or a specific antibody in the case of HP1.

MALDI-TOF Analysis. To purify the methylated peptides from contaminating salts, the peptide solution was passed

over a pipet tip containing small amounts of C18 reversed phase material (ZipTip, Millipore). After three 10 μL wash steps with 0.1% TFA, the bound peptides were eluted with 1 μL of prepared matrix solution (saturated α-cyanohydroxy-cinnamic-acid (Sigma) dissolved in 50% ACN (v/v)/0.3% TFA (v/v)) directly onto the target plate. Samples were air-dried to allow cocrystallization of the peptides and the matrix, and the target plate was loaded in a Voyager DE STR spectrometer and analyzed.

RESULTS

Full-Length dSU(VAR)3−9 Is an Active Methyltransferase. To analyze the enzymatic properties of dSU(VAR)3−9, we expressed a recombinant full-length protein containing six histidine residues at the N-terminus in bacteria and purified it by affinity chromatography (Figure 1A). Recombinant dSU(VAR)3−9 methylates histone H3 in a mixture of histones as well as in reconstituted nucleosomes (Figure 1B). We defined the site of methylation using by using peptides premodified at lysine 4 or lysine 9 (Figure 1C). As lysine 27 is surrounded by almost identical amino acids and can be methylated by methyltransferases that also methylate lysine 9 (*30*, *41*, *42*), we also tested whether dSU(VAR)3−9 is able to methylate a histone H3 molecule carrying a mutation at lysine 9 or at lysine 27. The fact that dSU(VAR)3−9 only methylates the wildtype H3 molecule and the H3 mutated at lysine 27 but does not methylate mutants in which lysine 9 is mutated further confirmed our specificity analysis (Figure 1D). This is in good agreement with the finding that dSU(VAR)3−9 isolated from *Drosophila* embryos (*43*) as well as a N-terminally truncated version of dSU(VAR)3−9 (*14*) are able to methylate lysine 9 within the N-terminus of H3.

dSU(VAR)3−9 Is a Nonprocessive Enzyme with Similar Affinity for Unmethylated and Monomethylated H3K9. Lysines within histones exist in mono-, di-, and trimethylated forms and the different isoforms can have different molecular functions (*44*). Experiments using antibodies specific for either di- or trimethylated lysine 9 demonstrate that dSU(VAR)3−9 function is required for di- as well as trimethylation of histone H3 in *Drosophila* polytene chromosomes (*14*, *30*). We therefore analyzed the reaction products of an in vitro methylation reaction using full-length dSU(VAR)3−9 and a H3 peptide by MALDI-TOF (Figure 2A). A time course experiment of the methylation reaction using unmodified peptide shows that after 5 min about 20% of the peptides are found to be monomethylated and none of it is dimethylated. The dimethylated form only appears after 10 min of reaction time when almost 50% of all peptide has been converted into the monomethylated form. After 80 min, almost all of the unmethylated peptide is converted into either the mono- or the dimethylated form. We have not observed a significant amount of trimethylation by dSU(VAR)3−9 under those conditions (Figure 2A). We also used peptides that were either mono- or dimethylated at lysine 9 as substrate to exclude the possibility that dSU(VAR)3−9 could trimethylate a peptide that is already premodified. In both cases, we do not observe significant trimethylation of the peptide (Figure 2B,C). Only at a very high enzyme-to-substrate ratio or at extended reaction times we could observe a small fraction (less than 1%) of trimethylated peptide (data not shown). This is in good agreement with experiments using the human orthologue of dSU(VAR)3−9 SUV39H1, which also methylates a dimethylated peptide only with a very low efficiency (*15*).

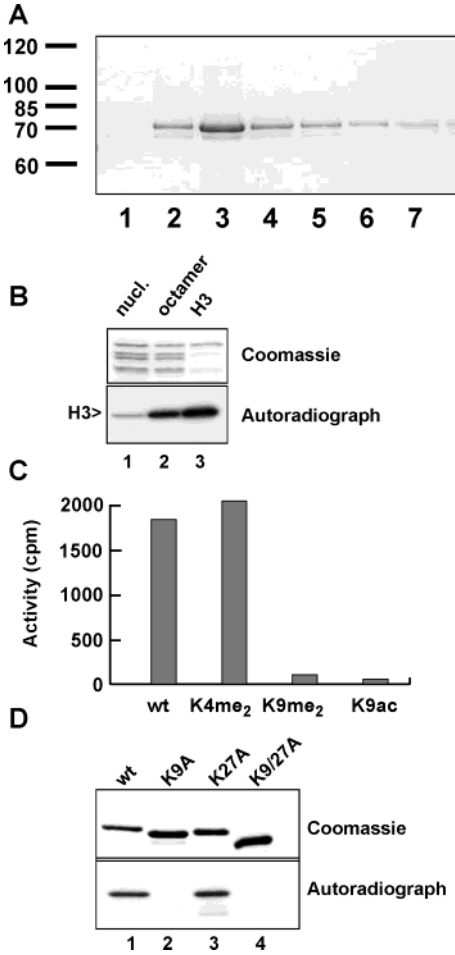

FIGURE 1: Characterization of recombinant dSU(VAR)3−9. (A) Elution of recombinant, His tagged dSU(VAR)3−9 from Talon beads. Ten microliters of the first eight fractions (lanes 1−8) was loaded onto a gel and subjected to 10% SDS−PAGE, and the gel was stained with Coomassie blue R250. (B) In vitro methylation reactions using different protein substrates. Nucleosomal arrays (lane 1) were reconstituted on pBS(KS) (Stratagene) by salt dialysis using recombinant octamers (lane 2), which were reconstituted from equimolar amounts of histones produced in *E. coli* and purified by gel-filtration chromatography. H3 (lane 3) was expressed and purified as described. The reaction products were then loaded and run on a 18% SDS PAA gel, and the gel was stained with Coomassie blue R250, dried, and exposed to a X-ray film (autoradiograph) for 24 h. (C) Peptides containing the first 19 amino acids of H3 were methylated by recombinant dSU(VAR)3−9 and radioactive SAM (Amersham). We used the unmodified peptide (wt), a peptide dimethylated at K4 ($K4me_2$) or at K9 ($K9me_2$) and a peptide acetylated at K9 (K9ac) as substrates. Incorporated radioactivity was measured by a filter-binding assay. (D) In vitro methylation reaction using either wt recombinant H3 (lane 1), H3 mutated at lysine 9 (lane 2), H3 mutated at lysine 27 (lane 3), or a H3 molecule mutated at both sites (lane 4). Histones were methylated by recombinant dSU(VAR)3−9 in the presence radioactive SAM, separated by SDS−PAGE, and analyzed by autoradiography.

A possible explanation for the slow appearance of the dimethylated peptide could be a dramatically reduced reaction velocity of the methylation reaction after the peptide has been monomethylated. To test this, we repeated the same experiments using the monomethylated peptide as a substrate and found very similar kinetics (Figure 2B,D). From these

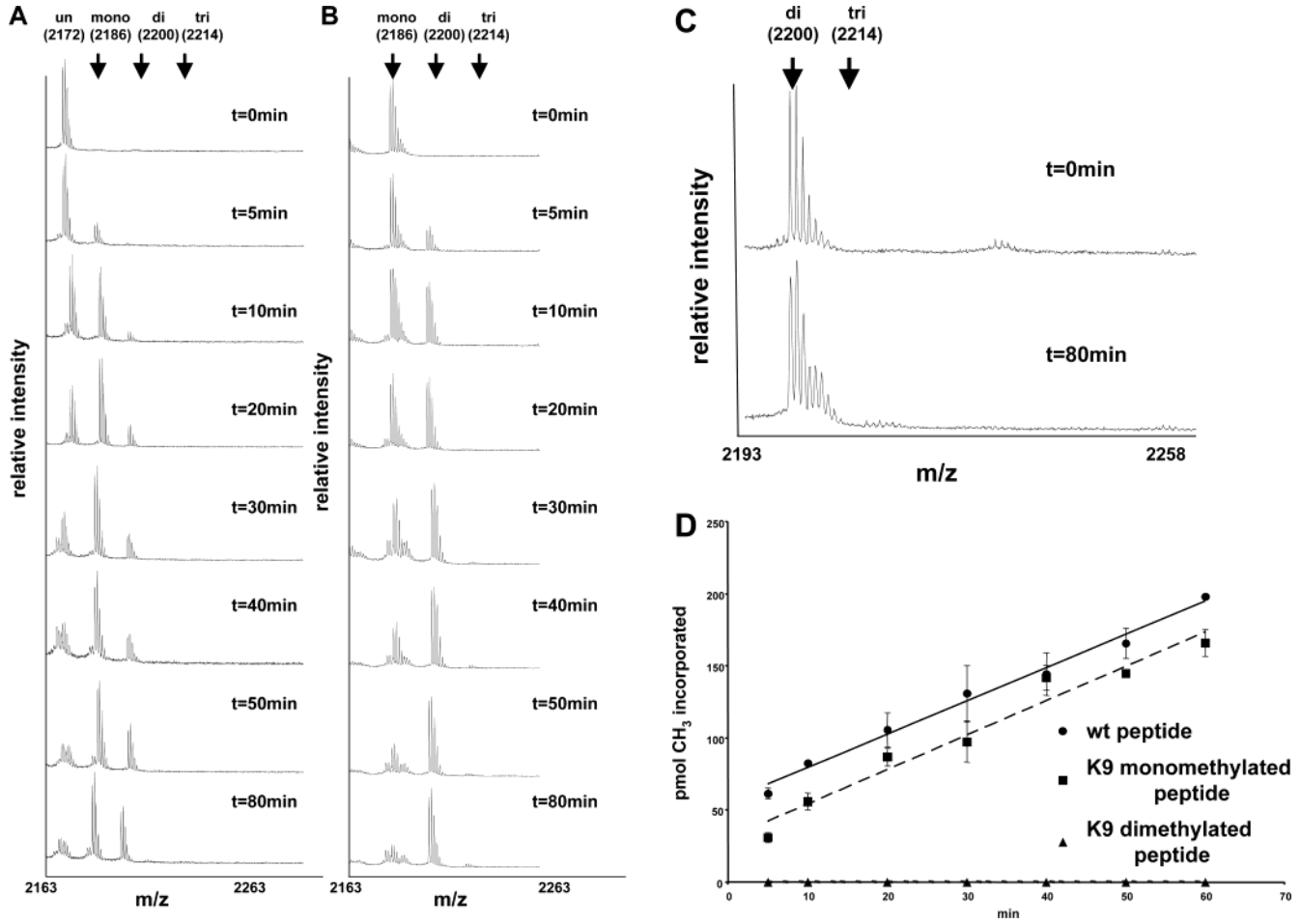

FIGURE 2: MALDI analysis of reaction products. MALDI-TOF analysis of the reaction products using 600 ng of dSU(VAR)3−9 and 460 pmol of a H3 peptide (see Figure 1), which was unmethylated (A), monomethylated (B), or dimethylated (C) at K9. The methylation reaction was stopped at different time points after starting the reaction and reaction products analyzed by MALDI-TOF. In case of the dimethylated peptide, only the 80-min time point is shown. (D) Time course of a methylation reaction as measured by a filter-binding assay.

experiments, we conclude that dSU(VAR)3−9 adds a single methyl group to the peptide, after which it dissociates from the SET domain and has to reassociate for a second methylation reaction. This behavior is in marked contrast to the trimethylase DIM5 of *Neurospora*, which processively methylates lysine 9 within a H3 peptide to the trimethylated form without releasing it into the solution (*45*) or to SET7/9, which has been shown to only monomethylate lysine 4 on the H3 tail (*25*).

The N-Terminus of dSU(VAR)3−9 Is Required for Full Catalytic Activity. To analyze the influence of the N-terminus of dSU(VAR)3−9 on its enzymatic activity, we expressed various mutant dSU(VAR)3−9 proteins in *E. coli* and studied their catalytic activity (Figure 3A,B). As expected, a mutation of dSU(VAR)3−9 in the SET domain (H561K) renders the enzyme inactive. Enzymes in which the N-terminal 152 or 213 amino acids were deleted are still able to methylate H3 peptides and histones albeit with an over all 10-fold lower methyltransferase activity (Figure 3C,D). Further deletion of the N-terminus including the chromo domain (Δ279) resulted in an additional decline of methylation activity, which we have not further analyzed.

Kinetic Parameters for Full-Length Recombinant dSU(VAR)3−9. To further quantify the effect of the N-terminus on the HMT activity of dSU(VAR)3−9, we used a standard filter-binding assay to analyze the kinetics of dSU(VAR)3−9 methyltransferase reaction. Under standard reaction conditions, the reaction is linear for at least 60 min (Figure 2D). To prevent possible product inhibition effects, we measured the incorporated radioactivity after 1 min, when less than 5% of product was formed (see Figure 2). In test experiments, we verified that this amount of *S*-adenosyl homocystein (SAH) or of the methylated H3 peptide did not significantly inhibit the reaction in our assays when added externally (data not shown). In the reminder of the paper, the reaction velocity is therefore expressed as pmol of CH_3 incorporated min^{-1}. Determination of the kinetic parameters of the full-length dSU(VAR)3−9 revealed a V_{max} for the methylation reaction of 95.2 nmol min^{-1} mg^{-1} and a K_m-[SAM] of 25.9 μM (Figure 4A), assuming that all molecules are active. This translates into a k_{cat} of 0.11 s^{-1}, which is 2-fold higher than the reported k_{cat} of the full-length Rubisco methyltransferase LSMT (0.05 s^{-1}) (*23*). More importantly, full-length dSU(VAR)3−9 is approximately 20 times faster than another SET containing histone methyltransferase enzyme SET9 (k_{cat} = 0.005 s^{-1}) (*23*). Deletion of the N-terminal domain does not change the K_m for SAM or the H3 peptide, indicating that there is no major change in substrate affinity. Strikingly, the V_{max} and the k_{cat} of the N-terminally truncated version Δ213 are about 20 times

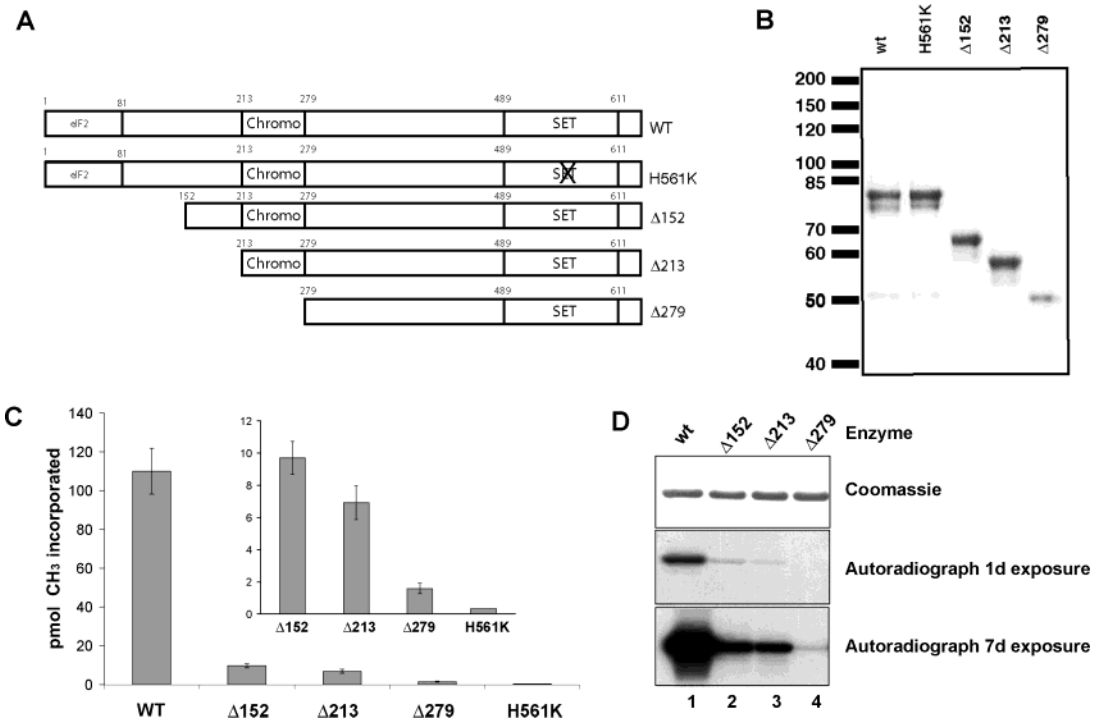

FIGURE 3: Expression and purification of dSU(VAR)3−9 mutants. (A) Scheme of dSU(VAR)3−9 mutants generated and expressed. In *Drosophila* dSU(VAR)3−9 mRNA is generated by alternative splicing of the translation initiation factor (eIF2) RNA leading to an additional 81 amino acids at the N-terminus of the protein, which are common between eIF2 and dSU(VAR)3−9. For the point mutation within the SET domain (H561K) histidine 561 was mutated into a lysine. (B) Coomassie-stained gel of Talon purified dSU(VAR)3−9 mutant proteins. (C) Comparison of HMT activity of various dSU(VAR)3−9 mutants on a H3 peptide and on recombinant H3 molecules (D). For a better comparison, the inset of panel C shows the activities of the N-terminal deletions and a point mutation within the SET domain only. To compare different activities on intact H3 molecules, an autoradiograph of a 1-day (top panel) and a 7-day (bottom panel) exposure is shown.

lower than the ones observed for the full-length enzyme and more similar to the kinetic parameters of SET9 (6.8 nmol min^{-1} mg^{-1} and 0.005 s^{-1}, respectively) (Figure 4A). This substantial increase in the catalytic efficiency of the full-length enzyme may be due to a conformational change or an association of monomeric enzymes into multimers. As multimeric enzymes often show a concentration-dependent increase of specific activity as expressed in substrate molecules converted per molecule of enzyme (*46*), we determined the relationship between the velocity of the reaction and the enzyme concentration. When the rate of methyl peptide formation was plotted against the corresponding enzyme concentration, a nonlinear plot was obtained (Figure 4B). This behavior is not observed when using the N-terminally truncated proteins, which only show a linear dependence of methyltransferase activity on enzyme concentration. Replotting the number of CH_3 groups incorporated per enzyme molecule revealed a steady increase of activity until the specific activity reached a plateau at an enzyme concentration of approximately 0.5 μM for the wild type. In contrast, virtually no change was observed for the N-terminally truncated enzyme (Figure 4C). On the basis of these observations, we reasoned that under our assay conditions the full-length enzyme is indeed able to form multimers, which have a higher specific activity than the monomers and that at a concentration of 0.5 μM and above virtually all molecules exist as multimers.

The N-Terminus Is Important for Dimerization and Activity of dSU(VAR)3−9 in Vitro. To test this hypothesis, we analyzed the molecular weight of the recombinant protein by gel filtration chromatography and density gradient centrifugation. The full-length dSU(VAR)3−9 elutes with an apparent molecular weight of 160 kDa, which is indicative of a dimer from a Superdex 200 gel filtration column (Figure 5A). The deletion of the N-terminus of dSU(VAR)3−9 results in a complete loss of this dimerization as the N-terminally truncated protein elutes with an apparent molecular weight of 60 kDa corresponding to a monomeric species (Figure 5A bottom panel). To further confirm the dimerization of dSU(VAR)3−9, we loaded the purified, recombinant enzyme on a 5−20% sucrose gradient under denaturing and nondenaturing conditions. As expected, under native conditions the full-length dSU(VAR)3−9 is found in fractions corresponding to higher molecular weight when compared to the Δ213, whereas it behaves virtually identical under denaturing conditions (Figure 5B). The N-terminally deleted protein as well as the BSA standard display a minor shift to an apparently smaller molecular weight in the presence of urea, which is probably due to a change in density of the denaturing solution (arrows in Figure 5B).

The N-Terminus Mediates Interactions within dSU(VAR)3−9. As the deletion of the first 152 amino acids leads to a loss of dimer formation, we expressed the N-terminal 152 amino acids of dSU(VAR)3−9 as a GST fusion protein in bacteria and used it as an affinity resin in GST pull-down experiments. The bound fusion protein was incubated either with recombinant HP1 or with in vitro translated dSU(VAR)3−9 proteins. As has been shown previously (*14*, *34*), the N-terminus is able to interact with HP1 in vitro (Figure 6A, right panel). This domain also inter-

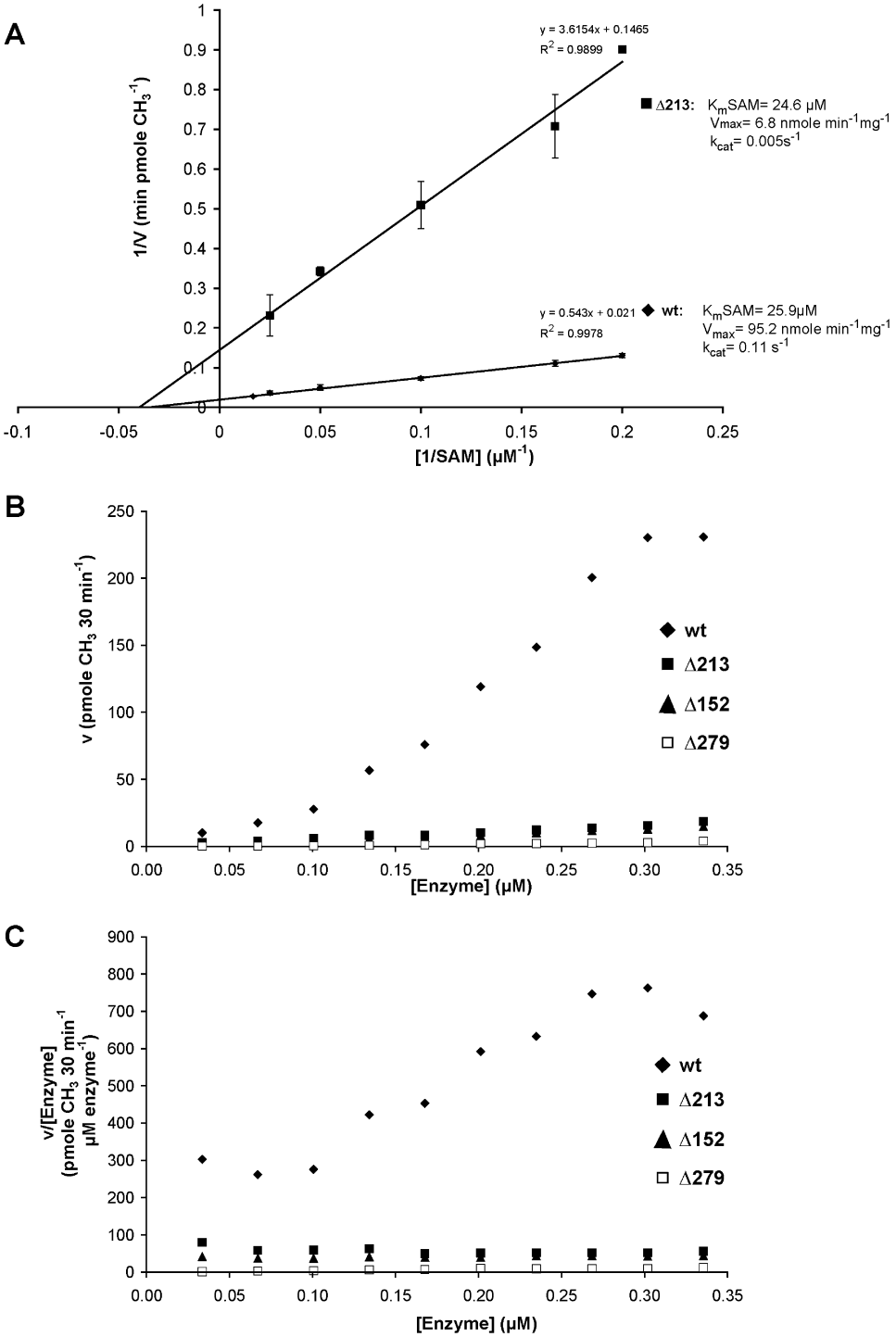

FIGURE 4: Kinetic properties of recombinant dSU(VAR)3−9. (A) Double reciprocal plots of in vitro methylation reactions using a H3 tail peptide and either wt (500 ng) or a N-terminally truncated protein (Δ213; 1 μg) using various concentrations of SAM under saturating peptide concentrations were used to determine the K_m for SAM. (B) Concentration-dependent increase of enzyme activity. Different concentrations of wt and N-terminally truncated dSU(VA)3−9 were incubated with H3 peptide and SAM at saturating concentrations for 30 min. After stopping the reaction, the amount of incorporated radioactivity was measured and plotted against the concentration of enzyme. (C) The ratio of the incorporated radioactivity to the concentration of enzyme present was replotted against the enzyme concentration to determine the increase in specific activity.

acts very efficiently with in vitro translated dSU(VAR)3−9, suggesting a role of this domain in inter- or intramolecular interactions. Surprisingly, this domain is also able to interact with a polypeptide lacking the first 152 amino acids. To map the region within dSU(VAR)3−9 that interacts with the first 152 amino acids, we have generated a series of mutations within dSU(VAR)3−9 and analyzed their capability to bind to the N-terminus (Figure 6A,B). Using these mutant proteins, we could narrow down the interaction domain to amino acids 152−213 (Figure 6C). This suggests the existence of a bipartite interaction motif that can potentially mediate a intra- as well as an intermolecular interaction. To further confirm this result, we expressed the amino acids 152−213 as a GST fusion protein and did another series of GST pull down experiments. As expected, the GST(152−213) protein is able to interact with the full-length protein

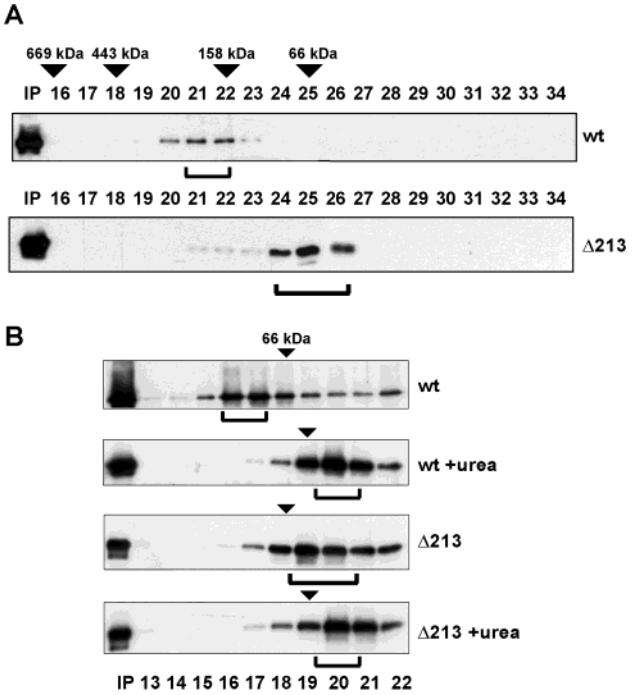

FIGURE 5: Molecular weight determination of dSU(VAR)3−9. (A) Elution profiles of wt dSU(VAR)3−9 (top) and the N-terminal deletion construct Δ213 (bottom). Retention of the molecular weight standards is indicated at the top. (B) Profile of a 5−20% sucrose gradient in the presence (panels 2 and 4) or absence of 3 M urea (panels 1 and 3). The position of the 66-kDa marker protein is indicated as a black triangle at the top of each gel. Note the slight shift (1 fraction) of the 66-kDa marker and the Δ213 protein, which is due to the presence of urea in the buffer compared to the significant shift in case of the wt protein (>3 fractions).

but only weakly binds to a protein lacking the first 152 amino acids (Figure 7A,B). On the basis of this result, we strongly favor a model in which dSU(VAR)3−9 interacts with itself via a domain swapping mechanism similar to what has been described for other dimeric proteins (*47*).

DISCUSSION

Recombinant dSU(VAR)3−9 is a catalytically active methyltransferase and is able to methylate lysine 9 within histone H3. The main conclusions from our experiments are that the full-length enzyme transfers two methyl groups to lysine 9 within an H3 tail peptide in a nonprocessive manner and that the enzyme requires the N-terminus for homodimerization and for full activity in vitro. The N-terminus of dSU(VAR)3−9 can be subdivided into two parts, which can interact with each other.

The initial rate kinetics of the methylation reaction show that dSU(VAR)3−9 has a very similar K_m for the protein substrate and a similar turnover rate as another SET containing methyltransferase, Rubisco LSMT (*23*), but a significantly higher K_m for SAM. This suggests that to have full catalytic activity the concentration of SAM has to be kept at a relatively high concentration within the cell. The intracellular SAM concentration varies between 20 and 40 μM (*48*) depending on the cell type used, which is in the range of the K_m of dSU(VAR)3−9. Under these conditions, the rate of methylation by dSU(VAR)3−9 is directly proportional to the SAM concentration and can therefore directly respond to variations of cofactor concentration. This high SAM concentration is maintained by the main SAM synthase enzyme, SU(Z)5, which, like dSU(VAR)3−9, is a suppressor for position effect variegation in *Drosophila* (*49*). It will be interesting to see whether the Su(z)5 gene product is randomly distributed throughout the cell or if it shows a specific localization maybe directing it to the sites of dSU(VAR)3−9 action. The concentration of SAM could therefore be an important regulator of heterochromatin spreading.

Recently several labs have characterized the processivity of various SET containing enzymes revealing remarkable differences in their ability to add one, two, or three methyl groups to their corresponding substrate (*25*, *45*). Furthermore, mono-, di-, and trimethylated histones have different functions (*44*). By analyzing the reaction products of recombinant dSU(VAR)3−9 in vitro, we find that it very efficiently adds two methyl groups to its substrate but is very poor in adding a third one. Moreover, we only see a trimethylated peptide (less than 1% of total product) at a high enzyme-to-substrate ratio (Figure 2D and data not shown). However, deletion of dSU(VAR)3−9 in vivo leads to a disappearance of trimethylated H3 molecules at the chromocenter of polytene chromosomes (*30*). The fact that we can observe a small trimethylating activity of recombinant dSU(VAR)3−9 argues against a sterical inhibition of trimethylation within the active center by the enzyme as it is the case for SET9 (*50*).

SET domain containing enzymes have been classified in several different classes based on their primary amino acid sequence (*51*). The only enzyme of the SU(VAR)3−9 class that has been kinetically characterized in detail is the *Neurospora* enzyme DIM5. Our experiments show that dSU(VAR)3−9, in contrast to DIM5, is not processive and mainly dimethylates a peptide containing lysine 9. Further analysis of additional point mutations within the SET domain will reveal the structural basis of this intriguing difference. An obvious candidate for an amino acid important for this difference is the R238 of DIM5, which is replaced by a histidine in dSU(VAR)3−9 and its orthologues in mouse and humans (*15*). In fact, it has been shown that a mutation within SUV39H1 converting H320 into an arginine residue strongly increases activity in vitro (*15*).

It has been speculated that a targeted recruitment of SET1 to the promoter region of an active gene can lead to a limited trimethylation due to a very high local concentration of enzyme (*44*, *52*), whereas the reminder of the chromatin is only dimethylated. As we observe a nonlinear increase of HMT activity dependent on the enzyme concentration in vitro, it is possible that comparable mechanisms of the regulation of the methylation state also affect the methylation capability of dSU(VAR)3−9 in vivo. Alternatively, the ability of dSU(VAR)3−9 to trimethylate may be regulated by phosphorylation of the protein (*19*, *53*), or through interaction with additional cofactors (*19*) as has been shown recently in the case of ESET (*54*). Furthermore, the trimethylation of K9 could be mediated by a different HMT enzyme, which is able to add a third methyl group to already dimethylated H3. One of the potential enzymes with such a trimethylating activity is the polycomb group protein enhancer of zeste (*30*).

Besides this kinetic observation, the most interesting observation we have made in analyzing the recombinant dSU(VAR)3−9 protein is the fact that it requires the

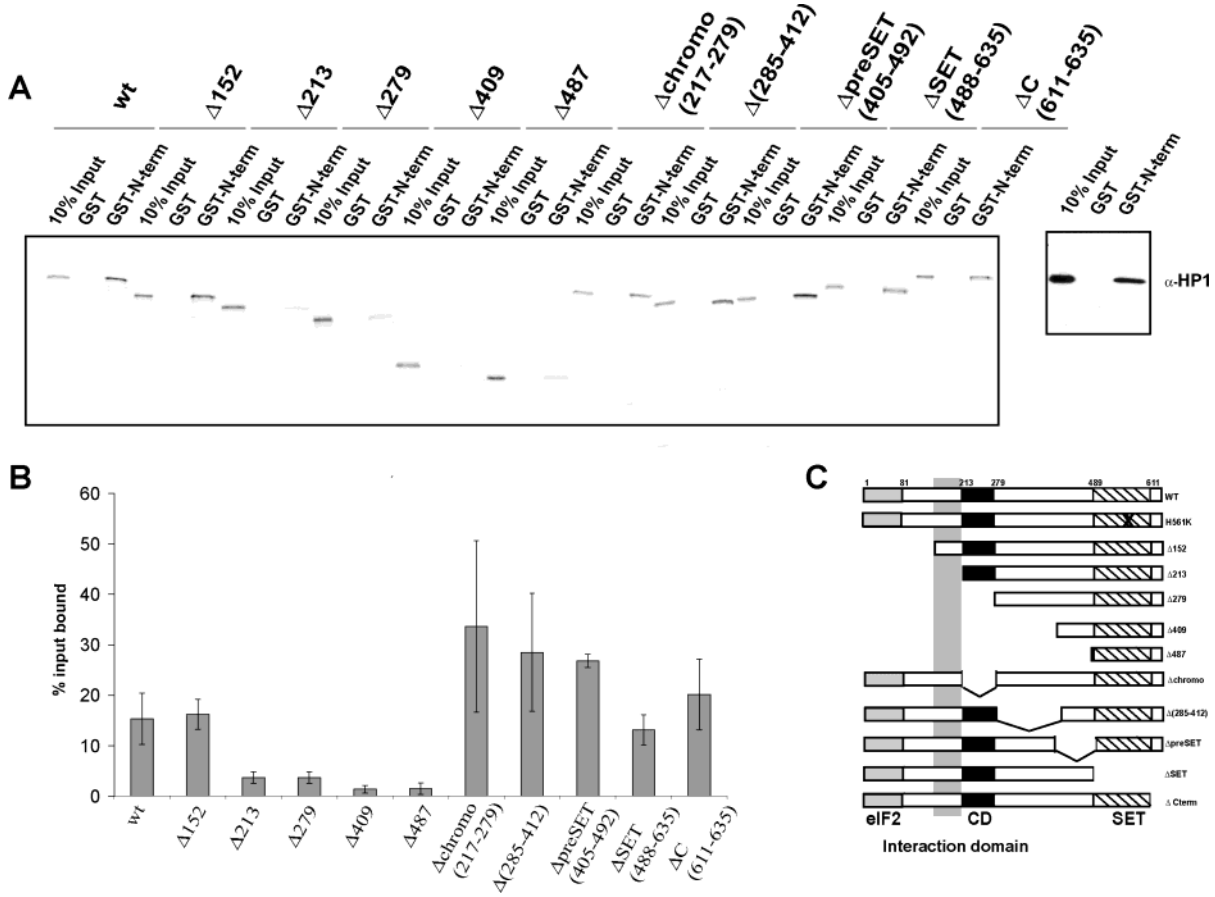

FIGURE 6: In vitro interaction assays to map the dimerization domain. The first 152 amino acids of dSU(VAR)3−9 are expressed as a GST fusion proteins and used to affinity purify either recombinant HP1 (A, right panel) or in vitro translated dSU(VAR)3−9 (A, left panel). HP1 was detected by Western blotting using a monoclonal antibody against HP1 (C1A9, kind gift of S. Elgin) and dSU(VAR)3−9 was detected by autoradiography. (B) Quantification of the binding affinities of the various dSU(VAR)3−9 proteins. Error bars represent the variations of at least three different experiments. (C) Schematic representations of the dSU(VAR)3−9 proteins used and the position of the dimerization domain.

N-terminus for its full in vitro activity. Our experiments strongly suggest that this N-terminus allows the recombinant protein to form dimers in solution, which greatly enhances its activity. However, we cannot fully exclude the possibility that intramolecular interactions within the N-terminus induce a major conformational shift that causes the full-length protein to migrate with an apparent molecular weight of a dimer on a gel filtration column as well as a density gradient. The observed concentration-dependent increase in specific enzyme activity, as expressed in molecules SAM converted per molecule of enzyme, argues against this possibility as the different conformation should not change as a function of enzyme concentration. Interestingly, the arginine methyltransferase PRMT1 and the SET domain containing lysine methyltransferase vSET also form oligomers in vitro (*26*, *55*, *56*). Both enzymes are nonprocessive and the multimerization of the protein has been suggested to facilitate the methylation reaction by increasing the probability of the monomethylated product to bind to a second enzyme molecule. This is in contrast to other SET domain proteins such as DIM-5 and SET7/9, which are either processive or only transfer one methyl group respectively and do not dimerize in vitro. Interestingly, the catalytic capacity of full-length dSU(VAR)3−9 is about 20 times higher than the one of SET9 or a N-terminally truncated version of dSU(VAR)3−9, which both fail to dimerize in solution suggesting that the dimerization can indeed be used to significantly enhance HMT activity.

The mapping of the dimerization domain via GST pull down experiments revealed a bipartite dimeriztaion motif. This organization points to a dimerization via a domain swapping mechanism in which identical domains are exchanged between two proteins to form a homodimer (*57*). On the basis of our experiments, we would suggest that the amino acids 1−152 can interact with the residues 152−213 either intra- or intermolecularly and that the domain swapped dimer has a higher catalytic capacity than the monomer. The different conformation of a loop between two swapped domains in the monomeric and the dimeric form of an enzyme can have a significant effect on the function of a remote active site (*47*). Such an induced conformational change may provide an alternative explanation for the higher activity of the dimeric form of dSU(VAR)3−9. Domain swapping has also been implicated in the formation of oligomeric assemblies of proteins (*58*). Although we have strong evidence for dimer formation and could not identify higher order oligomers in gel filtration chromatography or density gradient experiments, at present we cannot fully exclude the existence of oligomeric species that may assembly from dimers and are disrupted in the course of our analysis.

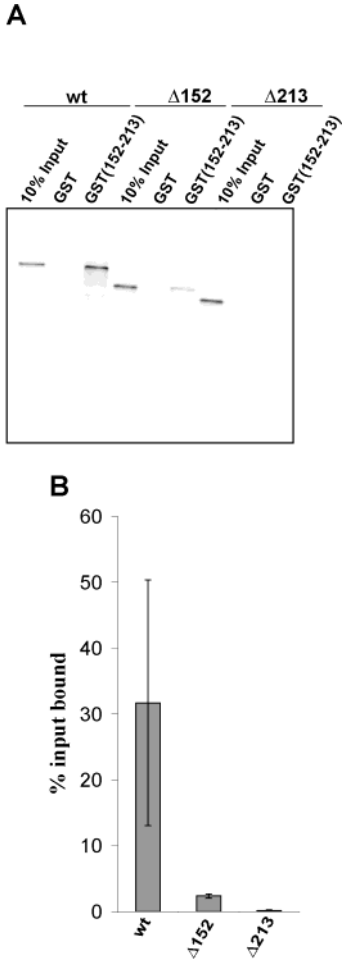

FIGURE 7: In vitro interaction assay using amino acids 152−213 as a GST fusion protein to affinity purify in vitro translated dSU(VAR)3−9, and two N-terminally truncated versions of dSU(VA)3−9 (A). (B) Quantification of the binding affinities of the various dSU(VAR)3−9 proteins. Error bars represent the variations of at least three different experiments.

The concentration-dependent self-interaction of dSU(VAR)3−9 may also be a way to regulate its function within the cell. One well-known features of dSU(VAR)3−9 is its strict dosage-dependent effect on PEV. Our observation that dSU(VAR)3−9's specific HMT activity increases in a nonlinear way provides a possible explanation for this effect. The human orthologue of dSU(VAR)3−9, SUV39H1, forms distinct nuclear bodies when overexpressed in tissue culture cells (*19*), which can be dispersed by modulating the phosphorylation state of the enzyme. From our in vitro experiments, we would suggest that the N-terminus plays an important role in the formation of those nuclear bodies.

ACKNOWLEDGMENT

We would like to thank Sally Elgin, Gunter Reuter, Danny Reinberg, and Joel Eissenberg for valuable reagents. We also would like to thank Peter Becker, Alex Brehm, and Josephine Sutcliffe for valuable comments on the manuscript and Felix Hartlepp for recombinant GST protein.

REFERENCES

1. Choo, K. H. (1997) Centromere DNA dynamics: latent centromeres and neocentromere formation. *Am. J. Hum. Genet. 61*, 1225−33.
2. Karpen, G. H., and Allshire, R. C. (1997) The case for epigenetic effects on centromere identity and function. *Trends Genet. 13*, 489−96.
3. Earnshaw, W. C., and Cooke, C. A. (1989) Proteins of the inner and outer centromere of mitotic chromosomes. *Genome 31*, 541−52.
4. Sugata, N., Li, S., Earnshaw, W. C., Yen, T. J., Yoda, K., Masumoto, H., Munekata, E., Warburton, P. E., and Todokoro, K. (2000) Human CENP-H multimers colocalize with CENP-A and CENP-C at active centromere−kinetochore complexes. *Hum. Mol. Genet. 9*, 2919−26.
5. Weimer, R., Haaf, T., Kruger, J., Poot, M., and Schmid, M. (1992) Characterization of centromere arrangements and test for random distribution in G0, G1, S, G2, G1, and early S′ phase in human lymphocytes. *Hum. Genet. 88*, 673−82.
6. Zalensky, A. O., Allen, M. J., Kobayashi, A., Zalenskaya, I. A., Balhorn, R., and Bradbury, E. M. (1995) Well-defined genome architecture in the human sperm nucleus. *Chromosoma 103*, 577−90.
7. Warburton, P. E., Dolled, M., Mahmood, R., Alonso, A., Li, S., Naritomi, K., Tohma, T., Nagai, T., Hasegawa, T., Ohashi, H., Govaerts, L. C., Eussen, B. H., Van Hemel, J. O., Lozzio, C., Schwartz, S., Dowhanick-Morrissette, J. J., Spinner, N. B., Rivera, H., Crolla, J. A., Yu, C., and Warburton, D. (2000) Molecular cytogenetic analysis of eight inversion duplications of human chromosome 13q that each contain a neocentromere. *Am. J. Hum. Genet. 66*, 1794−806.
8. Depinet, T. W., Zackowski, J. L., Earnshaw, W. C., Kaffe, S., Sekhon, G. S., Stallard, R., Sullivan, B. A., Vance, G. H., Van Dyke, D. L., Willard, H. F., Zinn, A. B., and Schwartz, S. (1997) Characterization of neo-centromeres in marker chromosomes lacking detectable alpha-satellite DNA. *Hum. Mol. Genet. 6*, 1195−204.
9. Richards, E. J., and Elgin, S. C. (2002) Epigenetic codes for heterochromatin formation and silencing: rounding up the usual suspects. *Cell 108*, 489−500.
10. Reuter, G., and Spierer, P. (1992) Position effect variegation and chromatin proteins. *Bioessays 14*, 605−12.
11. Henikoff, S. (1992) Position effect and related phenomena. *Curr. Opin. Genet. Dev. 2*, 907−12.
12. Choo, K. H. (2000) Centromerization. *Trends Cell Biol. 10*, 182−8.
13. Pidoux, A. L., and Allshire, R. C. (2000) Centromeres: getting a grip of chromosomes. *Curr. Opin. Cell Biol. 12*, 308−19.
14. Schotta, G., Ebert, A., Krauss, V., Fischer, A., Hoffmann, J., Rea, S., Jenuwein, T., Dorn, R., and Reuter, G. (2002) Central role of Drosophila SU(VAR)3−9 in histone H3−K9 methylation and heterochromatic gene silencing. *EMBO. J. 21*, 1121−31.
15. Rea, S., Eisenhaber, F., O'Carroll, D., Strahl, B. D., Sun, Z. W., Schmid, M., Opravil, S., Mechtler, K., Ponting, C. P., Allis, C. D., and Jenuwein, T. (2000) Regulation of chromatin structure by site-specific histone H3 methyltransferases. *Nature 406*, 593−9.
16. Schotta, G., Ebert, A., Dorn, R., and Reuter, G. (2003) Position-effect variegation and the genetic dissection of chromatin regulation in Drosophila. *Semin. Cell Dev. Biol. 14*, 67−75.
17. Ivanova, A. V., Bonaduce, M. J., Ivanov, S. V., and Klar, A. J. (1998) The chromo and SET domains of the Clr4 protein are essential for silencing in fission yeast. *Nat. Genet. 19*, 192−5.
18. Peters, A. H., O'Carroll, D., Scherthan, H., Mechtler, K., Sauer, S., Schofer, C., Weipoltshammer, K., Pagani, M., Lachner, M., Kohlmaier, A., Opravil, S., Doyle, M., Sibilia, M., and Jenuwein, T. (2001) Loss of the Suv39h histone methyltransferases impairs mammalian heterochromatin and genome stability. *Cell 107*, 323−37.
19. Firestein, R., Cui, X., Huie, P., and Cleary, M. L. (2000) Set domain-dependent regulation of transcriptional silencing and growth control by SUV39H1, a mammalian ortholog of Drosophila Su(var)3−9. *Mol. Cell Biol. 20*, 4900−9.
20. Snowden, A. W., Gregory, P. D., Case, C. C., and Pabo, C. O. (2002) Gene-Specific Targeting of H3K9 Methylation Is Sufficient for Initiating Repression In Vivo. *Curr. Biol. 12*, 2159−66.
21. Min, J., Zhang, X., Cheng, X., Grewal, S. I., and Xu, R. M. (2002) Structure of the SET domain histone lysine methyltransferase Clr4. *Nat. Struct. Biol. 9*, 828−32.
22. Zhang, X., Tamaru, H., Khan, S. I., Horton, J. R., Keefe, L. J., Selker, E. U., and Cheng, X. (2002) Structure of the Neurospora SET domain protein DIM-5, a histone H3 lysine methyltransferase. *Cell 111*, 117−27.

23. Trievel, R. C., Beach, B. M., Dirk, L. M., Houtz, R. L., and Hurley, J. H. (2002) Structure and catalytic mechanism of a SET domain protein methyltransferase. *Cell 111*, 91−103.
24. Wilson, J. R., Jing, C., Walker, P. A., Martin, S. R., Howell, S. A., Blackburn, G. M., Gamblin, S. J., and Xiao, B. (2002) Crystal structure and functional analysis of the histone methyltransferase SET7/9. *Cell 111*, 105−15.
25. Xiao, B., Jing, C., Wilson, J. R., Walker, P. A., Vasisht, N., Kelly, G., Howell, S., Taylor, I. A., Blackburn, G. M., and Gamblin, S. J. (2003) Structure and catalytic mechanism of the human histone methyltransferase SET7/9. *Nature 421*, 652−6.
26. Manzur, K. L., Farooq, A., Zeng, L., Plotnikova, O., Koch, A. W., Sachchidanand, and Zhou, M. M. (2003) A dimeric viral SET domain methyltransferase specific to Lys27 of histone H3. *Nat. Struct. Biol. 10*, 187−96.
27. Cao, R., Wang, L., Wang, H., Xia, L., Erdjument-Bromage, H., Tempst, P., Jones, R. S., and Zhang, Y. (2002) Role of histone H3 lysine 27 methylation in Polycomb-group silencing. *Science 298*, 1039−43.
28. Muller, J., Hart, C. M., Francis, N. J., Vargas, M. L., Sengupta, A., Wild, B., Miller, E. L., O'Connor, M. B., Kingston, R. E., and Simon, J. A. (2002) Histone methyltransferase activity of a Drosophila Polycomb group repressor complex. *Cell 111*, 197−208.
29. Kuzmichev, A., Nishioka, K., Erdjument-Bromage, H., Tempst, P., and Reinberg, D. (2002) Histone methyltransferase activity associated with a human multiprotein complex containing the Enhancer of Zeste protein. *Genes Dev. 16*, 2893−905.
30. Czermin, B., Melfi, R., McCabe, D., Seitz, V., Imhof, A., and Pirrotta, V. (2002) Drosophila enhancer of Zeste/ESC complexes have a histone H3 methyltransferase activity that marks chromosomal Polycomb sites. *Cell 111*, 185−96.
31. Fang, J., Feng, Q., Ketel, C. S., Wang, H., Cao, R., Xia, L., Erdjument-Bromage, H., Tempst, P., Simon, J. A., and Zhang, Y. (2002) Purification and Functional Characterization of SET8, a Nucleosomal Histone H4-Lysine 20-Specific Methyltransferase. *Curr. Biol. 12*, 1086−99.
32. Nishioka, K., Rice, J. C., Sarma, K., Erdjument-Bromage, H., Werner, J., Wang, Y., Chuikov, S., Valenzuela, P., Tempst, P., Steward, R., Lis, J. T., Allis, C. D., and Reinberg, D. (2002) PR-Set7 is a nucleosome-specific methyltransferase that modifies lysine 20 of histone H4 and is associated with silent chromatin. *Mol. Cell 9*, 1201−13.
33. Melcher, M., Schmid, M., Aagaard, L., Selenko, P., Laible, G., and Jenuwein, T. (2000) Structure−function analysis of SUV39H1 reveals a dominant role in heterochromatin organization, chromosome segregation, and mitotic progression. *Mol. Cell Biol. 20*, 3728−41.
34. Yamamoto, K., and Sonoda, M. (2003) Self-interaction of heterochromatin protein 1 is required for direct binding to histone methyltransferase, SUV39H1. *Biochem. Biophys. Res. Commun. 301*, 287−92.
35. Melnick, A., and Licht, J. D. (1999) Deconstructing a disease: RARalpha, its fusion partners, and their roles in the pathogenesis of acute promyelocytic leukemia. *Blood 93*, 3167−215.
36. Kentsis, A., Gordon, R. E., and Borden, K. L. (2002) Control of biochemical reactions through supramolecular RING domain self-assembly. *Proc. Natl. Acad. Sci. U.S.A. 99*, 15404−9.
37. Henikoff, S. (1996) Dosage-dependent modification of position-effect variegation in Drosophila. *Bioessays 18*, 401−9.
38. Zhao, T., and Eissenberg, J. C. (1999) Phosphorylation of heterochromatin protein 1 by casein kinase II is required for efficient heterochromatin binding in Drosophila. *J. Biol. Chem. 274*, 15095−100.
39. Luger, K., Mader, A. W., Richmond, R. K., Sargent, D. F., and Richmond, T. J. (1997) Crystal structure of the nucleosome core particle at 2.8 Å resolution. *Nature 389*, 251−60.
40. Brackertz, M., Boeke, J., Zhang, R., and Renkawitz, R. (2002) Two highly related p66 proteins comprise a new family of potent transcriptional repressors interacting with MBD2 and MBD3. *J. Biol. Chem. 277*, 40958−66.
41. Ogawa, H., Ishiguro, K., Gaubatz, S., Livingston, D. M., and Nakatani, Y. (2002) A complex with chromatin modifiers that occupies E2F- and Myc-responsive genes in G0 cells. *Science 296*, 1132−6.
42. Tachibana, M., Sugimoto, K., Fukushima, T., and Shinkai, Y. (2001) Set domain-containing protein, G9a, is a novel lysine-preferring mammalian histone methyltransferase with hyperactivity and specific selectivity to lysines 9 and 27 of histone H3. *J. Biol. Chem. 276*, 25309−17.
43. Czermin, B., Schotta, G., Hulsmann, B. B., Brehm, A., Becker, P. B., Reuter, G., and Imhof, A. (2001) Physical and functional association of SU(VAR)3−9 and HDAC1 in Drosophila. *EMBO Rep. 2*, 915−9.
44. Santos-Rosa, H., Schneider, R., Bannister, A. J., Sherriff, J., Bernstein, B. E., Emre, N. C., Schreiber, S. L., Mellor, J., and Kouzarides, T. (2002) Active genes are tri-methylated at K4 of histone H3. *Nature 419*, 407−11.
45. Tamaru, H., Zhang, X., McMillen, D., Singh, P. B., Nakayama, J. I., Grewal, S. I., Allis, C. D., Cheng, X., and Selker, E. U. (2003) Trimethylated lysine 9 of histone H3 is a mark for DNA methylation in Neurospora crassa. *Nat. Genet. 34*, 75−9.
46. Bheemanaik, S., Chandrashekaran, S., Nagaraja, V., and Rao, D. N. (2003) Kinetic and catalytic properties of dimeric KpnI DNA methyltransferase. *J. Biol. Chem. 278*, 7863−74.
47. Schymkowitz, J. W., Rousseau, F., Wilkinson, H. R., Friedler, A., and Itzhaki, L. S. (2001) Observation of signal transduction in three-dimensional domain swapping. *Nat. Struct. Biol. 8*, 888−92.
48. Hoffman, D. R., Marion, D. W., Cornatzer, W. E., and Duerre, J. A. (1980) S-Adenosylmethionine and S-adenosylhomocystein metabolism in isolated rat liver. Effects of L-methionine, L-homocystein, and adenosine. *J. Biol. Chem. 255*, 10822−7.
49. Larsson, J., and Rasmuson-Lestander, A. (1994) Molecular cloning of the S-adenosylmethionine synthetase gene in Drosophila melanogaster. *FEBS Lett. 342*, 329−33.
50. Zhang, X., Yang, Z., Khan, S. I., Horton, J. R., Tamaru, H., Selker, E. U., and Cheng, X. (2003) Structural basis for the product specificity of histone lysine methyltransferases. *Mol. Cell 12*, 177−85.
51. Baumbusch, L. O., Thorstensen, T., Krauss, V., Fischer, A., Naumann, K., Assalkhou, R., Schulz, I., Reuter, G., and Aalen, R. B. (2001) The *Arabidopsis thaliana* genome contains at least 29 active genes encoding SET domain proteins that can be assigned to four evolutionarily conserved classes. *Nucleic Acids Res. 29*, 4319−33.
52. Ng, H. H., Robert, F., Young, R. A., and Struhl, K. (2003) Targeted recruitment of Set1 histone methylase by elongating Pol II provides a localized mark and memory of recent transcriptional activity. *Mol. Cell 11*, 709−19.
53. Aagaard, L., Schmid, M., Warburton, P., and Jenuwein, T. (2000) Mitotic phosphorylation of SUV39H1, a novel component of active centromeres, coincides with transient accumulation at mammalian centromeres. *J. Cell Sci. 113*, 817−29.
54. Wang, H., An, W., Cao, R., Xia, L., Erdjument-Bromage, H., Chatton, B., Tempst, P., Roeder, R. G., and Zhang, Y. (2003) mAM facilitates conversion by ESET of dimethyl to trimethyl lysine 9 of histone H3 to cause transcriptional repression. *Mol. Cell 12*, 475−87.
55. Tang, J., Frankel, A., Cook, R. J., Kim, S., Paik, W. K., Williams, K. R., Clarke, S., and Herschman, H. R. (2000) PRMT1 is the predominant type I protein arginine methyltransferase in mammalian cells. *J. Biol. Chem. 275*, 7723−30.
56. Tang, J., Gary, J. D., Clarke, S., and Herschman, H. R. (1998) PRMT 3, a type I protein arginine *N*-methyltransferase that differs from PRMT1 in its oligomerization, subcellular localization, substrate specificity, and regulation. *J. Biol. Chem. 273*, 16935−45.
57. Newcomer, M. E. (2002) Protein folding and three-dimensional domain swapping: a strained relationship? *Curr. Opin. Struct. Biol. 12*, 48−53.
58. McGee, A. W., Dakoji, S. R., Olsen, O., Bredt, D. S., Lim, W. A., and Prehoda, K. E. (2001) Structure of the SH3-guanylate kinase module from PSD-95 suggests a mechanism for regulated assembly of MAGUK scaffolding proteins. *Mol. Cell 8*, 1291−301.

BI035964S

MOLECULAR AND CELLULAR BIOLOGY, Jan. 2007, p. 453–465 Vol. 27, No. 2
0270-7306/07/$08.00+0 doi:10.1128/MCB.01576-06

HP1 Binding to Chromatin Methylated at H3K9 Is Enhanced by Auxiliary Factors[▽]

Ragnhild Eskeland, Anton Eberharter, and Axel Imhof*

Adolf-Butenandt Institut, University of Munich, Schillerstr. 44, 80336 Muenchen, Germany

Received 23 August 2006/Returned for modification 2 October 2006/Accepted 1 November 2006

A large portion of the eukaryotic genome is packaged into transcriptionally silent heterochromatin. Several factors that play important roles during the establishment and maintenance of this condensed form have been identified. Methylation of lysine 9 within histone H3 and the subsequent binding of the chromodomain protein heterochromatin protein 1 (HP1) are thought to initiate heterochromatin formation in vivo and to propagate a heterochromatic state lasting through several cell divisions. For the present study we analyzed the binding of HP1 to methylated chromatin in a fully reconstituted system. In contrast to its strong binding to methylated peptides, HP1 binds only weakly to methylated chromatin. However, the addition of recombinant SU(VAR) protein, such as ACF1 or SU(VAR)3-9, facilitates HP1 binding to chromatin methylated at lysine 9 within the H3 N terminus (H3K9). We propose that HP1 has multiple target sites that contribute to its recognition of chromatin, only one of them being methylated at H3K9. These findings have implications for the mechanisms of recognition of specific chromatin modifications in vivo.

Chromatin within the eukaryotic nucleus can be cytologically divided into active euchromatin and silent heterochromatin (19, 32, 56). Genetic analysis of position effect variegation in *Drosophila melanogaster* identified the methylation of lysine 9 within the H3 N terminus (H3K9) as a crucial factor for heterochromatin formation (60, 61, 68). The main histone methyl transferase (HMTase) responsible for this mark is SU(VAR)3-9 (60). This modification can be found at pericentric heterochromatin in virtually all higher eukaryotes and is currently viewed as a hallmark of silenced chromatin (13, 29, 56). Methylation at H3K9 (H3K9Me) is essential for the binding of heterochromatin protein 1 (HP1), a major constituent of heterochromatin (5, 40). HP1 homologues can be found in almost all eukaryotes ranging from *Schizosaccharomyces pombe* (18, 39, 43) to mammals and higher plants (26, 58, 62). Higher eukaryotes have at least three different isoforms of HP1 (HP1α, HP1β, and HP1γ in mammals and HP1a, HP1b, and HP1c in *Drosophila*) (47, 63), which differ in their subnuclear localization. HP1α/a and HP1β/b are primarily found within centromeric heterochromatin, whereas HP1γ/c is enriched at euchromatic sites (27, 48, 63). All HP1 molecules share a conserved architecture consisting of a chromo domain (CD), a flexible hinge region, and a chromo shadow domain (CSD) (2, 38). Genetic complementation assays (54) as well as structural data (67) showed that both globular domains (CD and CSD) are required for proper targeting of HP1. This is confirmed by experiments showing that a chimeric protein containing the CD of polycomb and the CSD of HP1 is targeted not only to heterochromatin but also to binding sites of the endogenous polycomb protein (53).

The CD of HP1 interacts specifically with a peptide resembling the N terminus of H3 that is di- or trimethylated at K9 (5, 34, 35, 40, 52). The interaction surface is highly conserved among different HP1 isoforms, and a mutation that abolishes binding results in a loss of function allele of HP1α/a (5, 40, 53). More recently, the CD of HP1 has also been shown to interact specifically with isoform 1.4 of the H1 linker histone when it is methylated at K26 (12). Although the CD of HP1 and its ability to recognize methylated histones are necessary for heterochromatin binding in vivo, they are not sufficient to support chromatin binding in vitro. Pulldown experiments using bacterially expressed glutathione *S*-transferase (GST)-HP1 showed that the CD alone could not efficiently pull down native soluble oligonucleosomes from chicken nucleated erythrocytes (46). The binding of recombinant HP1 to mononucleosomes required the presence of the full-length protein, suggesting that individual domains are not able to maintain a stable binding to a nucleosome (74). Moreover, in contrast to what is seen in vivo, the interaction of HP1 with chromatin is independent of the histone tails (46, 74) and could be mediated by an interaction between HP1 and the core region of H3 (51). This type of binding is contradictory to most data obtained in vivo that point out H3K9Me as a major factor in targeting. However, alternate ways of binding of HP1 to chromatin in vivo have been suggested as well. Treatment of nuclei with RNAses leads to a release of bound HP1 in mammalian tissue culture cells (45, 49). The putative RNA binding activity of HP1 could be assigned to a conserved region within the hinge domain, which binds RNA in vitro (49). The involvement of an RNA component in the targeting of HP1 to heterochromatin is further strengthened by the observation that mutations in components of the RNA interference (RNAi) machinery prevent SWI6/HP1-mediated formation of heterochromatin in fission yeast (30). The hinge region of HP1α has also been shown to directly interact with the linker histone H1 (51) and with native H1 containing chromatin (46). In addition, HP1α was shown to interact with the histone variant H2A.Z when incorporated into a nucleosomal array (21).

Besides the CD and the hinge domain, the CSD of HP1 is

* Corresponding author. Mailing address: Histone Modifications Group, Adolf-Butenandt Institut, University of Munich, Schillerstr. 44, 80336 Muenchen, Germany. Phone: 49 89 218075420. Fax: 49 89 218075440. E-mail: Imhof@lmu.de.

▽ Published ahead of print on 13 November 2006.

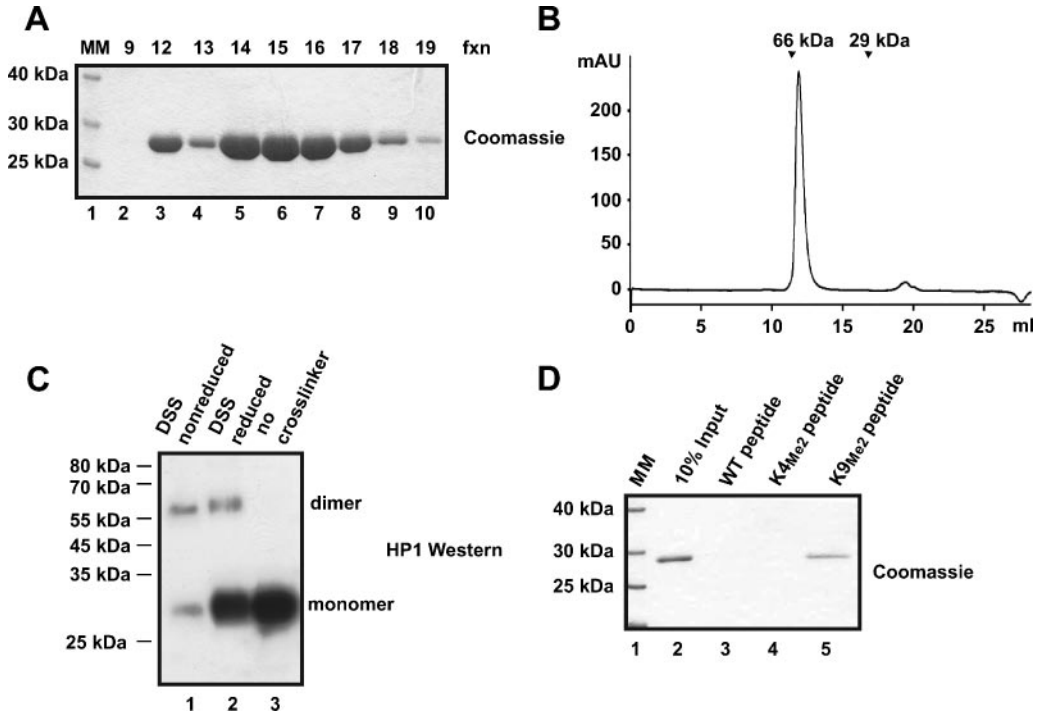

FIG. 1. Bacterially expressed HP1 dimerizes and binds H3 peptides methylated at lysine 9. (A) Untagged recombinant HP1 was purified over four successive columns. A Coomassie-stained SDS–12% polyacrylamide (PAA) gel of 5 μl of fractions 9 to 19 from the last column, a MonoQ, is depicted. fxn, fractions. (B) Purified recombinant HP1 was loaded onto a gel filtration column (Superdex 200), and the elution profile (A_{280}) of HP1 is shown. Molecular mass (MM) standards (bovine serum albumin [66 kDa] and carbonic anhydrase [29 kDa]) are labeled with arrows. (C) In vitro cross-linking of HP1 using DTSSP (DSS). Recombinant HP1 before (lane 3) or after (lanes 1 and 2) cross-linking was subjected to SDS–12% PAGE, transferred to a PVDF membrane, and detected with HP1 (C1A9) antibody. The DTSSP cross-linking can be partially reversed by reductive cleavage of the disulfide-containing cross-linking molecule (lane 2). The cross-linking revealed dimeric HP1. (D) Recombinant HP1 was assayed for binding to H3 peptides containing the first 19 amino acids of H3 immobilized onto Sulfolink Sepharose. The substrates were unmodified peptide (lane 3), peptide dimethylated at K4 ($K4_{Me2}$; lane 4), and peptide dimethylated at K9 ($K9_{Me2}$; lane 5). Bound HP1 was visualized by Coomassie staining.

also crucial for targeting of HP1 to its site of action. The CSD mediates dimerization of HP1 and its binding to small peptide regions that can be recognized by key residues at the surface of an HP1 dimer (8). A consensus sequence that interacts with the CSD of HP1a has been identified by using a phage display method to enrich for peptides that have a high affinity to the CSD (64). This small motif can be found in many proteins, several of which have been shown to interact with the CSD and are thought to target HP1 to specific promoters (42, 65) in order to establish a silenced chromatin domain. The CSD of HP1α is also required to mediate its interaction with the large subunit of CAF1 (50). This interaction provided a link to the replication machinery and led to a model in which HP1 is targeted to replication foci by its interaction with CAF-1 and subsequently "handed over" to methylated chromatin (50).

Our goal was to reconstitute highly H3K9-methylated chromatin in vitro and to study the binding of recombinant *Drosophila* HP1a to methylated and nonmethylated chromatin. We found that HP1a binds to a unmodified chromatin array only weakly even though more than 85% of all H3 molecules within the reconstituted array were methylated at K9. The addition of auxiliary factors such as ACF1 or SU(VAR)3-9, which interact with the CSD of HP1a, facilitated its binding to methylated chromatin. Mutations inhibiting the interaction between HP1a and these factors abolished the binding, suggesting a bimodal binding of HP1 to methylated chromatin.

MATERIALS AND METHODS

Plasmids and cloning. J. C. Eissenberg kindly provided HP1a in expression vector pET11a. Site-directed mutagenesis of full-length HP1a was performed using the QuickChange kit (Stratagene). To generate HP1 (V26M) we used primers HP1V26MNcoIfwd (5′-GAGGAGGAGTACGCCATGGAAAAGA TCATCG-3′) and HP1V26MNcoIrew (5′-CGATGATCTTTTCCATGGCGT ACTCCTCCTC-3′), and to generate HP1 (W200A) we used primers HP1aW200ABstNI (5′-CGAAGAGCGCCTATCCGCGTACTCTGATAAT GAAG-3′) and HP1aW200ABstNIrev (5′-CTTCATTATCAGAGTACGCG GATAGGCGCTCTTCG-3′). HP1a (amino acids [aa] 2 to 206) was subcloned into XmaI and XhoI sites of pGEX4T-1 (Amersham) using primers pgexHP1aNtXmaI5 (5′-GTAGACCCGGGTGGCAAGAAAATCG-3′) and pgexHP1aCtXhoI3 (5′-TCTCACTCGAGTTAATCTTCATTATC-3′). SU(VAR)3-9 constructs were previously described in reference 20.

Antibodies and immunoblotting. The HP1 (C1A9) mouse monoclonal antibody (36) and the HP1 rabbit polyclonal antibody (58) were kind gifts from S. C. R. Elgin. Dilutions for Western blots were 1:200 for C1A9 and 1:1,500 for polyclonal HP1. For all quantifications the HP1 polyclonal antibody was used. The FLAG antibody (Sigma) was used at a concentration of 1:2,000. SU(VAR)3-9 rat monoclonal antibody (SU3D9) was generated by E. Kremmer against purified His-tagged SU(VAR)3-9 Δ213. The supernatant was used at a concentration of 1:5. Proteins were transferred onto polyvinylidene fluoride (PVDF) membranes (Millipore), probed with the indicated antibodies, detected with fluorescently labeled secondary antibodies, and quantified with an Odyssey system (Li-Cor). For quantification the background method was set to median with a border of 1 and a Top/Bottom segment. In Fig. 1C, the secondary antibody

was conjugated to horseradish peroxidase (Amersham), and the detection was performed with chemiluminescence (Amersham).

Expression and purification of recombinant *Drosophila* HP1 and SU(VAR)3-9. Bacterially expressed HP1 and point mutants were purified according to the method detailed in reference 73 and dialyzed against BC100 (25 mM HEPES [pH 7.6], 100 mM NaCl, 1 mM $MgCl_2$, 0.5 mM EGTA, 0.1 mM EDTA, 10% [vol/vol] glycerol, 1 mM dithiothreitol [DTT], and 0.2 mM phenylmethylsulfonyl fluoride [PMSF]). All HP1s were quantified by Bradford (Bio-Rad), and Coomassie-stained proteins were quantified using the ImageMaster 1D Elite version 3.01 software package (Amersham), with bovine serum albumin (BSA) as a standard. SU(VAR)3-9 wild type (WT) and Δ213 were expressed and purified as described in reference 20.

H1 purification. H1 was purified from *Drosophila* embryos (0 to 12 h) according to the method of Croston et al. (11a), and its identity was verified by mass spectrometry. For incorporation into chromatin, H1 was added after chromatin assembly, when the chromatin was linked to paramagnetic beads. H1 incubation with chromatin or DNA was performed for 1 h at 26°C. Washing steps were the same as those described below for HP1.

Histone purification and nucleosome assembly by salt dialysis. Recombinant *Drosophila* histones were expressed and purified from *Escherichia coli* BL21(DE3)pLys and reconstituted into octamers as described previously (44). Nucleosomes were reconstituted by salt dialysis overnight at 4°C using NaCl concentrations of 2 M to 0.1 M (44). The dialysis buffer contained 10 mM Tris-HCl (pH 8), 1 mM EDTA, 0.1 M NaCl, 0.05% (vol/vol) NP-40, and 1 mM β-mecaptoethanol. Two micrograms of nucleosome particles was digested with 45 Boehringer units of micrococcal nuclease (MNase; Sigma), and reactions were stopped at 20, 60, and 120 s with 0.2 volumes of stop buffer (4% sodium dodecyl sulfate [SDS] and 10 mM EDTA). The reaction mixtures were digested with proteinase K (Genaxxon), and the DNA was separated on a 1.3% agarose gel.

Gel filtration. Recombinant HP1 (128 μM/145 μg) was loaded onto a Superdex 200 column (HR 10/30; Amersham Pharmacia). The column was run isocratically with 0.2 ml/min in BC200 buffer at 1.4 column volumes, and 0.5-ml fractions were collected.

Cross-linking assay. Bacterially expressed HP1 (0.17 μM) was cross-linked using 250 μM DTSSP [3,3′-dithiobis(sulfosuccinimydal propionate)] (Pierce) and incubated on ice for 2 h in BC100 buffer without DTT. The reaction was stopped by adding 100 mM Tris-HCl (pH 7.6) and boiled in SDS-polyacrylamide gel electrophoresis (PAGE) sample buffer with or without β-mercaptoethanol. After separation by SDS electrophoresis, the proteins were transferred to a PVDF membrane (Millipore) and incubated with α-HP1 (C1A9).

Peptide pulldown. Various H3 peptides (aa 1 to 19) were coupled to Thiolink beads (Bio-Rad) and resuspended as 1:1 slurry in BC100. Twenty microliters of this slurry was incubated with 1 μg of recombinant HP1 in a total volume of 200 μl BC100. The incubation was performed on a rotating wheel at 4°C for 2 h. After washing three times with BC100 (containing 0.05% [vol/vol] NP-40) for 10 min each, the bound protein was eluted with 30 μl acidic elution buffer (100 mM Glycine [pH 2.5], 500 mM NaCl) for 20 min at 4°C. The eluted proteins were analyzed by SDS–12% PAGE and Coomassie stained. One microgram of biotinylated H3 peptides, unmodified from aa 1 to 21 (WT) and trimethylated at K9 aa 1 to 21 (Upstate), were mixed with 2 μg HP1 (WT or mutant proteins) and incubated for 1 h at 4°C. Then 10 μl of a 1:1 slurry of paramagnetic beads (Dynal) (preblocked in BSA) was added and incubated for 1 h at 26°C in BC100 (containing 0.05% [vol/vol] NP-40). The paramagnetic beads were concentrated on a magnetic concentrator (Dynal) and washed once with BC100 plus 0.05% (vol/vol) NP-40 and twice with BC200 plus 0.05% (vol/vol) NP-40. Bound proteins were separated on an SDS–12% PAGE gel and Coomassie stained.

H3K9-methylated octamer. One hundred twenty micrograms of recombinant octamer was incubated in the presence of 9 μg of active recombinant *Drosophila* SU(VAR)3-9 (20) to retrieve 60 μg of a 70 to 80% H3K9 di- and trimethylated octamer. The reaction mixture was incubated at 30°C for 90 min in the presence of 40 μM *S*-adenosylmethionine (New England BioLabs) as methyl donor and 40 mM NaCl. After incubation concentrations were adjusted to 100 mM NaCl, and 0.2 mM PMSF and 2 mM DTT were added. To a 1-ml total volume, 80 μl (1:1 slurry) of Biorex70 beads (Bio-Rad) was added. The reaction mixture was rotated at 4°C for 4 h and washed five times with TEN200 (200 mM NaCl, 10 mM Tris, 1 mM EDTA, 0.2 mM PMSF, 1 mM DTT) and five times with TEN400. The methylated octamer was eluted with TEN2500, and 4 μl (2 μg) was analyzed by SDS–15% PAGE and stained with Coomassie blue.

MALDI-TOF analysis. The Coomassie stained band corresponding to H3 was excised and subjected to chemical modification by treating with propionic anhydride to convert free amino groups to propionic amides of lysine residues as described (66). H3 was digested over night with 100 ng of sequencing-grade trypsin (Promega) in a total volume of 40 μl according to manufacturers protocol. In order to purify the methylated peptides from contaminating salts or acryl amide the peptide solution was passed over a pipette tip containing SCX material (ZipTip, Millipore) and eluted as previously described (20). The matrix-assisted laser desorption ionization–time of flight (MALDI-TOF) spectra were acquired and analyzed according to the method described in reference 7. Quantification was performed as previously described in reference 28.

Chromatin assembly extract. S150 chromatin assembly extract was prepared from 0- to 90-min *Drosophila* embryos according to the method described in reference 6.

Chromatin assembly on immobilized DNA and micrococcal nuclease digestion. The assembly reactions for immobilized DNA were performed according to reference 57. In short, 2 μg DNA was immobilized to 0.8 mg paramagnetic streptavidin beads (Dynal) and, after extensive washing, blocked for 30 min at 4°C with BSA (1 μg/μl) in EX50 (10 mM HEPES [pH 7.6], 50 mM NaCl, 1.5 mM $MgCl_2$, 0.5 mM EGTA, 10% [vol/vol] glycerol, 0.2 mM PMSF, 1 mM DTT) containing 0.05% (vol/vol) NP-40 before assembly. Unmodified or H3K9Me histone octamers (2 μg) were mixed with the assembly extract at time point zero together with an ATP regenerating system (3 mM ATP, 30 mM creatine phosphate, 10 μg creatine kinase/ml, 3 mM $MgCl_2$, and 1 mM DTT). HP1 was then added at a concentration of 2 μg (8.3 ng/μl), and the reaction mixture was left to rotate for 6 h at 26°C. MNase digestions was performed as described in reference 57, with 30 Boehringer units of MNase (Sigma). For MNase digestion of chromatin assembled onto circular DNA, 150 Boerhringer units were used. A 123-bp ladder (Invitrogen) was used as a size marker.

Immobilization of salt-assembled chromatin and HP1 binding assays. Salt-assembled unmodified or H3K9Me chromatin (1 μg) was immobilized onto 0.4-mg paramagnetic streptavidin beads (Dynal) in TEN100 buffer containing 0.05% (vol/vol) NP-40 and 250 ng/μl BSA. After 2 h of rotation at 4°C, the chromatin on paramagnetic beads was concentrated on a magnetic concentrator (Dynal) and washed once with EX100 buffer containing 0.05% (vol/vol) NP-40. Chromatin was immediately resuspended in a total volume of 80 μl containing 60 μl EX100 plus 0.05% (vol/vol) NP-40, BSA (100 ng/μl), ATP regenerating system (3 mM ATP, 30 mM creatine phosphate, 10 μg creatine kinase/ml, 3 mM $MgCl_2$, and 1 mM DTT) and 2 μg (25 ng/μl) HP1. Purified SU(VAR3-9) WT and Δ213 were added in a total concentration of 100 ng in the presence of 1 μM Chaetocin dissolved in dimethyl sulfoxide or an equal volume of dimethyl sulfoxide only. FLAG-eluted ACF at a total concentration of 50 ng was added in the presence or absence of ATP. *Drosophila* assembly extract was added at a concentration of 100 μg in the presence of ATP or nonhydrolyzable ATP-γ-S analog.

Chromatin washes and HP1 detection. Assembled chromatin was concentrated on a magnetic concentrator (Dynal), and the supernatant was removed. The chromatin beads were washed once with 100 μl EX100 (10 mM HEPES [pH 7.6], 100 mM NaCl, 1.5 mM $MgCl_2$, 0.5 mM EGTA, 10% [vol/vol] glycerol, 0.2 mM PMSF, 1 mM DTT) containing 0.05% (vol/vol) NP-40 and twice with the same buffer containing 200 mM NaCl. The bound proteins were eluted with 10 μl SDS loading dye and separated by SDS–15% PAGE. The proteins on the gel that were smaller than 20 kDa, including the histones, were subjected to Coomassie staining, whereas the rest of the gel was transferred to a PVDF membrane (Millipore). Blots were probed with HP1 polyclonal rabbit antibody and incubated with fluorescently labeled secondary antibodies and visualized using the Odyssey system (Li-Cor) as described above.

ACF and ACF1 pulldowns. ACF1-FLAG and imitation switch (ISWI) were expressed in Sf9 cells as described previously (15) The ACF complex was generated by coexpression of ACF1-FLAG with untagged ISWI. Sf9 cells were suspended in BC500 containing 0.05% (vol/vol) NP-40, 1 mM DTT, 0.2 mM PMSF, and protease inhibitors. The cells incubated on ice were sonicated two times for 15 s at 50% amplitude and centrifuged at maximum speed on a tabletop centrifuge for 30 min. A total of 500 ng of the expressed proteins was immobilized on M2 anti-FLAG agarose beads, washed with BC500 and BC1000 containing 0.05% (vol/vol) NP-40, and blocked with 1-μg/μl BSA. Recombinant HP1 or HP1 mutants were added at a concentration of 1 μg in a total volume of 200 μl BC100 containing 0.05% (vol/vol) NP-40, 100 μg BSA, and 5 μg ethidium bromide. After 30 min of incubation at room temperature, the beads were washed two times in the same buffer without ethidium bromide and BSA, containing 100 mM NaCl, and four times in a buffer containing 200 mM NaCl. The bound proteins were eluted with SDS sample buffer, analyzed by SDS-PAGE, and transferred onto a PVDF membrane (Millipore).

GST pulldowns. GST pulldowns were performed as described in reference 20. ACF1 constructs were translated in vitro according to the method described in reference 31.

RESULTS

In order to generate chromatin fibers that contain HP1, we have expressed *Drosophila* HP1a (HP1) in bacteria and purified it to homogeneity over four consecutive columns (74) (Fig. 1A). Throughout the present article we will refer to this recombinant HP1a protein as HP1 unless stated otherwise. The purified HP1 dimerizes and interacts specifically with peptides that resemble the H3 N terminus dimethylated at K9 (Fig. 1). For the chromatin binding studies, we assembled recombinant *Drosophila* histones (16) onto DNA fragments containing 11 repeats of the 5S nucleosome positioning sequence using salt dialysis (9). The level of assembly was tested by micrococcal nuclease digestion (Fig. 2B, right panel). The DNA fragments were asymmetrically labeled with biotin and immobilized using streptavidin-coupled paramagnetic beads. Fully assembled arrays were coupled and used for binding assays after washing with a buffer containing 100 mM salt. The addition of the highly purified HP1 dimer at a 4:1 molar ratio of HP1/nucleosome to the immobilized chromatin fiber resulted in only weak binding (Fig. 2C, lane 2) of HP1. This is consistent with previous observations that report binding of HP1 only at HP1-to-nucleosome ratios of more than 500:1 (74). In contrast to HP1, the linker histone H1 binds very efficiently to chromatin fibers even at a molar ratio of 2:1 (Fig. 2D, lane 3). From these experiments we concluded that HP1 requires high-affinity docking sites in order to bind with a recognizable strength to chromosomal arrays.

One of the best-characterized binding sites for HP1 in vivo is an H3 molecule that is methylated at K9 (40, 52). The enzyme responsible for creating the site in a living cell is the histone methyltransferase SU(VAR)3-9, which interacts with HP1 and has been suggested to create an autoregulatory loop that helps in maintaining the methylated state of heterochromatin (60). We wanted to generate a high-affinity binding site for HP1 by reconstituting chromatin using in vitro-methylated recombinant histones. To do this we used recombinant SU(VAR)3-9 (20) to methylate a mixture of four recombinant expressed core histones that were reconstituted into octamers (44). Subsequently, the recombinant SU(VAR)3-9 as well as the cofactors *S*-adenosylmethionine and *S*-adenosylhomocysteine were separated from the histone octamer using a cation exchange resin (70). Only histone preparations that contained no detectable SU(VAR)3-9 protein (as measured by Western blotting) were used for subsequent experiments. The purified histones were analyzed by mass spectrometry, which showed that more than 85% of all H3 molecules were methylated at K9, with more than 80% carrying two or three methyl groups (Fig. 2A, right panel and MALDI-TOF spectrum). No other lysine in H3, H2A, H2B, or H4 was found to be methylated, and no SU(VAR)3-9 was detectable in the purified histones (data not shown). The highly methylated histone octamers were then used to assemble chromatin fibers as described above. Micrococcal nuclease digestion showed that the methylated chromatin has a similar spacing and sensitivity toward the nuclease (Fig. 2B, right panel, compare lanes 2 to 4 and 5 to 7). However, despite the high content of methylated H3, recombinant HP1 showed only a weak binding that was independent of histone methylation and was even weaker than its affinity to free DNA (Fig. 2C). From these experiments we concluded that HP1 either binds to methylated histones before assembly of chromatin or it requires additional factors for the binding to its substrate.

In addition to its interaction with the methylated H3 tail, HP1 has also been shown to interact with core residues of H3 and H1 (51), which are buried within chromatin, suggesting that HP1 may bind to H3 before assembly. In order to test this hypothesis, we had to use a different assembly method, as we reasoned that the HP1 binding would not sustain the high salt concentration during the salt assembly reaction. Therefore, we used a S150 chromatin assembly extract from early *Drosophila* embryos (6) that allowed us to assemble chromatin at lower salt concentrations (less than 100 mM) (Fig. 3A). However, even though recombinant HP1 was added at the same time as the assembly extract, we could detect only a weak association of HP1 with the assembled chromatin (Fig. 3C, lane 3). As we have previously shown that histones from early *Drosophila* embryos contain less than 5% H3K9 methylation (7), we added either unmodified or in vitro-methylated histones to the extract before the assembly reaction (Fig. 3C, lanes 4 and 5). The addition of exogenous histones led to a slight decrease in sensitivity towards MNase (Fig. 3B, compare lanes 2, 3, and 4 with lanes 6, 7, 8, 10, 11, and 12). However, we could not observe any difference in nucleosomal repeat length when supplementing the S150 with either unmodified or H3K9Me octamers. MS analysis of the chromatin after assembly showed that it contained K9-methylated chromatin only when the in vitro-methylated histones were added (data not shown), indicating that the exogenously added histones are incorporated by the assembly extract. Under these conditions, HP1 bound to chromatin arrays where methylated octamers were added before the assembly reaction but only weakly interacted with chromatin to which unmodified histones were added (Fig. 3C, compare lanes 4 and 5). A quantification of this experiment is shown in Fig. 3D. There is 10 times more HP1 bound to H3K9Me chromatin than to unmodified chromatin. As we assembled chromatin using a heterogeneous extract we could not directly conclude from these experiments whether HP1 bound to the methylated H3 before the assembly or whether the binding was enhanced by the action of accessory factors. To distinguish between these two possibilities, we assembled chromatin from unmodified or methylated histones by salt dialysis and added S150 extract together with recombinant HP1 after the assembly reaction. It turned out that the S150 extract was able to facilitate HP1 binding to methylated chromatin even at concentrations that were not sufficient to assemble nucleosomes in vitro (Fig. 4). As chromatin assembly is ATP dependent, we wondered whether the loading process required ATP hydrolysis. The addition of ATP stimulated binding of HP1 to the nucleosomal array irrespective of its methylation state (Fig. 4B, compare lanes 4 and 6). The stimulation of HP1 binding to the methylated chromatin, however, was not dependent on ATP hydrolysis (Fig. 4B, compare lanes 5 and 7). A quantification of this HP1 binding experiment is shown in Fig. 4C. In the presence of an assembly extract HP1 is bound more than 11 times better to H3K9Me chromatin compared to unmodified chromatin. From these results we reckoned that the assembly extract does indeed contain factors that facilitated HP1

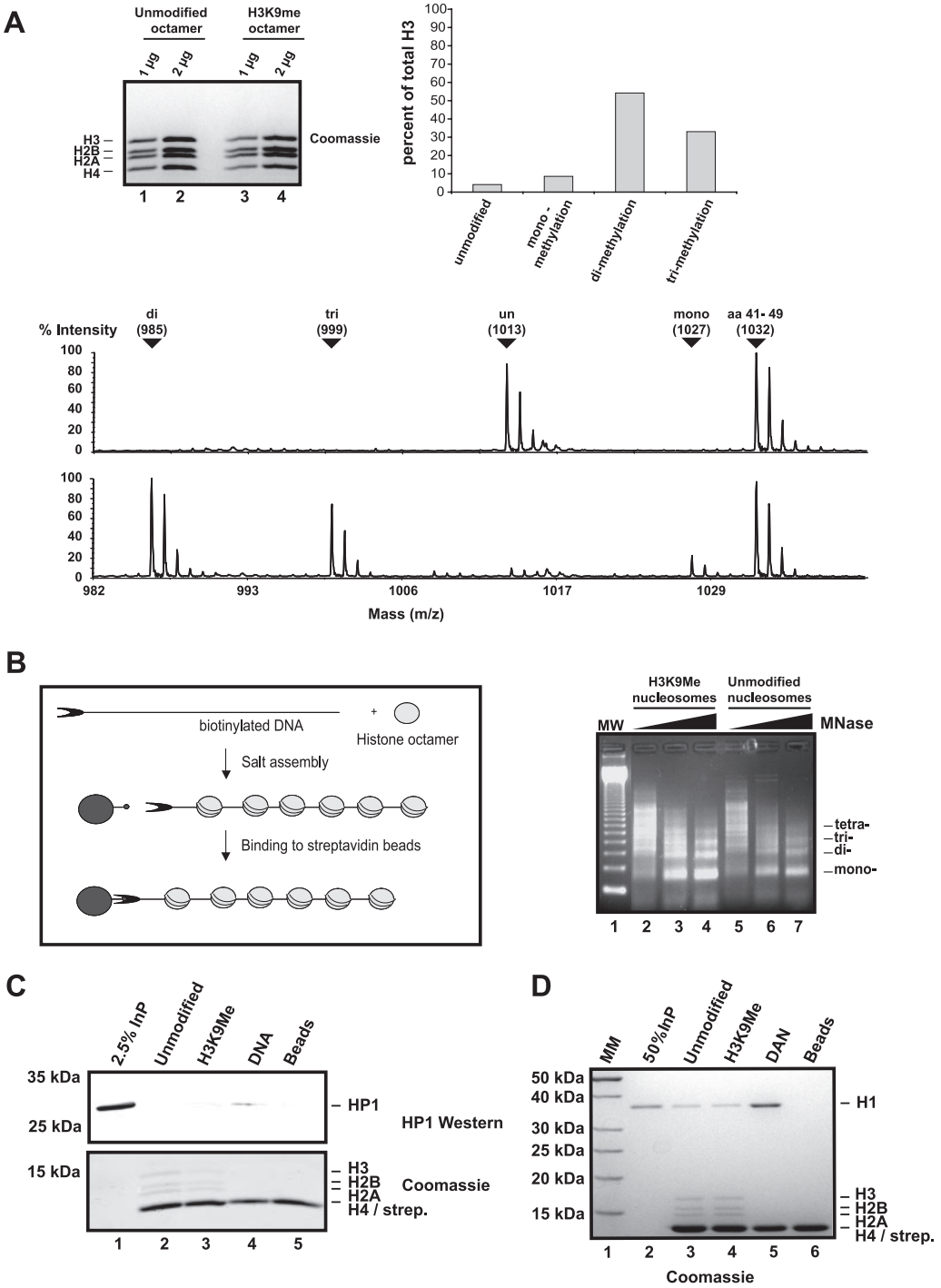

FIG. 2. Generation of H3K9-methylated chromatin. (A) To the left is a Coomassie blue-stained SDS–15% PAA gel of reconstituted unmodified (lanes 1 and 2) and H3K9-methylated (lanes 3 and 4) octamers. Displayed in the lower panel is a MALDI-TOF analysis of H3 peptide 9-17 from unmodified H3 (top) and H3 methylated at K9 (bottom). As an internal standard we show H3 peptide 41-49. Unmodified and mono-, di-, and trimethylated peptides with corresponding mass are labeled with arrows. The masses of unmodified and monomethylated peptide 9-17 are higher than those of di- and trimethylated peptide because the free N-terminal amines are propionylated. The quantification of the MALDI-TOF analysis is shown in the upper right panel. (B) Scheme of our chromatin reconstitution protocol. The DNA used for chromatin reconstitution is a linearized biotinylated fragment containing 12 repeats of the 5S nucleosome positioning sequence (69). A micrococcal digestion pattern of salt-reconstituted chromatin with unmodified or in vitro methylated histones is shown on the right. MW, molecular weight. (C) HP1 was assayed for binding to unmodified chromatin (lane 2), H3K9Me chromatin (lane 3), DNA immobilized on paramagnetic beads (lane 4), and beads alone (lane 5). Bound HP1 was separated by SDS–15% PAGE and visualized with an HP1 polyclonal antibody. The bottom panel shows the corresponding histones stained with Coomassie blue. Boiling of the streptavidin-coated beads resulted in the release of a strongly stained band with an apparent molecular weight similar to that of H4, which is therefore labeled H4/streptavidin (strep.). InP, input. (D) The same assay as described for panel C was performed with histone H1, also visualized by Coomassie blue. MM, molecular mass.

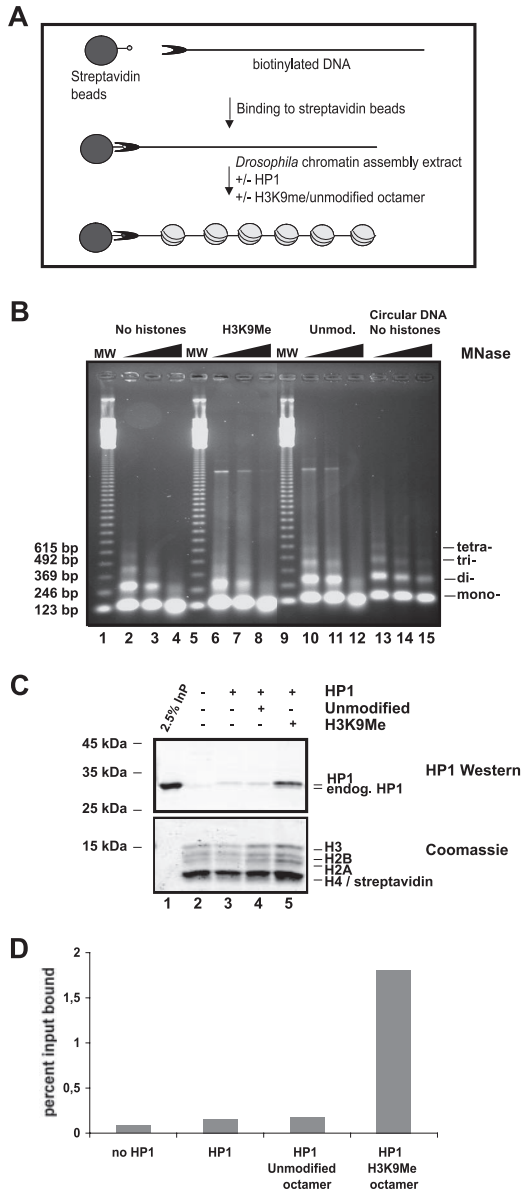

FIG. 3. Reconstitution of methylated chromatin using an S150 *Drosophila* assembly extract and HP1 binding. (A) Scheme of the assay. (B) Micrococcal digestion pattern of chromatin assembly reactions as described for panel C, without HP1 added. MNase digestions were stopped after 30, 60, and 300 s. Assembly of circular DNA was used as a control. MW indicates lanes containing the 123-bp ladder as size marker. Unmod., unmodified. (C) Chromatin was reconstituted on a 2-μg linearized biotinylated fragment containing 12 repeats of the 5S nucleosome positioning sequence bound to paramagnetic beads in the presence or absence of 2 μg of HP1 for 6 h at 26°C. Before assembly, 2 μg of unmodified (lane 4) or H3K9Me (lane 5) histone octamers was supplemented to the extract. The paramagnetic beads were washed, and proteins remaining on the beads were separated on an SDS–15% polyacrylamide gel. HP1 was visualized with an HP1 polyclonal antibody. The corresponding histones were stained by Coomassie blue. Endogenous (endog.) HP1 from the assembly extract and recombinantly added HP1 are labeled. InP, input. (D) The graph corresponds to quantification of bound HP1 from panel C. Recombinant and endogenous HP1 are included in the quantification. The *y* axis displays the percentage of input bound. The graph is representative of three or more different experiments.

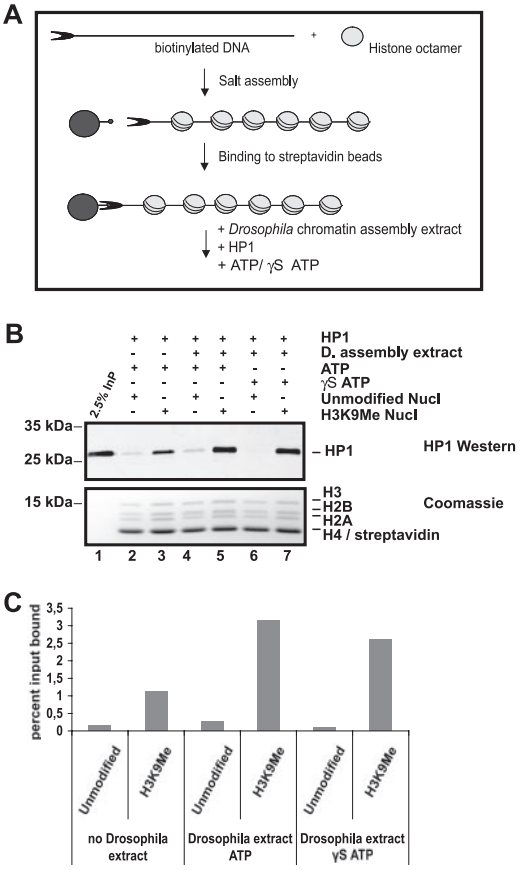

FIG. 4. HP1 is bound to salt-assembled chromatin in the presence of *Drosophila* assembly extract. (A) Scheme of the assay. (B) Salt-assembled unmodified or H3K9Me chromatin attached to paramagnetic beads was incubated for 1 h at 26°C with HP1, plus and minus *Drosophila* (D.) assembly extract. The reactions were carried out in the presence of ATP or nonhydrolyzable ATP-γ-S analog (γS ATP). The assembly extract added was less than 5% of what is needed for the assembly reaction in Fig. 3. HP1 was detected with HP1 polyclonal antibody, and corresponding histones were detected with Coomassie blue. Nucl, nucleosome. (C) The graph corresponds to quantification of bound HP1 as shown in Fig. 3B. The *y* axis displays the percentage of input bound. The graph is representative of at least four individual experiments.

binding to the methylated H3 tail and that can assist HP1 binding to assembled chromatin. The presence of ATP in the reaction moderately stimulates the affinity of HP1 to chromatin but does not increase the specific binding to methylated chromatin.

As discussed above, HP1 has three domains, all of which are involved in HP1 function. The CD binds histone H3 methylated at K9, the hinge domain is important for DNA and RNA binding, and the CSD carries a protein-protein interaction domain. In order to get more insight into the nature of HP1 binding to methylated chromatin, we expressed and purified mutant HP1 proteins (Fig. 5A and B) and added them to a chromatin assembly reaction as shown in Fig. 3A. As has been reported before (35), a V26M mutation within the CD of HP1 prevented binding to a peptide containing methylated K9 (Fig. 5C, lane 7). This mutation also resulted in a reduction of HP1 binding to the methylated chromatin (Fig. 5D, lane 6). A point mutation of W to A at position 200 in the CSD of HP1 that has

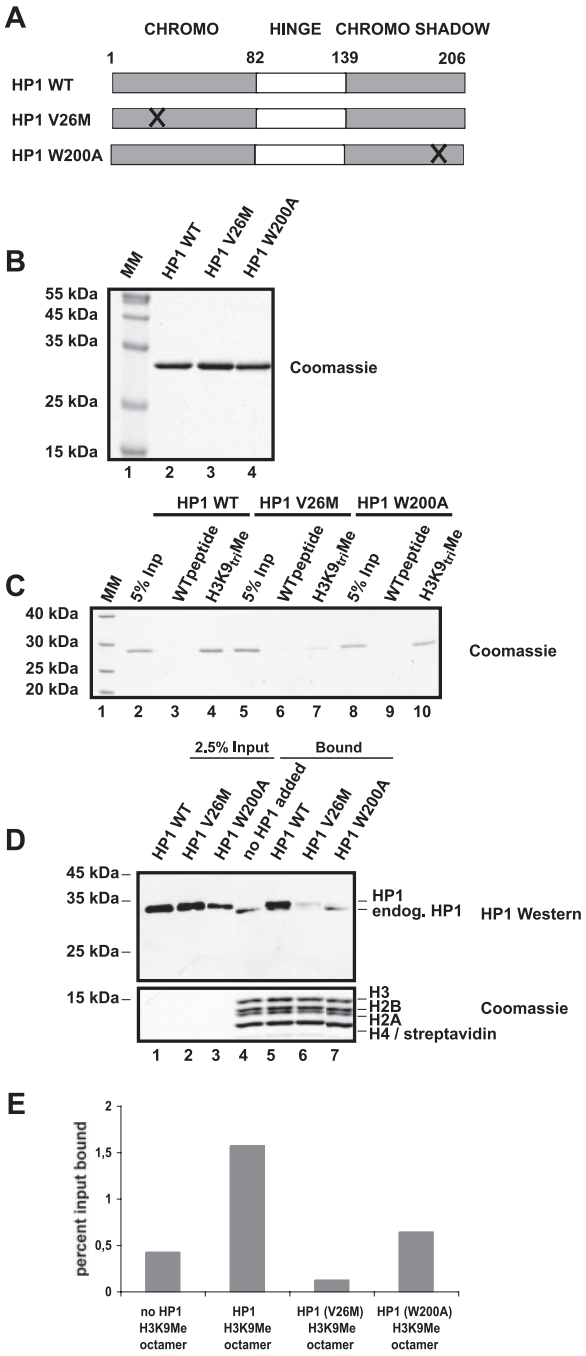

FIG. 5. Expression of HP1 mutant proteins and binding of these to H3K9Me chromatin during assembly. (A) Scheme of HP1 mutants generated. (B) Coomassie blue-stained 15% SDS-polyacrylamide gel of the purified HP1 proteins. MM, molecular mass. (C) Peptide pulldown of the recombinant HP1 WT and mutants using H3 peptide aa 1 to 21, unmodified (WT) versus trimethylated at K9 ($H3K9_{tri}Me$). Bound HP1s were visualized by use of Coomassie blue. InP, input. (D) *Drosophila* assembly reaction with 2 μg H3K9Me octamer as described for Fig. 3A. In lanes 1 to 3, 2.5% HP1 input was used. Lanes 4 to 7 correspond to proteins bound after 6 h of incubation. HP1 was detected with HP1 polyclonal antibody, and the corresponding histones were stained with Coomassie blue. Bound exogenous and endogenous (endog.) HP1 present in the *Drosophila* assembly extract are labeled. (E) The graph corresponds to quantification of bound HP1 from panel D. Recombinant and endogenous HP1 are included in the quantification. The *y* axis displays percentage of input bound. This quantification is representative of at least three different experiments.

been shown to selectively interfere with the interaction between HP1 and associated proteins (8) also resulted in a loss of HP1 binding to methylated chromatin (Fig. 5D, lane 7), despite its ability to interact with the methylated peptide (Fig. 5C, lane 10). A quantification of this experiment is shown in Fig. 5E. These results pointed towards a protein-protein interaction rather than an HP1 DNA or HP1 RNA interaction playing a key role in the loading of HP1 to heterochromatin.

Several chromatin-associated factors have been suggested to play a role in heterochromatin formation and its function (55, 59). The chromatin-remodeling factor ACF consisting of the ISWI ATPase and the regulatory ACF1 protein is very abundant in early *Drosophila* embryos. A mutation in the gene *ACF1* of *Drosophila* has been identified as a suppressor of position effect variegation, which places ACF1 in the same genetic pathway as HP1 (24). Mammalian ACF1 has been shown to colocalize with HP1β in NIH 3T3 cells and is suggested to have a role in replication of heterochromatin (11). As we have observed a strong impairment of chromatin binding of HP1 mutants that carry a mutation within the CSD, we first investigated whether recombinant ACF was able to interact directly with HP1 and whether this interaction was mediated by the CSD. We purified an ACF complex using a baculoviral system expressing a FLAG-tagged ACF1 protein together with untagged ISWI (Fig. 6A), and the immobilized complex was then incubated with various HP1 mutant proteins. We could detect binding of HP1 to the reconstituted ACF complex (Fig. 6B) as well as to the isolated ACF1 subunit (Fig. 6C). Consistent with previous findings showing that most heterotypic protein-protein interactions with HP1 are mediated by the CSD (67), the ACF1-HP1 interaction was also mediated by this domain, as the point mutation within the CSD motif impaired the interaction (Fig. 6B and C, compare lanes 3 and 6 with lane 9). The fact that the isolated ACF1 subunit is sufficient for the HP1 binding may explain the specific effect of an *ACF1* mutation on heterochromatin formation (24). In order to map the interaction domain within ACF1 that is responsible for the HP1 interaction, we performed GST pulldown experiments using GST-HP1 and in vitro-translated ACF1 fragments (Fig. 6D). In these experiments we could detect binding of all fragments containing amino acids 202 to 468 (Fig. 6E and F).

The region responsible for ACF1 binding to HP1 contains the evolutionarily conserved DDT motif (14), suggesting that this motif most likely represents an HP1 interaction domain. For *Drosophila* ACF1, the region containing the DDT motif has been shown to be required for ISWI interaction (16, 25).

Another prominent factor that is known to interact with HP1 in vivo and which plays an important role in heterochromatin formation is the histone methyltransferase SU(VAR)3-9 (1, 60). We performed protein-protein interaction assays using different SU(VAR)3-9 or HP1 mutants in order to biochemically map the interaction regions for each protein. The N terminus of SU(VAR)3-9 was necessary for its association with HP1 (Fig. 7A), while the CSD of HP1 was required for SU(VAR)3-9 binding (Fig. 7B). This further demonstrated the importance of the HP1 CSD for protein-protein interaction (8, 41, 72). The in vivo target loci of HP1 and SU(VAR)3-9 have been mapped in *Drosophila* Kc cells

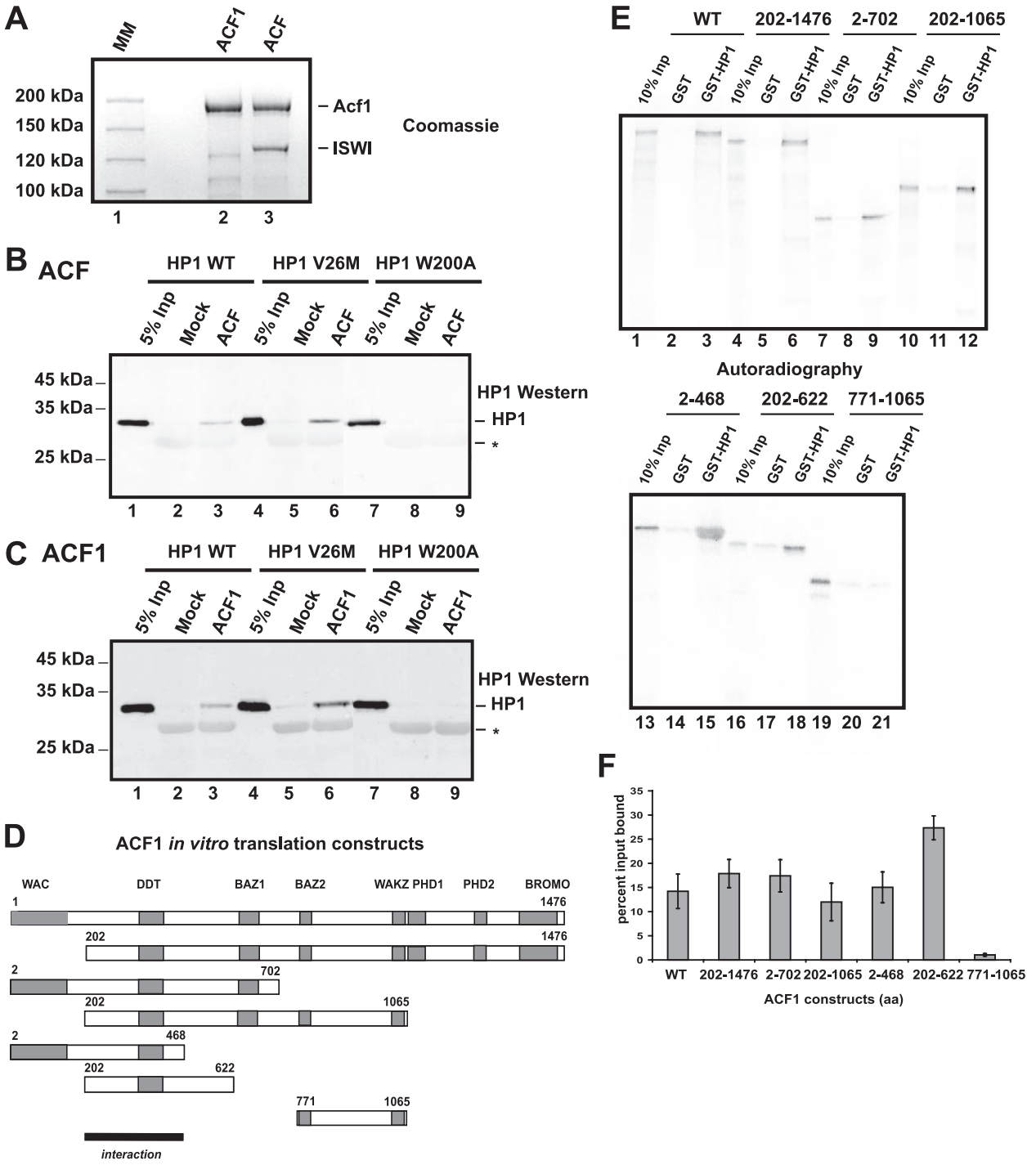

FIG. 6. HP1 interacts with the ACF complex and ACF1. (A) Coomassie-stained SDS–8% PAA gel of FLAG affinity-purified recombinant ACF1 and ACF complex from Sf9 cells coinfected with FLAG-ACF1 in the presence or absence of untagged ISWI. MM, molecular mass. (B) HP1 pulldown with FLAG beads incubated with mock Sf9 extract or extract containing FLAG-ACF1 and untagged ISWI. After extensive washing, the protein remaining on the beads was separated by SDS–12% PAGE, imunoblotted, and detected with HP1 antibody. Asterisks indicate FLAG antibody light chains. Inp, input. (C) Western blot of HP1 pulldown using FLAG beads incubated with mock Sf9 extract or extract containing FLAG-ACF1. Asterisks indicate FLAG antibody light chains. (D) ACF1 constructs used for in vitro translation. (E) GST and GST-HP1 pulldown with in vitro translated ACF1 constructs. (F) Quantification of the binding affinities of the various ACF constructs. Error bars represent standard deviations from three independent pulldown experiments.

(27). HP1 and SU(VAR)3-9 colocalized at multiple sites, suggesting a possible targeting of HP1 by SU(VAR)3-9, but the fact that HP1 can also be found at other chromatin sites supports the idea that SU(VAR)3-9 binding is not the sole way of stabilizing HP1 binding to chromatin. We therefore tested whether the known SU(VAR) proteins ACF1 and SU(VAR)3-9 could facilitate HP1 binding to methylated chromatin in vitro. In order to do this, we used salt-assembled

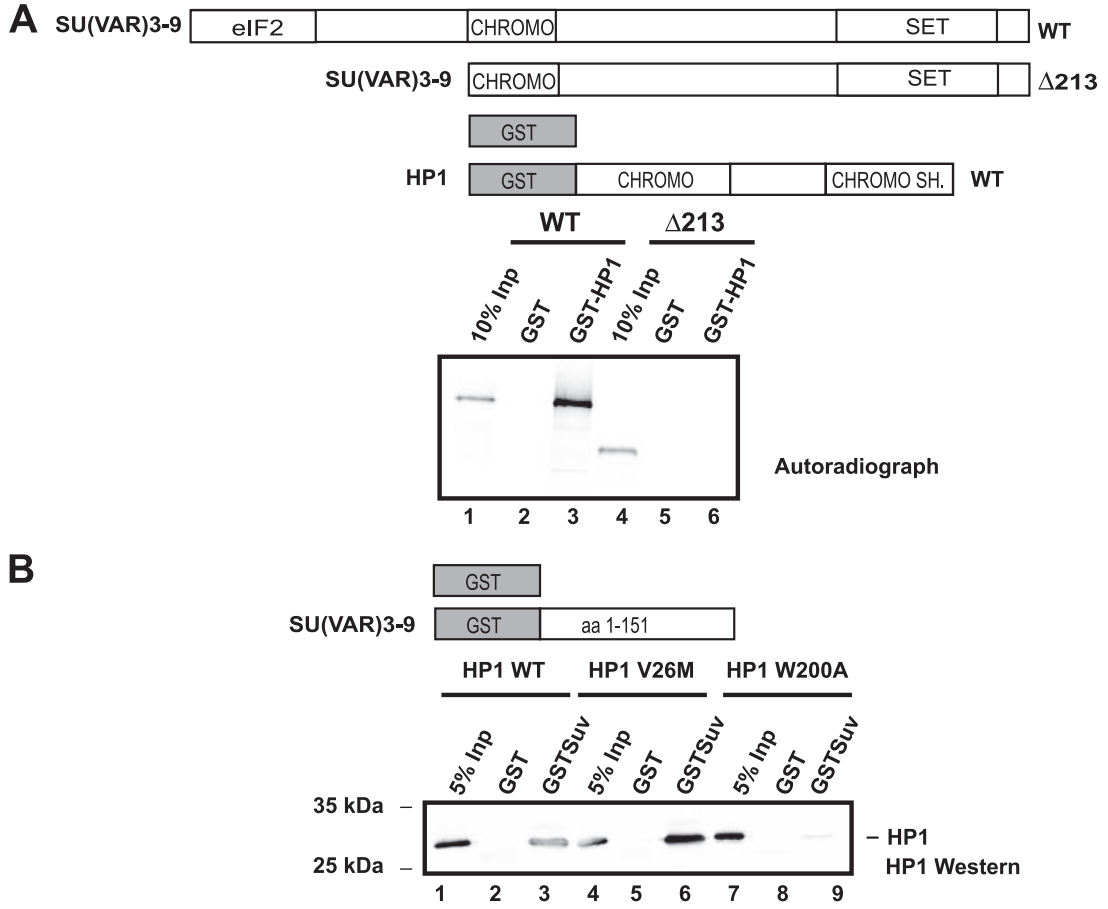

FIG. 7. HP1 interacts with SU(VAR)3-9. (A) SU(VAR)3-9 constructs used for in vitro translation and GST constructs are shown at the top. The GST pulldown is shown at the bottom. SU(VAR)3-9 was detected by autoradiography. CHROMO SH., chromo shadow. (B) The upper panel shows GST constructs used for the pulldown experiment. The lower panel represents an HP1 Western blot of GST pulldown with recombinant HP1 WT (lanes 1 to 3), HP1 (V26M) (lanes 4 to 6), and HP1 (W200A) (lanes 7 to 9). HP1 was detected with HP1 polyclonal antibody.

chromatin that contained either methylated or nonmethylated histones and added recombinant HP1 together with recombinant SU(VAR)3-9 or ACF (Fig. 8A). Consistent with the model that HP1 requires multiple binding sites for efficient chromatin binding, we observed an increased association of HP1 with methylated chromatin when ACF complex (Fig. 8B, lane 5, and 8C [quantification]) or SU(VAR)3-9 (Fig. 8D, lane 5, and 8E [quantification]) was present. This was not due to an intrinsically higher affinity of the auxiliary factors to methylated chromatin, as both bound efficiently to the chromatin fiber independently from its modification state (Fig. 8B, compare lanes 4 and 5, and 8D, compare lanes 4 and 5). We also found that neither ATP nor HMTase activity was required for preferential binding of HP1 to methylated chromatin (Fig. 8B and 8D, compare lanes 5 and 7).

This evidence suggests that only the protein-protein interaction served as a second binding site within chromatin and stabilized the interaction of HP1 and the methylated chromatin. This finding is further strengthened by the observation that a mutation in the CSD of HP1 (W200A) that no longer interacts with SU(VAR)3-9 has a reduced binding affinity towards methylated chromatin (Fig. 8F, compare lanes 3 and 9).

DISCUSSION

It is of critical importance to understand how epigenetic information is stored and maintained. The finding that a combinatorial aspect of histone modification can contribute to this epigenetic information processing therefore represents a very attractive model (37, 71). However, it has not been shown so far how epigenetic marks in the form of specific histone modifications can be "read" within a defined chromatin context and how the factors that can bind specifically to these marks access them. We reconstituted HP1 containing chromatin fibers in the test tube using a highly purified reconstituted system containing unmodified histones with H3 molecules that are methylated at K9, recombinant HP1 and two known SU(VAR) proteins, ACF and SU(VAR)3-9. Both factors bind chromatin in a methylation-independent manner and can interact simultaneously with HP1 via the CSD of HP1. These findings suggest a bimodal interaction of HP1 with chromatin, in which a single binding site is not sufficient to stably anchor HP1 to chromatin. It is important to mention that the binding assay we are using throughout the study is not an equilibrium binding assay. As HP1 could bind to methylated chromatin with high affinity but

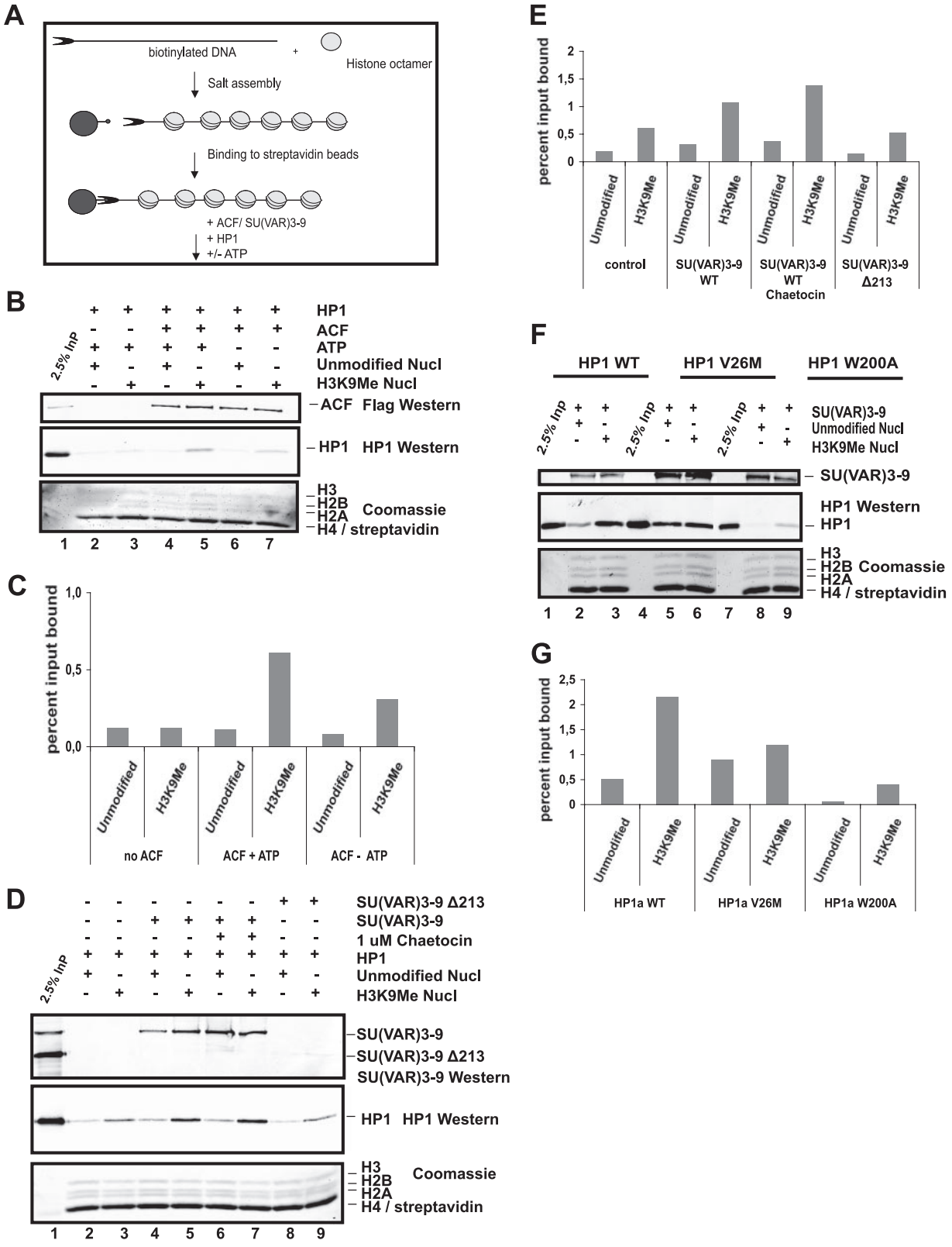

FIG. 8. SU(VAR) 3-9 and ACF facilitate HP1 binding to H3K9Me chromatin. (A) Scheme of the assay. (B) Salt-assembled unmodified or H3K9Me chromatin bound to paramagnetic beads was incubated with HP1 in the presence or absence of ACF and ATP for 1 h at 26°C. After washing, the proteins remaining on the paramagnetic beads were separated by SDS–15% PAGE. ACF1 was detected with FLAG antibody, and HP1 was detected with HP1 polyclonal antibody (upper panels). The corresponding histones were detected with Coomassie blue (bottom panel). Lane 1 corresponds to 50% ACF input (InP) and 2.5% HP1 input. Nucl, nucleosome. (C) The graph displays bound HP1 as a percentage of input as shown in panel B. The *y* axis corresponds to percent input bound. The graph is representative of at least two individual experiments.

with rapid association and dissociation rates, we actually detected the rate of dissociation of HP1 from chromatin. The auxiliary factors may increase the average time HP1 resides at methylated chromatin, which may be essential for heterochromatin formation.

These findings are in accordance with observations in vivo showing that HP1 can be released from its binding sites either by a peptide resembling the H3 N terminus that is methylated at K9 (5, 49), by treatment with RNase (45), or by a peptide that mediates the interaction with an associated factor (4). Our data provide a biochemical explanation for these seemingly contradictory observations.

HP1 is considered a major component of constitutive heterochromatin (56). Despite an enormous wealth of data regarding the localization of HP1 in vivo, the molecular details of how HP1 recognizes pericentric heterochromatin have been sparse. Our data show that even though HP1 is able to bind histones that are methylated at K9 when they are incorporated into chromatin, the affinity is rather weak and presumably not sufficient to maintain a heterochromatic structure in vivo or in vitro. This is in perfect agreement with biophysical studies that have measured a dissociation constant for H3K9-methylated peptides between 2 μM (nuclear magnetic resonance) (52) and 100 μM (isothermal titration calorimetry) (34), which is rather high compared to other protein-protein or protein-DNA interactions. Considering the picomolar constant for dissociation of a histone tail from the DNA (33) and the fact that histone tails can be UV cross-linked to DNA in vivo and in vitro (3), it is difficult to envision efficient binding of HP1 to the methylated tail only. The weak interaction and the corresponding low occupancy time at a given binding site is presumably also the reason for the dynamic nature of HP1 in the nuclei of eukaryotic cells (10, 23).

Our data also suggest that an efficient binding of HP1 to chromatin can be achieved only when several binding sites are present within the chromatin substrate. It had previously been reported that the general affinity of HP1 to mononucleosomes is rather low and independent of the histone tails (74). In contrast to this, native chromosomal fibers can be purified with reasonably efficiency using immobilized HP1 molecules (46). In our fully defined reconstituted system we also detected only weak binding of HP1 to chromatin that was moderately stimulated when the H3 tail is fully methylated at K9. This binding of HP1 to methylated chromatin was stimulated by the addition of factors that were able to bind HP1 and chromatin at the same time, thereby enhancing the affinity of HP1 to chromatin. A mutational analysis of the ability of the factors to load HP1 to methylated chromatin showed that the physical interaction with HP1 is required for their activity to assist HP1 binding. It may be that the native fibers still contain such additional factors and therefore increase the affinity of HP1 for heterochromatin.

HP1 has been shown to interact with several factors via its CSD (64), and the binding site is reconstituted by both HP1 molecules within the HP1 dimer (67). This interaction domain is required for heterochromatin localization in vivo as mutant HP1 proteins that can no longer form this domain also do not associate stably with centromeric heterochromatin or telomeric regions (22, 67). We also observe this failure of a HP1 mutant in the CSD to bind K9-methylated chromatin when assisted by a *Drosophila* S-150 chromatin assembly extract. This observation led us to the conclusion that HP1 has to interact with a factor present in this extract to bind methylated chromatin.

The two candidate factors that we used in order to test their ability to assist HP1 in its binding to K9-methylated chromatin both show a SU(VAR) phenotype when mutated in *Drosophila melanogaster* (24, 68). One, ACF1, has been shown to be a major chromatin assembly factor in *Drosophila* and has an effect on position effect variegation (24). In human cells, ACF1 has also been shown to colocalize with HP1β (11). ACF1 has been shown to bind DNA via its WAC domain (25) and to interact with histone molecules via its PHD fingers (16). Those two domains are presumably responsible for its interaction with the chromatin template. It is intriguing that the region spanning the DDT motif, which we found crucial for interaction with HP1, does not seem to be involved in binding to the chromatin substrate and could therefore be used to recruit HP1 to chromatin. It is tempting to speculate that ACF1-HP1 interaction may increase the local concentration of HP1 within heterochromatin, where the binding could be stabilized by its interaction via the CD with chromatin methylated at K9.

The second factor that we have tested is the histone methyltransferase SU(VAR)3-9. SU(VAR)3-9 is responsible for methylating H3 at K9 (60), thereby generating a potential binding site for HP1 within heterochromatin. SU(VAR)3-9 interacts with HP1 via the N terminus, and it has been suggested that this interaction serves as an autoregulatory loop, helping to maintain the methylated state of heterochromatin (60). We observed a high affinity of full-length SU(VAR)3-9 for in vitro assembled chromatin irrespective of its methylation state. Similar to our observations for ACF, described above, we also see increased binding of HP1 after adding SU(VAR)3-9 that is independent of its ability to methylate H3. However, when the interaction between SU(VAR)3-9 and HP1 was impaired due to a mutation either in HP1 or in SU(VAR)3-9, no increase in binding of HP1 to methylated chromatin could be observed. This additional function of SU(VAR)3-9 in stabiliz-

(D) SU(VAR)3-9 couples HP1 to chromatin. HP1 was incubated with unmodified or H3K9Me chromatin in the presence of recombinant SU(VAR)3-9 WT (lanes 4 to 7) or Δ213 (lanes 8 and 9). The SU(VAR)3-9-specific HMTase inhibitor Chaetocin was added to a concentration of 1 μM (lanes 6 and 7). The remaining SU(VAR)3-9 and HP1 on paramagnetic beads was detected by Western analysis, and the histones were detected with Coomassie blue. Lane 1 corresponds to 100% SU(VAR)3-9 input and 2.5% HP1 input. (E) Quantification of HP1 bound as shown in panel D. The graph is representative of at least three individual experiments and displays percent input bound. (F) SU(VAR)3-9 was added in the presence of HP1 WT (lanes 1 to 3), HP1 (V26M) (lanes 4 to 6), and HP1 (W200A) (lanes 7 to 9) to unmodified and H3K9Me chromatin. Bound SU(VAR)3-9 and HP1 were detected by Western analysis, and histones were detected with Coomassie blue. (G) The graph corresponds to total HP1 binding as shown in panel F. The *y* axis displays percent input bound. The graph is representative of at least two individual experiments.

ing HP1 binding could help explain the strong dose dependency the gene has, which is rather unusual for enzymatic activity. This may also be an explanation that some hypomorphic alleles of SU(VAR)3-9 can be isolated that show a Su(var) phenotype despite having normal HMTase activity (17).

The finding that HP1 binding is not only dependent on methylation at H3K9 but also requires additional auxiliary factors explains many in vivo observations that have been previously considered to be contradictory. It would also enable a cell to fine-tune its level of heterochromatin in response to external signals by modulating the different binding sites of HP1 within chromatin. We tested two known chromatin-associated factors for their ability to help increasing the affinity of HP1 to methylated chromatin. However, there may be additional factors and probably redundant mechanisms that can help loading HP1 to chromatin. It will be interesting to see whether the different targeting factors have different contributions to the localization of HP1 at different stages of the cell cycle, during different stages of development, or in different cell types. Our in vitro system for looking at HP1 binding to methylated chromatin will certainly be useful for identification of additional targeting factors in the future.

ACKNOWLEDGMENTS

We acknowledge Sally Elgin for the HP1 antibodies and Joel Eisenberg for the HP1 plasmid, Jeff Hansen for the 208-12 plasmid, Elisabeth Kremmer for generation of the SU(VAR)3-9 antibody, Gernot Langst and Peter Becker for helpful discussions and advice, and Josephine Sutcliffe for critical reading of the manuscript.

This work was supported by a grant from the Deutsche Forschungsgemeinschaft (IM23/4-3).

REFERENCES

1. **Aagaard, L., G. Laible, P. Selenko, M. Schmid, R. Dorn, G. Schotta, S. Kuhfittig, A. Wolf, A. Lebersorger, P. B. Singh, G. Reuter, and T. Jenuwein.** 1999. Functional mammalian homologues of the Drosophila PEV-modifier Su(var)3-9 encode centromere-associated proteins which complex with the heterochromatin component M31. EMBO J. **18:**1923–1938.
2. **Aasland, R., and A. F. Stewart.** 1995. The chromo shadow domain, a second chromo domain in heterochromatin-binding protein 1, HP1. Nucleic Acids Res. **23:**3168–3173.
3. **Angelov, D., J. M. Vitolo, V. Mutskov, S. Dimitrov, and J. J. Hayes.** 2001. Preferential interaction of the core histone tail domains with linker DNA. Proc. Natl. Acad. Sci. USA **98:**6599–6604.
4. **Badugu, R., M. M. Shareef, and R. Kellum.** 2003. Novel Drosophila heterochromatin protein 1 (HP1)/origin recognition complex-associated protein (HOAP) repeat motif in HP1/HOAP interactions and chromocenter associations. J. Biol. Chem. **278:**34491–34498.
5. **Bannister, A. J., P. Zegerman, J. F. Partridge, E. A. Miska, J. O. Thomas, R. C. Allshire, and T. Kouzarides.** 2001. Selective recognition of methylated lysine 9 on histone H3 by the HP1 chromo domain. Nature **410:**120–124.
6. **Becker, P. B., and C. Wu.** 1992. Cell-free system for assembly of transcriptionally repressed chromatin from *Drosophila* embryos. Mol. Cell. Biol. **12:**2241–2249.
7. **Bonaldi, T., A. Imhof, and J. T. Regula.** 2004. A combination of different mass spectroscopic techniques for the analysis of dynamic changes of histone modifications. Proteomics **4:**1382–1396.
8. **Brasher, S. V., B. O. Smith, R. H. Fogh, D. Nietlispach, A. Thiru, P. R. Nielsen, R. W. Broadhurst, L. J. Ball, N. V. Murzina, and E. D. Laue.** 2000. The structure of mouse HP1 suggests a unique mode of single peptide recognition by the shadow chromo domain dimer. EMBO J. **19:**1587–1597.
9. **Carruthers, L. M., C. Tse, K. P. Walker III, and J. C. Hansen.** 1999. Assembly of defined nucleosomal and chromatin arrays from pure components. Methods Enzymol. **304:**19–35.
10. **Cheutin, T., A. J. McNairn, T. Jenuwein, D. M. Gilbert, P. B. Singh, and T. Misteli.** 2003. Maintenance of stable heterochromatin domains by dynamic HP1 binding. Science **299:**721–725.
11. **Collins, N., R. A. Poot, I. Kukimoto, C. Garcia-Jimenez, G. Dellaire, and P. D. Varga-Weisz.** 2002. An ACF1-ISWI chromatin-remodeling complex is required for DNA replication through heterochromatin. Nat. Genet. **32:**627–632.

11a. **Croston, G. E., L. M. Lira, and J. T. Kadonaga.** 1991. A general method for purification of H1 histones that are active for repression of basal RNA polymerase II transcription. Protein Expr. Purif. **2:**162–169.

12. **Daujat, S., U. Zeissler, T. Waldmann, N. Happel, and R. Schneider.** 2005. HP1 binds specifically to Lys26-methylated histone H1.4, whereas simultaneous Ser27 phosphorylation blocks HP1 binding. J. Biol. Chem. **280:**38090–38095.
13. **Dillon, N., and R. Festenstein.** 2002. Unravelling heterochromatin: competition between positive and negative factors regulates accessibility. Trends Genet. **18:**252–258.
14. **Doerks, T., R. Copley, and P. Bork.** 2001. DDT—a novel domain in different transcription and chromosome remodeling factors. Trends Biochem. Sci. **26:**145–146.
15. **Eberharter, A., S. Ferrari, G. Langst, T. Straub, A. Imhof, P. Varga-Weisz, M. Wilm, and P. B. Becker.** 2001. Acf1, the largest subunit of CHRAC, regulates ISWI-induced nucleosome remodelling. EMBO J. **20:**3781–3788.
16. **Eberharter, A., I. Vetter, R. Ferreira, and P. B. Becker.** 2004. ACF1 improves the effectiveness of nucleosome mobilization by ISWI through PHD-histone contacts. EMBO J. **23:**4029–4039.
17. **Ebert, A., G. Schotta, S. Lein, S. Kubicek, V. Krauss, T. Jenuwein, and G. Reuter.** 2004. Su(var) genes regulate the balance between euchromatin and heterochromatin in Drosophila. Genes Dev. **18:**2973–2983.
18. **Ekwall, K., J. P. Javerzat, A. Lorentz, H. Schmidt, G. Cranston, and R. Allshire.** 1995. The chromodomain protein Swi6: a key component at fission yeast centromeres. Science **269:**1429–1431.
19. **Elgin, S. C., and S. I. Grewal.** 2003. Heterochromatin: silence is golden. Curr. Biol. **13:**R895–R898.
20. **Eskeland, R., B. Czermin, J. Boeke, T. Bonaldi, J. T. Regula, and A. Imhof.** 2004. The N-terminus of Drosophila SU(VAR)3-9 mediates dimerization and regulates its methyltransferase activity. Biochemistry **43:**3740–3749.
21. **Fan, J. Y., D. Rangasamy, K. Luger, and D. J. Tremethick.** 2004. H2A.Z alters the nucleosome surface to promote HP1alpha-mediated chromatin fiber folding. Mol. Cell **16:**655–661.
22. **Fanti, L., G. Giovinazzo, M. Berloco, and S. Pimpinelli.** 1998. The heterochromatin protein 1 prevents telomere fusions in Drosophila. Mol. Cell **2:**527–538.
23. **Festenstein, R., S. N. Pagakis, K. Hiragami, D. Lyon, A. Verreault, B. Sekkali, and D. Kioussis.** 2003. Modulation of heterochromatin protein 1 dynamics in primary mammalian cells. Science **299:**719–721.
24. **Fyodorov, D. V., M. D. Blower, G. H. Karpen, and J. T. Kadonaga.** 2004. Acf1 confers unique activities to ACF/CHRAC and promotes the formation rather than disruption of chromatin in vivo. Genes Dev. **18:**170–183.
25. **Fyodorov, D. V., and J. T. Kadonaga.** 2002. Binding of Acf1 to DNA involves a WAC motif and is important for ACF-mediated chromatin assembly. Mol. Cell. Biol. **22:**6344–6353.
26. **Gaudin, V., M. Libault, S. Pouteau, T. Juul, G. Zhao, D. Lefebvre, and O. Grandjean.** 2001. Mutations in *LIKE HETEROCHROMATIN PROTEIN 1* affect flowering time and plant architecture in *Arabidopsis*. Development **128:**4847–4858.
27. **Greil, F., I. van der Kraan, J. Delrow, J. F. Smothers, E. de Wit, H. J. Bussemaker, R. van Driel, S. Henikoff, and B. van Steensel.** 2003. Distinct HP1 and Su(var)3-9 complexes bind to sets of developmentally coexpressed genes depending on chromosomal location. Genes Dev. **17:**2825–2838.
28. **Greiner, D., T. Bonaldi, R. Eskeland, E. Roemer, and A. Imhof.** 2005. Identification of a specific inhibitor of the histone methyltransferase SU(VAR)3-9. Nat. Chem. Biol. **1:**143–145.
29. **Grewal, S. I., and J. C. Rice.** 2004. Regulation of heterochromatin by histone methylation and small RNAs. Curr. Opin. Cell Biol. **16:**230–238.
30. **Hall, I. M., G. D. Shankaranarayana, K. Noma, N. Ayoub, A. Cohen, and S. I. Grewal.** 2002. Establishment and maintenance of a heterochromatin domain. Science **297:**2232–2237.
31. **Hartlepp, K. F., C. Fernandez-Tornero, A. Eberharter, T. Grune, C. W. Muller, and P. B. Becker.** 2005. The histone fold subunits of *Drosophila* CHRAC facilitate nucleosome sliding through dynamic DNA interactions. Mol. Cell. Biol. **25:**9886–9896.
32. **Henikoff, S.** 2000. Heterochromatin function in complex genomes. Biochim. Biophys. Acta **1470:**O1–O8.
33. **Hong, L., G. P. Schroth, H. R. Matthews, P. Yau, and E. M. Bradbury.** 1993. Studies of the DNA binding properties of histone H4 amino terminus. Thermal denaturation studies reveal that acetylation markedly reduces the binding constant of the H4 "tail" to DNA. J. Biol. Chem. **268:**305–314.
34. **Jacobs, S. A., and S. Khorasanizadeh.** 2002. Structure of HP1 chromodomain bound to a lysine 9-methylated histone H3 tail. Science **295:**2080–2083.
35. **Jacobs, S. A., S. D. Taverna, Y. Zhang, S. D. Briggs, J. Li, J. C. Eissenberg, C. D. Allis, and S. Khorasanizadeh.** 2001. Specificity of the HP1 chromo domain for the methylated N-terminus of histone H3. EMBO J. **20:**5232–5241.
36. **James, T. C., J. C. Eissenberg, C. Craig, V. Dietrich, A. Hobson, and S. C. Elgin.** 1989. Distribution patterns of HP1, a heterochromatin-associated nonhistone chromosomal protein of Drosophila. Eur. J. Cell Biol. **50:**170–180.

37. **Jenuwein, T., and C. D. Allis.** 2001. Translating the histone code. Science **293:**1074–1080.
38. **Kellum, R.** 2003. HP1 complexes and heterochromatin assembly. Curr. Top. Microbiol. Immunol. **274:**53–77.
39. **Klar, A. J., and M. J. Bonaduce.** 1991. swi6, a gene required for mating-type switching, prohibits meiotic recombination in the mat2-mat3 "cold spot" of fission yeast. Genetics **129:**1033–1042.
40. **Lachner, M., D. O'Carroll, S. Rea, K. Mechtler, and T. Jenuwein.** 2001. Methylation of histone H3 lysine 9 creates a binding site for HP1 proteins. Nature **410:**116–120.
41. **Lechner, M. S., D. C. Schultz, D. Negorev, G. G. Maul, and F. J. Rauscher III.** 2005. The mammalian heterochromatin protein 1 binds diverse nuclear proteins through a common motif that targets the chromoshadow domain. Biochem. Biophys. Res. Commun. **331:**929–937.
42. **Li, Y., J. R. Danzer, P. Alvarez, A. S. Belmont, and L. L. Wallrath.** 2003. Effects of tethering HP1 to euchromatic regions of the Drosophila genome. Development **130:**1817–1824.
43. **Lorentz, A., K. Ostermann, O. Fleck, and H. Schmidt.** 1994. Switching gene swi6, involved in repression of silent mating-type loci in fission yeast, encodes a homologue of chromatin-associated proteins from Drosophila and mammals. Gene **143:**139–143.
44. **Luger, K., T. J. Rechsteiner, and T. J. Richmond.** 1999. Preparation of nucleosome core particle from recombinant histones. Methods Enzymol. **304:**3–19.
45. **Maison, C., D. Bailly, A. H. Peters, J. P. Quivy, D. Roche, A. Taddei, M. Lachner, T. Jenuwein, and G. Almouzni.** 2002. Higher-order structure in pericentric heterochromatin involves a distinct pattern of histone modification and an RNA component. Nat. Genet. **30:**329–334.
46. **Meehan, R. R., C. F. Kao, and S. Pennings.** 2003. HP1 binding to native chromatin in vitro is determined by the hinge region and not by the chromodomain. EMBO J. **22:**3164–3174.
47. **Minc, E., Y. Allory, H. J. Worman, J. C. Courvalin, and B. Buendia.** 1999. Localization and phosphorylation of HP1 proteins during the cell cycle in mammalian cells. Chromosoma **108:**220–234.
48. **Minc, E., J.-C. Courvalin, and B. Buendia.** 2000. HP1γ associates with euchromatin and heterochromatin in mammalian nuclei and chromosomes. Cytogenet. Cell Genet. **90:**279–284.
49. **Muchardt, C., M. Guilleme, J. S. Seeler, D. Trouche, A. Dejean, and M. Yaniv.** 2002. Coordinated methyl and RNA binding is required for heterochromatin localization of mammalian HP1alpha. EMBO Rep. **3:**975–981.
50. **Murzina, N., A. Verreault, E. Laue, and B. Stillman.** 1999. Heterochromatin dynamics in mouse cells: interaction between chromatin assembly factor 1 and HP1 proteins. Mol. Cell **4:**529–540.
51. **Nielsen, A. L., M. Oulad-Abdelghani, J. A. Ortiz, E. Remboutsika, P. Chambon, and R. Losson.** 2001. Heterochromatin formation in mammalian cells: interaction between histones and HP1 proteins. Mol. Cell **7:**729–739.
52. **Nielsen, P. R., D. Nietlispach, H. R. Mott, J. Callaghan, A. Bannister, T. Kouzarides, A. G. Murzin, N. V. Murzina, and E. D. Laue.** 2002. Structure of the HP1 chromodomain bound to histone H3 methylated at lysine 9. Nature **416:**103–107.
53. **Platero, J. S., T. Hartnett, and J. C. Eissenberg.** 1995. Functional analysis of the chromo domain of HP1. EMBO J. **14:**3977–3986.
54. **Powers, J. A., and J. C. Eissenberg.** 1993. Overlapping domains of the heterochromatin-associated protein HP1 mediate nuclear localization and heterochromatin binding. J. Cell Biol. **120:**291–299.
55. **Reuter, G., and P. Spierer.** 1992. Position effect variegation and chromatin proteins. Bioessays **14:**605–612.
56. **Richards, E. J., and S. C. Elgin.** 2002. Epigenetic codes for heterochromatin formation and silencing: rounding up the usual suspects. Cell **108:**489–500.
57. **Sandaltzopoulos, R., T. Blank, and P. B. Becker.** 1994. Transcriptional repression by nucleosomes but not H1 in reconstituted preblastoderm Drosophila chromatin. EMBO J. **13:**373–379.
58. **Saunders, W. S., C. Chue, M. Goebl, C. Craig, R. F. Clark, J. A. Powers, J. C. Eissenberg, S. C. Elgin, N. F. Rothfield, and W. C. Earnshaw.** 1993. Molecular cloning of a human homologue of Drosophila heterochromatin protein HP1 using anti-centromere autoantibodies with anti-chromo specificity. J. Cell Sci. **104** (Pt. 2)**:**573–582.
59. **Schotta, G., A. Ebert, R. Dorn, and G. Reuter.** 2003. Position-effect variegation and the genetic dissection of chromatin regulation in Drosophila. Semin. Cell Dev. Biol. **14:**67–75.
60. **Schotta, G., A. Ebert, V. Krauss, A. Fischer, J. Hoffmann, S. Rea, T. Jenuwein, R. Dorn, and G. Reuter.** 2002. Central role of Drosophila SU(VAR)3-9 in histone H3-K9 methylation and heterochromatic gene silencing. EMBO J. **21:**1121–1131.
61. **Schotta, G., A. Ebert, and G. Reuter.** 2003. SU(VAR)3-9 is a conserved key function in heterochromatic gene silencing. Genetica **117:**149–158.
62. **Singh, P. B., J. R. Miller, J. Pearce, R. Kothary, R. D. Burton, R. Paro, T. C. James, and S. J. Gaunt.** 1991. A sequence motif found in a Drosophila heterochromatin protein is conserved in animals and plants. Nucleic Acids Res. **19:**789–794.
63. **Smothers, J. F., and S. Henikoff.** 2001. The hinge and chromo shadow domain impart distinct targeting of HP1-like proteins. Mol. Cell. Biol. **21:** 2555–2569.
64. **Smothers, J. F., and S. Henikoff.** 2000. The HP1 chromo shadow domain binds a consensus peptide pentamer. Curr. Biol. **10:**27–30.
65. **Stewart, M. D., J. Li, and J. Wong.** 2005. Relationship between histone H3 lysine 9 methylation, transcription repression, and heterochromatin protein 1 recruitment. Mol. Cell. Biol. **25:**2525–2538.
66. **Taipale, M., S. Rea, K. Richter, A. Vilar, P. Lichter, A. Imhof, and A. Akhtar.** 2005. hMOF histone acetyltransferase is required for histone H4 lysine 16 acetylation in mammalian cells. Mol. Cell. Biol. **25:**6798–6810.
67. **Thiru, A., D. Nietlispach, H. R. Mott, M. Okuwaki, D. Lyon, P. R. Nielsen, M. Hirshberg, A. Verreault, N. V. Murzina, and E. D. Laue.** 2004. Structural basis of HP1/PXVXL motif peptide interactions and HP1 localisation to heterochromatin. EMBO J. **23:**489–499.
68. **Tschiersch, B., A. Hofmann, V. Krauss, R. Dorn, G. Korge, and G. Reuter.** 1994. The protein encoded by the Drosophila position-effect variegation suppressor gene Su(var)3-9 combines domains of antagonistic regulators of homeotic gene complexes. EMBO J. **13:**3822–3831.
69. **Tse, C., and J. C. Hansen.** 1997. Hybrid trypsinized nucleosomal arrays: identification of multiple functional roles of the H2A/H2B and H3/H4 N-termini in chromatin fiber compaction. Biochemistry **36:**11381–11388.
70. **Wade, P. A., P. L. Jones, D. Vermaak, and A. P. Wolffe.** 1999. Purification of a histone deacetylase complex from Xenopus laevis: preparation of substrates and assay procedures. Methods Enzymol. **304:**715–725.
71. **Wang, Y., W. Fischle, W. Cheung, S. Jacobs, S. Khorasanizadeh, and C. D. Allis.** 2004. Beyond the double helix: writing and reading the histone code. Novartis Found. Symp. **259:**3–17, 17–21, 163–169.
72. **Yamamoto, K., and M. Sonoda.** 2003. Self-interaction of heterochromatin protein 1 is required for direct binding to histone methyltransferase, SUV39H1. Biochem. Biophys. Res. Commun. **301:**287–292.
73. **Zhao, T., and J. C. Eissenberg.** 1999. Phosphorylation of heterochromatin protein 1 by casein kinase II is required for efficient heterochromatin binding in Drosophila. J. Biol. Chem. **274:**15095–15100.
74. **Zhao, T., T. Heyduk, C. D. Allis, and J. C. Eissenberg.** 2000. Heterochromatin protein 1 binds to nucleosomes and DNA in vitro. J. Biol. Chem. **275:**28332–28338.

nature chemical biology

Identification of a specific inhibitor of the histone methyltransferase SU(VAR)3-9

Dorothea Greiner[1], Tiziana Bonaldi[1], Ragnhild Eskeland[1], Ernst Roemer[2,3] & Axel Imhof[1]

Histone methylation plays a key role in establishing and maintaining stable gene expression patterns during cellular differentiation and embryonic development. Here, we report the characterization of the fungal metabolite chaetocin as the first inhibitor of a lysine-specific histone methyltransferase. Chaetocin is specific for the methyltransferase SU(VAR)3-9 both *in vitro* and *in vivo* and may therefore be used to study heterochromatin-mediated gene repression.

During the life of every multicellular organism, totipotent cells have to acquire specific functions and maintain their differentiated state. The differentiated state of a cell is determined by its specific pattern of gene expression, which in turn is established and maintained through the differential packaging of DNA into chromatin. The basic unit of chromatin is the nucleosome, a nucleoprotein particle that consists of 147 base pairs of DNA that are wrapped around a proteinaceous core of the four core histones H2A, H2B, H3 and H4 (ref. 1). It is widely accepted that the post-translational modifications of the histone N-terminal tails, as well as modifications within the globular domain, regulate the level of chromatin condensation and are therefore important in regulating gene expression[2]. Inhibitors of histone acetyltransferases can affect the heritable changes in gene expression of specific genes and are used as drugs for cancer therapy[3]. In addition to histone acetylation, histone methylation has also been shown to be important in establishing stable gene-expression patterns. Some of the known histone methyltransferases (HMTs) are misregulated in tumors[4], and methyltransferase-induced heterochromatin formation could be involved in neurodegenerative diseases[5].

To find small molecules that affect HMT function, we screened a small library of compounds for their ability to inhibit the activity of recombinant *Drosophila melanogaster* SU(VAR)3-9 protein. SU(VAR)3-9 is a key player in establishing condensed heterochromatin by specifically methylating Lys9 of histone H3 (ref. 6) and is conserved in most higher eukaryotes. The screening was done by pooling eight individual compounds and testing the pooled mixtures in a standard radioactive filter-binding assay (**Supplementary Methods** online). Every pool that reduced HMT activity by more than 60% was considered inhibitory, and the individual compounds were retested for activity (**Fig. 1a**). Of the 2,976 compounds screened, 22 reduced HMT activity by more than 80% under standard conditions. To verify the activity, and to exclude a possible peptide-specific effect, we further tested the most active inhibitors using intact recombinant H3 molecules as substrates (**Fig. 1b**). One of the strongest inhibitors was the fungal mycotoxin chaetocin (**Fig. 1c**, **1**), which was initially isolated from the fermentation broth of *Chaetomium minutum*[7] and belongs to the class of 3-6 epidithio-diketopiperazines (ETPs). It has a half-maximal inhibitory

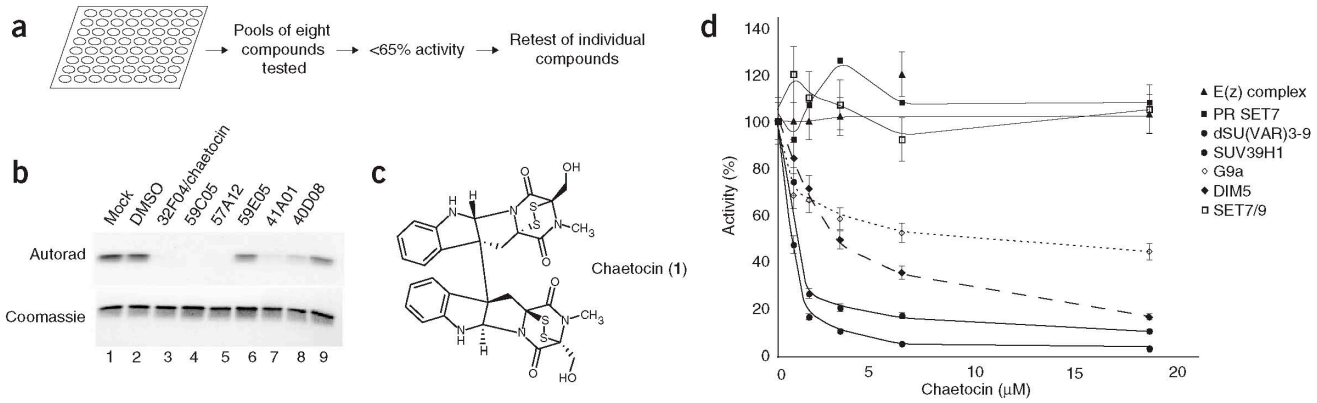

Figure 1 *In vitro* inhibition of dSU(VAR)3-9. (**a**) Schematic outline of the inhibitor screen. (**b**) SDS-PAGE analysis of *in vitro* methylated H3 in the presence or absence of 10 μg of inhibitor. (**c**) Structure of chaetocin. The chaetocin used in all reactions was >95% pure (**Supplementary Fig. 2** online). (**d**) Inhibition curves for various recombinant HMTs. Methyltransferase assays were performed as described previously[13]. Reactions were done in duplicate and error bars reflect the standard deviation from at least two different experiments.

[1]Adolf Butenandt Institute, Department of Molecular Biology, Histone Modifications Group, Ludwig-Maximillians University of Munich, Schillerstr. 44, 80336 Munich, Germany. [2]Leibniz-Institut für Naturstoff-Forschung und Infektionsbiologie–Hans-Knöll-Institut für Naturstoff-Forschung, Abteilung Molekulare Naturstoff-Forschung, Beutenbergstrasse 11a, 07745 Jena, Germany. [3]Present address: Institut für Pflanzenbiochemie, Universität Halle, Weinberg 3, Halle (Saale) 06120, Germany. Correspondence should be addressed to A.I. (imhof@lmu.de).

Published online 17 July 2005; doi:10.1038/nchembio721

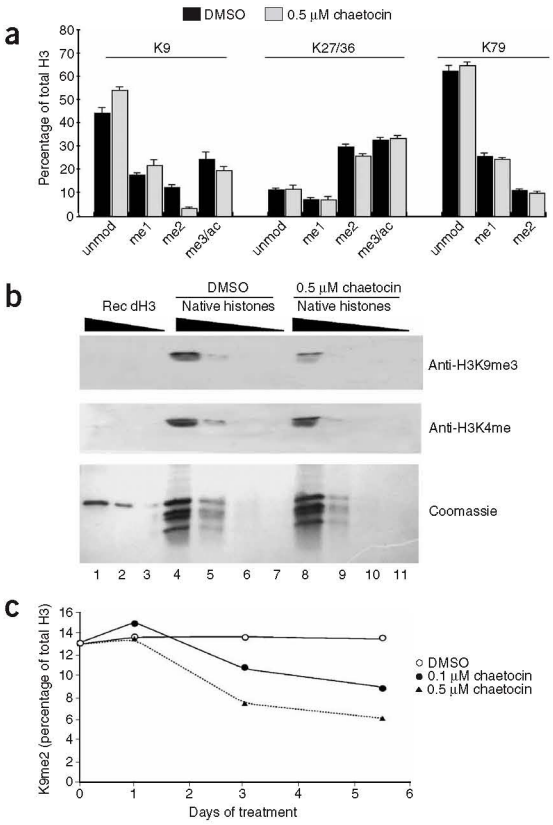

Figure 2 *In vivo* inhibition of SU(VAR)3-9. (**a**) SL-2 cells were grown in the absence (dark bars) or presence (light bars) of chaetocin. Methylation levels were measured by quantitative MALDI-TOF MS as described previously[11,14]. Shown are the relative values for the differentially modified peptides as a fraction of the total H3 (=100%). (**b**) To study Lys4 dimethylation and Lys9 trimethylation, increasing amounts of recombinant histones (lanes 1–3) or histones isolated from SL-2 cells treated (lanes 8–11) or not treated (lanes 4–7) with chaetocin were loaded on an 18% SDS PAA gel and analyzed by western blotting with specific antibodies against H3K9me3 and H3 dimethylated at Lys4 (H3K4me2). (**c**) Effect of chaetocin on H3 Lys9 methylation as a function of time. H3 Lys9 methylation levels of histones extracted from nuclei of SL-2 cells at 1, 3 and 5 d after induction were measured by quantitative MALDI-TOF MS. Shown are the relative values for H3K9me2 peptide from histones that were untreated (open circles) and treated with 0.1μM chaetocin (filled circles) or 0.5 μM chaetocin (filled triangles).

concentration (IC_{50}) for SU(VAR)3-9 of 0.6 μM and acts as a competitive inhibitor for *S*-adenosylmethionine (SAM, **Supplementary Fig. 1** online). As SU(VAR)3-9 has a cluster of cysteine residues in its active site[6], and as we have observed a drop in activity with thiol-reactive substances such as DTT at high doses (>10 mM), we wondered whether the disulfide bond of chaetocin is important for its inhibitory activity. To examine this, we performed the inhibition assays in the presence of increasing amounts of DTT to reduce the disulfide bonds within chaetocin but did not see a substantial decrease in inhibition by SU(VAR)3-9 (**Supplementary Fig. 1**).

To test the enzyme specificity of chaetocin, we also tested other known HMT enzymes that contain a SU(VAR)3-9, enhancer-of-zeste, trithorax-homology (SET) domain for their sensitivity to chaetocin (**Fig. 1d**). We found that although chaetocin inhibited the human ortholog of dSU(VAR)3-9 with a similar IC_{50} value (0.8 μM), it inhibited other known Lys9-specific HMTs such as mouse G9a and *Neurospora crassa* DIM5 with a higher IC_{50} value (2.5 and 3 μM, respectively). We also tested the recombinant *Drosophila* E(z)-complex (expressed and purified in a baculoviral expression system), which preferentially methylates H3 at Lys27, the bacterially expressed H4 Lys20–specific HMT PRSET7 and the Lys4-specific lysine methyltransferase SET7/9. In all three cases we found IC_{50} values that were much higher than for the other enzymes (>90 μM for the dE(Z) complex and >180 μM for PRSET7 and SET7/9). This suggests that chaetocin is an inhibitor of enzymes belonging to the class of the SUV39 family with the strongest inhibitory potential for SU(VAR)3-9 and is a weaker inhibitor of more distantly related enzymes of this family, such as G9a or DIM5 (ref. 8), with a higher IC_{50} value. HMTs that do not belong to the SU(VAR)3-9 class of enzymes, such as E(z), PRSET7 or SET7/9, are not inhibited, despite having a recognizable SET domain. Taking this together with the finding that chaetocin acts as a competitive inhibitor for SAM, we suggest that the SAM-binding cleft of E(z) and PRSET7 is too divergent from the SU(VAR)3-9 class of enzymes to be bound by chaetocin.

To study the effectiveness of chaetocin at inhibiting SU(VAR)3-9 *in vivo*, we cultivated SL-2 *Drosophila* tissue culture cells in the presence or absence of the inhibitor. The chaetocin used was >95% pure and stable during the course of the experiment (**Supplementary Fig. 2** online). Like other ETPs, chaetocin has a toxic effect on cells grown in culture[9]. When cultivating SL-2 cells, we observed that the toxicity is highly dependent on the initial cell density when chaetocin is added to the culture. Cells seeded at low density ($<5 \times 10^5$ cells per ml) are very sensitive to chaetocin treatment, whereas cells seeded at higher density ($>2 \times 10^6$ cells per ml) can be treated with up to 0.5 μM chaetocin, which causes only a growth retardation of 24–48 h (**Supplementary Fig. 3** online). The toxicity of other known ETPs, such as gliotoxin, has been attributed to their ability to form mixed thiols with various cellular proteins[9]. From these results, and based on the observation that a fly strain deficient for SU(VAR)3-9 is viable[10], we suggest that the toxic effects are not caused by the inhibition of SU(VAR)3-9, as the disulfide bonds are not required for HMT inhibition. Therefore, we seeded cells at a density of 2.5×10^6 cells per ml, treated the culture with different concentrations of the inhibitor (0.1 μM and 0.5 μM) for several days and took aliquots after 1, 3 and 5 d of culture to study the level of histone modification. Histone modification patterns were analyzed by MS, as previously shown[11]. Consistent with the inhibition of SU(VAR)3-9 *in vitro*, the number of H3 molecules dimethylated at Lys9 (H3K9me2) was markedly reduced when cells were grown in medium containing 0.5 μM chaetocin (**Fig. 2a**) after 5 d. Histones isolated from cells treated with 0.1 μM and for a shorter time also showed a drop in Lys9 methylation, but not as strongly as with the higher concentration (**Fig. 2b**). Because of the similar mass shift of a trimethyl and an acetyl group, the quantification of the H3 isoform trimethylated at Lys9 (H3K9me3) is obscured by the acetylated form. Therefore, we used an antibody that is specific for trimethylated Lys9 (ref. 12) to selectively investigate the effect of chaetocin on Lys9 trimethylation (**Fig. 2c**). Using this antibody, we also observed a substantial drop in Lys9 trimethylation in the chaetocin-treated cells. These findings are consistent with observations in flies that lack a functional dSU(VAR)3-9 enzyme. The histones isolated from these flies show a marked loss of di- and trimethylation at Lys9 but not of any other lysine[10]. Accordingly, chaetocin does not influence the degree of methylation of other lysines such as Lys27, Lys36, Lys79 or Lys4 when analyzed by MS or western blotting (**Fig. 2**).

As chaetocin also inhibits G9a *in vitro*, we cannot exclude the possibility that the reduction of H3K9me2 is due to the inhibition of the *Drosophila* ortholog of mammalian G9a. However, we consider this to be unlikely because of the similar reduction of H3K9me2 in flies deficient in dSU(VAR)3-9. The specificity of chaetocin for HMTs that target Lys9 within the H3 tail not only will allow a detailed analysis of methyltransferase-mediated gene repression but also provides an excellent tool to mechanistically dissect the processes that lead to the formation of mono-, di- and trimethylated H3 by dSU(VAR)3-9. Despite showing toxic effects in a tissue-culture system, the analysis of derivatives of chaetocin that lack the disulfide bond and therefore have lower toxicity should allow the use of these molecules for various therapeutic or experimental applications.

Accession codes. BIND identifiers (http://bind.ca/): 300892–300895.

Note: Supplementary information is available on the Nature Chemical Biology website.

ACKNOWLEDGMENTS

Work in A.I.'s laboratory is funded by grants from the Deutsche Forschungsgemeinschaft (IM23/4-1). D.G. is supported by a predoctoral grant from the University of Munich (FöFoLe #12). T.B. is funded by a long-term postdoctoral fellowship from the European Molecular Biology Organisation (ALTF 642-2003). We thank T. Jenuwein, E. Selker, Y. Shinkai, Y. Cho and P. Singh for valuable reagents, B. Czermin and L. Israel for help with the protein expression and MS analysis, and J. Sutcliffe for critical reading of the manuscript.

COMPETING INTERESTS STATEMENT

The authors declare that they have no competing financial interests.

Received 10 March; accepted 22 June 2005
Published online at http://www.nature.com/naturechemicalbiology/

1. Wolffe, A.P. *Chromatin Structure and Function* (Academic Press, San Diego, USA, 1998).
2. Jenuwein, T. & Allis, C.D. *Science* **293**, 1074–1080 (2001).
3. Mei, S., Ho, A.D. & Mahlknecht, U. *Int. J. Oncol.* **25**, 1509–1519 (2004).
4. Hake, S.B., Xiao, A. & Allis, C.D. *Br. J. Cancer* **90**, 761–769 (2004).
5. Saveliev, A., Everett, C., Sharpe, T., Webster, Z. & Festenstein, R. *Nature* **422**, 909–913 (2003).
6. Rea, S. *et al. Nature* **406**, 593–599 (2000).
7. Hauser, D., Weber, H.P. & Sigg, H.P. *Helv. Chim. Acta* **53**, 1061–1073 (1970).
8. Baumbusch, L.O. *et al. Nucleic Acids Res.* **29**, 4319–4333 (2001).
9. Gardiner, D.M., Waring, P. & Howlett, B.J. *Microbiology* **151**, 1021–1032 (2005).
10. Schotta, G. *et al. EMBO J.* **21**, 1121–1131 (2002).
11. Bonaldi, T., Imhof, A. & Regula, J.T. *Proteomics* **4**, 1382–1396 (2004).
12. Tamaru, H. *et al. Nat. Genet.* **34**, 75–79 (2003).
13. Eskeland, R. *et al. Biochemistry* **43**, 3740–3749 (2004).
14. Fraga, M.F. *et al. Nat. Genet.* **37**, 391–400 (2005).

Published online 8 September 2006 *Nucleic Acids Research, 2006, Vol. 34, No. 16* ***4609–4621***
doi:10.1093/nar/gkl640

The *Drosophila G9a* gene encodes a multi-catalytic histone methyltransferase required for normal development

Marianne Stabell, Ragnhild Eskeland[1], Mona Bjørkmo, Jan Larsson[2], Reidunn B. Aalen, Axel Imhof[1] and Andrew Lambertsson*

Department of Molecular Biosciences, University of Oslo, PO Box 1041, Blindern, NO-0316 Oslo, Norway, [1]Adolf-Butenandt Institute, Department of Molecular Biology, Histone Modifications Group and Protein Analysis Unit, Ludwig-Maximillians University of Munich, Schillerstrasse 44, DE-80336 Munich, Germany and [2]UCMP, Umeå University, SE-901 87 Umeå, Sweden

Received June 6, 2006; Revised July 24, 2006; Accepted August 17, 2006

ABSTRACT

Mammalian G9a is a histone H3 Lys-9 (H3–K9) methyltransferase localized in euchromatin and acts as a co-regulator for specific transcription factors. G9a is required for proper development in mammals as *g9a*$^{-}$/*g9a*$^{-}$ mice show growth retardation and early lethality. Here we describe the cloning, the biochemical and genetical analyses of the *Drosophila* homolog dG9a. We show that dG9a shares the structural organization of mammalian G9a, and that it is a multi-catalytic histone methyltransferase with specificity not only for lysines 9 and 27 on H3 but also for H4. Surprisingly, it is not the H4–K20 residue that is the target for this methylation. Spatiotemporal expression analyses reveal that dG9a is abundantly expressed in the gonads of both sexes, with no detectable expression in gonadectomized adults. In addition we find a low but clearly observable level of dG9a transcript in developing embryos, larvae and pupae. Genetic and RNAi experiments reveal that dG9a is involved in ecdysone regulatory pathways.

INTRODUCTION

Modifications of histones are an important mark for transcriptional regulation during embryonic development. The protruding tales of the histones are modified by acetylation, phosphorylation, ubiquitination and arginine and lysine methylation, and the combinations are hypothesized to form a histone code (1,2). The best-characterized substrates for lysine methylation in eukaryotic cells are histone proteins, although methylation of several non-histone proteins, such as the tumor suppressor p53, has been reported as well (3).

Histone H3 has been shown to be methylated on lysine residues K4, K9, K27, K36 and K79 whereas in histone H4, K20 is methylated (4,5). Each of these lysine side chains can be mono-, di- or tri-methylated by histone lysine methyltransferases (HKMTases), which, except for Dot1 (6), carry a catalytic SET [Su(var), Enhancer of Zeste, Trithorax] domain (7). The SET domain is a conserved ~130 amino acid sequence, which is flanked by the less conserved pre-SET and post-SET regions at the amino and C-termini, respectively. The specificity of a HKMTase, as well as the number of methyl residues that attaches to a lysine residue, depends on the structure of the HKMTase or the presence of additional co-factor proteins (8). On the other hand Ezh2 requires the presence of the co-factors suppressor of zeste-12 (SUZ12) and embryonic ectoderm development (Eed) for tri-methylation of H3–K27 (9). The HKMTase ERG-associated protein (ESET) di-methylates H3–K9, but is converted into a tri-methylating enzyme by its association with a mouse-activating transcription-factor-associated modulator (mAM) (10). The methylated histones recruit proteins that carry CHROMO, TUDOR or WD40 domains and are capable of specific interactions with differently methylated lysine residues reviewed in Ref. (11). This recruitment step is likely to define a unique functional readout for individual lysine methylations. Thus, tri-methylation of lysine 9 in histone H3 by Suv39H1 and Suv39H2 creates a binding site for the chromodomain-containing heterochromatic protein HP1 which is thought to induce heterochromatin formation (12). Di-methylation of H3–K9 by G9a is associated with the silencing of euchromatic genes (13).

Mammalian G9a mono- and di-methylates H3–K9 at euchromatic loci (14,15), and has recently also been found at heterochromatic loci (16). In g9a^{-}/g9a^{-} mice H3–K9

*To whom correspondence should be addressed. Tel: +47 22 85 48 94; Fax: +47 22 85 47 26; Email: g.a.lambertsson@imbv.uio.no
Present address:
Mona Bjørkmo, The Biotechnology Centre of Oslo, University of Oslo, NO-0317 Oslo, Norway

methylation is drastically reduced resulting in severe growth retardation and early lethality (17). The loss of G9a primarily affects the methylation of H3–K9 in euchromatic regions (14). G9a is the major euchromatic histone H3–K9 methyltransferase in higher eukaryotes but in *Drosophila* the euchromatic H3–K9 HKMTase has not been characterized. Although the H3–K9 methylation is strongly reduced in *Su(var)3–9* null mutants, a small amount of H3 molecules remain methylated at K9 suggesting the existence of other K9 specific HKMTases in *Drosophila* (18).

There are several reports demonstrating the silencing effects from H3–K9 methylation, including the inactive X chromosome of female mice and humans (19), and developmentally regulated genes (20).

In a search for SET domain containing genes in *Drosophila* that might code a K9 specific HKMTase, we performed a bioinformatics search of the *Drosophila melanogaster* genome and found the gene *CG2995* which share significant homology to mammalian *G9a*. In this paper we describe the cloning, and the biochemical and genetical analyses of *CG2995*. We show that it encodes a histone methyltransferase specific for H3–K9, K27 and H4, and that it shares the structural organization of mammalian G9a. Therefore, we suggest that CG2995 is renamed *dG9a*. It adds up to three methyl groups to unmethylated H3 and H4. Our results indicate a role for *dG9a* in germ cell formation. Using RNAi we show that *dG9a* is critical for development, very likely by being involved in the ecdysone regulated gene expression.

MATERIALS AND METHODS

Fly handling and generation of transgenic flies

All genetic crosses were carried out at 25°C. Fly lines were obtained from the Bloomington *Drosophila* stock centre.

Generation of double stranded (ds) RNA was performed by using the pHIBS and pUds-GFP vectors as described in Ref. (21). A 756 bp fragment of *dG9a* cDNA was PCR amplified with the 2995UBamHI (5′-CAAGGATCCTGTCGCACTTCTCGTTCATC-3′) and 2995LKpnI (5′-TGCGGTACCTGCTGGATAATGCATTGTGTT-3′) primers.

Transgenic flies were generated by P-element mediated transformation, and nine independent lines on different chromosomes were established, including the 2995-18 line used in this study. The GAL4-UAS system (22) was used to express dG9a.IR construct, and *Act5C-GAL4* (BL 4414), *da-GAL4* (BL 5460), *P{GawB}c698a* (BL 3739), and *ap-GAL4* (BL 3041) were used as drivers. As control the 2995-18 line without driver was used.

The *ap-GAL4,UAS-dG9a.IR/EcR*^{M554fs} flies were generated by standard genetic procedures.

Bioinformatics tools

Database searches were performed using BLASTP, TBLASTN and PSI-BLAST (http://www.ncbi.nlm.nih.gov/BLAST/). Protein domains were identified using the programs RPS-BLAST (NCBI) and ProfileScan (http://hits.isb-sib.ch/cgi-bin/PFSCAN) searching the Pfam-A, Prosite profiles and Smart databases (NCBI). Nuclear localization signal was detected by using PredictNLS (http://cubic.bioc.columbia.edu/predictNLS/). Amino acid sequence alignments were created using ClustalX 1.8 (http://www-igbmc.u-strasbg.fr/BioInfo/ClustalX) with default parameters and manual adjustments from GeneDoc 2.6.001 (http://www.psc.edu/biomed/genedoc/).

Rapid amplification of cDNA ends (RACE) analyses

5′-RACE and 3′-RACE were performed using a Marathon™ cDNA Amplification Kit (Clontech) with 2 μg of total RNA isolated from adult female flies as template and Advantage® 2 Polymerace Mix in accordance with the manufacturer's recommendations. RACE PCR products were sequenced using a MegaBACE 1000 sequencer.

Sequences of primers used for RACE analyses are available on request. DNA and amino acid sequences derived from the cDNAs were compared and analyzed with the GenBank database.

RT–PCR

Testes and ovaries from adults were dissected in Ringer's solution (6.5 g NaCl, 0.14 g KCl, 0.2 g $NaHCO_3$, 0.12 g $CaCl_2$ and 0.01 g NaH_2PO_4 per liter). Total RNA was isolated from indicated tissues or stages by the use of TRIzol® reagent (Invitrogen), and 5 μg of total RNA were reverse transcribed with SuperScript III RNase H-free reverse transcriptase (RT) (Invitrogen). A random primer pd$(N)_6$ was used for first-strand synthesis. PCR was performed with 2995left (5′-GATGAACGAGAAGTGCGACA-3′, located in exon 5) and 2995right (5′-GATGAACGAGAAGTGCGACA-3′, located in exon 9) primers and with rp49 primers (23) as loading control for 35 cycles at an annealing temperature of 56°C.

Immunostainings and immunofluorescence

The anti-dG9a polyclonal antiserum was raised in rabbits (Eurogentec S.A) against a synthetic peptide containing dG9a residues 1623–1637. The antiserum was affinity purified.

Polytene chromosomes from the salivary glands of third instar larvae were prepared and stained essentially as described in Ref. (24).

Tissues were stained with anti-dG9a (1:25). As secondary antibodies, goat anti-rabbit IgG, conjugated with AlexaFluor 555 (MedProbe, diluted 1:200) were used. Materials were co-stained with DAPI for visualization of DNA. Preparations were analyzed by using a Zeiss Axiophot microscope equipped with a KAPPA DX20C charge-coupled device camera. Staining of larval tissues, ovaries and embryos were performed using standard techniques with anti-dG9a, as described above. Preparations were analyzed by using a ZeissAxioplan2 microscope equipped with a Zeiss AxioCam HRc camera, software: AxioVision3.1. Images were assembled, contrasted and merged electronically by using Photoshop 7.0 (Adobe Systems).

Whole-mount *in situ* hybridization

RNA *in situ* hybridization using digoxigenin-labeled antisense RNA probes was performed as described previously (25,26). A cDNA containing *dG9a* was linearized with

BamHI and used as template to make a 674 bp *dG9a* RNA probe.

Western analysis

Nuclear extract from 0–12 h dechorionated embryos (27) was separated on a SDS–PAGE (8%). Proteins were transferred onto PVDF membrane (Amersham) and probed with an anti-dG9a antibody (1:500) using standard procedures. Secondary antibodies conjugated to HRP (Amersham) were used according to the manufacturer's instructions. Detection of antibody signals was performed with chemiluminescence (Pierce).

Generation of baculovirus, viral transfection and dG9a purification

Amino acids 789–1637 of dG9a was PCR amplified with the primers 2995 SpeIFlag (5′-GACTACAAGGACGACGATG-ACAAGATTTGTCTATGTCAGAAGCCTTCC-3′, FLAG tag sequence underlined) and 2995 KpnI (5′-TGCGGTACCCTA-CGCGTGTCCAATTTTCT-3′) cloned into pFastBac(tm)1 (Invitrogen) as a SpeI/KpnI fragment. Site-directed mutagenesis of flag-dG9a (789–1637 amino acid) was performed using the QuickChange kit (Stratagene) with primers CG2995H1536KBstNIfwd (5′-ATGGAAATGTAACCAGG-TTTTTTAACAAGTC GTGTGAGCCGAATG-3′) and CG2995H1536KBstNIrew (5′-CATTCGG CTCACACGAC-TTGTTAAAAAACCTGGTTACATTTCCAT-3′).

FLAG tagged dG9a in pFastBac^{TM}1 was transformed into DH10Bac (Invitrogen) and bacemid purified according to protocol (Invitrogen). A monolayer of SF9 (*Spodoptera frugiperda*) (9×10^5) was transfected with 1 μg of bacemid using Cellfectin Reagent (Invitrogen) and cells were left for 7 days at 26°C. The supernatant was amplified 2–3 times and recombinant viruses were used for test expression. Cell extracts were checked, 48 h post-transfection, for fusion protein expression using anti-FLAG monoclonal antibody (Sigma). For routine protein expression 10 × 150 mm Petri dishes were infected and the cells kept at 26°C. The cells were harvested 48 h post-infection and washed once with 1× phosphate-buffered saline. For purification of FLAG-dG9A protein, infected cells (1.2×10^8) were resuspended in 4 ml of BC300 [25 mM HEPES (pH 7.6), 300 mM NaCl, 1 mM $MgCl_2$, 0.5 mM EGTA, 0.1 mM EDTA, 10% (v/v) glycerol, 1 mM DTT and protease inhibitors] containing 0.05% (v/v) NP40. The cells were sonicated on ice two times for 15 s at 50% amplitude using a Branson sonifier and centrifuged at 15 000 r.p.m. for 30 min and 100 μl 1:1 slurry of M2 anti-FLAG agarose beads (Sigma) was added to the supernatant followed by incubation for 2 h at 4°C. After washing three times with BC300 [containing 0.05% (v/v) NP40] for 10 min each, and once with BC100 [0.05% (v/v) NP40] the bound protein was eluted with 0.5 mg/ml FLAG peptide BC100 [0.05% (v/v) NP40] for 2 h. The purity of the protein was checked by SDS–PAGE. Eluates were stored at −80°C.

Histone purification and nucleosome assembly

Recombinant *Drosophila* histones were expressed and purified from *Escherichia coli* BL21(DE3)pLys, and reconstituted into octamers as described previously (28). Recombinant histone H3 carrying the mutations K9A, K27A or K9A/K27A were expressed from plasmids kindly provided by D. Reinberg, and histone H4 carrying a K20A mutation was expressed from a plasmid given by T. Jenuwein. Recombinant H4 N-terminal mutant proteins Δ5, Δ10, Δ15, Δ19 were expressed and purified as described previously (29). Native histones were purified from 0–12 h *Drosophila* embryos essentially as described in Ref. (30). Nucleosomes were reconstituted on circular pBS(KS) (Stratagene) by salt dialysis over night from 2 to 0.1 M NaCl (31).

Histone methyltransferase assay

Histone methyltransferase assays were performed as described in Ref. (32). In short, 100 ng of eluted dG9a was mixed with 1 or 2 μg of histone H3, H4, octamer or nucleosomes and S-adenosyl-[methyl-^{3}H]-l-methionine (25 μCi/ml) (Amersham) in a buffer containing 12.5 mM Tris–HCl, pH 8.8, 1 mM DTT, 50 mM NaCl, 50 ng/μl BSA and 2.5 mM $MgCl_2$. The reaction was incubated at 30°C for 1 h and stopped by adding SDS–PAGE loading buffer. The histones were separated by 15% SDS–PAGE, Coomassie stained, amplified and dried. The autoradiograph was developed after 1 and 2 weeks. For experiments with mouse G9a, we used 250 ng of protein and the incubation time was 30 min. Exposure time for autoradiograph was 1 and 2 days.

MALDI-TOF analysis

Methylation reactions were carried out as described above with 0.5 μg of histone H3 or H4 and 250 μM of S-Adenosylmethionine (New England BioLabs). The reaction was stopped by addition of SDS–PAGE loading buffer and the histones were separated by 15% SDS–PAGE. The Coomassie stained bands corresponding to H3 and H4 were excised and subjected to chemical modification to derive free amino groups of lysine residues as described previously (33). H3 and H4 were digested over night with 100 ng of sequencing-grade trypsin (Promega) in a total volume of 40 μl according to manufacturer's protocol. In order to purify the methylated peptides from contaminating salts or acrylamide the peptide solution was passed over a pipette tip containing C18 material (ZipTip, Millipore) and eluted as described previously (32). The MALDI spectra were acquired and analyzed as described previously (34). Reaction mix without enzyme was used for calibration. Quantification was performed as previously described in Ref. (35).

Ecdysone feeding experiments

The feeding experiments were performed essentially as described in Ref. (36).

RESULTS

CG2995 is the *Drosophila* homolog of the mouse G9a HKMTase

We performed a bioinformatics search of the *D. melanogaster* genome with the Su(var)3–9, E(Z) and Trithorax SET domains and found novel genes encoding putative SET proteins. Performing a BLASTP search with the SET domain of one of these proteins, the annotated CG2995 protein,

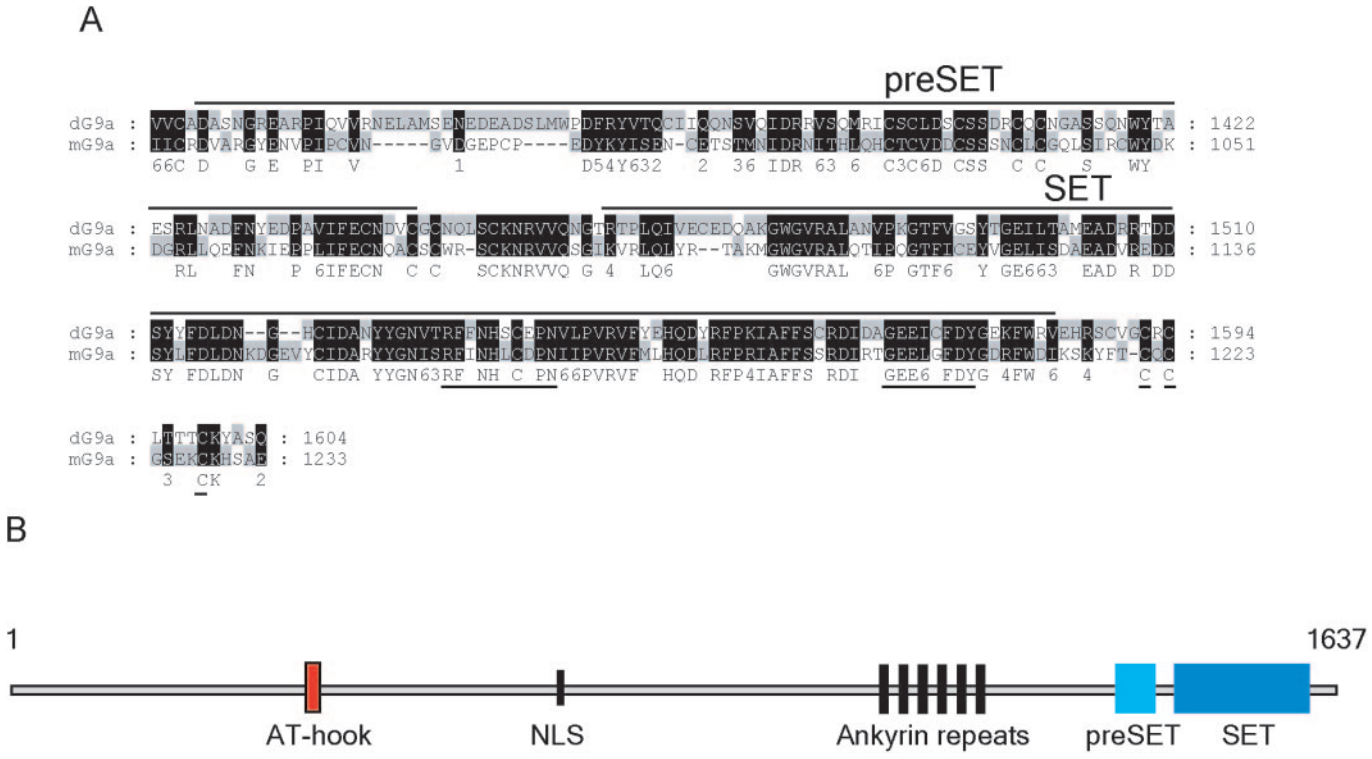

Figure 1. The domain organization is conserved between dG9a and G9a. (**A**) Alignment of SET domains and flanking cysteine-rich regions of mouse and *Drosophila* dG9a protein. The degree of conservation is distinguished at four levels (100, 80 and 60%, and not conserved), where 100% has the darkest shade of grey. The upper and lower case letters in the consensus line indicate 100 and 80% conservation within all groups, respectively. Numbers in the consensus line represent conserved similarity groups as defined by the Blossum 62 scoring table. The conserved R(H)ΦΦNHSC and the FDYG motifs are underlined. (**B**) Domain organization within *Drosophila* protein dG9a. An AT-hook and an ankyrin motif are found in addition to the SET domain.

against the mouse and human database identified it as the *Drosophila* homolog of the G9a protein. This SET domain alone shares 61% identity (76% similarity) with the corresponding domain of the mouse G9a protein (Figure 1A). In comparison, the SET domain of CG2995 shares 45% identity with the SET domain of the Su(var)3–9 protein of *Drosophila*, suggesting that CG2995 is the only homolog of G9a in the *Drosophila* genome. This is emphasized when looking at the pre-SET/SET/post-SET regions, where it is notable that CG2995 is more similar to mouse G9a than to Su(var)3–9 or dSET2. Thus, dSu(var)3–9 versus G9a shows 37% identity, 55% similarity, dSET2 versus G9a displays 36% identity, 50% similarity, and CG2995 versus G9a has 47% identity, 68% similarity. *CG2995* is located as the third gene in region 1A1 on the X chromosome, and a further comparative analysis of the CG2995 protein with the mouse G9a shows that the CG2995 has 33% identity and 49% similarity to the mouse protein (1172–1263 amino acid). The fly protein is longer at the N-terminus but otherwise shares the same module organization as its mouse counterpart. The CG2995 protein contains multiple putative domains in addition to the SET domain, like the adjacent cysteine-rich regions [the pre-SET (also called SAC); (37)], and conserved cysteine residues in the C-terminal region of the SET domain that corresponds to the post-SET domain (Figure 1A), which has shown to be required for enzymatic activity (38). Within the SET domain, a H(R)ΦΦNHSC motif (where Φ indicates a hydrophobic residue) has previously been shown to be an important catalytic site. For SUV39H1 protein, a histidine-to-arginine mutation of the first histidine (His^{320}) in the ^{320}HΦΦNHSC^{326} motif resulted in a 20-fold higher catalytic activity (38). This observation suggests that the H(R)ΦΦNHSC motif is correlated with the HKMTase activity. The CG2995 protein contains a ^{1532}RΦΦNHSC^{1538} motif (Figure 1A, underlined), together with another motif reported to be needed for HKMTase activity, $GE(x)_5Y$, located in the C-terminal end of the SET domain (38; Figure 1A, underlined).

In addition, the CG2995 protein harbors contiguous copies of a 33-amino acid repeat (Figure 1B). This repeat, originally identified in the Notch protein of *Drosophila* and known as the ankyrin repeat, is also found in G9a and in a number of other proteins involved in intracellular protein–protein interactions (39).

An AT-hook also is found in the N-terminus part of the CG2995 protein. The AT-hook is a small DNA-binding protein motif that was first described in the high mobility group non-histone chromosomal protein HMG-I(Y). Since its discovery, this motif has been observed in other DNA-binding proteins from a wide range of organisms. Furthermore, AT-hook motifs are frequently associated with known functional domains seen in chromatin proteins and in DNA-binding proteins (e.g. histone folds, homeodomains and zinc fingers). In general, it appears that the AT-hook motif is an auxiliary protein motif co-operating with other DNA-binding activities and facilitating changes in the structure of the DNA either as a polypeptide on its own [e.g. HMG-I(Y)] (40) or as part of a multidomain protein

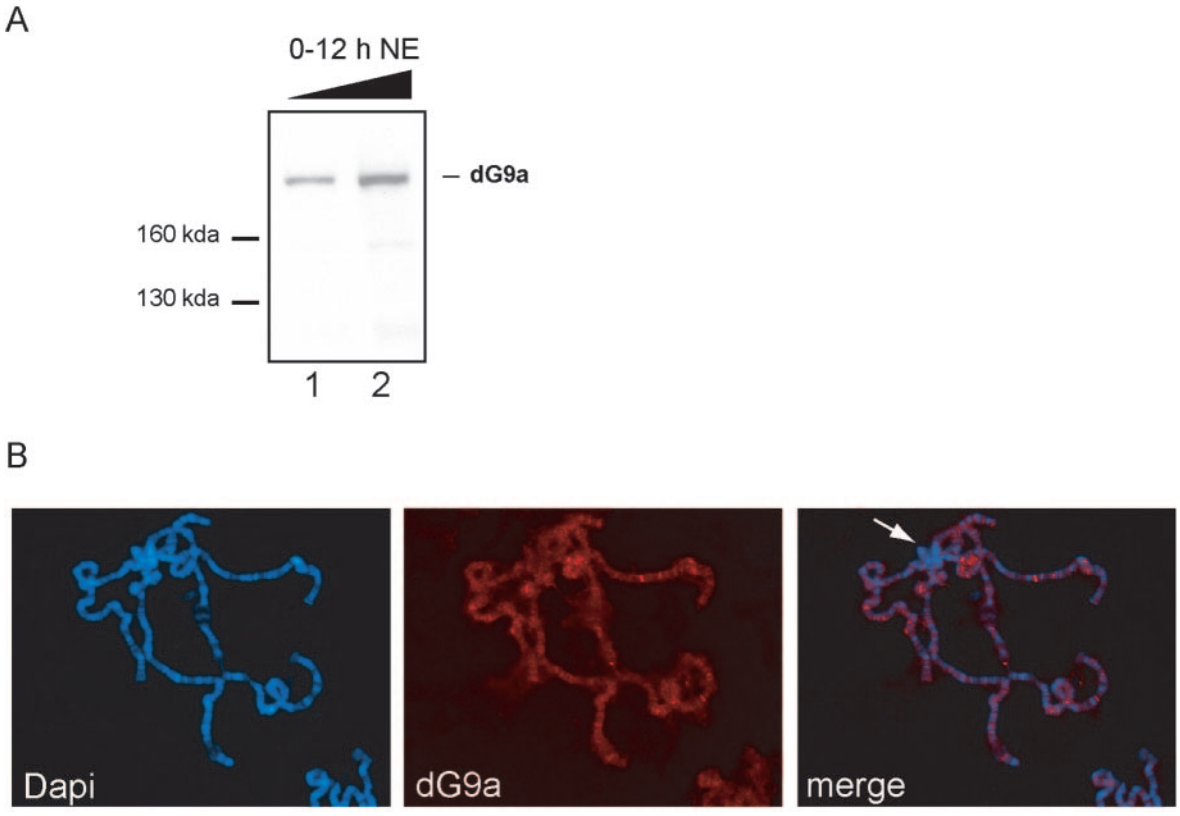

Figure 2. The dG9a protein localizes to distinct chromosome bands. (**A**) Antibodies against dG9a raised in rabbit are specific and recognize a single band of ~180 kDa as predicted on a western blot of *Drosophila* nuclear extract. (**B**) dG9a protein (in red) localizes to chromatin and gives a distinct banding pattern on polytene chromosomes. There is no staining in the chromocenter (arrow), and dG9a localizes predominantly to euchromatic regions. DNA is counterstained with DAPI (in blue).

[e.g. Swi2p in *Saccharomyces cerevisiae* or HRX (ALL-1) in *Homo sapiens*] (41). It is most interesting that this motif seems to be specific to known or predicted chromosomal/DNA-binding proteins, suggesting that it may act as a versatile minor groove tether (41). A nuclear localization signal is found in the N-terminal of the protein. In conclusion, CG2995 has a high level of similarity to mouse G9a and we suggest CG2995 is the *Drosophila* homolog of G9a and will refer to it as dG9a.

Full-length cDNA was cloned by RACE and RT–PCR. This cDNA revealed that the *dG9a* gene consists of 10 exons with a 4911 bp open reading frame (ORF) encoding a protein of 1637 amino acid. The coding region ends by an in-frame stop codon that is followed by a poly(A) signal 1173 downstream, suggesting that it is full-length and consistent with the annotated sequence in FlyBase (http://flybase.bio.indiana.edu/; Figure 1B). Northern analysis also showed that there is only one transcript of expected size (data not shown).

The dG9a protein localizes to euchromatin

Antibodies specific to dG9a were generated by immunization of rabbits with a peptide corresponding to the last 14 amino acids (1623 through 1637 amino acid). This antibody recognized a band of the predicted size of ~180 kDa (Figure 2A). The localization of dG9a protein was investigated by analysis of polytene chromosomes from salivary glands (Figure 2B). The immunostaining showed discrete banding pattern in euchromatic regions with no staining observed in the chromocenter.

Spatiotemporal expression of *dG9a*

To investigate the spatiotemporal expression of *dG9a* we first used semi-quantitative RT–PCR. As shown in Figure 3A, a low but measurable amount of *dG9a* transcript is present in 0–3-h-old embryos. In 3–6-h-old embryos the expression of *dG9a* is barely detectable, indicating that the *dG9a* transcripts seen in 0–3-h-old embryos are of maternal origin. Between 6 and 21 h of embryogenesis the expression of *dG9a* is low but clearly discernible, and about the same level of expression is observed throughout larval development, with a slightly elevated expression during the third larval instar. Then, in 12–46-h-old pupae there is no or very little expression of *dG9a*. In adult flies the expression of *dG9a* is restricted to the gonads in both sexes (Figure 3A, last four lanes). However, we cannot rule out the possibility that *dG9a* is expressed in one or more tissues of the gonadectomized flies, but at a level too low to be detected by the RT–PCR settings used here.

Next, in order to study the spatiotemporal expression of dG9a in more detail, we stained ovaries and embryos with the dG9a antibody. The immunostainings revealed that dG9a is expressed in all cells of the ovary, including the germarium (Figure 3C) where especially the nurse cells,

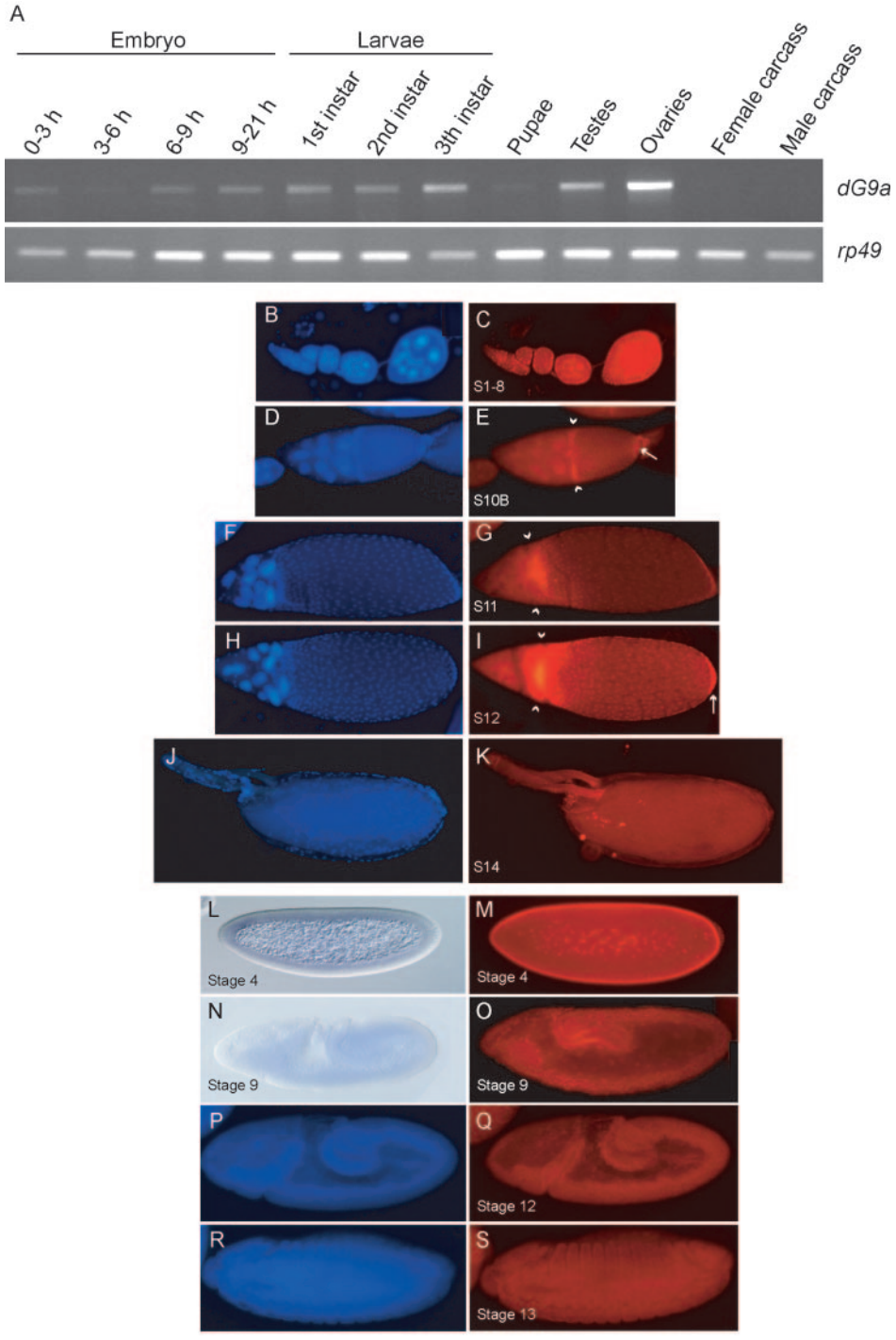

Figure 3. Spatiotemporal expression of dG9a. (**A**) Developmental RT–PCR shows that *dG9a* is maternally deposited in the egg, and that there is moderate expression during the larval development. dG9a is present in all developmental stages investigated. (B–K) dG9a is present from the very start of oogenesis through the end of oogenesis in wild-type ovarioles. Anterior is to the left, posterior to the right. dG9a in red (right column) and the nuclei is counter stained with DAPI in blue (left column). (**B** and **C**) The early stages of oogenesis development. The dG9a protein is present from the very start. (**D** and **E**) Stage 10B ovaries. dG9a localizes to nuclei in both nurse and follicle cells. An accumulation of protein is observed in the region where the anterior polar cells and the centripetal follicle cells are located, arrowheads and in the posterior follicle cells, arrow. (**F** and **G**) Stage 11. Shortly after centripetal migration (stage 10B), the nurse cells rapidly transfer their contents into the oocyte (stage 11) then begin to degenerate and undergo apoptosis (stages 12–14). (**H** and **I**) Stage 12. Dumping complete, no or very little dG9a is detectable in the degenerating nurse cell nuclei, but is still present in the follicle cells. Notice the accumulation of dG9a protein in the extreme posterior part of the egg, arrowheads, where the posterior polar cells located. (**J** and **K**) Stage 14. The egg is fully developed and dG9a protein is maternally deposited. (L–S) Lateral views of wild-type embryos hybridized with digoxigenin-labeled RNA probes (L and N with Nomarski optics) or with a dG9a antibody (**M, O, Q** and **S**). Anterior is to the left and dorsal is up. The nuclei are counter stained with DAPI in blue. (**L** and **M**) Embryo at syncytial blastoderm stage (stage 4, ~1.5–2.5 h). dG9a is localized to the nuclei. In early embryos the message and the protein are ubiquitously distributed due to its maternal contribution. (**N** and **O**) Embryo during germband extension (stage 9). (**P** and **Q**) Stage 12. In late-stage embryos, expression is strongest in the CNS and the neuroectoderm. (**K** and **S**) Stage 13. Surface view of embryo at the completion of germband shortening.

which undergo a dramatic endoreplication, stain heavily. It also clearly shows that dG9a is localized to the nucleus. In stage 10B egg chambers it appears that dG9a is markedly upregulated in what appears to be the centripetal follicle cells (Figure 3E, arrowheads). At this stage, a moderate upregulation is also discernible in the posterior follicle cells (arrow). During stage 11 nurse start dumping their content into the oocyte, which is revealed by an accumulation of dG9a at the border between the growing oocyte and the degenerating nurse cells (Figure 3G). At this stage an increased expression of dG9a is also found in the posterior follicle cells (Figure 3G, arrow head). In stage 12 the amount of dG9a has increased considerably and has started to move into the oocyte. An accumulation in the posterior follicle cells is now prominent (Figure 3I, arrow). At stage 14, dG9a appears to be evenly distributed in the mature oocyte (Figure 3K).

In blastoderm embryos (stage 4, ~1.5–2.5 h) *dG9a* transcript as well as protein are present in the syncytial nuclei (Figure 3L and M). During stages 9 and 12, dG9a expression appears to be more abundant in the central nervous system (CNS) and the neuroectoderm (Figure 3N, O and Q). Figure 3S shows a surface view of embryo at the completion of germband shortening, with all cells evenly stained.

Expression and purification of recombinant histone methyltransferase dG9a

In order to investigate the enzymatic properties of dG9a we expressed a FLAG tagged N-terminal fragment (789–1637 amino acid) using a baculovirus expression system. The purified dG9a was soluble and had the expected molecular size of 95 kDa (Figure 4A). To confirm that dG9a has HKMTase activity we incubated it in presence of H^3-S-adenosylmethionine (SAM) and different substrates (Figure 4B). dG9a methylates H3 and H4 present as free histones but had no detectable activity on nucleosomal arrays. In contrast to the recombinant dG9a, mouse G9a only methylates H3 even when other histones are present (Figure 4C). In order to exclude the possibility that the unexpected H4 HMT activity is due to a contaminating activity co-purifying with the recombinant dG9a we expressed the enzyme carrying a point mutation within the SET domain (H1536K) that dramatically impairs its catalytic activity. The mutated enzyme was not able to methylate either H3 or H4 indicating that both methylations are a result of dG9a activity (Figure 4D). In order to determine the substrate specificity we performed a quantitative MALDI-TOF analysis of H3 molecules methylated by dG9a. Similarly to the activity of the mouse ortholog (42), dG9a methylates exclusively K9 and K27 with K9 being the preferred substrate in wild-type (wt) H3. As shown for mG9a (43) dG9a is able to add up to three methyl groups to H3 (Figure 4H). This finding is confirmed by using H3 molecules carrying a lysine to alanine replacement at position 9 and 27 or both (Figure 4E). We observe decreased methylation efficiency on H3 K9A and H3 K27A compared to wt H3. In a filter binding assay we observed a 70% reduction when K9 was mutated and a 50% reduction when K27 was mutated. When both H3 lysine residues were mutated (K9A and K27A) we observe a lower activity (efficiency of 27%) indicating that in absence of K9 and K27 dG9a is also able to methylate other lysines. Mouse G9a also showed a decreased activity (27%) towards the double mutant (K9A/K27A) (Figure 4F). When we use highly active mG9a (43), it methylates wt H3 and the H3 molecules carrying a single mutation on K9 or K27 with a similar efficiency. However, as we use relatively long reaction times we can not exclude the possibility that K9 is methylated faster than K27, which explains the larger differences observed in previous publications (16,44).

Interestingly dG9a was also able to methylate histone H4 (Figure 4B). This is in marked contrast to the mouse G9a where we do not observe such an activity (Figure 4C) (42). The only lysine residue of H4 shown to be methylated *in vivo* is K20 and the first HKMTase identified with this activity was hPR-Set7/dSET8 (45,46). Other HKMTases in *Drosophila* shown to methylate H4 lysine 20 are Ash1 and Suv4–20 (47,48). Ash1 is in addition able to methylate lysine 4 and 9 in histone H3 (47). From these experiments we concluded that dG9a also is a multi-catalytic histone methyltransferase with specificity for lysine 9 and 27 on H3 and possibly lysine 20 on histone H4. However, when we incubated dG9a with H4 carrying a mutation of lysine 20 to alanine we observed no reduction of activity (Figure 4G). To further investigate the specificity, we tested whether dG9a was able to methylate H4 molecules carrying different N-terminal deletions (29). We observed that dG9a could methylate the H4 N-terminus when the first five amino acids were deleted, excluding K5 as a possible substrate. However, the activity was lost when we used the H4 Δ10 mutant (Figure 4G). This suggests that the substrate is K8, but considering that the minimal substrate specificity for mG9a surrounding K9 contains seven amino acids (TARKSTG) (49) we cannot exclude that another downstream lysine can serve as a substrate. MALDI-TOF analysis of H4 methylated by dG9a, showed that only the peptide containing amino acids 4–17 was methylated *in vitro* (Figure 4H). We conclude from these experiments that dG9a can methylate lysine 8, 12 or 16 of H4 *in vitro*. It remains to be seen to what level these lysines are methylated *in vivo* and what the function of this methylation is.

dG9a is required for normal development

To investigate the *in vivo* function of dG9a, transgenic flies with an inverted-repeat *UAS-dG9a.IR* construct were crossed to different GAL4-driver lines (22). The vector used for making the inverted repeats has an independent UAS-GFP marker so that a tissue exposed to RNAi will simultaneously show GFP expression [pUds-GFP; (21)] as an internal control to RNAi expression. In addition, down regulation of *dG9a* was confirmed by RT–PCR (Figure 5A).

Using the ubiquitously expressed *da-GAL4* driver with the *UAS-dG9a*.IR flies, the progeny developed normally until the end of the third larval instar. However, these RNAi larvae did not form their puparium and crawling larvae were found after 7–8 days (Figure 5B). The majority of these larvae developed melanotic tumors, either one or two larger ones or several smaller. The larvae finally stopped moving, and in the few cases where 'pseudo-prepupae' were formed,

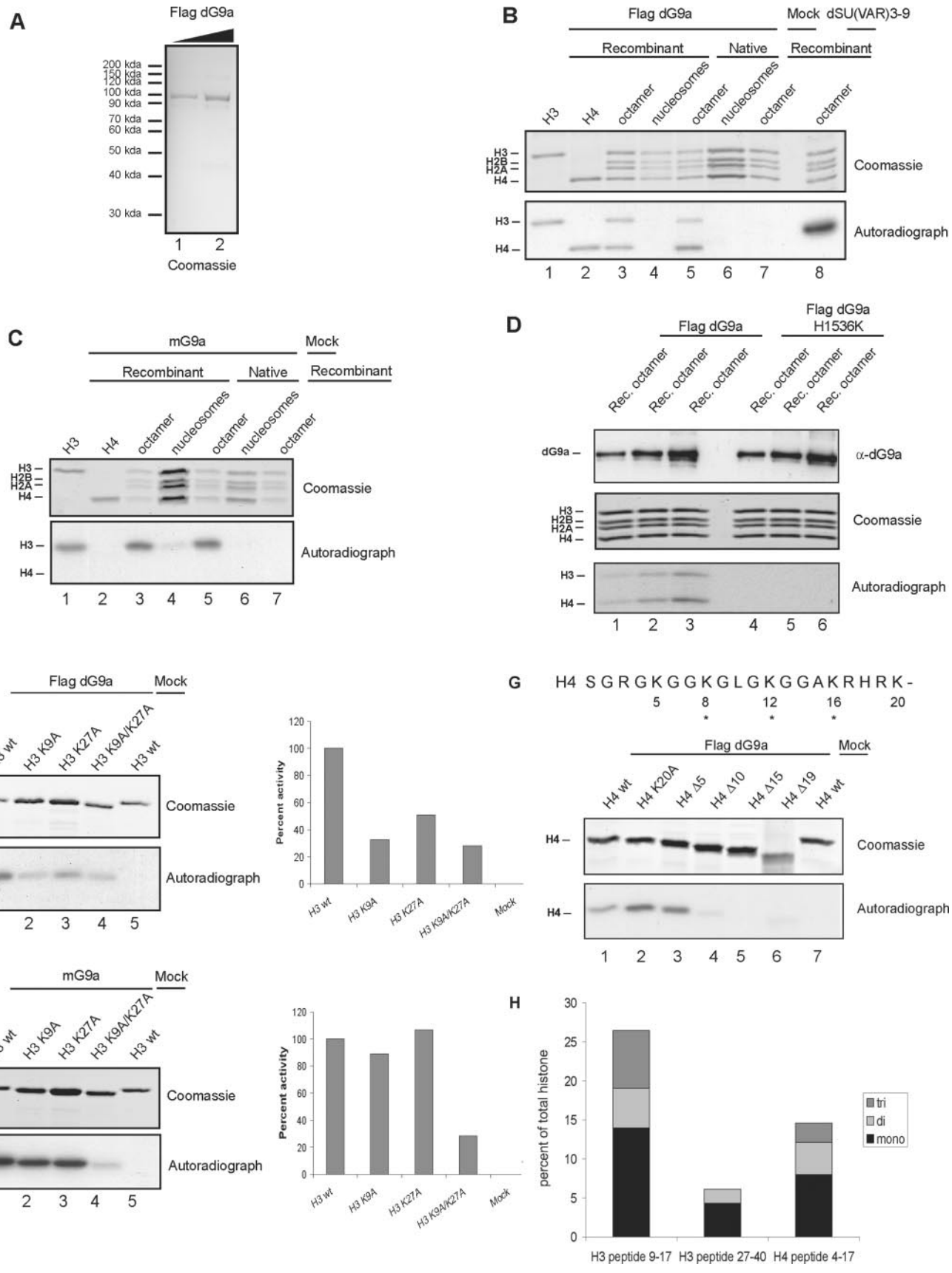
A
Flag dG9a
200 kda
150 kda
120 kda
100 kda
90 kda
70 kda
60 kda
50 kda
40 kda
30 kda
1 2
Coomassie
B
Flag dG9a
Mock dSU(VAR)3-9
Recombinant
Native
Recombinant
H3
H4
octamer
nucleosomes
octamer
nucleosomes
octamer
octamer
H3
H2B
H2A
H4
Coomassie
Autoradiograph
1 2 3 4 5 6 7 8
C
mG9a
Mock
Recombinant
Native
Recombinant
H3
H4
octamer
nucleosomes
octamer
nucleosomes
octamer
Coomassie
Autoradiograph
1 2 3 4 5 6 7
D
Flag dG9a
Flag dG9a H1536K
Rec. octamer
dG9a
α-dG9a
Coomassie
Autoradiograph
1 2 3 4 5 6
E
Flag dG9a
Mock
H3 wt
H3 K9A
H3 K27A
H3 K9A/K27A
H3 wt
Coomassie
Autoradiograph
1 2 3 4 5
Percent activity
H3 wt
H3 K9A
H3 K27A
H3 K9A/K27A
Mock
F
mG9a
Mock
H3 wt
H3 K9A
H3 K27A
H3 K9A/K27A
H3 wt
Coomassie
Autoradiograph
1 2 3 4 5
Percent activity
G
H4 S G R G K G G K G L G K G G A K R H R K -
5 8 12 16 20
Flag dG9a
Mock
H4 wt
H4 K20A
H4 Δ5
H4 Δ10
H4 Δ15
H4 Δ19
H4 wt
Coomassie
Autoradiograph
1 2 3 4 5 6 7
H
percent of total histone
tri
di
mono
H3 peptide 9-17
H3 peptide 27-40
H4 peptide 4-17

these maintained the elongated larval form and failed to evert the anterior spiracles; there was only slight melanization of these 'pseudo-prepupae' (Figure 5C).

The defects in puparium formation seen in *dG9a* RNAi animals could result from either a decrease in the ecdysone titer or a decrease in the ability of the ecdysone signal to be transduced. To distinguish between these possibilities we examined the effects of feeding ecdysone to *dG9a* RNAi larvae. This method has been shown to effectively rescue phenotypes associated with ecdysone-deficient mutations (36). Mid- and late-third instar larvae were transferred to food either with or without 20-hydroxyecdysone (20E) for 6–8 h and scored on a 12-h basis. Feeding 20E to *dG9a* RNAi larvae did not rescue them to puparium formation. Therefore, we conclude that ecdysone is not limiting in the *da-GAL4/UAS-dG9a.IR* animals and that *dG9a* functions downstream of ecdysone biosynthesis and release.

When the ubiquitously expressed, but weaker, *Act5C-GAL4* driver was used, development of progeny of genotype *Act5C-GAL4/UAS-dG9a.IR* proceeded up to and through puparium formation (data not shown). However, most of the pupal cases were only lightly tanned and no flies eclosed from these cases. Upon dissection, dead and partially differentiated pharates with no eye pigmentation or legs were found (data not shown). Development appeared to have proceeded further in the posterior part of fly. Of all pupae formed ($N = 133$), ~17% developed normally, and the eclosed flies were without exception females.

As immunostaining indicated a role for dG9a in neuroectoderm and CNS, a driver which expresses GAL4 in brain and throughout CNS, but not in discs, of third instar larvae, P{GawB}c698a, was used. The phenotypes observed were similar to those observed with the *Act5C-GAL4* driver. Here, however, most of the pupae were partly more melanized (Figure 5D), without differentiation proceeding any further than that described for the *Act5C-GAL4* driver (Figure 5E). A small portion (~5%) of the pupae actually developed normally but of these almost all failed to escape from the pupal case. The very few that succeeded were all normal females and lived for at least 2 weeks.

The results described above strongly suggest a defect in ecdysone responses at puparium formation, similar to those reported earlier for mutants in the ecdysone pathway (50). Also, using RNAi very similar results were obtained with the H3–K36 HKMTase *dSet2* gene (M. Stabell, unpublished data).

Ecdysone controls wing morphogenesis and cell adhesion by regulating integrin expression during metamorphosis (51). Therefore, to test further the possible involvement of dG9a in the ecdysone regulation hierarchy, we triggered *dG9a* RNAi in the wing disc by the *ap-GAL4* driver. This resulted in slightly held-out/up wings with an anterior–posterior compression (Figure 5F), and occasionally in blister formation (Figure 5G). We next generated flies of genotype *ap-GAL4,UAS-dG9a.IR/EcR*^{M554fs}. *EcR*^{M554fs} is a loss of function mutation where only half the amount of the ecdysone receptor is present in mutant flies. As shown in Figure 5I, these animals show a wing phenotype of a more extreme character, with both wings having a blister and being clearly smaller than normal, most likely because the wings never completely unfold. This phenotype has 100% penetrance. Taken together, these results support the notion that dG9a functions in ecdysone signaling pathways during development.

DISCUSSION

dG9a is a euchromatic histone methyltransferase

In this study we show that CG2995 is the *Drosophila* homolog of the HKMTase G9a, and that it specifically mono-, di- and trimethylates H3–K9, H3–K27 and K8, 12 or 16 in H4. This methylation pattern is mainly correlated with silencing (11) suggesting that dG9a is involved in transcriptional repression. Further, we showed that dG9a methylates free histones but has no detectable activity on nucleosomal arrays. As revealed by the staining of polytene chromosomes, the centromeric region, where Su(var)3–9 predominantly stains (52), is devoid of dG9a. We therefore conclude that dG9a is a euchromatic histone methyltransferase that acts on loosely packed DNA and that methylation by dG9a may occur on pre-assembled histones.

Figure 4. Characterization of recombinant dG9a. (**A**) Eluted FLAG tagged dG9a (789–1637 amino acid) was separated on a 12% SDS–PAGE and stained with Coomassie blue G250. (**B**) *In vitro* methylation reactions using dG9a (lanes 1–6), no enzyme (lane 7) and dSu(var)3–9 (lane 8). In the reaction we used 1 μg of different histones: recombinant histone H3 (lane 1), recombinant histone H4 (lane 2), recombinant (lane 3) and native histone octamer (lane 5) and recombinant and native nucleosomes (lanes 4 and 6) reconstituted on circular pBS(KS) from equimolar amounts of histones. The upper panel shows Coomassie stained gel and the lower panel the autoradiograph. (**C**) Activity of recombinant mouse G9a expressed in baculovirus infected cells (a kind gift from S. Pradhan). HKMTase activity on 1 μg of different histone substrates: recombinant histone H3 (lane 1), recombinant histone H4 (lane 2), recombinant and native histone octamers (lanes 3 and 5) and recombinant and native nucleosomes (lanes 4 and 6). Mock control (lane 7) is incubation of recombinant octamer without enzyme. The Coomassie gel is shown at the top and the corresponding autoradiograph at the bottom. (**D**) FLAG dG9a wild type versus H1536K mutation of the conserved region of the SET domain. The upper panels shows a western blot of the two proteins. Recombinant octamer (2 μg) was used as substrate for 25. 50 and 100 ng of wt (lanes 1–3) and H1536K mutant (lanes 4–6). The corresponding autoradiograph is shown in the lower panel. (**E**) *In vitro* methylation of 2 μg of recombinant H3 (lane 1), H3 mutated at lysine 9 (lane 2), H3 mutated at lysine 27 (lane 3) or both (lane 4) using dG9a and a mock purification. Coomassie stained H3 is shown in the upper panel and a corresponding autoradiography in lower panel. A corresponding filter binding assay is shown to the right. The *y*-axis displays the percent radioactivity incorporated on 2 μg of histone H3 and H3 mutants K9A, K27A and K9/K27A with radioactivity incorporated on wt H3 set to 100% and the background is subtracted. (**F**) HKMTase activity of mG9a on histone H3 molecules and H3 K9A, H3 K27A and the double mutant K9A/K27A. A gel of Coomassie stained histones and the corresponding autoradiography is shown. On the right, a filter binding assay showing percent radioactivity incorporated on 2 μg of histone H3 and H3 mutants K9A, K27A and K9/K27A. The *y*-axis displays the percent radioactivity incorporated with activity on wt H3 set to 100% and the background is subtracted (**G**) Amino acid sequence of the H4 N-terminus is shown at the top. Asterisks indicate possible substrates for dG9a *in vitro*. Methylation of 2 μg of recombinant H4 (lane 1), H4 K20A (lane 2), H4Δ5 (lane 3), H4Δ10 (lane 4), H4Δ15 (lane 5) and globular H4 (lane 6). Mock control (lane 7) is incubation of wt H4 without enzyme. (**H**) Quantitative MALDI-TOF analysis of 500 ng of H3 and H4 methylated by 100 ng of dG9a. Peptides spanning amino acids 9–17 and 27–40 of H3 and 4–17 of H4 is represented by graphs. No signals were observed in other peptides. Mono-, di- and trimethylation are shown as percent of total H3 or H4. This figure is representative for at least three different methyltranferase assays.

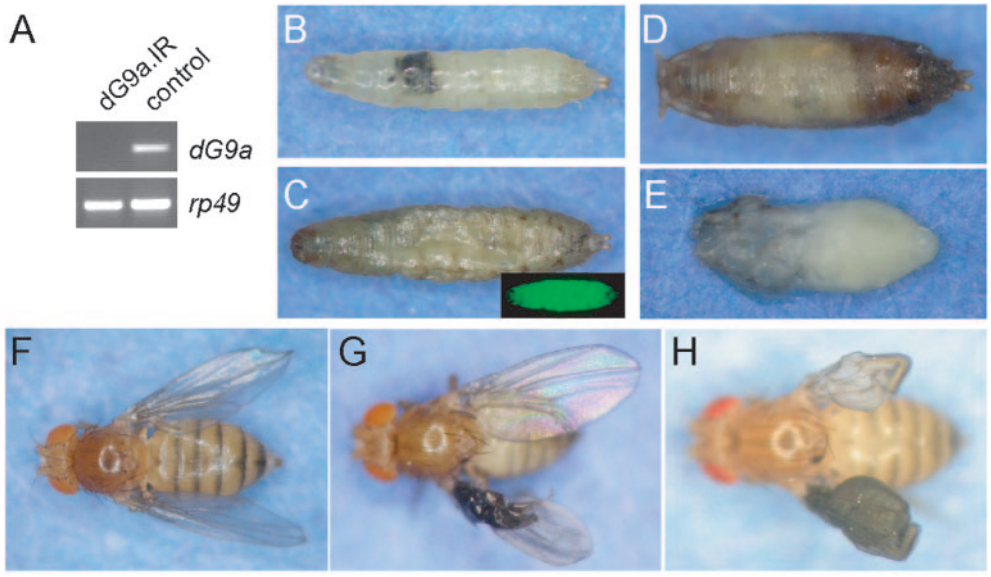

Figure 5. Knock down of *dG9a* give phenotypic effects. RNAi experiments show that dG9a is important for development. (**A**) RT–PCR shows that *dG9a* is down regulated by RNAi; *rp49* is used as loading control. (**B** and **C**) Using a ubiquitously expressed driver, *da-GAL4*, to induce the IR construct shows that dG9a is required for proper transition from larva to pupa. Penetrance is 100%. In (B) the larva is 6 days, in (C) 8 days. The IR construct is tagged with an independent UAS-GFP, which can be used as control (insert). Melanotic tumors are frequently observed in these larvae. (**D** and **E**) Using a larval *CNS-GAL4* (BL 3739) driver the progeny makes it up to and through pupariation (**F**), but fails to hatch. Differentiation seems more complete in posterior part of the animal (**G**). A similar phenotype is observed when using *Act5C-GAL4* as driver. Remarkably, in both cases, the escapers observed to hatch (~10%) are females. (**H** and **I**) When using the *ap-GAL4* driver defects in the wings are observed. This phenotype is highly pleiotropic, with one or both wings affected. Among the phenotypes are narrow wings held in a Dichaeate-like fashion, wings standing straight up and blistered wings. Progeny with no apparent defects are also observed. (**J**) Progeny of genotype *ap-GAL4,UAS-dG9a.IR*/EcR^{M544fs} show a wing phenotype of severe character and 100% penetrance.

dG9a is expressed throughout development

Immunostaining revealed that the dG9a protein is found throughout oogenesis, embryogenesis, and larval development. During these stages, large cells (like nurse cells and salivary gland cells) are metabolically very active, and having multiple copies of genes (polyteny) permits a high level of gene expression; that is, abundant transcription and translation to produce the gene products. (53). In adult flies the *dG9a* transcript and protein are solely found in the gonads, where cells are undergoing extensive endo- and mitotic replication. One can assume that is important that certain genes are kept silent in these cells, and one possible function of dG9a could be to maintain repression of a subset of genes in cells that otherwise have a high gene expression level.

In the RNAi knock down studies, no lethality was observed during embryogenesis, but this can be ascribed to the fact that the RNAi construct was made using a pUAST based vector that is defect in the germline during oogenesis (22). Conditional knock down of dG9a in the female germline was therefore not possible in this study, but should be subject for future investigation. An interesting observation is that the escapers from the RNAi studies are exclusively females. This result suggests that dG9a may have different roles in males versus females. It is possible that conditional depletion of dG9a in transgenic flies may affect the expression of genes that are required for chromatin stability, chromosome segregation and proper histone modifications resulting in a preferential lethality in male flies. This has recently been reported for *Su(var)205* (also called *HP1*) (54), and *bonus* (*bon*), encoding a homolog of the vertebrate TIF1 transcriptional cofactors and required for male viability (55). Interestingly, bon is associated with genes that are implicated in the ecdysone pathway.

dG9a is involved in ecdysone mediated signaling

Next, we provide evidence that dG9a is required for important transitions during *Drosophila* development. Our results suggest a role for dG9a in regulation of genes, especially during the onset of metamorphosis, and wing development, processes tightly correlated to ecdysone responsive signaling (56). Additional evidence for dG9a being involved in the ecdysone hierarchy is the formation of melanotic tumors in the larvae that do not form their puparium. Several chromatin-modifying or chromatin-associated complexes (57) as well as ecdysone have been implicated in hemocyte development and melanotic tumor formation (58,59). Furthermore, our genetic studies revealed that the EcR^{M544fs} is able to dominantly affect the wing phenotype in *ap-GAL4,UAS-dG9a.IR*/EcR^{M554fs} flies. Genetic interactions between mutant alleles of different genes are indicative of these genes belonging to the same functional pathway. Thus, the genetic studies support the results from the RNAi experiments, and together provide strong evidence of dG9a being involved in the ecdysone signaling hierarchy. As the RNAi mutants are not rescued by hormone feeding, dG9a must exert its effect downstream of ecdysone biosynthesis and metabolism. One possible scenario is that dG9a acts as a co-regulator for the ecdysone receptor mediating downstream gene regulation as a response to ecdysone pulses. A similar scenario has been reported for mammalian G9a, where a reduction of endogenous G9a reduced hormonal activation of an endogenous target gene by the androgen receptor (60).

The genetic interaction between EcR^{M554fs} and *ap-GAL4,UAS-dG9a.IR* on wing development may suggest a molecular interaction between the EcR receptor and dG9a. Activation and repression of transcription involve the recruitment of many co-regulator (co-repressor or co-activator) proteins to the regulated gene promoter by sequence-specific DNA binding transcription factors. As dG9a contains an AT-hook, it could tether the ecdysone receptor to the DNA, or, more plausible, the DNA binding activity of EcR by could bring dG9a to the promoter. Two models could explain the EcR-dG9a relationship observed:

(i) dG9a act as a co-repressor of the early puffs according to the Ashburner model for the hormonal control of polytene chromosome puffing (61). Briefly, this model proposed that ecdysone, bound to its specific receptor, directly induces the expression of a small set of early regulatory genes. The protein products of these genes, in turn, repress their own expression and induce a much larger set of late target genes. dG9a could be involved in this repression.
(ii) dG9a act as a co-activator coupled to the transcription apparatus during activation of ecdysone regulated genes.

Vakoc and co-workers (62) reported recently that H3–K9 methylation was found at high levels in the transcribed region of four genes while they were transcribed. This observation is rather remarkable in that it implies a coupling of the traditionally accounted H3–K9 silencing mark to active transcription. Therefore, the possibility that dG9a plays a role in maintaining transcription should be further investigated. In addition, there are observations that murine G9a acts both as a co-repressor (63–65), and a co-activator (60), depending on promoter context and/or regulatory environment, along with the observation that the zinc finger protein wiz links G9a/GLP histone methyltransferases to the co-repressor molecule CtBP (66). Furthermore, NSD1, which methylates both H3–K36 and H4–K20 *in vitro* (67), acts as a co-activator and a co-repressor for NRs (37).

As a complement to the RNAi approach, we have tried to generate null mutants (deletions) by re-mobilization of the P-element inserted in the 5′-untranslated region (5′-UTR) of *dG9a* in the $dG9a^{13414}$ stock. Whereas several independent lines with precise excision of the P-element were obtained we failed to find any imprecise excision (deletion) events (M. Stabell, unpublished data). During the course of the preparation of this manuscript, Mis *et al*. (68) also identified CG2995 as being the *Drosophila* homolog of mammalian G9a. This group also reported unsuccessful mobilization of the P-element, and suggested that this may be due to a defective P-element. Instead, they investigated the $dG9a^{13414}$/$dG9a^{13414}$ mutant and report only a minor phenotype without characterizing the nature of the mutant. On the other hand, they showed that this $dG9a^{13414}$ mutant suppresses position effect variegation (PEV) and that it interacts genetically with Su(var)3–9, suggesting that the two proteins have an overlapping role in heterochromatic gene silencing and may be members of protein complexes involved gene silencing. In contrast to Mis *et al*. (68) who concluded that dG9a is a H3–K9 HKMTase, we provide evidence that dG9a (i) methylates H4 as well as H3, (ii) is able to add three methyl groups, (iii) methylates K9 and K27 on histone H3 with a preference for K9 and (iv) has a specificity towards K8, K12 or K16 on the H4 N-terminus. In polytene chromosomes dG9a is excluded from the chromocenter (Figure 3), indicating a euchromatic role for dG9a. But as the majority of full-length GFP-mG9a fusion proteins has been found in pericentric heterochromatin (16), we cannot rule out a conceivable function for dG9a during facultative heterochromatinization in other tissues and/or stages of development.

ACKNOWLEDGEMENTS

We would like to thank Sriharsa Pradhan for providing the mouse G9a baculoviral protein, Danny Reinberg for H3 mutant plasmids, Thomas Jenuwein for the H4 K20A plasmid, Cedric R. Clapier and Peter Becker for the H4 N-terminal deletion proteins, Daisy Schwarzlose for providing SF9 cells, Anette Preiss for the pHIBS and pUds-GFP vectors, and Ann Mari Voie at the EMBL injection service for the transgenic lines. This study was supported by a grant from the Norwegian Research Council to R.B.A. and A.L., from the Swedish Research Council to J.L., and from the Deutsche Forsghungsgemeinschaft (IM23/4-3) to A.I. Funding to pay the Open Access publication charges for this article was provided by Norwegian Research Council.

Conflict of interest statement. None declared.

REFERENCES

1. Jenuwein,T. and Allis,C.D. (2001) Translating the histone code. *Science*, **293**, 1074–1080.
2. Strahl,B.D. and Allis,C.D. (2000) The language of covalent histone modifications. *Nature*, **403**, 41–45.
3. Chuikov,S., Kurash,J.K., Wilson,J.R., Xiao,B., Justin,N., Ivanov,G.S., McKinney,K., Tempst,P., Prives,C., Gamblin,S.J. *et al*. (2004) Regulation of p53 activity through lysine methylation. *Nature*, **432**, 353–360.
4. Fischle,W., Wang,Y. and Allis,C.D. (2003) Histone and chromatin cross-talk. *Curr. Opin. Cell Biol*., **15**, 172–183.
5. Lachner,M., O'Sullivan,R.J. and Jenuwein,T. (2003) An epigenetic road map for histone lysine methylation. *J. Cell Sci*., **116**, 2117–2124.
6. Ng,H.H., Feng,Q., Wang,H., Erdjument-Bromage,H., Tempst,P., Zhang,Y. and Struhl,K. (2002) Lysine methylation within the globular domain of histone H3 by Dot1 is important for telomeric silencing and Sir protein association. *Genes Dev*., **16**, 1518–1527.
7. Jenuwein,T., Laible,G., Dorn,R. and Reuter,G. (1998) SET domain proteins modulate chromatin domains in eu- and heterochromatin. *Cell Mol. Life Sci*., **54**, 80–93.
8. Zhang,X., Yang,Z., Khan,S.I., Horton,J.R., Tamaru,H., Selker,E.U. and Cheng,X. (2003) Structural basis for the product specificity of histone lysine methyltransferases. *Mol. Cell*, **12**, 177–185.
9. Cao,R. and Zhang,Y. (2004) SUZ12 is required for both the histone methyltransferase activity and the silencing function of the EED–EZH2 complex. *Mol. Cell*, **15**, 57–67.
10. Wang,H., An,W., Cao,R., Xia,L., Erdjument-Bromage,H., Chatton,B., Tempst,P., Roeder,R.G. and Zhang,Y. (2003) mAM facilitates conversion by ESET of dimethyl to trimethyl lysine 9 of histone H3 to cause transcriptional repression. *Mol. Cell*, **12**, 475–487.
11. Martin,C. and Zhang,Y. (2005) The diverse functions of histone lysine methylation. *Nat. Rev. Mol. Cell. Biol*., **6**, 838–849.
12. Aagaard,L., Laible,G., Selenko,P., Schmid,M., Dorn,R., Schotta,G., Kuhfittig,S., Wolf,A., Lebersorger,A., Singh,P.B. *et al*. (1999) Functional mammalian homologues of the *Drosophila* PEV-modifier Su(var)3–9 encode centromere-associated proteins which complex with the heterochromatin component M31. *EMBO J*., **18**, 1923–1938.

13. Stewart,M.D., Li,J. and Wong,J. (2005) Relationship between histone H3 lysine 9 methylation, transcription repression, and heterochromatin protein 1 recruitment. *Mol. Cell. Biol.*, **25**, 2525–2538.
14. Peters,A.H., Kubicek,S., Mechtler,K., O'Sullivan,R.J., Derijck,A.A., Perez-Burgos,L., Kohlmaier,A., Opravil,S., Tachibana,M., Shinkai,Y. *et al.* (2003) Partitioning and plasticity of repressive histone methylation states in mammalian chromatin. *Mol. Cell*, **12**, 1577–1589.
15. Rice,J.C., Briggs,S.D., Ueberheide,B., Barber,C.M., Shabanowitz,J., Hunt,D.F., Shinkai,Y. and Allis,C.D. (2003) Histone methyltransferases direct different degrees of methylation to define distinct chromatin domains. *Mol. Cell*, **12**, 1591–1598.
16. Esteve,P.O., Patnaik,D., Chin,H.G., Benner,J., Teitell,M.A. and Pradhan,S. (2005) Functional analysis of the N- and C-terminus of mammalian G9a histone H3 methyltransferase. *Nucleic Acids Res.*, **33**, 3211–3223.
17. Tachibana,M., Sugimoto,K., Nozaki,M., Ueda,J., Ohta,T., Ohki,M., Fukuda,M., Takeda,N., Niida,H., Kato,H. *et al.* (2002) G9a histone methyltransferase plays a dominant role in euchromatic histone H3 lysine 9 methylation and is essential for early embryogenesis. *Genes Dev.*, **16**, 1779–1791.
18. Schotta,G., Ebert,A., Krauss,V., Fischer,A., Hoffmann,J., Rea,S., Jenuwein,T., Dorn,R. and Reuter,G. (2002) Central role of *Drosophila* SU(VAR)3–9 in histone H3-K9 methylation and heterochromatic gene silencing. *EMBO J.*, **21**, 1121–1131.
19. Mermoud,J.E., Popova,B., Peters,A.H., Jenuwein,T. and Brockdorff,N. (2002) Histone H3 lysine 9 methylation occurs rapidly at the onset of random X chromosome inactivation. *Curr. Biol.*, **12**, 247–251.
20. Litt,M.D., Simpson,M., Gaszner,M., Allis,C.D. and Felsenfeld,G. (2001) Correlation between histone lysine methylation and developmental changes at the chicken beta-globin locus. *Science*, **293**, 2453–2455.
21. Nagel,A.C., Maier,D. and Preiss,A. (2002) Green fluorescent protein as a convenient and versatile marker for studies on functional genomics in *Drosophila*. *Dev. Genes Evol.*, **212**, 93–98.
22. Brand,A.H. and Perrimon,N. (1993) Targeted gene expression as a means of altering cell fates and generating dominant phenotypes. *Development*, **118**, 401–415.
23. McGuire,S.E., Le,P.T., Osborn,A.J., Matsumoto,K. and Davis,R.L. (2003) Spatiotemporal rescue of memory dysfunction in *Drosophila*. *Science*, **302**, 1765–1768.
24. Larsson,J., Chen,J.D., Rasheva,V., Rasmuson-Lestander,A. and Pirrotta,V. (2001) Painting of fourth, a chromosome-specific protein in *Drosophila*. *Proc. Natl Acad. Sci. USA*, **98**, 6273–6278.
25. Jiang,J., Hoey,T. and Levine,M. (1991) Autoregulation of a segmentation gene in *Drosophila*: combinatorial interaction of the even-skipped homeo box protein with a distal enhancer element. *Genes Dev.*, **5**, 265–277.
26. Tautz,D. and Pfeifle,C. (1989) A non-radioactive in situ hybridization method for the localization of specific RNAs in *Drosophila* embryos reveals translational control of the segmentation gene hunchback. *Chromosoma*, **98**, 81–85.
27. Sandaltzopoulos,R., Mitchelmore,C., Bonte,E., Wall,G. and Becker,P.B. (1995) Dual regulation of the *Drosophila* hsp26 promoter *in vitro*. *Nucleic Acids Res.*, **23**, 2479–2487.
28. Luger,K., Mader,A.W., Richmond,R.K., Sargent,D.F. and Richmond,T.J. (1997) Crystal structure of the nucleosome core particle at 2.8 A resolution. *Nature*, **389**, 251–260.
29. Clapier,C.R., Nightingale,K.P. and Becker,P.B. (2002) A critical epitope for substrate recognition by the nucleosome remodeling ATPase ISWI. *Nucleic Acids Res.*, **30**, 649–655.
30. Kornberg,R.D., LaPointe,J.W. and Lorch,Y. (1989) Preparation of nucleosomes and chromatin. *Methods Enzymol.*, **170**, 3–14.
31. Luger,K., Rechsteiner,T.J. and Richmond,T.J. (1999) Preparation of nucleosome core particle from recombinant histones. *Methods Enzymol.*, **304**, 3–19.
32. Eskeland,R., Czermin,B., Boeke,J., Bonaldi,T., Regula,J.T. and Imhof,A. (2004) The N-terminus of *Drosophila* SU(VAR)3–9 mediates dimerization and regulates its methyltransferase activity. *Biochemistry*, **43**, 3740–3749.
33. Taipale,M., Rea,S., Richter,K., Vilar,A., Lichter,P., Imhof,A. and Akhtar,A. (2005) hMOF histone acetyltransferase is required for histone H4 lysine 16 acetylation in mammalian cells. *Mol. Cell. Biol.*, **25**, 6798–6810.
34. Bonaldi,T., Regula,J.T. and Imhof,A. (2004) The use of mass spectrometry for the analysis of histone modifications. *Methods Enzymol.*, **377**, 111–130.
35. Greiner,D., Bonaldi,T., Eskeland,R., Roemer,E. and Imhof,A. (2005) Identification of a specific inhibitor of the histone methyltransferase SU(VAR)3–9. *Nature Chem. Biol.*, **1**, 143–145.
36. Bialecki,M., Shilton,A., Fichtenberg,C., Segraves,W.A. and Thummel,C.S. (2002) Loss of the ecdysteroid-inducible E75A orphan nuclear receptor uncouples molting from metamorphosis in *Drosophila*. *Dev. Cell*, **3**, 209–220.
37. Huang,N., vom Baur,E., Garnier,J.M., Lerouge,T., Vonesch,J.L., Lutz,Y., Chambon,P. and Losson,R. (1998) Two distinct nuclear receptor interaction domains in NSD1, a novel SET protein that exhibits characteristics of both corepressors and coactivators. *EMBO J.*, **17**, 3398–3412.
38. Rea,S., Eisenhaber,F., O'Carroll,D., Strahl,B.D., Sun,Z.W., Schmid,M., Opravil,S., Mechtler,K., Ponting,C.P., Allis,C.D. *et al.* (2000) Regulation of chromatin structure by site-specific histone H3 methyltransferases. *Nature*, **406**, 593–599.
39. Mosavi,L.K., Cammett,T.J., Desrosiers,D.C. and Peng,Z.Y. (2004) The ankyrin repeat as molecular architecture for protein recognition. *Protein Sci.*, **13**, 1435–1448.
40. Reeves,R. (2000) Structure and function of the HMGI(Y) family of architectural transcription factors. *Environ. Health Perspect.*, **108**, 803–809.
41. Aravind,L. and Landsman,D. (1998) AT-hook motifs identified in a wide variety of DNA-binding proteins. *Nucleic Acids Res.*, **26**, 4413–4421.
42. Tachibana,M., Sugimoto,K., Fukushima,T. and Shinkai,Y. (2001) Set domain-containing protein, G9a, is a novel lysine-preferring mammalian histone methyltransferase with hyperactivity and specific selectivity to lysines 9 and 27 of histone H3. *J. Biol. Chem.*, **276**, 25309–25317.
43. Patnaik,D., Chin,H.G., Esteve,P.O., Benner,J., Jacobsen,S.E. and Pradhan,S. (2004) Substrate specificity and kinetic mechanism of mammalian G9a histone H3 methyltransferase. *J. Biol. Chem.*, **279**, 53248–53258.
44. Collins,R.E., Tachibana,M., Tamaru,H., Smith,K.M., Jia,D., Zhang,X., Selker,E.U., Shinkai,Y. and Cheng,X. (2005) *In vitro* and *in vivo* analyses of a Phe/Tyr switch controlling product specificity of histone lysine methyltransferases. *J. Biol. Chem.*, **280**, 5563–5570.
45. Fang,J., Feng,Q., Ketel,C.S., Wang,H., Cao,R., Xia,L., Erdjument-Bromage,H., Tempst,P., Simon,J.A. and Zhang,Y. (2002) Purification and functional characterization of SET8, a nucleosomal histone H4-lysine 20-specific methyltransferase. *Curr. Biol.*, **12**, 1086–1099.
46. Rice,J.C., Nishioka,K., Sarma,K., Steward,R., Reinberg,D. and Allis,C.D. (2002) Mitotic-specific methylation of histone H4 Lys 20 follows increased PR-Set7 expression and its localization to mitotic chromosomes. *Genes Dev.*, **16**, 2225–2230.
47. Beisel,C., Imhof,A., Greene,J., Kremmer,E. and Sauer,F. (2002) Histone methylation by the *Drosophila* epigenetic transcriptional regulator Ash1. *Nature*, **419**, 857–862.
48. Schotta,G., Lachner,M., Sarma,K., Ebert,A., Sengupta,R., Reuter,G., Reinberg,D. and Jenuwein,T. (2004) A silencing pathway to induce H3–K9 and H4–K20 trimethylation at constitutive heterochromatin. *Genes Dev.*, **18**, 1251–1262.
49. Chin,H.G., Pradhan,M., Esteve,P.O., Patnaik,D., Evans,T.C. Jr and Pradhan,S. (2005) Sequence specificity and role of proximal amino acids of the histone H3 tail on catalysis of murine G9A lysine 9 histone H3 methyltransferase. *Biochemistry*, **44**, 12998–13006.
50. Gates,J., Lam,G., Ortiz,J.A., Losson,R. and Thummel,C.S. (2004) Rigor mortis encodes a novel nuclear receptor interacting protein required for ecdysone signaling during *Drosophila* larval development. *Development*, **131**, 25–36.
51. D'Avino,P.P. and Thummel,C.S. (2000) The ecdysone regulatory pathway controls wing morphogenesis and integrin expression during *Drosophila* metamorphosis. *Dev. Biol.*, **220**, 211–224.
52. Ebert,A., Schotta,G., Lein,S., Kubicek,S., Krauss,V., Jenuwein,T. and Reuter,G. (2004) Su(var) genes regulate the balance between euchromatin and heterochromatin in *Drosophila*. *Genes Dev.*, **18**, 2973–2983.
53. Edgar,B.A. and Orr-Weaver,T.L. (2001) Endoreplication cell cycles: more for less. *Cell*, **105**, 297–306.

54. Liu,L.P., Ni,J.Q., Shi,Y.D., Oakeley,E.J. and Sun,F.L. (2005) Sex-specific role of *Drosophila melanogaster* HP1 in regulating chromatin structure and gene transcription. *Nat. Genet.*, **37**, 1361–1366.
55. Beckstead,R., Ortiz,J.A., Sanchez,C., Prokopenko,S.N., Chambon,P., Losson,R. and Bellen,H.J. (2001) Bonus, a *Drosophila* homolog of TIF1 proteins, interacts with nuclear receptors and can inhibit betaFTZ-F1-dependent transcription. *Mol. Cell*, **7**, 753–765.
56. King-Jones,K. and Thummel,C.S. (2005) Nuclear receptors—a perspective from *Drosophila*. *Nature Rev. Genet.*, **6**, 311–323.
57. Badenhorst,P., Xiao,H., Cherbas,L., Kwon,S.Y., Voas,M., Rebay,I., Cherbas,P. and Wu,C. (2005) The *Drosophila* nucleosome remodeling factor NURF is required for Ecdysteroid signaling and metamorphosis. *Genes Dev.*, **19**, 2540–2545.
58. Irving,P., Ubeda,J.M., Doucet,D., Troxler,L., Lagueux,M., Zachary,D., Hoffmann,J.A., Hetru,C. and Meister,M. (2005) New insights into *Drosophila* larval haemocyte functions through genome-wide analysis. *Cell Microbiol.*, **7**, 335–350.
59. Meister,M. and Lagueux,M. (2003) *Drosophila* blood cells. *Cell Microbiol.*, **5**, 573–580.
60. Lee,D.Y., Northrop,J.P., Kuo,M.H. and Stallcup,M.R. (2006) Histone H3 lysine 9 methyltransferase G9a is a transcriptional coactivator for nuclear receptors. *J. Biol. Chem.*, **281**, 8476–8485.
61. Ashburner,M., Chihara,C., Meltzer,P. and Richards,G. (1974) Temporal control of puffing activity in polytene chromosomes. *Cold Spring Harb. Symp. Quant. Biol.*, **38**, 655–662.
62. Vakoc,C.R., Mandat,S.A., Olenchock,B.A. and Blobel,G.A. (2005) Histone H3 lysine 9 methylation and HP1gamma are associated with transcription elongation through mammalian chromatin. *Mol. Cell*, **19**, 381–391.
63. Gyory,I., Wu,J., Fejer,G., Seto,E. and Wright,K.L. (2004) PRDI-BF1 recruits the histone H3 methyltransferase G9a in transcriptional silencing. *Nature Immunol.*, **5**, 299–308.
64. Nishio,H. and Walsh,M.J. (2004) CCAAT displacement protein/cut homolog recruits G9a histone lysine methyltransferase to repress transcription. *Proc. Natl Acad. Sci. USA*, **101**, 11257–11262.
65. Roopra,A., Qazi,R., Schoenike,B., Daley,T.J. and Morrison,J.F. (2004) Localized domains of G9a-mediated histone methylation are required for silencing of neuronal genes. *Mol. Cell*, **14**, 727–738.
66. Ueda,J., Tachibana,M., Ikura,T. and Shinkai,Y. (2006) Zinc finger protein wiz links G9a/GLP histone methyltransferases to the co-repressor molecule CtBP. *J. Biol. Chem.*, **281**, 20120–20128.
67. Rayasam,G.V., Wendling,O., Angrand,P.O., Mark,M., Niederreither,K., Song,L., Lerouge,T., Hager,G.L., Chambon,P. and Losson,R. (2003) NSD1 is essential for early post-implantation development and has a catalytically active SET domain. *EMBO J.*, **22**, 3153–3163.
68. Mis,J., Ner,S.S. and Grigliatti,T.A. (2006) Identification of three histone methyltransferases in *Drosophila*: dG9a is a suppressor of PEV and is required for gene silencing. *Mol. Genet. Genomics*, **275**, 513–526.